



Philipps-Universität Marburg
Fachbereich Biologie
-Genetik-

Genomic Analysis of Secondary Metabolism in *U. maydis*

Dissertation

zur

Erlangung des Doktorgrades
der Naturwissenschaften
(Dr. rer. nat.)

dem

Fachbereich Biologie
der Philipps-Universität Marburg
vorgelegt von

Esmeralda Za-nicthé Reyes Fernández
aus Culiacan, Sinaloa/Mexico

Marburg/Lahn 2016

Die in der vorliegenden Arbeit durchgeführten Untersuchungen wurden von Oktober 2011 bis Oktober 2016 am Institut für Genetik der Philipps-Universität Marburg unter der Leitung von Prof. Dr. Michael Bölker angefertigt.

Vom Fachbereich Biologie der Philipps-Universität Marburg als Dissertation am angenommen
am: 14.12.2016

Erstgutachter: Prof. Dr. Michael Bölker
Zweitgutachter: Prof. Dr. Alfred Batschauer

Tag der mündlichen Prüfung am: 21.12.2016

Declaration

I hereby declare that the dissertation entitled “**Genomic Analysis of Secondary Metabolism in *Ustilago maydis***” submitted to the Department of Biology, Philipps-Universität Marburg, is the original and independent work carried out by me under the guidance of the PhD committee, and the dissertation is not formed previously on the basis of any award of Degree, Diploma or other similar titles.

Marburg, 1st. October 2016.

Esmeralda Za-nicthé Reyes Fernández.

Dedicated to my beloved family and friends for always supported me.

I love you all dearly

Summary

Ustilago maydis is a well established model organism for the study of plant-microbe interactions although its biosynthetic potential has not been totally explored. Therefore, in this work we focused our attention on identifying potential secondary metabolite (SM) gene clusters by mining *U. maydis* genome. The combination of different strategies as manual annotation and bioinformatic approaches allowed us the detection of 4 potential SM gene clusters (A-D). The further selection of cluster A as a subject of this study, was based on its chromosomal location and the analysis of gene expression profiles among members of each cluster. Such analysis was possible due to the construction of an excel table in which all available *U. maydis* gene expression data from Gene Expression Omnibus were compiled and normalized. Overexpression of the transcription factor Mtf1 in cluster A resulted in the activation of at least 12 genes including three polyketide synthases (*pks3*, *pks4* and *pks5*), a cytochrome P450 (*cyp4*) and a versicolorin B synthase (*vbs1*), among others. Prolonged induction of cluster A triggered the production of a black-greenish pigment mainly composed of 1,3,6,8-tetrahydroxynaphthalene (T4HN), therefore cluster A was named as the melanin-like cluster. This result showed that *U. maydis* synthesizes melanin using an unusual pathway, since most fungal melanins are derived from DHN, whose precursor is T4HN. Mutants defective for *pks3*, *pks4*, *pks5* and *cyp4* did not accumulate melanin, indicating a crucial role of these genes at the first stages of its biosynthesis. Deletion of *cyp4* produced orsellinic acid (OA) and two of its derivatives. Interestingly, a feeding experiment with OA rescued the melanization defect of *pks3* and *pks4* deletion mutants. Moreover, the simultaneous expression of the *pks3* and *pks4* genes produced OA, suggesting that both genes are involved in OA biosynthesis, which is then used as a substrate for further chemical conversion into T4HN, a reaction presumably catalyzed by Cyp4 and/or Pks5. Overexpression of *pks1*, a polyketide synthase gene in *U. maydis* previously reported to play a role in melanization together with *pks2* and *lac1*, could rescue the phenotype in the strain MB215 $\Delta pks3$ *Pcrg::mtf1*, suggesting that Pks3 and Pks1 have complementary functions. Maize seedlings infected with single deletion mutants of the melanin-like cluster genes showed no effect on spore coloration and had only a minor effect on virulence, supporting the previous finding that *pks1* and *pks2* are the major contributors of melanization during sporulation. On the other hand, SG200 $\Delta pks3$, SG200 $\Delta pks4$ and SG200 $\Delta pks5$ showed no significant differences compared to the wild type (SG200) when exposed to hydrogen peroxide, indicating that melanin-like cluster genes may be involved in other kind of

stress responses, hence further experiments need to be performed to understand the conditions under which the melanin-like cluster is activated.

Zusammenfassung

Obwohl *Ustilago maydis* ein gut etablierter Modellorganismus zur Erforschung von Interaktionen zwischen Pflanzen und Mikroben ist, ist sein biosynthetisches Potenzial nur unvollständig untersucht. Deshalb wurde in dieser Arbeit das Hauptaugenmerk auf die Identifizierung potenzieller Sekundärmetabolit (SM)-Gencluster im Genom gelegt. Die Kombination von verschiedenen Strategien, wie manuelle Annotation und bioinformatische Ansätze, erlaubte die Identifizierung von 4 potentiellen SM Genclustern (A-D). Die Auswahl von Cluster A für die weiteren Untersuchungen in dieser Arbeit beruhte auf seiner chromosomalen Lokalisation und der Analyse von Genexpressionsprofilen der Clustergene. Zur Analyse der Genexpression in *U. maydis* wurden alle verfügbaren Daten der öffentlich zugänglichen Datenbank „Gene Expression Omnibus“ in einer Excel-Tabelle zusammengefügt und normalisiert. Die Überexpression des Transkriptionsfaktors Mtf1 in Cluster A führte zu einer Aktivierung von mindestens 12 Genen, unter denen sich auch drei Polyketidsynthasen (*pks3*, *pks4* und *pks5*), ein Cytochrom P450 (*cyp4*) und eine Versicolorin B-Synthase (*vbs1*) waren. Längere Induktion von Cluster A führte zur Produktion eines schwarz-grünen Pigments, das hauptsächlich aus 1,3,6,8-Tetrahydroxynaphthalin (T4HN) besteht. Daher wurde Cluster A Melanin-ähnlicher Cluster genannt. Dieses Ergebnis zeigte bereits, dass *U. maydis* Melanin über einen ungewöhnlichen Weg synthetisiert, da die meisten pilzlichen Melanine auf DHN, dessen Vorstufe T4HN ist, basieren. Mutanten mit fehlenden *pks3*, *pks4*, *pks5* und *cyp4*-Genen zeigten keine Melaninanreicherung, was auf eine essentielle Funktion dieser Gene bei den ersten Schritten der Biosynthese hindeutet. Die Deletion von *cyp4* führte zur Produktion von Orsellinsäure (OA) und zwei ihrer Derivate. Interessanterweise konnte durch Zugabe von zum Medium OA der Melanisierungsdefekt der *pks3/pks4*-Deletionsmutante ausgeglichen werden. Außerdem resultierte die simultane Überexpression der *pks3* und *pks4*-Gene in der Produktion von OA, was darauf hindeutet, dass beide Gene an der OA-Synthese beteiligt sind. OA stellt daher ein wichtiges Zwischenprodukt dar, das in nachfolgenden Reaktionsschritten als Substrat für weitere Umwandlungen zu T4HN verwendet wird. Diese Reaktionen werden vermutlich von Cyp4 und/oder Pks5 katalysiert. Überexpression von *pks1*, einer weiteren Polyketidsynthase-Gen in *U. maydis*, für das in früheren Arbeiten zusammen mit *pks2* und *lac1* eine Rolle bei der Melanisierung der Sporen beschrieben wurde, konnte den Phänotyp des Stammes MB215 $\Delta pks3$ *Pcrg::mtf1* ausgleichen. Dies deutet darauf hin, dass Pks3 und Pks1 eine vergleichbare biochemische Funktion ausüben. Maiskeimlinge, die mit Stämmen mit Einzelgendeletionen des Melanin-ähnlichen Clusters infiziert wurden, zeigten keinen Effekt auf

die Sporenfarbe und hatten nur einen geringen Einfluss auf die Virulenz. Dies unterstützt das vorherige Ergebnis, wonach *pks1* und *pks2* hauptsächlich zur Melanisierung während der Sporenbildung beitragen. Da die Deletionsmutanten SG200 $\Delta pks3$, SG200 $\Delta pks4$ und SG200 $\Delta pks5$ bei Wachstum auf Wasserstoffperoxid keine signifikanten Unterschiede zum Wildtyp (SG200) aufwiesen, deutet dies darauf hin, dass die Bildung dieses Melanin-ähnlichen Farbstoffs vermutlich eine Rolle bei anderen Stressantworten spielen könnte. Daher sind weitere Experimente nötig, um Bedingungen zu finden, bei denen die Gene dieses Clusters exprimiert sind.

Abbreviations

aa	Aminoacids
Amp	Ampicillin
BLAST	Basic Local Alignment Search Tool
bp	Base pair
<i>cbx</i>-locus	Gene locus of the iron-sulphur subunit of the succinate-dehydrogenase from <i>U. maydis</i>
Cbx^R	Carboxin resistance
cm	Centimeter
<i>crg</i>-Promoter	Arabinose-inducible promoter
C-terminal	Carboxy-terminal
ddH₂O	Doubled distilled water
DHN	1,8-dihydroxynaphthalene
DMAT	Dimethylallyl transferase
DMSO	Dimethylsulfoxide
DNA	Deoxyribonucleic acid
DNase	Deoxyribonuclease
dpi	Days post infection
dNTP	Deoxyribonucleotide
EDTA	Ethylendiamintetraacetic acid
FPP	Farnesyl pyrophosphate
GFP	Green fluorescent protein
GGPP	Geranylgeranyl pyrophosphate
GPP	Geranyl pyrophosphate
G418^R	Geneticin resistance
h	Hour
Hyg^R	Hygromycin resistance
kb	Kilobase
L	Liter
LB	Light broth
m	meter
M	Molar
min	Minute
ml	Milliliter
mM	Millimolar
MOPS	3-(N-Morpholino)-propanesulfonic acid
MS	Mass spectrometry
Nat^R	Nourseothricin resistance
NCBI	National Center for Biotechnology Information
NRPS	Non-ribosomal peptide synthetase
nt	Nucleotide
N-terminal	Amino-terminal
OD	Optical density
ON	Over night
<i>otef</i>-Promoter	Promoter of the translation elongation factor 1 of <i>U. maydis</i>
ORF	Open reading frame
PCR	Polymerase chain reaction
PD	Potato dextrose

PEG	Polyethylene glycol
PIPES	Piperazin-N-N'-bis-(2-ethansulfonat)
PKS	Polyketide synthase
PPO	Polyphenol oxidases
RNA	Ribonucleic acid
mRNA	Messenger RNA
rRNA	Ribosomal RNA
RT	Room temperature
SAP	Shrimp alkaline phosphatase
SDS	Sodium dodecyl sulfate
sec	Second
TAE	Tris base + acetic acid + EDTA
TC	Terpene cyclase
TE	Tris-Cl + Na ₂ -EDTA
TPS	Terpene synthase
Tris	Tris(hydroxymethyl)aminomethane
T4HN	1,3,6,8-tetrahydroxynaphthalene
T3HN	1,3,8-trihydroxynaphthalene
µg	Microgram
µl	Microliter
µm	Micrometer
rpm	Revolutions per minute
URA	Uracil
UV	Ultra-Violet
wt	Wild type
w/v	Weight per volume
YEP	Yeast extract + peptone
YEPD	Yeast extract + peptone + dextrose
YPD	Yeast extract + peptone + dextrose
YEPS	Yeast extract + peptone + sucrose
YNB	Yeast nitrogen base
%	Percent
°C	Degree Celsius

Table of contents

Summary.....	I
Zusammenfassung.....	III
Abbreviations.....	V
Table of contents.....	VII
Table of figures.....	X
1 Introduction.....	1
1.1 Secondary metabolism.....	1
1.2 Secondary metabolites in filamentous fungi.....	1
1.2.1 Classification of secondary metabolites.....	1
1.2.1.1 Polyketides (PKs).....	2
1.2.1.2 Non-ribosomal peptides (NRPs).....	9
1.2.1.3 Hybrid metabolites.....	11
1.2.1.4 Terpenes.....	13
1.2.1.5 Alkaloids.....	15
1.2.2 Strategies to elicit natural products from silent biosynthetic gene clusters.....	16
1.2.2.1 Cultivation based approaches.....	16
1.2.2.2 Molecular approaches.....	18
1.2.2.2.1 Ribosome engineering.....	18
1.2.2.2.2 Manipulation of global and cluster-specific regulators.....	19
1.2.2.2.3 Heterologous expression.....	20
1.2.2.2.4 Epigenetic mining.....	22
1.2.2.3 Mining for novel compounds and their biosynthetic genes.....	23
1.3 Secondary metabolism in <i>Ustilago maydis</i>.....	24
1.3.1 <i>U. maydis</i> as a model organism.....	24
1.3.2 Secondary metabolites identified in <i>U. maydis</i>	25
1.3.3 Melanization process in <i>U. maydis</i>	27
1.4 Aims of this work.....	29
2 Results.....	30
2.1 Identification of potential SM gene clusters in <i>U. maydis</i>.....	30
2.1.1 Manual annotation.....	30
2.1.2 Gene expression data.....	36
2.1.3 Analysis of the expression profiles of gene clusters identified by manual annotation.....	40
2.2 Upregulation of the Cluster A genes triggers the production of a black-greenish pigment.....	41
2.3 Deletion of the <i>pks3</i>, <i>pks4</i>, <i>pks5</i> and <i>cyp4</i> genes abolishes the melanin-like pigment production.....	46
2.4 Metabolic profiles of strains overexpressing single and multiple genes of the melanization gene cluster.....	51
2.5 Can the overexpression of the <i>pks1</i> and/or <i>pks2</i> genes rescue the phenotype in the strains MB215 $\Delta pks3$ <i>P_{erg}::mtf1</i>, MB215 $\Delta\Delta pks4$ <i>P_{erg}::mtf1</i> and MB215 $\Delta pks5$ <i>P_{erg}::mtf1</i>?.....	56
2.6 Orsellinic acid feeding experiment.....	65

2.7	Effect of tricyclazole on the melanin synthesis.....	68
2.8	Pathogenicity assays.....	69
2.9	H ₂ O ₂ sensitivity assay in <i>U. maydis</i>	73
3	Discussion.....	75
3.1	Identification of a coregulated polyketide synthase gene cluster in <i>U. maydis</i>	75
3.2	Identification of an alternative melanization pathway in <i>U. maydis</i>	77
3.3	Inactivation of <i>pks3</i> , <i>pks4</i> , <i>pks5</i> and <i>cyp4</i> genes abolishes melanin pigment biosynthesis.....	80
3.4	Inactivation of <i>vbs1</i> , <i>omt1</i> , <i>pmo1</i> and <i>deh1</i> genes influences the biosynthesis of the melanin-like pigment in <i>U. maydis</i>	91
3.5	Role of the melanin clusters in <i>U. maydis</i>	94
3.6	Conclusions and Outlook.....	104
4	Materials and Methods.....	106
4.1	<i>E. coli</i> , <i>S. cerevisiae</i> and <i>U. maydis</i> strains.....	106
4.1.1	<i>E. coli</i> strains.....	106
4.1.2	<i>S. cerevisiae</i> strains.....	106
4.1.3	<i>U. maydis</i> strains.....	106
4.1.3.1	Lab collection.....	106
4.1.3.2	<i>U. maydis</i> strains generated in this work.....	107
4.2	Plasmids and primers.....	112
4.2.1	Standard plasmids.....	112
4.2.2	Plasmids created in this study for the transformation of <i>U. maydis</i>	112
4.2.3	Primers.....	125
4.3	Materials and their sources of supply.....	125
4.3.1	Laboratory equipment.....	125
4.3.2	General materials.....	126
4.3.3	Chemicals.....	126
4.3.4	Enzymes.....	128
4.3.5	Kits used in this study.....	128
4.4	Cultivation methods.....	129
4.4.1	Cultivation of <i>E. coli</i>	129
4.4.2	Cultivation of <i>S. cerevisiae</i>	129
4.4.3	Cultivation of <i>U. maydis</i>	130
4.5	Molecular biological methods.....	131
4.5.1	Competent cell preparation and transformation of <i>E. coli</i>	131
4.5.2	Plasmid preparation from <i>E. coli</i>	131
4.5.3	Restriction enzymatic cleavage of DNA.....	132
4.5.4	Dephosphorylation of cut plasmid-DNA.....	133
4.5.5	Agarose gel electrophoresis.....	133
4.5.6	DNA extraction from agarose gel.....	133
4.5.7	Ligation of DNA fragments.....	134
4.5.8	PCR amplification of DNA.....	134
4.5.9	Sequencing of DNA.....	135
4.5.10	Competent cell preparation and transformation of <i>S. cerevisiae</i>	135
4.5.11	Protoplast preparation and transformation of <i>U. maydis</i>	136
4.5.12	Genomic DNA isolation of <i>U. maydis</i>	137
4.5.13	<i>U. maydis</i> total RNA isolation from axenic culture.....	138
4.5.14	DNA blotting and hybridization (Southern analysis).....	139
4.5.15	RNA blotting and hybridization (Northern analysis).....	139

4.5.16	Probe labeling	141
4.5.17	Pathogenicity assays	141
4.6	Genetic methods	142
4.6.1	Generation of deletion mutants in <i>U. maydis</i>	142
4.6.2	Integration of overexpressing constructs into the <i>ip</i> -locus in <i>U. maydis</i>	143
4.7	Analytical methods	144
4.7.1	Tricyclazole experiment	144
4.7.2	H ₂ O ₂ sensitivity assay	144
4.7.3	Orsellinic acid (OA) feeding experiment	144
4.7.4	Preparation of the extracts for HPLC analysis	145
4.7.5	HPLC-MS	145
4.8	Bioinformatic analysis	145
4.8.1	Sequence analysis of DNA and proteins	145
4.8.2	Compilation of gene expression data in <i>U. maydis</i>	146
5	References	147
6	Supplementary data	173

Table of figures

Figure 1. Basic mechanism involved in fatty acid and polyketide biosynthesis.....	3
Figure 2. Catalytic cycle of a representative minimal module	4
Figure 3. Three types of PKSs.....	5
Figure 4. Domain organization of the erythromycin polyketide synthase	6
Figure 5. The biosynthetic pathway of the fungal polyketide 6-methylsalicylic acid (6-MSA).....	7
Figure 6. Products of type II polyketide synthases from <i>Streptomyces</i> sp.....	8
Figure 7. Fungal nonribosomal peptides	9
Figure 8. NRP domain organization and NRPS mechanism	10
Figure 9. Simplified mechanism of action for NRPS and PKS modules within the hybrid synthase involved in the biosynthesis of zwittermicin A	12
Figure 10. Molecular structures of tenuazonic acid and lovastatin.....	13
Figure 11. Terpene biosynthetic pathway.....	14
Figure 12. Reaction catalyzed by DMATS and structures of ergot alkaloids.....	15
Figure 13. Pathway-specific strategies to induce the expression of silent biosynthetic gene clusters	21
Figure 14. Epigenetic perturbation as a strategy to activate silent gene clusters	23
Figure 15. Life cycle of <i>Ustilago maydis</i>	25
Figure 16. Major compounds of secondary metabolism in <i>U. maydis</i>	26
Figure 17. Melanin biosynthesis pathways in fungi	28
Figure 18. Melanized tumor of <i>U. maydis</i> and the proposed precursor for the melanin biosynthesis	28
Figure 19. Secondary metabolite gene clusters identified by manual annotation and bioinformatic approaches	35
Figure 20. Gene expression plots of three different biosynthetic gene clusters.....	38
Figure 21. Expression analysis of coregulated genes in <i>U. maydis</i> under a variety of conditions	39
Figure 22. Gene expression plots of biosynthetic clusters identified by manual annotation in <i>U. maydis</i>	40
Figure 23. Domain structure of the transcription factors Mtf1 and Mtf2 located within the cluster A	42
Figure 24. Induction of the silent gene cluster A results in the production of a black-greenish pigment.....	44
Figure 25. Serial 10 fold-dilutions of cell suspension of MB215, MB215 <i>Pcrg::mtf1</i> and MB215 <i>Pcrg::mtf2</i> strains on agar inducing medium.....	45
Figure 26. Overexpression of <i>mtf1</i> results in the production of many complex compounds derived from T4HN	46
Figure 27. The single deletion of the <i>pks4</i> gene has no effect on melanin production	48
Figure 28. Metabolic profiling of the melanin cluster deletion mutants.....	49
Figure 29. Molecular structure of orsellinic acid and its derivatives identified in the MB215 $\Delta cyp4$ <i>Pcrg::mtf1</i> strain	50
Figure 30. Metabolic profiles of MB215 $\Delta vbs1$ <i>Pcrg::mtf1</i> , MB215 $\Delta cyp4$ <i>Pcrg::mtf1</i> and MB215 $\Delta cyp4\Delta vbs1$ <i>Pcrg::mtf1</i>	50
Figure 31. Metabolic profiling of strains overexpressing single genes of the melanin gene cluster	52
Figure 32. Domain organization of polyketide synthases of the melanin-like gene cluster in <i>U. maydis</i>	53

Figure 33. Double overexpression of the <i>pks3</i> and <i>pks4</i> genes produces orsellinic acid (OA)	54
Figure 34. Metabolic profiles of the extracts from the double overexpression strains MB215 <i>Pcrg::pks3+Petef::cyp4</i> , MB215 <i>Pcrg::pks4+Petef::cyp4</i> and MB215 <i>Pcrg::pks5+Petef::cyp4</i> as detected by UV absorption at 272 nm.	55
Figure 35. <i>Mtf1</i> does not control the expression of the <i>pks1</i> and <i>pks2</i> genes	57
Figure 36. Domain structure of the polyketide synthases identified in the SM gene clusters A and D in <i>U. maydis</i>	57
Figure 37. HPLC profiles of the extracts from the double overexpressing strains MB215 <i>Pcrg::pks1+Pcrg::pks2</i> , MB215 <i>Pcrg::pks1+Petef::cyp4</i> and MB215 <i>Pcrg::pks2+Petef::cyp4</i> as detected by UV absorption at 272 nm	60
Figure 38. HPLC profiles of the extracts from the double overexpressing strains MB215 <i>Pcrg::pks1+Pcrg::pks3</i> , MB215 <i>Pcrg::pks1+Pcrg::pks4</i> and MB215 <i>Pcrg::pks1+Pcrg::pks5</i> as detected by UV absorption at 272 nm	61
Figure 39. HPLC profiles of the extracts from the double overexpressing strains MB215 <i>Pcrg::pks2+Pcrg::pks3</i> , MB215 <i>Pcrg::pks2+Pcrg::pks4</i> and MB215 <i>Pcrg::pks2+Pcrg::pks5</i> as detected by UV absorption at 272 nm	62
Figure 40. Phenotype of complementation strains MB215 $\Delta pks3$ <i>Pcrg::mtf1+Pcrg::pks1</i> , MB215 $\Delta pks3$ <i>Pcrg::mtf1+Pcrg::pks2</i> , MB215 $\Delta\Delta pks4$ <i>Pcrg::mtf1+Pcrg::pks1</i> , MB215 $\Delta\Delta pks4$ <i>Pcrg::mtf1+Pcrg::pks2</i> , MB215 $\Delta pks5$ <i>Pcrg::mtf1+Pcrg::pks1</i> and MB215 $\Delta pks5$ <i>Pcrg::mtf1+Pcrg::pks2</i>	64
Figure 41. Orsellinic acid feeding experiment in YNB liquid medium	66
Figure 42. Orsellinic acid feeding experiment on YNB agar plate	68
Figure 43. Effect of tricyclazole on the melanin biosynthesis pathway in <i>U. maydis</i>	69
Figure 44. Virulence of the <i>mtf1</i> and <i>mtf2</i> mutant strains	70
Figure 45. Virulence of the melanin-like single deletion mutants	72
Figure 46. Virulence of the SG200 $\Delta pks3\Delta cyp4$ strain	73
Figure 47. Sensitivity of <i>U. maydis</i> wild-type (SG200) and <i>pks3</i> , <i>pks4</i> and <i>pks5</i> mutant strains to oxidative stress	74
Figure 48. Domain organization of polyketide synthases in <i>U. maydis</i> , <i>U. hordei</i> , <i>S. reilianum</i> and <i>S. scitamineum</i>	79
Figure 49. Domain organization of polyketide synthases (PKSs)	82
Figure 50. Modular organization of type I polyketide synthases (PKSs)	82
Figure 51. Biosynthetic reaction scheme for T4HN and the by-product orsellinic acid produced by the heterologous expression of the <i>C. lagenarium</i> PKS1 gene in <i>A. oryzae</i>	84
Figure 52. Product identification of the wild-type PKS1 and its mutant in <i>C. lagenarium</i>	85
Figure 53. Sequence alignment of the PksA from <i>A. flavus</i> and Pks3 from <i>U. maydis</i>	86
Figure 54. Proposed HPQ melanin biosynthesis pathway in <i>Streptomyces griseus</i>	88
Figure 55. Proposed mechanisms for the first biosynthetic reactions in the melanin pathway in <i>U. maydis</i>	90
Figure 56. Teliospore development in maize plants induced by the wild-type, $\Delta pks2$, $\Delta pks3$ and $\Delta pks2\Delta pks3$ mutant strains.	97
Figure 57. RNA-Seq data of the PKSs and melanin-like cluster genes in <i>U. maydis</i> when cultivated in axenic culture and during maize plant infection	101
Figure 58. Strategy for creating deletion constructs in <i>S. cerevisiae</i> .	142
Figure 59. Integration of overexpressing plasmids into the genomic <i>ip</i> -locus in <i>U. maydis</i>	143

1 Introduction

1.1 Secondary metabolism

Secondary metabolites (SMs) are bioactive molecules, usually of low molecular weight, that play nonessential roles in growth, development, and reproduction of a living organism (Vining, 1992). They include antibiotics, antitumor agents, cholesterol-lowering drugs, toxins, and others. Secondary metabolites are produced in bacteria, fungi and plants often as a result of depletion of nutrients, absence of light, development of reproductive structures, or changes in ambient pH, just to mention some examples (Calvo *et al.*, 2002, Yu and Keller, 2005). Genes involved in the production of secondary metabolites are generally fast-evolving, often clustered, and coregulated through common transcription factors or at the level of chromatin organization (Brakhage, 2013). In many cases, the biosynthetic potential of secondary metabolite producers has been underestimated, since most of those gene clusters remain silent under normal laboratory conditions (Chiang *et al.*, 2011). Therefore, one of the biggest challenges is to understand where, when and how secondary metabolites are synthesized.

1.2 Secondary metabolites in filamentous fungi

Sequencing of fungal genomes has revealed that many fungi contain large numbers of genes involved in secondary metabolism that are typically arranged in gene clusters (Keller *et al.*, 2005). However, the identity, structure and function of most of the metabolites produced by enzymes that are encoded by these clusters remain unknown. In the next paragraphs, it will be described which types of secondary metabolites have been identified in fungi and some of the strategies to elicit the production of these compounds.

1.2.1 Classification of secondary metabolites

SMs are divided into classes according to their chemical nature and biosynthetic origin: polyketides (PKs), synthesized by polyketide synthases (PKSs); nonribosomal peptides (NRPs), produced by nonribosomal peptide synthetases (NRPSs); alkaloids and terpenes, which are generated by dimethylallyl tryptophan synthases (DMATs) and terpene cyclases (TCs), respectively. As a part of the classification, the hybrid metabolites produced by the enzymes

PKS-NRPSs are also included. A general description of each class of compounds together with the enzymes involved in their biosynthesis is included on the next pages.

1.2.1.1 Polyketides (PKs)

Polyketides are a remarkably diverse group of secondary metabolites that are enzymatically produced by polyketide synthases (PKSs) (Hertweck, 2009). Their structural diversity includes macrolides, polyphenols, polyenes, and numerous other structural scaffolds (Hertweck, 2009). Analogous to fatty acid synthases (FASs), PKSs catalyze the biosynthesis of polyketides through repetitive C-C bond-forming reactions between selected acyl-CoA derived building blocks (Cane *et al.*, 1999; Smith *et al.*, 2007). However, polyketide biosynthesis deviates in many ways from fatty acid biosynthesis. PKSs clearly differ from FASs not only in their ability to use a broader range of biosynthetic building blocks but also in the formation of various chain lengths (Hertweck, 2009). In addition, FASs catalyze the full reduction of each β -keto moiety prior to further chain extension in every cycle (Cox and Simpson, 2009). In contrast, PKSs synthesize polyketides with a higher degree of complexity, since the reduction steps following condensation can be fully, or partially omitted, giving a functionalized chain (Figure 1). The catalytic process on both FASs and PKSs can be divided into three steps: initiation, elongation and termination. Prior the initiation step, the acyl carrier protein (ACP) domain needs to be activated by an ACP synthase or 4'-phosphopantetheine transferase (4'-PPTase), which attaches a phosphopantetheine group from CoA onto the conserved serine of ACP to tether the acyl intermediate as thiol ester (Lim *et al.*, 2012). Once activated, the ACP domain shuttles the growing polyketide chain between various partner enzymes or catalytic domains of the PKS. Afterwards, the acyltransferase (AT) domain catalyzes the transfer of an extender unit such as malonyl- or (2S)-methylmalonyl-CoA, from the coenzyme A carrier to the phosphopantetheine side chain of the ACP domain (Figure 2). Since structural diversity of polyketides is strongly influenced by extender unit choices made by AT domains, these enzymes have been obvious targets for engineering of novel polyketides (Dunn *et al.*, 2013). After initiation, the ketosynthase (KS) domain carries out the decarboxylative Claisen condensation to form carbon-carbon bond between the growing polyketide chain and the ACP-bound extender unit (Figure 2). At this stage, diversity can be introduced through the installation of noncanonical extender units (Kapur *et al.*, 2012). Since KS is the most highly conserved domain in PKSs, it is often chosen for building up evolutionary trees of these enzymes (Gontang *et al.*, 2010). AT, KS and ACP constitute a minimal set of domains required for a functional PKS (Hopwood, 1997). Other domains such as ketoreductase (KR), dehydratase

(DH), enoyl reductase (ER), methyltransferase (MT) and cyclase (CYC) may be present to form different polyketide structures (Figure 1).

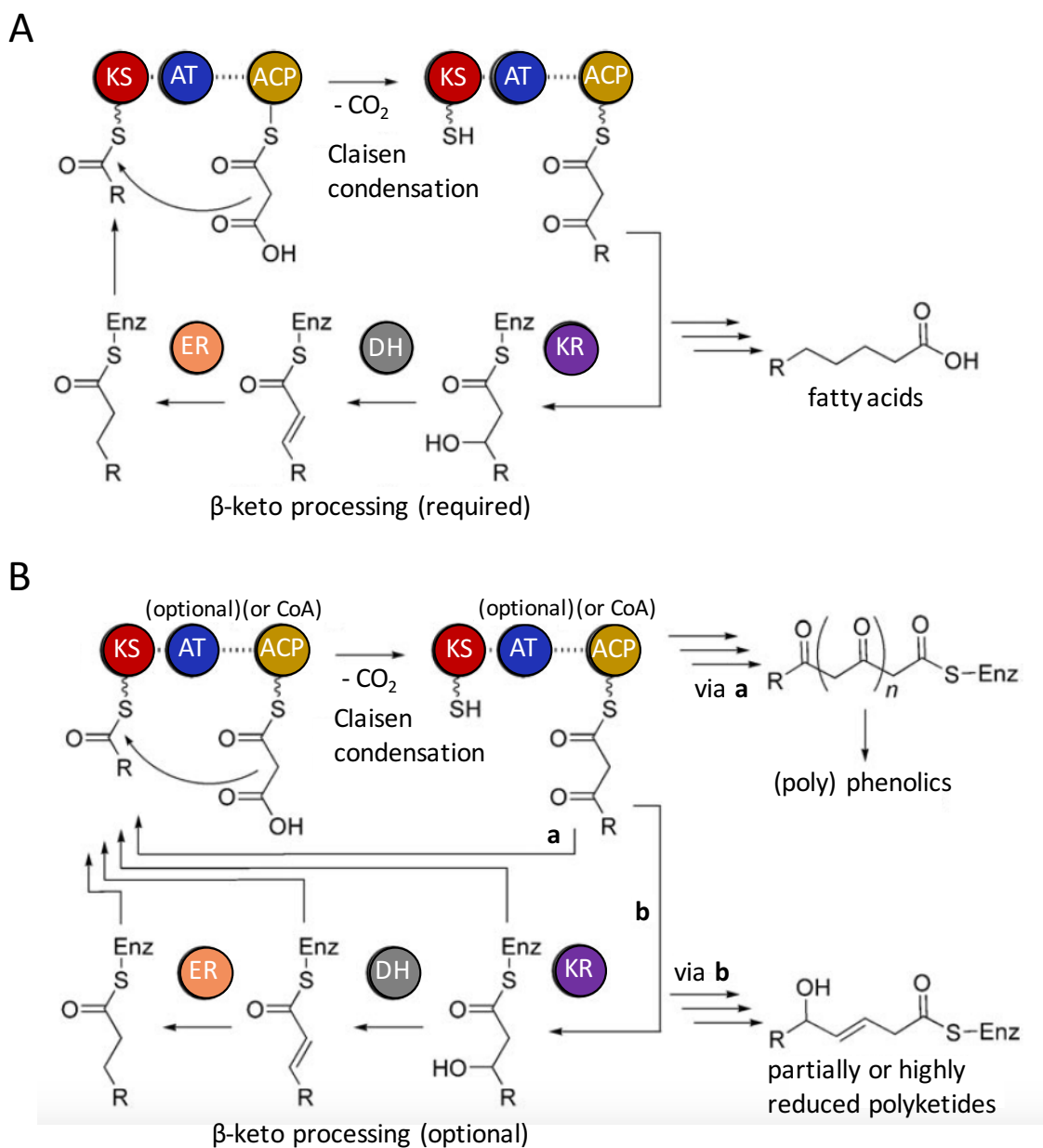


Figure 1. Basic mechanism involved in fatty acid and polyketide biosynthesis. (A) Fatty acid biosynthesis. A starter unit is condensed with a malonyl unit that undergoes decarboxylative Claisen condensation to furnish the electrons for the new carbon-carbon double bond. The resulting β-keto ester is successively reduced to hydroxy, dehydrated and finally reduced again to give a saturated chain longer than the original by two methylene units. **(B)** Polyketide biosynthesis. Unlike fatty acids, polyketides show a higher degree of complexity as the reduction steps following condensation can fully or partially (via **b**) or omitted (via **a**), giving highly functionalized chains. Enz: enzyme, KS: ketosynthase; AT: acyltransferase; ACP: acyl carrier protein; ER: enoyl reductase; DH: dehydratase; KR: ketoreductase. Adapted from Hertweck, 2009.

The termination step of polyketide biosynthesis is carried out by the thioesterase (TE) domain once the polyketide chain has reached the desired size. The polyketide product can be offloaded by different mechanisms as hydrolysis or macrocyclization (Bok *et al.*, 2009; Schroeckh *et al.*, 2009; Argyropoulos *et al.*, 2016).

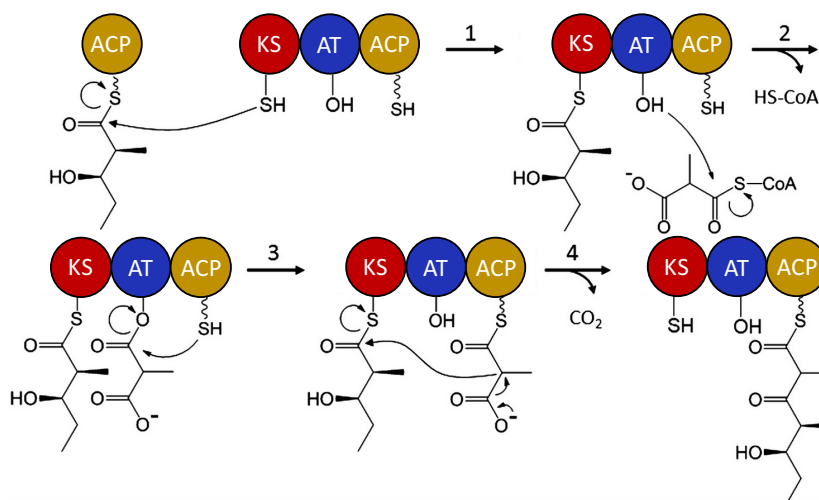


Figure 2. Catalytic cycle of a representative minimal module. Every module of an assembly line PKS catalyzes the following sequence reactions: (1) the polyketide chain is translocated from the ACP domain of the preceding module onto the KS domain of the target module. (2 and 3) Separately, the AT domain catalyzes transfer of a selected extender unit (in this case, a methylmalonyl group) onto the ACP domain. (4) The KS domain then catalyzes chain elongation via decarboxylative condensation, leading to the formation of an ACP-tethered β -ketoacyl product. The oxidation state and stereochemistry of this product is then set by an appropriate combination of KR, dehydratase, and enoyl reductase domains (not shown). Eventually, the chain is translocated of the downstream KS as in 1, although it is never translocated back to its own KS. AT: acyltransferase; ACP: acyl carrier protein; KS: ketosynthase. Adapted from Kapur *et al.*, 2012.

PKSs have been the subject of extensive review and are currently divided into three general classes according to their catalytic activities (type I, type II, and type III), although the exchange and evolution of genetic information among organisms has led to mixed classes (Shen, 2003). Type I PKSs are contained within multidomain polypeptides (Keatinge-Clay, 2012) and can be divided into iterative and modular PKSs, which are usually associated with fungi and bacteria, respectively. In a modular type I PKS each domain of a module corresponds to one biosynthetic step and the arrangement of domains in the genome reflects the molecular structure of the final product, which is known as the "co-linearity rule" (Staunton and Weissman, 2001; Moss *et al.*, 2004). The modules are not necessarily coded in a single gene; some are separated into multiple open reading frames, as in the case of the macrolide antibiotic erythromycin (Staunton, 1997), whose synthesis is carried out by three PKS genes (*eryAI-eryAIII*) (Figure 3A and 4). In some other cases, the complexity of a polyketide can be compared with the number of reactions needed for its synthesis, as it was previously reported for the

stambomycin gene cluster of *Streptomyces ambofaciens*, which is composed of 25 genes (nine of which encode PKSs), making it one of the largest PKS gene cluster described to date (Laureti *et al.*, 2011).

On the other hand, iterative type I PKSs conduct the synthesis of polyketides in multiple rounds of chain extension and appropriate β -ketoprocessing (Moss *et al.*, 2004). Mammalian fatty acid synthase (FAS) is an example of an iterative type I PKS, its catalytic domains are employed multiple times to condense two-carbon building blocks into the 16-carbon fatty acid palmitate (Keatinge-Clay, 2012).

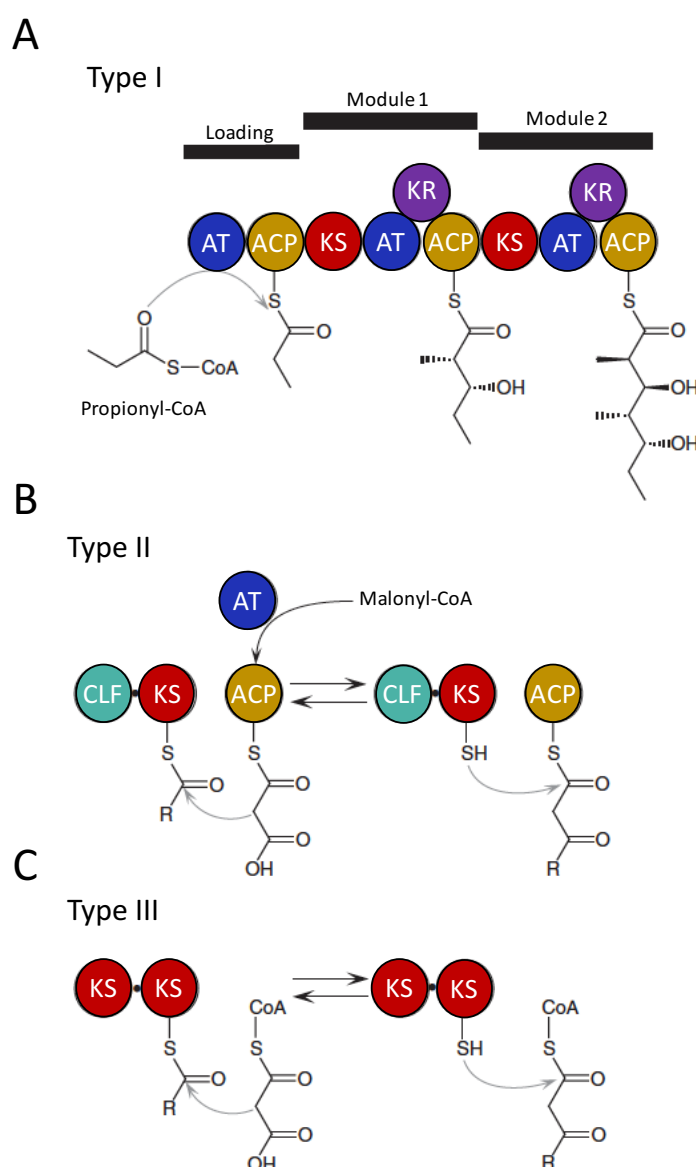


Figure 3. Three types of PKSs. (A) Type I PKS is a multifunctional peptide that is divided into modules and domains. (B) Type II PKS is a complex of discrete enzymes that possess an individual function. (C) Type III PKS is a simple homodimer of ketosynthase. AT: acyltransferase; KS: ketosynthase; ACP: acyl carrier protein; CLF: chain length factor. Adapted from Katsuyama and Horinouchi, 2010.

Iterative PKSs (IPKSs) can be still further subdivided according to their architecture and the presence or absence of additional β -keto processing domains into: non-reducing or aromatic PKSs (NR-PKSs), such as those involved in the production of norsolorinic acid (Zhou and Linz 1999), tetrahydroxynaphthalene (T4HN) (Wheeler, 1983) and bikaverin (Limón *et al.*, 2010); partially reducing PKSs (PR-PKSs), like 6-methylsalicylate (6-MSA) synthase from *Penicillium patulum* (Yalpani *et al.*, 2001), and highly reducing PKSs (HR-PKSs), as LovB and LovC for lovastatin biosynthesis (Ma *et al.*, 2009). Figure 5 illustrates the biosynthetic mechanism of 6-MSA synthase.

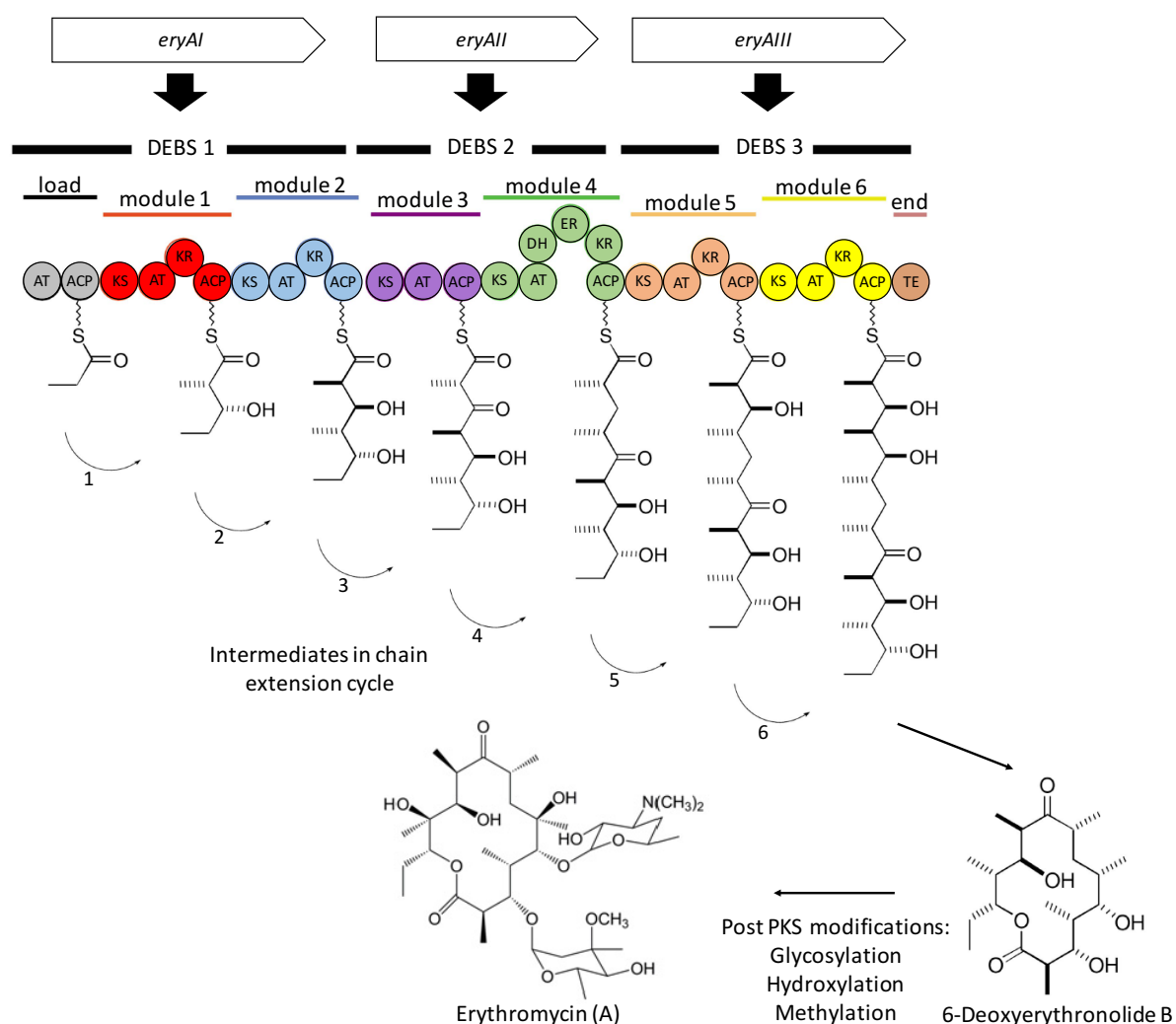


Figure 4. Domain organization of the erythromycin polyketide synthase. Putative domains are represented as circles and the structural residues are ignored. Each module incorporates the essential KS, AT and ACP domains, while all but one include optional reductive activities (KR, DH, ER). The one-to-one correspondence between domains and biosynthetic transformations explains how programming is achieved in this modular PKS. KS: ketosynthase; AT: acyltransferase; ACP: acyl carrier protein. Taken from Staunton and Weissman, 2001.

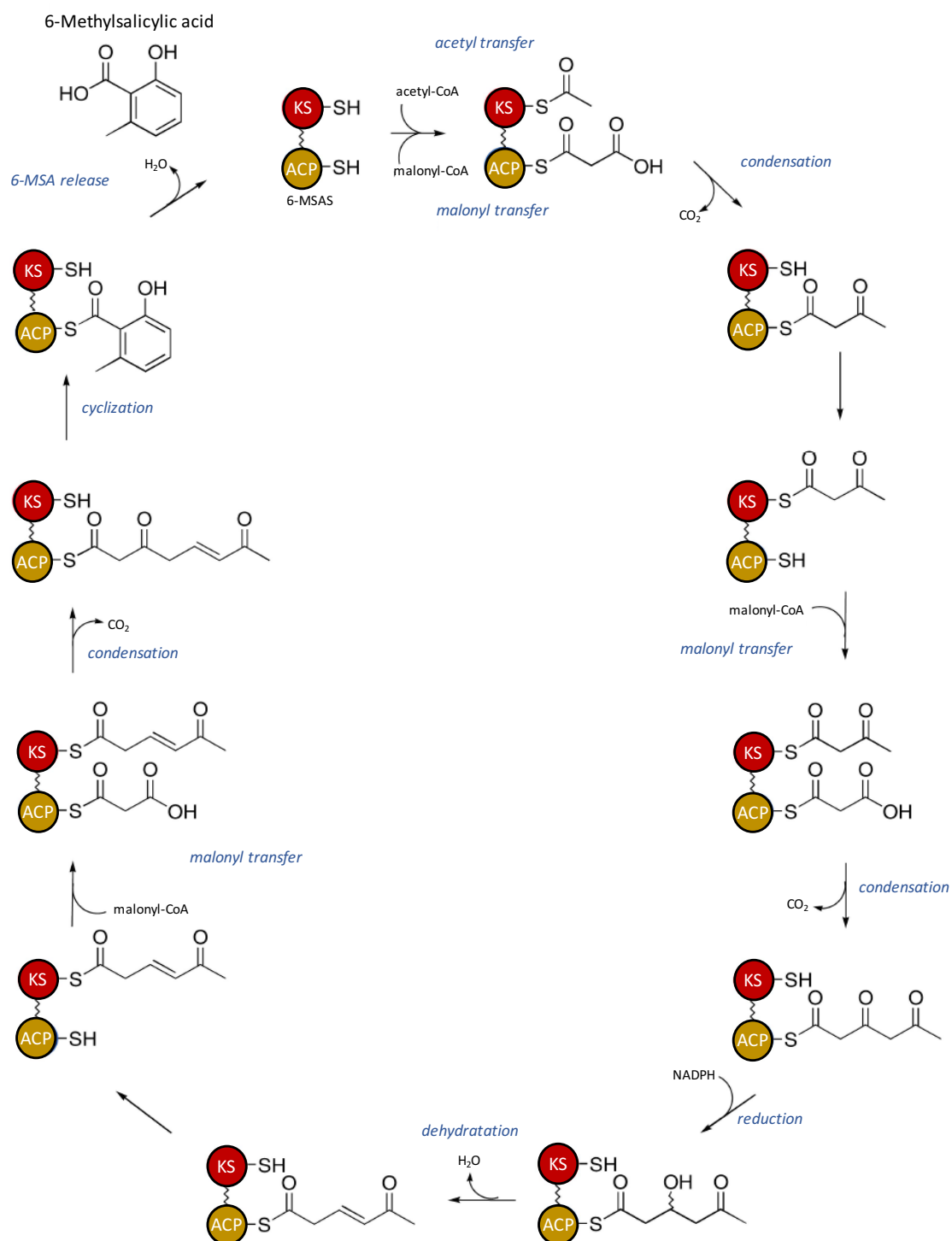


Figure 5. The biosynthetic pathway of the fungal polyketide 6-methylsalicylic acid (6-MSA). The 6-methylsalicylic acid synthase (6-MSAS) is an iterative type I PKS responsible for the biosynthesis of 6-MSA in *Penicillium patulum*. 6-MSAS catalyzes the three successive condensations required to make the eight carbon molecule. All of the active sites required for a total of 11 transformations are carried on a single multifunctional protein, and catalysis involves repeated use of these active sites. Adapted from Staunton and Weissman, 2001.

Type II PKSs carry each catalytic domain on separate polypeptides that form multiprotein complexes, analogous to type II FASs in bacteria and plants (Jenke-Kodama *et al.*, 2005), (Figure 3B). Type II PKSs have been shown to catalyze the biosynthesis of several compounds in bacteria, especially in *Streptomyces* sp., including the blue pigment antibiotic actinorhodin in *S. coelicolor* A3 (2) (Okamoto *et al.*, 2009), the antineoplastic agent dihydrogranaticin from *S. violaceoruber* T-22 (Taguchi *et al.*, 2001) and tetracenomycin, the antitumor antibiotic of *S. glaucescens* (Motamedi *et al.*, 1987) (Figure 6).

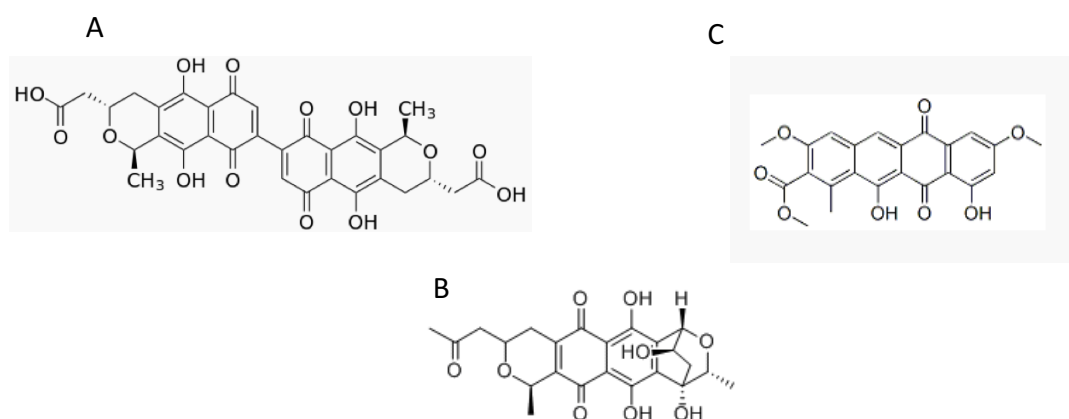


Figure 6. Products of type II polyketide synthases from *Streptomyces* sp. (A) Actinorhodin. (B) Dihydrogranaticin. (C) Tetracenomycin.

Moreover, type III PKSs (Figure 3C), also known as chalcone synthase-like PKSs, are homodimeric enzymes that produce a wide array of compounds as pyrones, acridones, phloroglucinols, stilbenes, and resorcinolic lipids. Their single active site in each monomer catalyzes the priming, extension, and cyclization reactions iteratively to form polyketide products (Yu *et al.*, 2012). Although type III PKSs are widely studied in plants and bacteria, their presence in fungi has only been realized in recent years (Hopwood, 1997). A previous analysis of PKS conserved domains suggested that most basidiomycetes PKS genes code for type I iterative polyketide synthases, putative type III PKS genes were found solely in three basidiomycete species (*P. brevispora*, *Dacyropinax* sp., and *Phanerochate chrysosporium*) (Lackner *et al.*, 2012).

Once the polyketides have been synthesized, they can undergo further modifications carried out by the so-called tailoring enzymes (TE), whose genes are normally located within the same biosynthetic gene cluster (BGC). Those enzymes include (de)hydratases, oxygenases, hydrolases, methylases, and others (Andersen *et al.*, 2013).

1.2.1.2 Non-ribosomal peptides (NRPs)

Instead of being synthesized by the rRNA- and tRNA-dependent ribosomal machinery, nonribosomal peptides (NRPs) are generated by nonribosomal peptide synthetases (NRPSs) (Finking and Marahiel, 2004). In addition to the 20 proteinogenic amino acids, NRPs are built from a huge number of nonproteinogenic amino acids, which are often essential for bioactivity (Marahiel and Essen, 2009). As it was previously described for PKSs, NRPSs possess a set of repetitive catalytic units called modules (Schwarzer and Marahiel, 2001). Mechanisms of NRPs biosynthesis are classified into three categories: (i) linear, the number and sequence of the modules in the NRPS matches the number and order of amino acids in the peptide; (ii) iterative, the modules or domains of the synthetase are used more than once to synthesize the peptide, and (iii) nonlinear, the arrangement of the modules does not match the sequence of amino acids (Cane and Walsh, 1999). Fungal NRPS pathways tend to be linear, as those involved in the biosynthesis of penicillin, cephalosporin, cyclosporin A and gliotoxin (Evans *et al.*, 2011) (Figure 7).

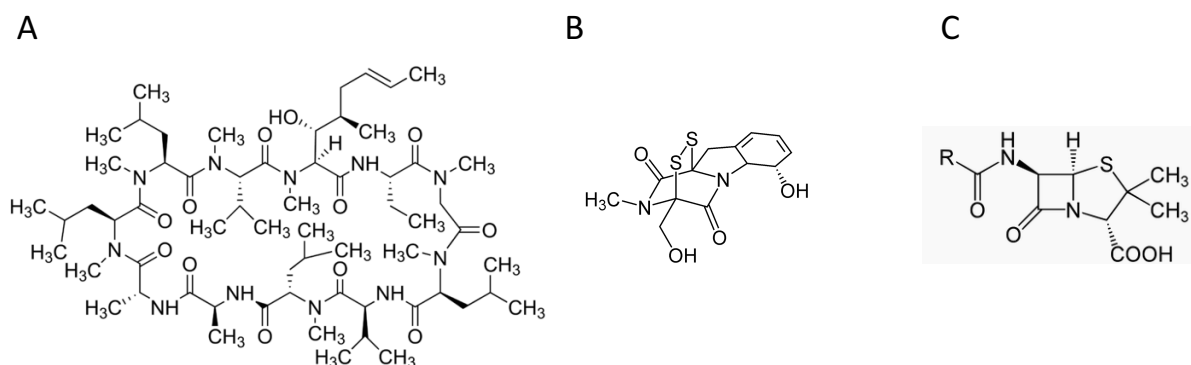
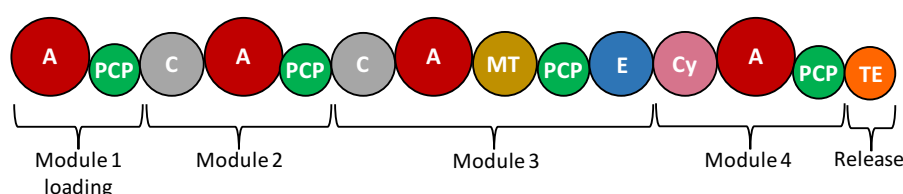


Figure 7. Fungal nonribosomal peptides. (A) Cyclosporin A, an NRP with a potent anti-inflammatory and immunosuppressant activity produced by the fungal species *Tolypocladium inflatum*. (B) Gliotoxin, an immunosuppressive mycotoxin long suspected to be a virulence factor of *Aspergillus fumigatus*. (C) Penicillin, a group of antibiotics which include penicillin G, penicillin V, procaine penicillin, and benzathine penicillin derived from *Penicillium* fungi. R: variable group.

A minimal chain elongation module contains three core domains: the condensation (C) domain, the adenylation (A) domain and the peptidyl carrier (PCP) domain (also known as the thiolation [T] domain) (Lautru and Challis, 2004). The A domain is responsible for the selection of the amino acids that make up the product and thus controls its primary sequence. The small peptidyl carrier protein (PCP) domain, located downstream of A-domain, is the site of cofactor binding (4'-phosphopantetheine), to which all substrates and intermediates of the NRPS assembly line are covalently bound. The condensation domain (C) catalyzes the peptide bond formation between two adjacent PCP-bound intermediates (Figure 8).

Several specialized C-terminal domains involved in chain termination and release of the final peptide product have also been identified (Keating and Walsh, 1999). Although the chain release is mostly carried out by a thioesterase (TE) domain in bacterial NRPSs (Schneider and Marahiel, 1998), only few NRPSs in fungi, such as the ACV synthetases, are known to release products via a TE domain (Bushley and Turgeon, 2010). Some other mechanisms include: 1) a terminal C domain, which catalyzes release by inter- or intramolecular amide bond formation (Keating *et al.*, 2001), and 2) a thioesterase NADP(H) dependent reductase (R) domain (Pospiech *et al.*, 1996; Silakowski *et al.*, 2000), which catalyzes reduction with NADPH to form an aldehyde.

A



B

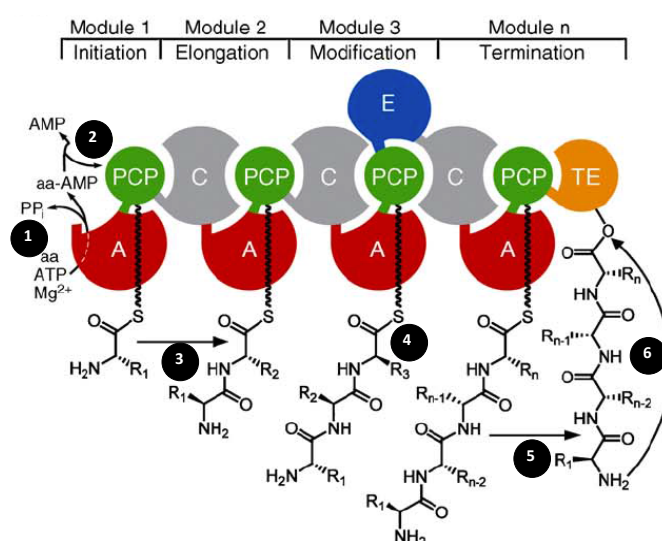


Figure 8. NRP domain organization and NRPS mechanism. (A) Domain organization of nonribosomal peptides (NRP). (B) Simplified mechanism of NRP synthesis. (1) The amino acid is activated as aminoacyl-AMP by the adenylation domain. (2) Transfer of the amino acid onto the PCP domain. (3) Condensation of PCP-bound amino acid. (4) Possibility of amino acid modifications, for example by epimerization domains. (5) Transesterification of the peptide chain from the terminal PCP onto the TE domain. (6) TE catalyzed product release by either hydrolysis or macrocyclization. The number of modification domains and modules is very variable. A: adenylation; PCP: peptidyl carrier protein; C: condensation; MT: methyltransferase; E: epimerization; Cy: cyclization; TE: thioesterase. Taken from Strieker *et al.*, 2010.

Aside from those enzymatic units required to build up a peptide, NRPSs may contain additional domains which modify the substrate during NRPS biosynthesis: 1) the epimerization (E) domain, which catalyzes the epimerization of the PCP-bound L-amino acid or C-terminal amino acid of the growing polypeptide (Linne *et al.*, 2001), 2) an N- or C-methylation (MT) domain (methyltransferase) which catalyzes the transfer of a methyl group from an S-adenosylmethionine to an α -amino of the amino acid substrate, and 3) the cyclization (Cy) domain which catalyzes the formation of oxazoline or thiazoline rings by internal cyclization of cysteine, serine, and threonine residues (Finking and Marahiel, 2004; Bushley and Turgeon, 2010) (Figure 8B). Some other tailoring enzymes (not included within the NRPSs) can further modify the nonribosomal peptides by glycosylation, hydroxylation, acylation or halogenation, as an essential contribution to their biological activity (Walsh *et al.*, 2001).

1.2.1.3 Hybrid metabolites

PKS domains also occur fused to NRPS domains, forming a PKS-NRPS hybrid (Hertweck, 2009). The interacting NRPS and PKS modules could physically reside on the same protein (type I hybrids) or separate proteins (type II hybrids). In order to be functional, both the PCP domains of the NRPS modules and the ACP domains of the PKS modules have to be converted from the inactive apo-form into the functional holo-form. Fungal PKS-NRPS products are produced via the action of two modules. A single type I, highly reducing PKS module acts iteratively to synthesize a complex polyketide core (Boettger and Hertweck, 2013), while the NRPS module is responsible for selecting the amino acid, synthesizing the peptide bond and, in some cases, conducting some other steps as for example Dieckmann cyclization to produce tetramic acids (Collemare *et al.*, 2008; Kakule *et al.*, 2014). An outstanding feature of fungal PKS-NRPS hybrid is the lack of an intact ER domain within the PKS module, either because the catalytic function is not essential for the product formation or because it is fulfilled by *trans*-acting ER (Boettger and Hertweck, 2013). In figure 9, a simplified mechanism of a PKS-NRPS system is described for zwittermicin A (Letzel *et al.*, 2013).

In fungi, the PKS-NRPS derived metabolites represent an important group of structurally complex molecules. Fusarin C constitutes the first PKS-NRPS identified in fungi by the group of Simpson and co-workers (Song *et al.*, 2004). Fusarin C is produced by several *Fusarium* species: *F. oxysporum*, *F. poae*, *F. sporotrichioides*, *F. acuminatum*, *F. crookwellense*, *F. dlamini* and *F. nygamai* (Golinski and Chelkowski, 1992).

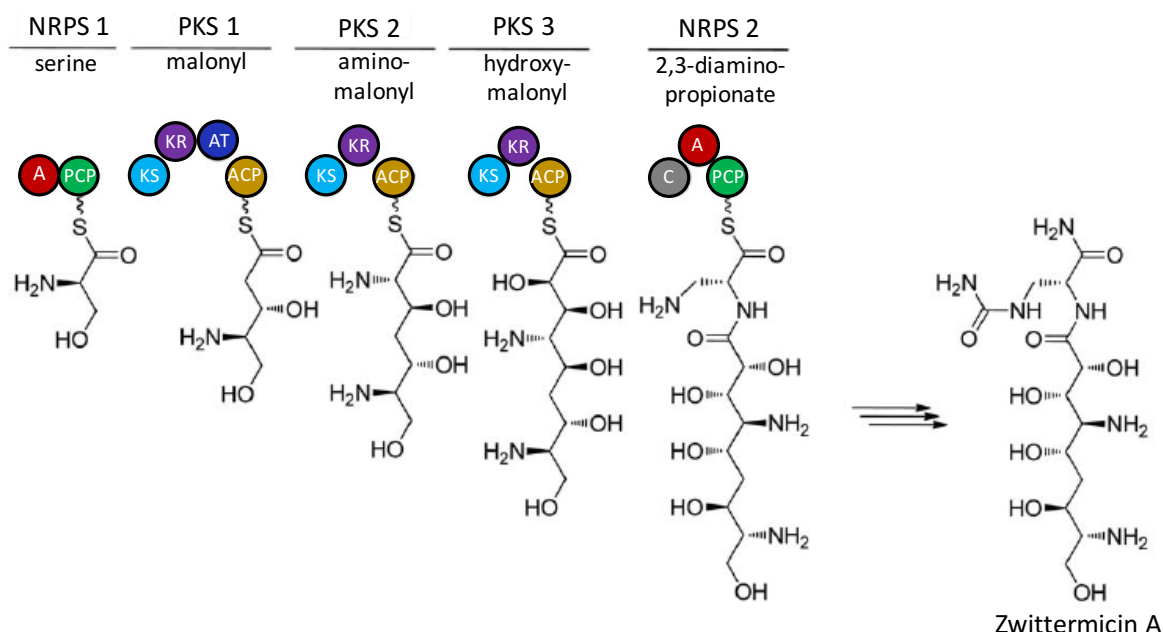


Figure 9. Simplified mechanism of action for NRPS and PKS modules within the hybrid synthase involved in the biosynthesis of zwittermicin A. The PKS-NRPS used in zwittermicin A synthesis utilizes modified extender units such as hydroxymalonyl-ACP, aminomalonyl-ACP and 2,3-diaminopropionate. Assembly begins by the activation of a serine residue, which is carried out by tethering the amino acid to a PCP via an NRPS. Subsequently, elongation of an activated malonyl unit covalently attached to an ACP by a ketosynthase occurs giving the five carbon unit. The next two elongation steps proceed in a similar manner using aminomalonyl and hydroxymalonyl units from a second and third ketosynthase. Finally, the zwittermicin A backbone is generated by the condensation of 2,3-diaminopropionate with the carried molecule by a second NRPS. A: adenylation; C: condensation; AT: acyltransferase; PCP; peptidyl carrier protein; ACP: acyl carrier protein; KS: ketosynthase; KR: ketoreductase. Taken from Letzel *et al.*, 2013.

On the other hand, tenuazonic acid (TeA) is a PKS-NRPS derived product generated by the plant pathogenic fungus *Alternaria tenuis* (Figure 9). Some of the biological properties described for TeA include antitumor, antibacterial, antiviral and phytotoxic activity (Miller *et al.*, 1963; Gitterman, 1965). In contrast to other PKS-NRPS hybrid enzymes, the PKS portion of TAS1 (TeA synthetase) has only a single KS domain, which is indispensable for TAS1 activity (Yun *et al.*, 2015). Important examples from *Aspergillus* sp. include the cholesterol lowering compound lovastatin (Figure 10), aspyridone A and pseurotin (Hendrickson *et al.*, 1999; Bergmann *et al.*, 2007; Maiya *et al.*, 2007). Other examples constitute equisetin synthesized by *F. heterosporum* (Fleck and Brock, 2010; Sims *et al.*, 2005), and tenellin, a PKS-NRPS yellow pigment produced by the insect pathogen *Beauveria bassiana* (Eley *et al.*, 2007).

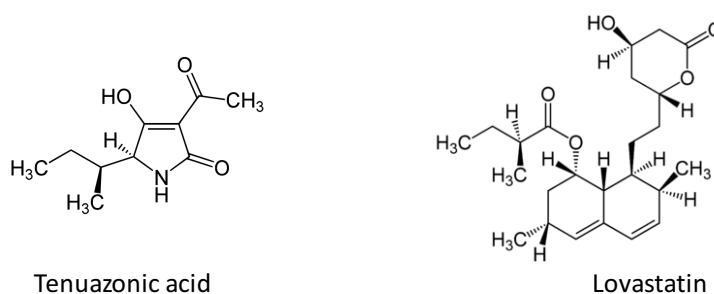


Figure 10. Molecular structures of tenuazonic acid and lovastatin.

1.2.1.4 Terpenes

Terpenes represent the largest class of secondary metabolites that are produced as volatile organic compounds in fungi by terpene cyclases (TCs) (Christianson, 2008). While polyketides and nonribosomal peptides are the major class of secondary metabolites discovered in filamentous fungi, terpenes appear to be a predominant class of secondary metabolites in Basidiomycota. Terpenes are derived from the basic five-carbon units isopentenyl diphosphate and its isomer dimethylallyl diphosphate, which are sequentially coupled via prenyltransferase enzymes to produce longer prenyl diphosphates, the direct precursors for terpene biosynthesis (Wawrzyn *et al.*, 2012). Terpenes are classified in monoterpenes, which are derived from geranyl pyrophosphate (GPP); sesquiterpenes, generated from farnesyl pyrophosphate (FPP); diterpenes and carotenoids, produced by geranylgeranyl pyrophosphate (GGPP) (Figure 11). In fungi, most of the different classes of terpenes has been observed, except for the monoterpenes (Shaw *et al.*, 2015). Botrydial is a sesquiterpenoid considered as the primary phytotoxic metabolite of *Botrytis cinerea*. It is mainly responsible for the development of necrotic lesions on tobacco and beans when applied to leaves (González-Collado *et al.*, 2007). Trichothecenes, also belonging to the class of sesquiterpenes, contain a common 12,13-epoxytrichothene skeleton and an olefinic bond with various side chain substitutions. *Fusarium* is the major genus producing such compounds like diacetoxscirpenol, deoxynivalenol and T2, which are considered as potent inhibitors of eukaryotic protein synthesis (Bennett and Klich, 2003). On the other hand, aristolochenes, from *A. terreus* and *P. roqueforti*, constitute an important group of sesquiterpenes (Cane *et al.*, 1993; Proctor and Hohn, 1993), which also likely serve as precursors for several sesquiterpenoid toxins produced by filamentous fungi (Hohn *et al.*, 1991), including PR-toxin produced by *P. roqueforti*. Related to diterpenes, many *Fusarium* species also synthesize the plant hormones gibberellins (GAs), which act as virulence factors for grain infection (Bomke and Tudzynski, 2009).

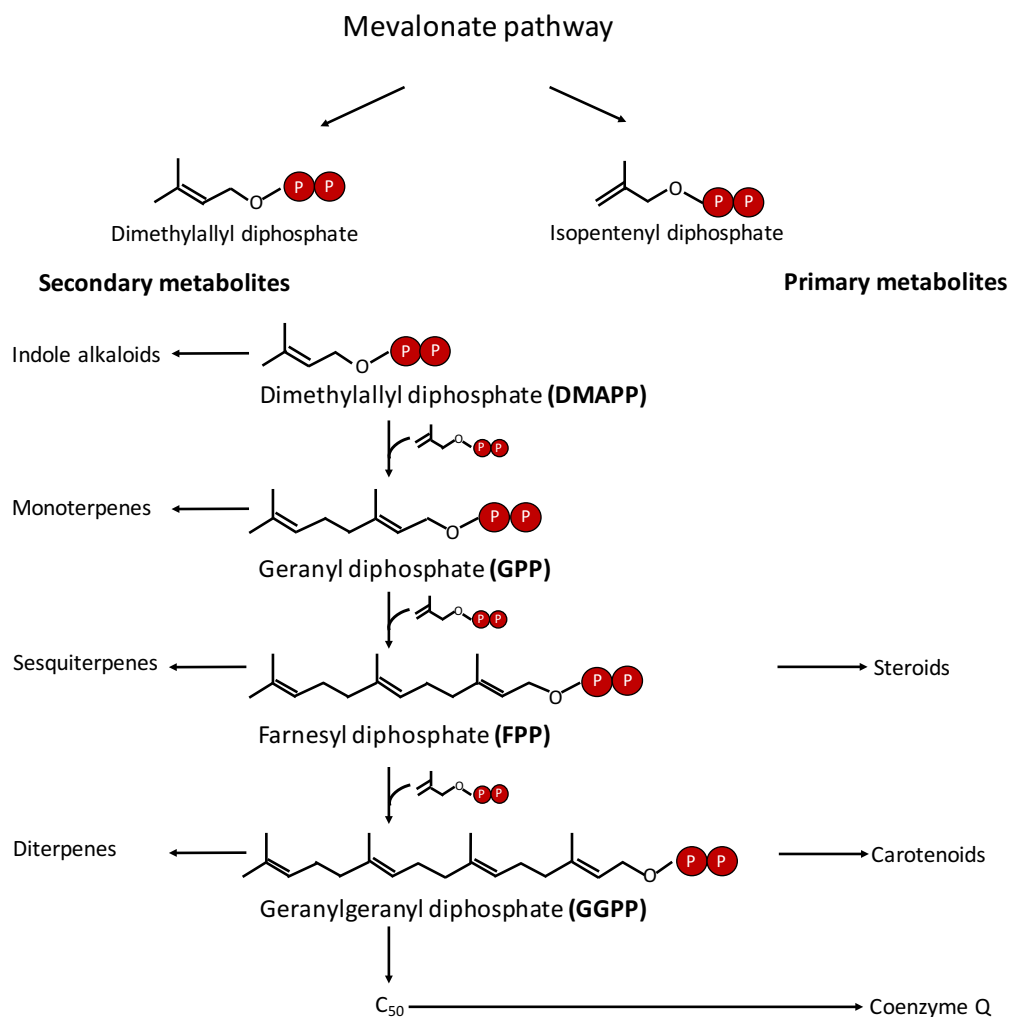


Figure 11. Terpene biosynthetic pathway. All terpenoids are derived from the basic five-carbon units isopentenyl diphosphate and its isomer dimethylallyl diphosphate (DMAPP), which are sequentially coupled via prenyltransferase enzymes to yield longer prenyl diphosphates, the direct precursors to terpene biosynthesis. Monoterpenes are derived from geranyl diphosphate (GPP, C₁₀), sesquiterpenes from farnesyl diphosphate (FPP, C₁₅), and diterpenes from geranylgeranyl diphosphate (GGPP, C₂₀). Adapted from Keller *et al.*, 2005.

Although the primary sequences of terpene cyclases are not well conserved between plants and fungi, the tertiary structure is conserved (Carruthers *et al.*, 2000; Fischer *et al.*, 2015). Last but not least, carotenoids also represent an important group of terpenoids produced by fungi. Best-known examples are those related to the production of β -carotene, astaxanthin and neurosporaxanthin. β -carotene has been reported in *S. sclerotiorum* (Georgiou *et al.*, 2001), *U. maydis* (Estrada *et al.*, 2010) and *Penicillium* sp. (Han *et al.*, 2005), just to mention some cases. Moreover, astaxanthin is synthesized from β -carotene by the basidiomycete yeast *X. dendrorhous* (Johnson, 2003), while the neurosporaxanthin, as the name implies, has been well studied in *N. crassa* mainly by its protective effect against UV irradiation (Schmidhauser *et al.*, 1990).

1.2.1.5 Alkaloids

Alkaloids have been reported as a group of basic organic substances of plant and microbial origin, containing at least one nitrogen atom in a ring structure in the molecule. Among these compounds, ergot alkaloids (EA) constitute a large family of fungal specialized metabolites derived from prenylated tryptophan with a characteristic ergoline ring system (Figure 12) in their structure (Flieger *et al.*, 1997; Hoffmeister and Keller, 2007). EA can be divided into 2 major classes: the amides of lysergic acid, which are produced by plant-associated fungi of the family Clavicipitaceae, and the clavine alkaloids, which are primarily produced by members of the fungal order Eurotiales such as *Aspergillus fumigatus* (Metzger *et al.*, 2009). The first committed step of ergot alkaloid biosynthesis is catalyzed by the 4-dimethylallyl tryptophan synthase (DMATS) (Tsai *et al.*, 1995). In this reaction, DMATS condenses L-tryptophan and dimethylallylpyrophosphate (DMAPP) to generate dimethylallyl tryptophan (DMAT), as it is shown in Figure 12.

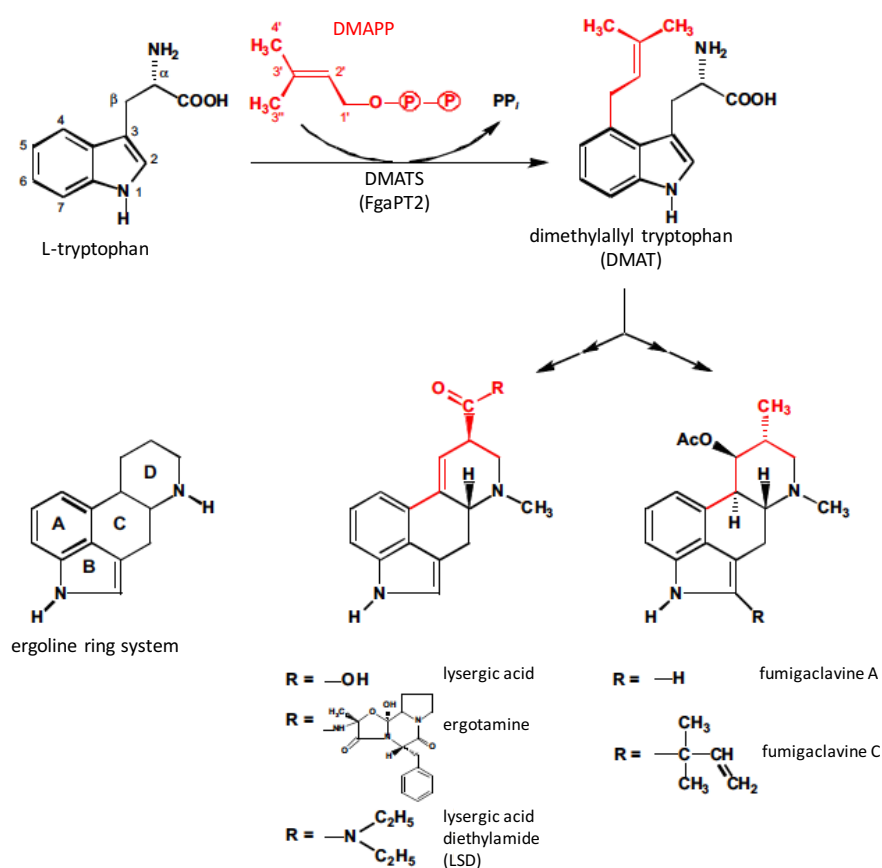


Figure 12. Reaction catalyzed by DMATS and structures of ergot alkaloids. FgaPT2 is a dimethylallyltryptophan synthase (DMATS) that catalyzes the first committed step of ergot alkaloid biosynthesis in *Aspergillus fumigatus*. FgaPT2 catalyzes the prenylation of L-tryptophan to generate dimethylallyltryptophan (DMAT). Taken from Metzger *et al.*, 2009.

The first biosynthetic gene cluster of ergot alkaloids was identified in *Claviceps purpurea* strain P1 by genome walking (Tudzynski *et al.*, 1999). In the same gene cluster, four NRPS genes and several putative oxidases were also identified (Haarmann *et al.*, 2005). In 2012, the group of Hywel-Jones isolated a new alkaloid, cordylactam, from the spider pathogenic fungus *Cordyceps* sp. BCC 12671 (Isaka *et al.*, 2012). Oxaline, from *Penicillium oxalicum*, is another alkaloid that has been studied due to its ability to arrest the cell cycle by inhibition of tubulin polymerization (Koizumi *et al.*, 2004). Moreover, the prenylated indole alkaloids 17-*epi*-notoamides Q and M, from *Aspergillus* sp., were found to have antibacterial activities (Chen *et al.*, 2013), while in some other cases, alkaloids as fumigaclavines and fumitremorgens, produced by *A. fumigatus*, showed toxic effects (dos Santo *et al.*, 2003).

1.2.2 Strategies to elicit natural products from silent biosynthetic gene clusters

Despite the large number of known bioactive compounds produced by fungi, the biosynthetic potential of these microorganisms is greatly underestimated since many of the genes involved in secondary metabolic pathways are silent under standard laboratory conditions. Methods to activate these silent biosynthetic pathways are thus of major interest. The key issue for the success of this approach is to find ways to induce or enhance the expression of cryptic or poorly expressed pathways. In the next paragraphs the most common strategies that have been applied in fungi for the production of secondary metabolites will be discussed.

1.2.2.1 Cultivation based approaches

Synthesis of various metabolites is dependent on culture conditions, such as surface or shake culture and pH of the fermentation medium. The OSMAC (one strain-many compounds) approach is an useful method, which functions under the concept "one fungus for the production of diverse secondary metabolites" (Bode *et al.*, 2002). In other words, the modification of different culture parameters can lead to the discovery of new metabolites that otherwise are not synthesized under standard laboratory conditions. By applying this strategy, six new polyketides (calbistrin F-H and dothideomynone A-C) were produced by the endophytic fungus *Dothideomycete* sp. CR17 after changing sources of potato and malt extract in culture media (Hewage *et al.*, 2014). Similarly, the cultivation of *Myxotrichum* sp. in a medium with rice led to the activation of three new polyketides myxotritones A-C, together with a new natural

product 7, 8-dihydro-7*R*, 8*S*-dihydroxy-3,7-dimethyl-2-benzopyran-6-one (Yuan *et al.*, 2016). Cultivation of the *Halichondria* sponge-derived fungus *Gymnacella dankaliensis* in malt extract medium resulted in the production of four unusual steroids (gymnasterones A-D), while the cultivation in a modified extract medium containing soluble starch instead of glucose synthesized two extremely unusual steroids, dankasterones A and B (Amagata *et al.*, 2007). Besides the medium composition, small modifications in the culture medium can bring about the discovery of new natural products. For instance, the replacement of the water used to make the media from tap water to distilled water resulted in the isolation of six new secondary metabolites, cytosporones F-I, quadrisepetin A, and 5'-hydroxymonocillin in *P. quadrisepitata* (Paranagama *et al.*, 2007).

Increasing evidence suggests that fungal secondary metabolism is not a stand-alone property but is tightly interconnected with morphological differentiation, stress response, and biotic interactions. The best understood example of the impact of environmental conditions that affect secondary metabolism are the pH-dependent expression of the penicillin/cephalosporin gene clusters (Brakhage *et al.*, 2009). The expression of the gliotoxin biosynthesis genes is affected by various factors as pH, temperature, the composition and aeration of the culture medium, biofilm formation (Bruns *et al.*, 2010), gliotoxin itself and other unknown factors (Cramer *et al.*, 2006; McDonagh *et al.*, 2008; Sugui *et al.*, 2008; Bruns *et al.*, 2010; Scharf *et al.*, 2012). In line with these findings, the depletion of molecular oxygen triggered the activation of the pseurotin A biosynthetic gene cluster *A. fumigatus* (Vödisch *et al.*, 2011).

Previous studies have revealed that the encounter of different microorganisms can stimulate the production of secondary metabolites and increase the biological activities of microbial extracts. However, it is important to take into account some factors before selecting cocultivation as a first strategy to uncover secondary metabolites: the optimum timing of inoculation of the cultivation partners and of extraction, the selection of the proper media, and the cell ratio. Once the experimental setups are ready, this technique can lead to the identification of novel compounds. Cocultivation of the marine fungus (strain CNL-365, *Pestalotia* sp.) with an unidentified marine bacterium led to the production of pestalone, a chlorinated benzophenone antibiotic (Cueto *et al.*, 2001). Similarly, the isolation of two antimicrobial cyclic depsipeptides, emericellamides A and B, occurred when the marine-derived fungus *Emericella* sp. and the marine actinomycete *Salinispora arenicola* were co-cultured (Oh *et al.*, 2007). In some cases, the microbial interactions are critical for survival and fitness, as it was reported for *A. fumigatus* and *Sphingomonas* bacterial strain KMK-001, whose cocultivation induced the production of glionitrin A (Park *et al.*, 2009).

Since both microbes were isolated from an acidic coal mine drainage, it is believed that glionitrin A may be synthesized in response to a survival mechanism of any of those strains. In another report, a tremendous increase in *Monascus* pigment production was detected when *Monascus* was co-cultivated in solid medium with either *Saccharomyces cerevisiae* or *Aspergillus oryzae* (Shin *et al.*, 1998). Further experiments revealed that hydrolytic enzymes (e.g., chitinase) from a variety of fungi were effective in enhancing *Monascus* pigment production (Shin *et al.*, 1998).

1.2.2.2 Molecular approaches

1.2.2.2.1 Ribosome engineering

Ribosome engineering is based on two different aspects, modulation of the translational apparatus by induction of a *str* (streptomycin) mutation, and modulation of the transcriptional apparatus by induction of a *rif* (rifampicin) mutation, thus increasing antibiotic productivity (Ochi *et al.*, 2004). Such increase is attributed to the ability of the mutants to accumulate ppGpp (guanosine 5'-diphosphate 3'-diphosphate), which is an important signaling molecule for the onset of antibiotic production (Hosoya *et al.*, 1998). Ribosome engineering is described as a new method for screening secondary metabolites with several advantages, including the ability to screen for drug resistance mutations by simple selection on drug-containing plates, even if the mutation frequency is extremely low, and the ability to select for mutations without prior genetic information (Tanaka *et al.*, 2013). The concept of ribosome engineering was first applied to bacteria but now it has been expanding to fungi (Ochi and Hosaka, 2013). Introduction of gentamycin resistance (GenR) into the marine-derived fungal strain *Penicillium purpurogenum* G59 activated the gene clusters responsible for the production of four antitumor secondary metabolites: janthinone, fructigenine A, aspterric acid methyl ester and citrinin (Chai *et al.*, 2012). In addition, the hygromycin B-resistant mutants of *Monascus pilosus* NBRC 4520 exhibited enhanced production of secondary metabolites (Ochi and Hosaka, 2013). Since hygromycin and gentamycin inhibit the synthesis of proteins, these studies suggest that by modulating the ribosomal function (ribosomal proteins or rRNA) it is possible to explore the biosynthetic potential in fungi. Even though this strategy has not been totally explored, it represents an alternative way to study the secondary metabolite potential in fungi.

1.2.2.2.2 Manipulation of global and cluster-specific regulators

A large number of known fungal secondary metabolites have been ascribed to the Ascomycete genus *Aspergillus*. Therefore, most of the studies on regulation of BGCs have been carried out in this genus, particularly on global regulators. LaeA is considered as a master regulator of secondary metabolism, as it is required not only for sterigmatocystin (ST) but also for penicillin (PN) biosynthesis, as well as for the biosynthesis of mycelial pigments in *A. nidulans* and *A. fumigatus* (Bok and Keller, 2004). Unlike other genes that regulate secondary metabolism, the loss of *laeA* has a negligible impact on morphological developmental processes. Another global regulator identified in *Aspergillus nidulans* is the protein PacC, which activates the expression of genes whose products are synthesized preferentially at alkaline pH. Mutations in *pacC* mimic the effects of growth at alkaline pH and lead to elevated levels of alkaline phosphatase, reduced levels of acid phosphatase and penicillin overproduction (Tilburn *et al.*, 1995). On the other hand, the *creA* gene in *A. nidulans* is a remarkable example of a global regulatory gene mediating carbon catabolite repression. Deletion of *creA* and surrounding DNA has an extremely severe effect on morphology under carbon catabolite repressing and nonrepressing conditions (Dowzer and Kelly, 1989). Also related to nutritional sources, the global nitrogen regulator AreA is responsible for nitrogen-induced repression of the gibberellin biosynthesis gene cluster in *F. fujikuroi* (Tudzynski *et al.*, 1999) but it is required for the production of fumonisin B1 in *F. verticillioides* (Kim and Woloshuk, 1998). Other global regulators that have been identified to affect SM gene cluster expression include development-related transcription factors such as StuA (Twumasi-Boateng *et al.*, 2009) and a bZIP transcription factor in *A. nidulans* (Yin *et al.*, 2011).

Many, but not all, clusters contain genes encoding transcriptional factors that positively or negatively regulate gene expression (Figure 13A and B). Therefore, one the simplest ways to activate a gene cluster is by inducing or repressing the expression of a regulator with a positive or negative effect on the cluster genes, respectively. Furthermore, it also helps to increase the amount of products, which is often necessary for structure elucidation. Overexpression of the *apdR* gene, coding for a Zn₂Cys₆ transcription factor in *A. nidulans*, resulted in the activation of a silent gene cluster responsible for the biosynthesis of the aspyridones A and B (Bergmann *et al.*, 2007). In the same year, Shimizu and co-workers identified an activator gene (*ctnA*) essential for the efficient production of citrinin (CT) in *Monascus purpureus*. CtnA was found in the upstream region of a gene encoding for a polyketide synthase (*pksCT*), which was shown to be expressed by *ctnA*. In addition, *ctnA* disruption drastically decreased CT production. In a similar way, the expression of the genes

involved in the biosynthesis of depudecin, a histone deacetylase inhibitor, in *Alternaria brassicicola* was shown to be controlled by the transcription factor *DEP6* located within the depudecin gene cluster (Wight *et al.*, 2009). Interestingly, *CtnA*, *DEP6* and *ApdR* belong to the largest cluster-specific family of transcription factors in fungi, Zn(II)₂Cys₆. Belonging to the same family of TFs are those regulating the biosynthesis of bikaverin (Bik5), cercosporin (CTB8), fumonisin (FUM21) and sirodesmin PL (Sir Z) (Wiemann *et al.*, 2009; Chen *et al.*, 2007; Brown *et al.*, 2007; Fox *et al.*, 2008). Other families of TFs involved in fungal secondary metabolism are: Cys₂His₂ (BMR1 and Cmr1 for melanin biosynthesis), bZip (ToxE for HC-toxin) and winged helix (CPR1 for cephalosporin C) (Knox and Keller, 2015).

1.2.2.2.3 Heterologous expression

To characterize the function of unknown genes, heterologous expression in well-defined hosts provides a promising option (Figure 13C). However, the application of this strategy shows some limitations that need to be taken into account when planning to express a gene encoding for a PKS or NRPS. First of all, the presence of introns and strain-specific splicing mechanism has to be considered; second, the ACP domains of PKSs and NRPSs require posttranslational 4-phosphopantetheinylation catalyzed by 4-phosphopantetheinyl transferases (PPTase), and third, the large sizes gene clusters containing SM genes could lead to unstable constructs (Schümann and Hertweck, 2006). For these reasons, using a host that is similar to the donor organism may increase the likelihood of synthesizing the desired compound.

Aspergillus oryzae has been considered as one of the most attractive fungal heterologous host due to its ability to secrete large amounts of protein (Pahirulzaman *et al.*, 2012). Such a system was used for Zhang and co-workers to overexpress the PKS gene involved in the biosynthesis of the squalene synthase inhibitor squalestatin S1 from *Phoma* sp. (Cox *et al.*, 2004). Following the same strategy, the entire citrinin (CT) biosynthetic cluster (20 kb) from *M. purpureus* was successfully introduced into *A. oryzae* with a high production rates (Sakai *et al.*, 2012). In addition to *A. oryzae*, *A. nidulans* has also served as a host for expressing secondary metabolite genes. A clear example was found in the PKS-encoding gene *atX* from *A. terreus*, which produced significant amounts of 6-methylsalicylic acid (6-MSA) when expressed in *A. nidulans* (Fujii *et al.*, 1996). Interestingly, two years later, the group of Barr and collaborators expressed the same PKS gene but used *E. coli* and *S. cerevisiae* as expression hosts (Kealey *et al.*, 1998). In both cases, polyketide production required coexpression of 6-MSA synthase and an heterologous phosphopantetheinyl transferase (PPTase) from *B. subtilis*, necessary for the conversion of the expressed apo-PKS to its holo form, thus indicating that it

is feasible to use such expression systems as long as those considerations are contemplated. Particularly in *E. coli*, there are more aspects to look at, as the unavailability of proper building blocks, difficulties in efficient translation and functional folding of key biosynthetic enzymes (Gao *et al.*, 2010). Meanwhile, *S. cerevisiae* does not produce some of the necessary acyl CoA polyketide precursors, such as methylmalonyl-CoA. In addition, yeast may have insufficient levels of some tRNAs needed for PKS expression (Mutka *et al.*, 2005). Despite some limitations, *S. cerevisiae* has served as an heterologous host for reconstituting fungal and plant biosynthetic pathways of the alkaloids cycloclavine and dihydrosanguinarine, respectively (Jakubczyk *et al.*, 2015; Fossati *et al.*, 2014). The latter, represents the longest reconstituted alkaloid pathway (10 genes) ever assembled in yeast (Fossati *et al.*, 2014).

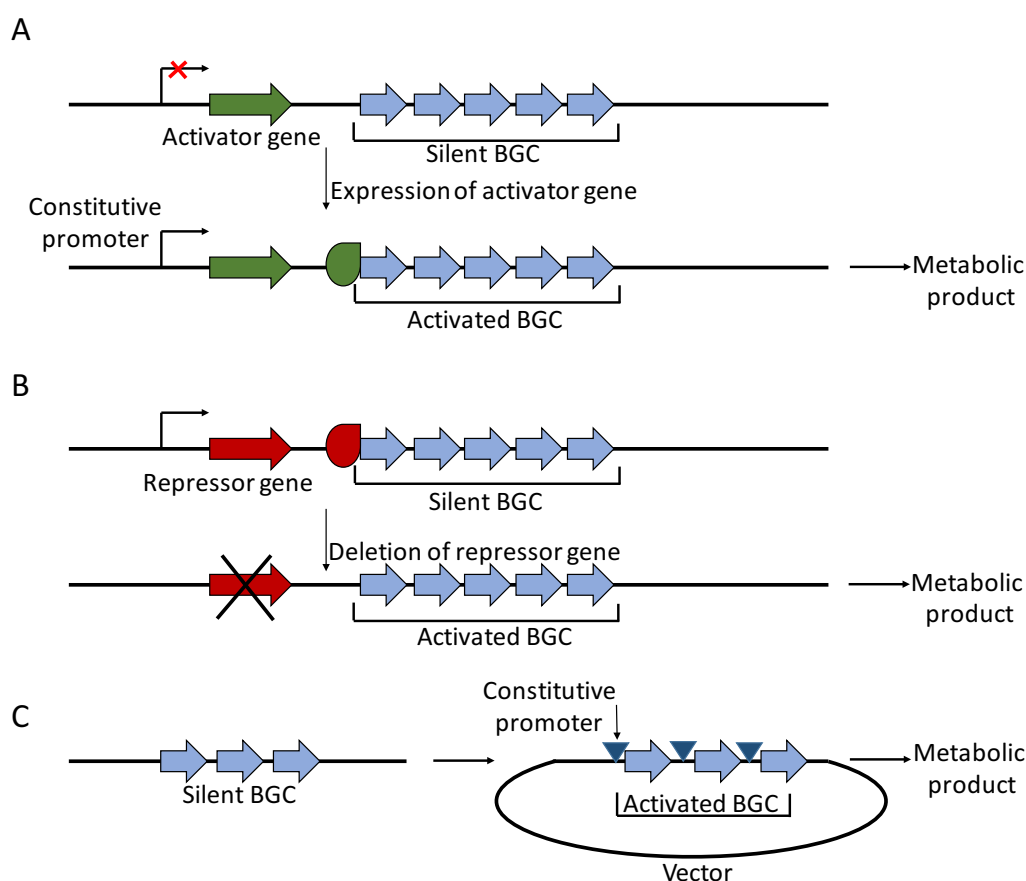


Figure 13. Pathway-specific strategies to induce the expression of silent biosynthetic gene clusters. (A) Overexpression of a pathway-specific activator gene has been used to induce expression of the corresponding biosynthetic gene cluster. **(B)** Deletion of a pathway-specific repressor gene has also been used to induce the expression of silent BGCs. **(C)** Refactoring, which refers to the replacement of native regulatory elements with constitutive or readily inducible promoter. Adapted from Rutledge and Challis, 2015.

Heterologous expression of fungal biosynthetic genes can be technically challenging and time consuming (Chiang *et al.*, 2011). Therefore, effective transformation protocols across fungal genera are necessary for the development of proper expression systems (Nevalainen *et al.*, 2005).

1.2.2.2.4 Epigenetic mining

Altering the chromatin landscape by either genetic or chemical manipulation of chromatin modifiers has shown to be a strategy to activate silent SM gene clusters in fungi (Gerke *et al.*, 2012; Szewczyk *et al.*, 2008; Wang *et al.*, 2010). For example, gene expression has been associated with acetylation of histone H3 lysine 9 (H3K9ac) and dimethylation of histone H3 lysine 4 (H3K4me2), whereas gene silencing has been associated with trimethylation of histone H3 lysine 9 (H3K9me3) (Wiemann and Keller, 2014) (Figure 14). Additionally, phosphorylation, ubiquitylation, and sumoylation can influence the expression of genes involved in secondary metabolism (Brakhage, 2013). Such epigenetic approaches are particularly useful in cases where any defined regulatory genes are present to control the expression of a SM gene cluster. Keller and co-workers demonstrated that deletion of *hdaA*, encoding an *A. nidulans* histone deacetylase (HDAC), caused transcriptional activation of two secondary metabolite gene clusters (Shwab *et al.*, 2007). Conversely, deletion of *gcnE*, encoding for the histone H3K9 acetyltransferase (HAT) of the SAGA/ADA complex in *A. nidulans*, abolished the production of orsellinic acid (Bok *et al.*, 2013). On the other hand, the use of chemical inhibitors of fungal histone methyltransferases (HMTs), as 5-azacytidine and 5-aza-2'-deoxycytidine, has shown to have an impact on different developmental and cellular processes in *C. albicans*, *Aspergillus* spp., *F. oxysporum* and *N. crassa* (Cichewicz, 2010). In conjunction with these results, the application of HDACs inhibitors such as suberoylanilide in *A. niger* and *D. stramonium* L. yielded the production of nygerone A and two derivatives of fusaric acid, respectively (Henrikson *et al.*, 2009; Chen *et al.*, 2013).

Both reports represent a good strategy to uncover new secondary metabolites in fungi, especially because it constitutes a low-cost technique and easy to apply in high-throughput screening operations.

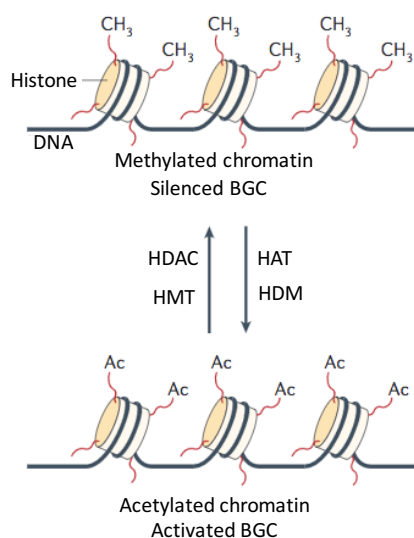


Figure 14. Epigenetic perturbation as a strategy to activate silent gene clusters. Histone acetyltransferases (HATs) and histone demethylases (HDMs) can convert methylated histones into acetylated histones, thus activating silent BGCs. On the other hand, histone deacetylases (HDACs) and histone methyltransferases (HMTs) convert acetylated chromatin into the methylated form, which silences BGCs. Taken from Rutledge and Challis, 2015.

1.2.2.3 Mining for novel compounds and their biosynthetic genes

Before automated tools became available, genome mining approaches have been undertaken by "manually " identifying key biosynthetic enzymes in genome data (Weber and Kim, 2016). Development of new bioinformatic technologies offered opportunities to increase the effectiveness of discovering and engineering fungal natural product(s) biosynthetic pathways. Some of the most popular available software programs used for this purpose are SMURF (Secondary Metabolite Unknown Regions Finder) and antiSMASH (antibiotics and Secondary Metabolite Analysis Shell). SMURF is based on three hallmarks of fungal SM biosynthetic pathways: (i) the presence of backbone genes (PKSs, NRPSs, PKS-NRPSs and DMATs), (ii) clustering, and (iii) characteristic protein domain content (Khaldi *et al.*, 2010). SMURF is capable of generating a comprehensive list of BGCs but with little detailed analysis. On the other hand, antiSMASH (Medema *et al.*, 2011; Blin *et al.*, 2013; Weber *et al.*, 2016) provides detection rules for 44 different classes and subclasses of secondary metabolites. In addition, it provides information related to the domain structures of PKSs and NRPSs, substrate predictions and comparative tools to identify similar gene clusters in other sequenced genomes, among others features. A combination of both bioinformatic sources, together with a manual analysis, represents a good strategy when there is not much information related to the biosynthetic potential of the desired microorganism. Other bioinformatic tools that can be used

for detection of secondary metabolite genes are: ClustScan (Starcevic *et al.*, 2008), NP. searcher (Li *et al.*, 2009) and SBSPKS (Anand *et al.*, 2010) focus on nonribosomal peptide and polyketide biosynthesis pathways. For a more detailed description on bioinformatic tools for detection of BGCs, reviews by Weber and Kim (Weber and Kim, 2016), and Medema and Fischbach (Medema and Fischbach, 2015) can be consulted.

1.3 Secondary metabolism in *Ustilago maydis*

1.3.1 *U. maydis* as a model organism

The fungus *Ustilago maydis* is the causative agent of smut disease on corn. In recent years *U. maydis* has emerged as an important model for plant pathogenic basidiomycetes, a large group of pathogens that causes smut and rust disease of plants (Kahmann and Kämper, 2004). It has also been used to study the molecular basis of such diverse phenomena as mating type determination, homologous recombination and signalling pathways (Bölker, 2001). *U. maydis* is dimorphic and grows in its haploid phase as a saprophytic yeast (Figure 15). Sexual development is initiated by the fusion of two compatible haploid yeast-like cells, a process controlled by the two mating type loci of *U. maydis*, the *a* and the *b* locus (Grandel *et al.*, 2000). The resulting dikaryon is filamentous, grows in close contact with the plant and is able to sense surface signals that trigger the formation of appressoria (Mendoza-Mendoza *et al.*, 2009; Lanver *et al.*, 2010). The plasma membrane of the plant cell invaginates and tightly surrounds the intracellular hyphae (Brefort *et al.*, 2009). An interaction zone develops between the plant and fungal membranes that is characterized by fungal deposits produced by exocytosis. At later stages, proliferation also occurs intercellularly and the dikaryotic mycelium grows towards bundle sheets (Doehlemann *et al.*, 2008). Proliferation is followed by sporogenesis where hyphal sections fragment, round up, and differentiate into heavily melanized diploid teliospores (Snetselaar and Mims, 1993) (Figure 15). These spores are distributed by air and can germinate under favourable conditions. During germination, meiosis occurs and results in the production of haploid, unicellular sporidia (Bölker, 2001).

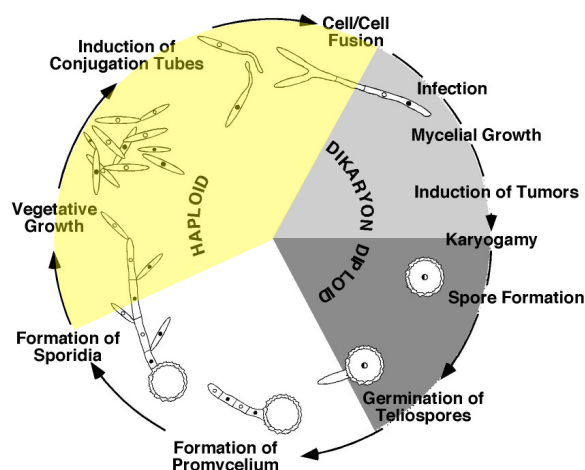


Figure 15. Life cycle of *Ustilago maydis*. In its saprophytic stage, *U. maydis* grows in the form of haploid budding yeast cells (sporidia). Sporidia of opposite mating types are able to fuse and give rise to the dikaryotic phase, which is the infective stage of the fungus. In the host tissues *U. maydis* grows in the form of mycelium, which eventually septates to form teliospores. At this stage, karyogamy occurs. Dark teliospores fill the galls characteristic of the disease. Upon germination of teliospores in the form of promycelium, meiosis and mitosis occur with the formation of basidiospores. Basidiospores bud off sporidia, which reproduce by budding, starting the life cycle again.

1.3.2 Secondary metabolites identified in *U. maydis*

Although *U. maydis* has not been considered as a commercial secondary metabolite producer, it secretes a number of interesting natural products (Bölker *et al.*, 2008). Ustilagic acid (UA) is a secondary metabolite produced in *U. maydis*, with a broad antibacterial and antifungal spectrum (Haskins, 1950; Haskins and Thorn, 1951). UA consists of 15,16-dihydroxypalmitic or 2,15,16-trihydroxypalmitic acid, which is O-glycosidically linked to cellobiose at its terminal hydroxyl group (Figure 16B). In addition, the cellobiose moiety is acetylated and acylated with a short-chain hydroxy fatty acid (Teichmann *et al.*, 2007). The SM gene cluster involved in the synthesis of UA consists of 12 ORFs, including a gene encoding for a transcriptional regulator (*rual1*) which controls its activation under nitrogen starvation conditions (Teichmann *et al.*, 2010). It was previously shown by the group of Bölker and collaborators in 2007, that UA production is critical during antagonistic interactions, since the co-inoculation of *U. maydis* with *B. cinerea* prevented the infection of the latter on tomato leaves (Teichmann *et al.*, 2007). Besides UA, *U. maydis* also secretes large amounts of mannosylerythritol lipids (MELs) under nitrogen starvation conditions (Hewald *et al.*, 2006). MELs consist of a mannosylerythritol disaccharide which is acylated with short-chain (C_2 to C_8) and medium-chain (C_{10} to C_{18}) fatty acids at the mannosyl moiety (Figure 17A). According to the number of acetyl groups, MELs can be differentiated into MEL A (fully acetylated), MEL

B and MEL C (monoacetylated at R-6 and R-4, respectively), and the fully deacetylated MEL D (Kitamoto *et al.*, 1990).

In particular, *U. maydis* served as the first organism for the molecular study of siderophore biosynthesis (Wang *et al.*, 1989). To recruit iron from the environment, *U. maydis* produces two siderophores (Figure 17C), ferrichrome and ferrichrome A, which are synthesized by non-ribosomal peptide synthetases (NRPSs) and contain the unusual amino acid δ -N-hydroxyornithine. Ferrichrome biosynthesis in *U. maydis* has been shown to be dependent on Sid1 (ornithine mono-oxygenase) and Sid2 (NRPS) (Mei *et al.*, 1993; Wang *et al.*, 1989; Yuan *et al.*, 2001).

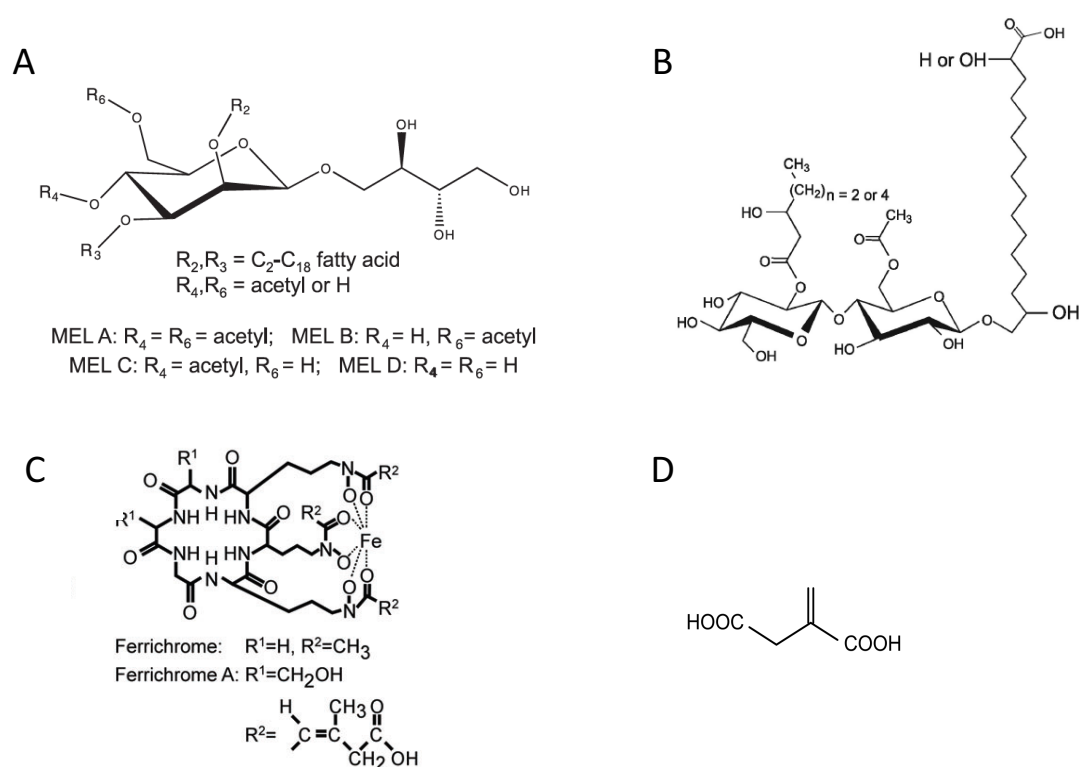


Figure 16. Major compounds of secondary metabolism in *U. maydis*. (A) Mannosylerythritol lipids (MELs). (B) Ustilagic acid (UA). (C) Ferrichrome and ferrichrome A. (D) Itaconic acid. Taken from Bölker *et al.*, 2008.

Recently, itaconic acid (IA) has been added to the list of secondary metabolites produced in *U. maydis* (Geiser *et al.*, 2016) (Figure 16D). IA is an unsaturated dicarboxylic organic acid that can be easily incorporated into polymers, and may serve as a substitute for petrochemical-based acrylic or methacrylic acid (Willke and Vorlop, 2001). IA production was first described in *Aspergillus itaconicus* and *Aspergillus terreus* and later on, in other microorganisms like *Candida* sp., *Rhodotorula* sp., *U. zea*, and *U. maydis* (Steiger *et al.*, 2013). As other organic acids in fungi, itaconate production enables the liberation of micronutrients, such as phosphate

and metals through chelating properties of the acids and a decrease of pH. Since fungi tolerate low pH, it provides a competitive advantage in carbon-rich environments (Cray *et al.*, 2013). In most of the described organisms, IA is generated by decarboxylation of the tricarboxylic acid (TCA) cycle intermediate *cis*-aconitate, while in *U. maydis*, IA is synthesized using a novel alternative pathway involving the isomerization of *cis*-aconitate into *trans*-aconitate and its subsequent decarboxylation to generate itaconate (Geiser *et al.*, 2016).

1.3.3 Melanization process in *U. maydis*

Typical examples of secondary metabolites are pigments, which absorb damaging ultraviolet radiation and thus protect the organism against DNA damage and oxidative stress (Brakhage and Liebmann, 2005). Among those pigments, melanin plays an important role in many organisms including, of course, fungi (Nosanchuk and Casadevall, 2003). Melanin contributes to the ability of fungi to survive in harsh environments. In addition, it plays a role in pathogenesis (Eisenman and Casadevall, 2012). Melanins are polymerized from phenolic and/or indolic compounds forming negatively charged, hydrophobic pigments of high molecular weight (White, 1958).

In fungi, two main melanin biosynthetic pathways have been described, DHN and L-DOPA. In the DHN pathway, precursor molecules (acetyl-CoA or malonyl-CoA) are produced endogenously and transformed into 1,3,6,8-tetrahydroxynaphthalene (T4HN) by the action of a polyketide synthase (PKS). Afterwards, a series of reduction and dehydration reactions produce the intermediates scytalone, 1,3,8-trihydroxynaphthalene (T3HN), vermelone, and finally 1,8-dihydroxynaphthalene (DHN). Subsequently, DHN is polymerized into melanin (Langfelder *et al.*, 2003) (Figure 17). In the L-3,4-dihydroxyphenylalanine (L-dopa) pathway, there are two possible starting molecules: L-dopa or tyrosine. If L-dopa is the precursor molecule, it is oxidized to dopaquinone by laccase. If tyrosine is the starting molecule, it is first converted to L-dopa and then to dopaquinone (Figure 17). Tyrosinase catalyzes both steps (Eisenman and Casadevall, 2012). Dopaquinone is a highly reactive intermediate and in the absence of thiol compounds it undergoes intramolecular cyclization, leading eventually to the formation of eumelanin (Figure 17). Although both melanin biosynthetic pathways are found in fungi, the DHN pathway is the most common one (Tsai *et al.*, 1999; Woo *et al.*, 2010).

The first studies of melanin in *U. maydis* suggested that catechol was the precursor for its biosynthesis since this compound was found in ethanol extracts from teliospores (Bell and Wheeler, 1986) (Figure 18). On the other hand, recent studies in *U. maydis* have shown that two PKS genes (*pks1* and *pks2*) and a laccase (*lac1*) are involved in the melanization process

of teliospores during plant infection (Islamovic *et al.*, 2015). This suggested that melanin in *U. maydis* is probably synthesized by the DHN pathway. However, whether the biosynthetic steps are carried out in the same way as for other fungi remains to be elucidated.

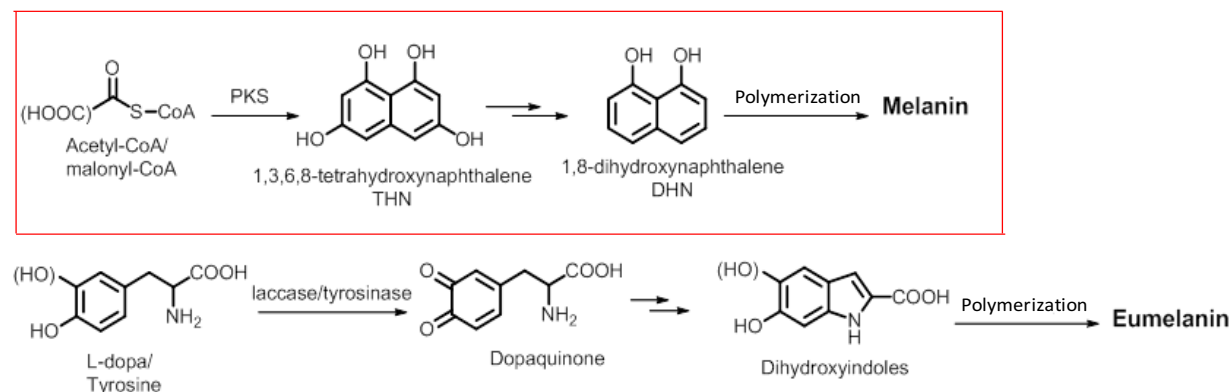


Figure 17. Melanin biosynthesis pathways in fungi. DHN and L-DOPA pathways are the two main routes for synthesizing melanin in fungi. In the DHN pathway (above), the starter molecule, acetyl-CoA or malonyl-CoA, is converted to 1,3,6,8-tetrahydroxynaphthalene by a polyketide synthase (PKS). Subsequently, series of reduction and dehydration reactions produce 1,8-dihydroxynaphthalene (DHN). Polymerization of DHN leads to the formation of melanin. On the other hand, few fungi synthesize melanin via L-3,4-dihydroxyphenylalanine (L-dopa) in a pathway that resembles mammalian melanin biosynthesis (below). The starter molecules can be either L-dopa or tyrosine. If the precursor molecule is L-dopa, it is oxidized to dopaquinone by laccase, while if tyrosine is the precursor, it is first converted to L-dopa and then dopaquinone. Tyrosinase, carries out both steps. Due to the high reactivity of dopaquinone, it forms dihydroxyindoles that polymerize into melanin.

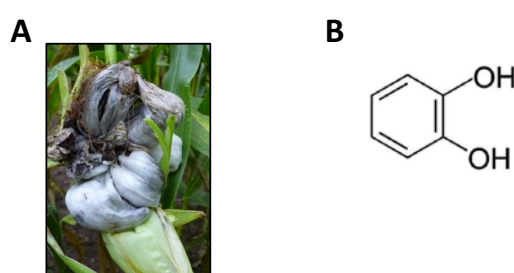


Figure 18. Melanized tumor of *U. maydis* and the proposed precursor for the melanin biosynthesis. (A) *U. maydis* tumor on field-grown maize plant (taken from Djamei and Kahmann, 2012). Teliospores of *U. maydis* contain dense deposits of melanin. (B) Molecular structure of catechol.

1.4 Aims of this work

The analysis of an increasing number of whole genome sequences indicates that fungi encode the genetic information for the biosynthesis of a plethora of compounds that are not observed when cultured under standard laboratory conditions. Although in *U. maydis* some biosynthetic pathways involved in the production of secondary metabolites have been elucidated, its metabolic potential has not been totally explored yet. Based on this premise, the general objectives of this project were:

1. Identification of potential secondary metabolite gene clusters in *U. maydis*, especially those that could be involved in plant-pathogen interaction.
2. Identification of novel metabolites by forced-expression of the selected gene clusters.
3. Elucidation of the biosynthetic steps associated with the production of these secondary metabolites.
4. Investigation of the biological role of the identified compounds in *U. maydis* life cycle.

2 Results

2.1 Identification of potential SM gene clusters in *U. maydis*

The first goal of the project was to identify potential SM gene clusters in *U. maydis*. For that reason, two different strategies were followed. The first one, manual annotation, consisted in a careful inspection of the *U. maydis* genome data base in order to seek for characteristic candidate genes involved in secondary metabolism. The second one, focused on the search of clusters of coregulated genes under different conditions by the analysis of existing expression data of *U. maydis* genes. Comparison of the output from both strategies, together with the data collected from bioinformatic algorithms as SMURF (Khaldi *et al.*, 2010) and antiSMASH (Medema *et al.*, 2011), led to the detection of several putative SM gene clusters. A detailed description of each strategy is presented below.

2.1.1 Manual annotation

The MIPS *Ustilago maydis* genome database (MUMDB) is a web-based resource that provides reliable information regarding molecular structure and functional annotation of the entirely sequenced genome of this basidiomycetous fungus (Kämper *et al.*, 2006). Taking advantage of the well annotated database, we searched for *U. maydis* genes implicated in the biosynthesis of secondary metabolites. For practical reasons, the search was restricted to genes coding for proteins belonging to any of these categories: backbone enzymes (BEs), tailoring enzymes (TEs), transcription factors (TFs) and transporters (TPs). A description of the classes of genes covered in each category is indicated in Table 1. Among the genes encoding backbone enzymes, PKSs were found in a higher number in comparison with NRPSs or DMATs. On the other hand, no terpene cyclases (TCs) were identified in this analysis (Table 1). Cytochrome P450 monooxygenases, dehydrogenases, transferases, hydroxylases and oxygenases were grouped into the category of tailoring enzymes, while all classes of TFs and TPs were included in this study. Selected genes were subsequently placed in a table with their respective ID number, putative function and chromosome location (Table S1). Genes located on the same chromosome and in close proximity to each other were considered to be part of a potential SM gene cluster. Since fungal secondary metabolite biosynthetic genes often occur in clusters that tend to be sub-telomerically located, we also took this criterion into account for selection of the

clusters. Based on this strategy, four putative SM gene clusters were identified, three of them contained at least one PKS and one contained an NRPS (Figure 19). Since none of the identified gene clusters has been previously characterized, they were tentatively named as cluster A (um04095-um11113), cluster B (um10532-um10539), cluster C (um10543-um05253) and cluster D (um06414-um11241). The arrangement of each gene cluster, its length and chromosome location is depicted in Figure 19.

Table 1. Putative secondary metabolite genes identified by manual inspection of *U. maydis* genome database.

Functional category	Gene families	Number of genes
BEs ^a	PKS	6
	NRPS	1
	DMAT	1
	TC	0
TEs ^b	Cytochrome P450	61
	Dehydrogenase	136
	Transferase	220
	Hydroxylase	9
	Oxygenase	34
TFs ^c	All families were considered	34
TPs ^d	All families were considered	104

a Backbone enzymes

b Tailoring enzymes

c Transcription factors

d Transporters

In order to define with more accuracy the borders of each gene cluster identified by manual annotation, we compared the clusters A-D with those detected by the algorithms SMURF and anti-SMASH (Table S2 and S3). All the clusters, except for cluster B, were somehow considered as potential candidates by both bioinformatic programs (Table 3). In the case of cluster A, SMURF detected their genes as part of two clusters located next to each other, cluster 7 (um04095-um04097) and cluster 8 (um04100-um04109) (Table 3). On the other hand, antiSMASH only detected a single cluster composed by three of its genes (cluster 10, um04095-

um04097). Moreover, a short version of cluster C was only shown by antiSMASH as cluster 13 (um10543-um05248). Related to cluster D, SMURF and antiSMASH could detect most of its genes in cluster 13 (um06407-um06430) and 14 (um06411-um06418), respectively (Table 3). These results suggested that even though the use of bioinformatic approaches to identify SM gene clusters constitutes a valuable option, we observed differences among both programs, particularly in assessing the length of the gene clusters. Therefore, we could not totally rely on these data, although they gave us a hint that most of our gene clusters (A, C and D) are potential candidates for being involved in secondary metabolism.

Table 2. Selected secondary metabolite genes identified by manual inspection of *U. maydis* genome database.

Backbone Enzymes (BEs)				Tailoring Enzymes (TEs)					Transcription Factors (TFs)	Transporters
PKS	NRPS	DMAT	TC	Cytochrome P450	Dehydrogenase	Transferase	Hydroxylase	Oxygenase	All categories	All categories
um04095 ^a				um04109 ^a	um11113 ^a	um04106 ^a		um04107 ^a	um04101 ^a	um04146
um04097 ^a				um04189	um04127	um04193			um04168	um04162
um04105 ^a				um42237	um04182	um04198			um10417	
					um04210	um04209			um10426	
					um04268	um10428				
					um04300	um04209				
						um10428				
						um04277				
um10532 ^b				um04362	um10846	um04353		um04348		um04347
					um04378	um11151				um04399
					um04441	um04374				um04410
					um10533 ^b	um04375				um04423
					um04480	um04406				um10528 ^b
						um04420				um04444
						um10539 ^b				um11977
										um04478
	um10543 ^c			um12083	um05252	um05293		um05329	um10544 ^c	um05260 ^c

					um05275	um05348			um10560	um10210
					um05407-A	um05355			um05338	um05396
					um05407-B	um05433				
					um05412					
um06414^d				um11005	um11241^d	um06426^d	um06466		um15103	um06461
um06418^d				um06459		um06462	um12340			
				um11812		um06467				

Genes highlighted in black were selected by manual annotation to be part of a secondary metabolite gene cluster.

a Genes located on chromosome 12

b Genes located on chromosome 14

c Genes located on chromosome 19

d Genes located on chromosome 23

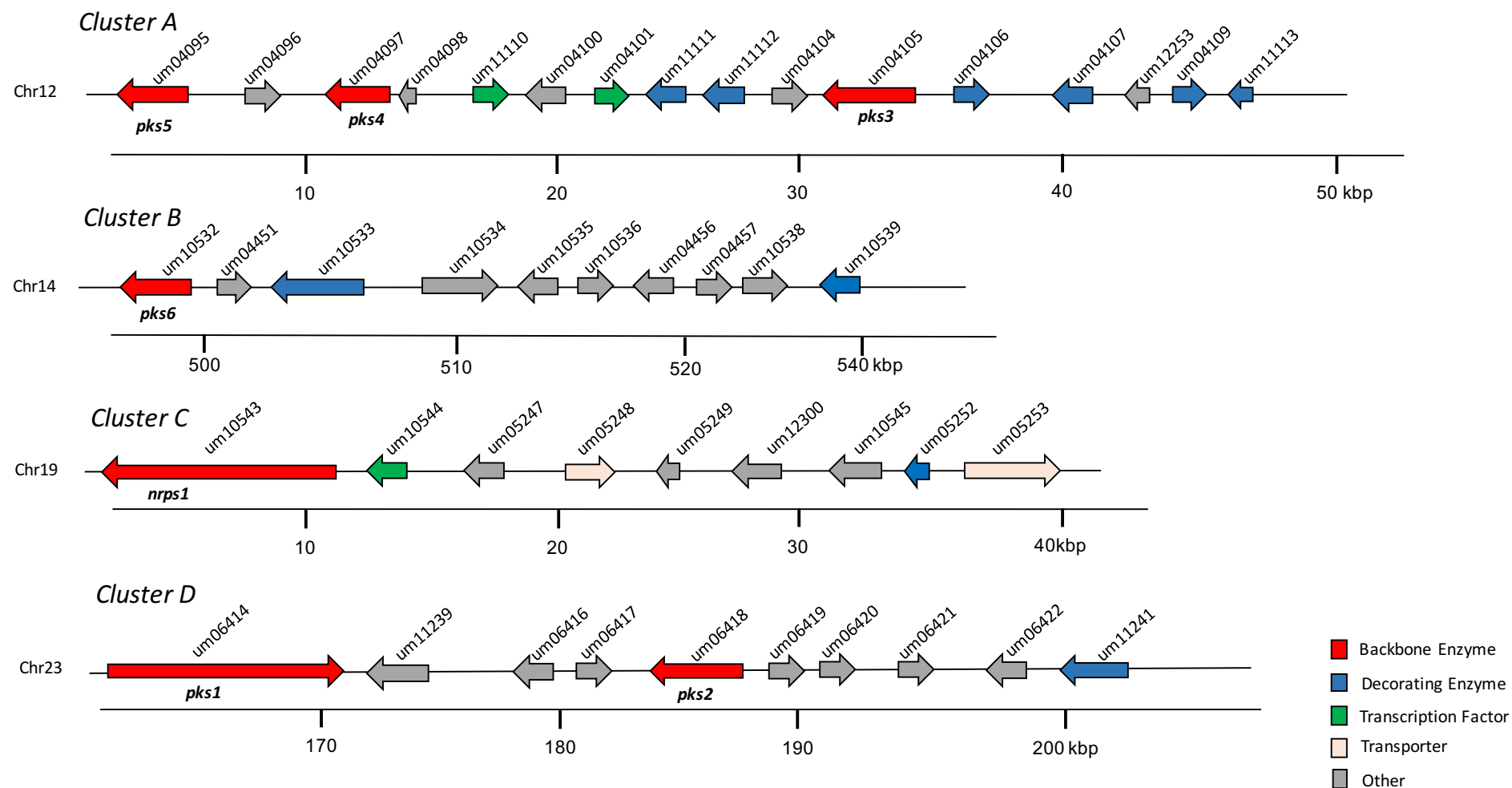


Figure 19. Secondary metabolite gene clusters identified by manual annotation and bioinformatic approaches. Four potential secondary metabolite gene clusters (A, B, C and D) were identified in *U. maydis* genome by manual annotation and bioinformatic sources as SMURF and antiSMASH. Genes are colored according to five categories: red (backbone enzyme), blue (tailoring enzyme), green (transcription factor), light pink (transporter) and gray (other). Chromosome location is indicated on the left side of each cluster.

Table 3. Comparison of the SM gene clusters identified by manual annotation with those detected by the SMURF and antiSMASH algorithms.

Manual annotation	SMURF ^a	antiSMASH ^b
Cluster A (um04095-um11113)	Cluster 7 (um04095-um04097) Cluster 8 (um04100-um04109)	Cluster 10 (um04095-um04097)
Cluster B (um10532-um10539)	-	-
Cluster C (um10543-um05253)	-	Cluster 13 (um10543-um05248)
Cluster D (um06414-um11241)	Cluster 13 (um06407-um06430)	Cluster 14 (um06411-um06418)

^a Secondary Metabolite Unknown Regions Finder

^b antibiotics and Secondary Metabolite Analysis SHell

2.1.2 Gene expression data

By measuring correlation among expression profiles of adjacent genes it is possible to detect coregulated gene clusters potentially involved in a common pathway. Examination of *U. maydis* gene expression data under a variety of conditions represents a strategy to identify potential secondary metabolite gene clusters. The GEO (Gene Expression Omnibus) database is a public functional genomics data repository for gene expression profiles that allows users to locate, review, and download studies of interest (<http://www.ncbi.nlm.nih.gov/geo/>). Therefore, we decided to explore the available gene expression data in *U. maydis* by downloading all 144 annotated experiments (platform GPL3681) and assembling them into an excel database (Table S4). Each sample (GSM105898, GSM105899, etc.) gene expression vector was added to a table column, thus creating an 8,682 (genes) vs. 144 (samples) excel table. The raw expression data were processed according to the following modifications: \log_2 transformation, normalization (z-score along each gene) and hierarchical clustering on the normalized data along samples and genes using Euclidean distance for column and row ordering (see Materials and Methods). In order to measure the similarity of expression profiles of a gene with its immediate upstream neighbor, we used the mean Pearson correlation coefficient (R). Mean R was calculated for the expression profiles of all possible pairs of 3 to 13 genes. Following this strategy, 40 clusters of coexpressed genes were identified (1GE-40GE) (Figure S1), including those important for the

production of mannosylerythritol lipid (MEL), ustilagic acid (UA) and ferrichrome A, which served as controls to validate the data processing strategy (Figure 20 and S1). From selected gene clusters, 52.5% contained 3 genes and 2.5% were formed by 9 genes, which represented the smallest and longest clusters identified by this method, respectively. Around 70% of the gene clusters seemed to be mostly upregulated during plant infection, 5 and 13 dpi (condition 4-9 and 15-16, respectively), suggesting that many of these genes could be involved in processes that would allow the fungus to cope with the adverse environment inside the plant (Figure S1, Table S4). In addition to the identification of coregulated genes located on the chromosome and with potential roles in secondary metabolism (Figure 21A), the constructed gene expression table also allows the analysis of coregulated genes involved in several metabolic processes that are not necessarily located on the same chromosome, which is possible to detect by ordering genes by hierarchical clustering of their expression profiles. A clear example can be noted for those genes involved in pheromone response in *U. maydis* (Figure 21B).

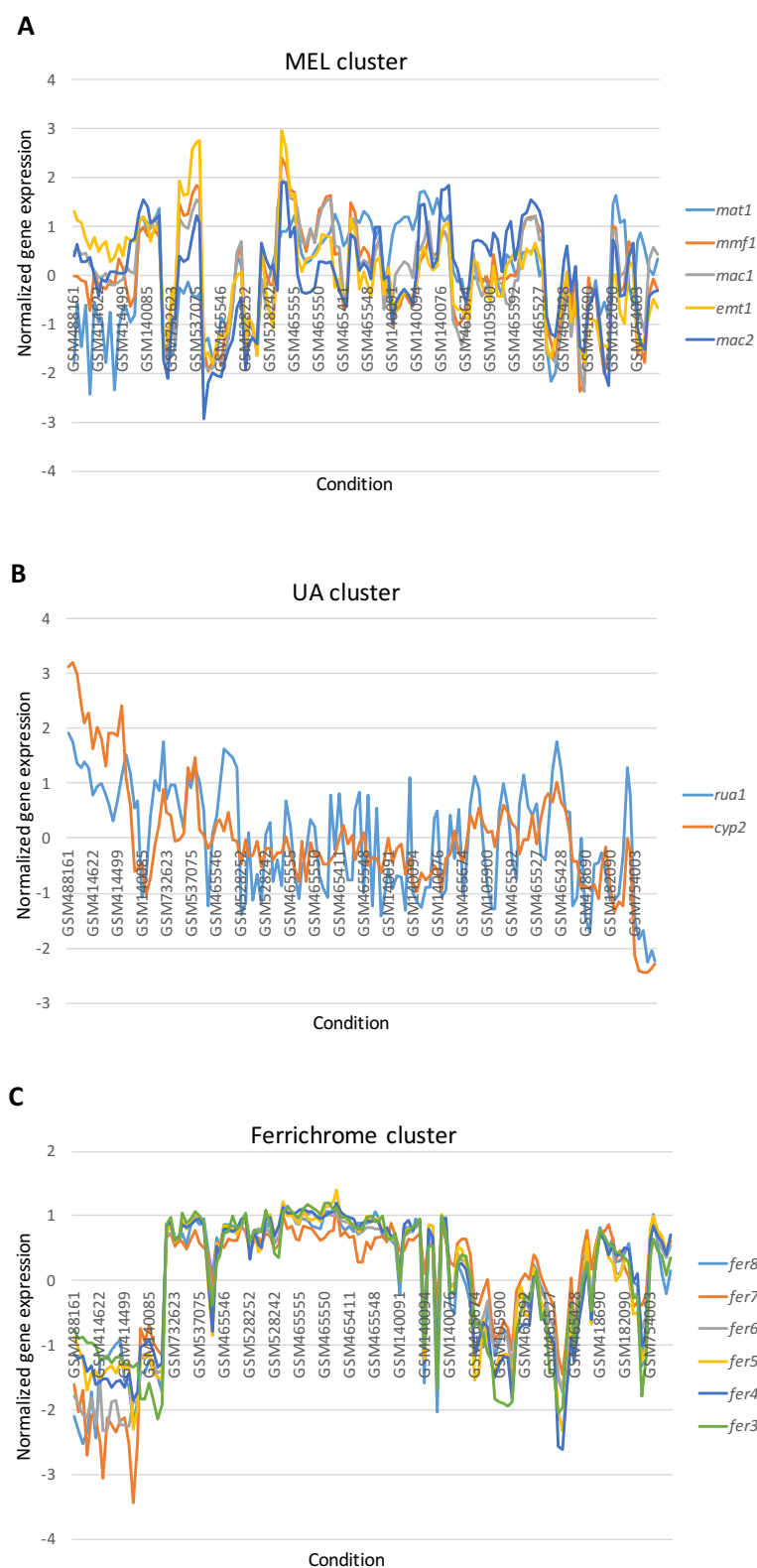
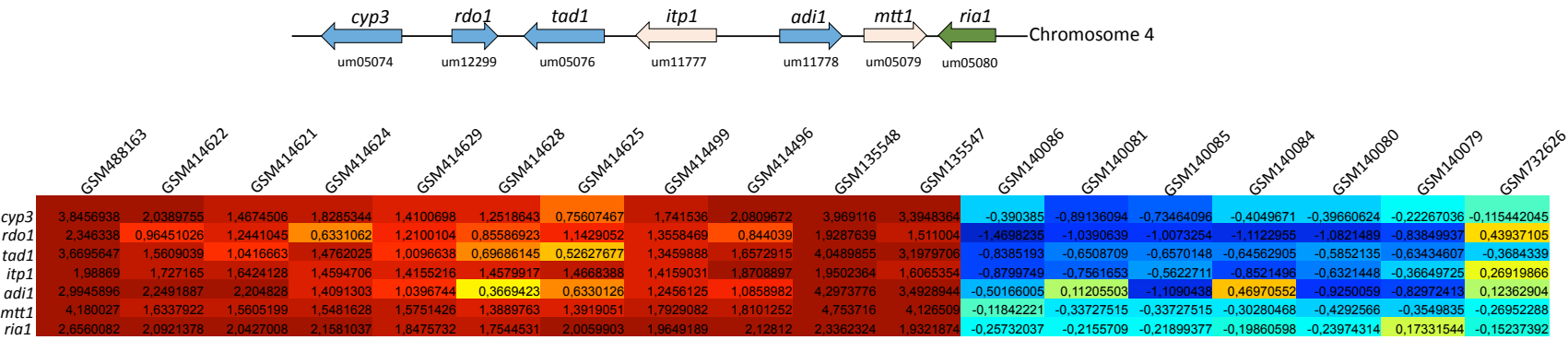


Figure 20. Gene expression plots of three different biosynthetic gene clusters. Analysis of the coregulation of the genes belonging to the (A) mannosylerythritol lipid, (B) ustilagic acid and (C) ferrichrome biosynthetic clusters serves as a control to validate the construction of the gene expression excel table. The x axis represents the experimental conditions downloaded from the platform GPL3681, and the y axis the normalized gene expression values.

A Coregulated genes located on the same chromosome



B Coregulated genes located on different chromosomes

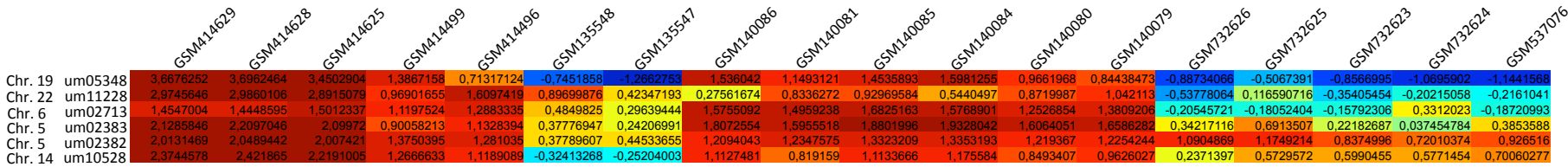


Figure 21. Expression analysis of coregulated genes in *U. maydis* under a variety of conditions. (A) Coregulated genes located on the same chromosome. Itaconic acid (IA) cluster genes (*cyp3*, *rdo1*, *tad1*, *itp1*, *adi1*, *mtt1* and *ria1*) located on chromosome 4 are coregulated under a variety of conditions. IA genes show a high expression level in tumor material from maize leaves 5 days post FB1/FB2 mixed infection at 28 °C (GSM488163) and a low expression level in the FB1 strain grown in CM-medium with 5 % of arabinose as a carbon source for 75 min (GSM140081). (B) Coregulated genes located on different chromosomes. Hierarchical clustering allows the identification of coregulated genes located on different chromosomes but involved in similar metabolic pathways or cellular processes as the pheromone response. Gene description: um05348, related to RAM1 protein farnesyltransferase; um11228, related to CAAX prenyl protease; um02713, pheromone response factor Prf1; um02383, α 2-pheromone receptor Pra1; um02382, α 1-specific pheromone (mating factor α 1) and um10528, related to STE6-ABC transporter. The different colors of the cells represent the level of expression of a gene under a given condition, indicated above each column. In the scale of colors, dark red indicates a highly expressed gene while a dark blue represents lowly expression.

2.1.3 Analysis of the expression profiles of gene clusters identified by manual annotation

In order to determine whether the genes manually identified as part of the clusters A, B, C and D were coregulated, the expression profile of each gene was analyzed and compared with the profiles of the other genes supposed to be part of the same cluster. Therefore, genes exhibiting similar expression profile under all given 144 experiments were considered to be coregulated. The corresponding expression graphs for the cluster genes are illustrated below (Figure 22).

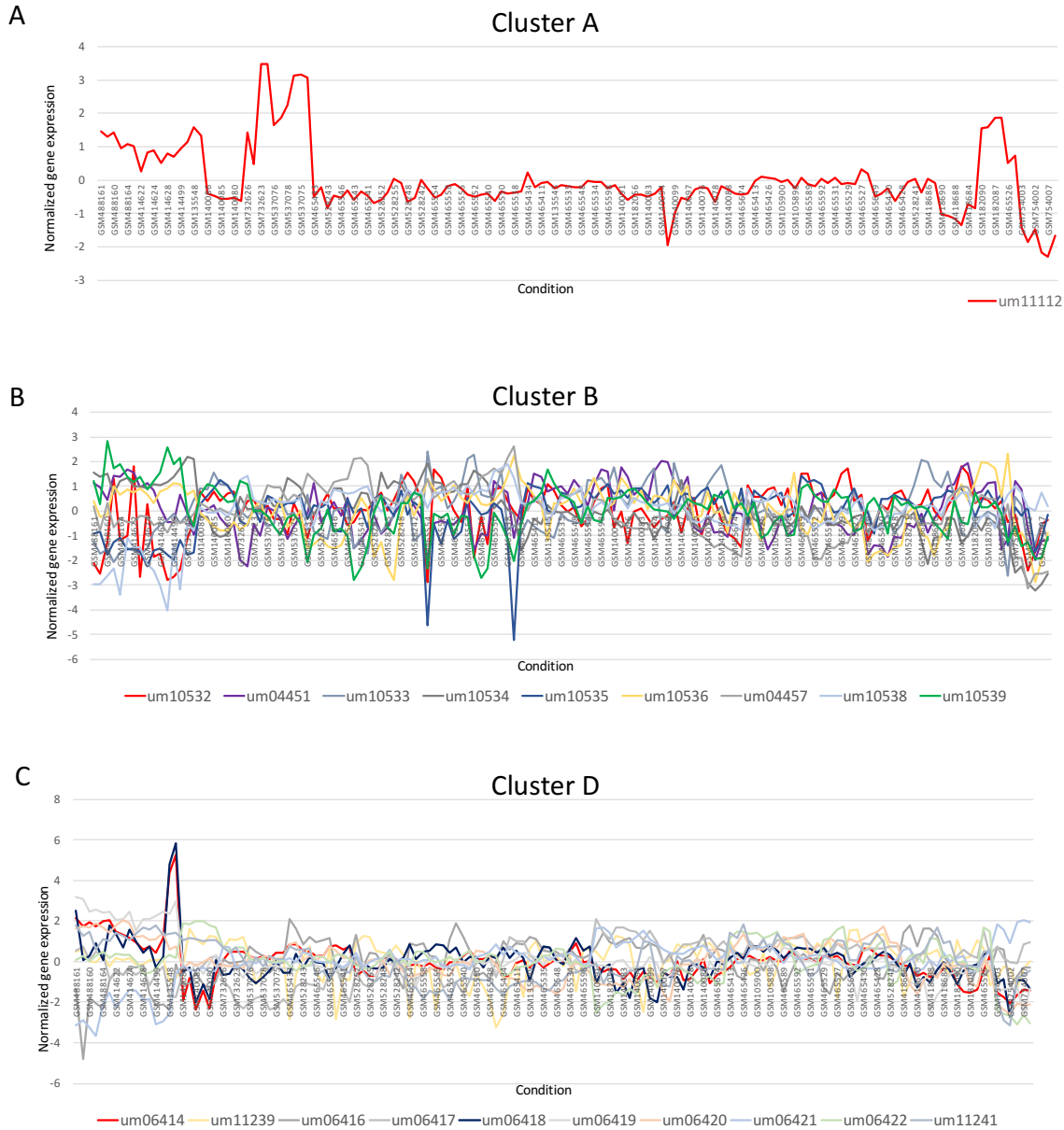


Figure 22. Gene expression plots of biosynthetic clusters identified by manual annotation in *U. maydis*. The y axis indicates the gene expression index on a log₂ scale, and the x axis represents the 144 experimental conditions included in the microarray excel table. **(A)** Cluster A. Gene expression profile of versicolorin B-synthase (um11112), the only member of the group with gene expression data available. **(B)** Cluster B (um10532-um10539). **(C)** Cluster D (um06414-um11241).

Microarray expression data of cluster A genes contained information only for the gene um11112, described as versicolorin B synthase (Figure 22A). A similar case was encountered for the cluster C, where nearly no expression was observed for any of their genes under most conditions, thus indicating that probably these genes were not sequenced or annotated when the DNA chips were designed.

Regarding cluster B, even though microarray data was available for all their genes, differences in expression profiles throughout the described conditions suggested no coregulation (Figure 22B). Therefore, cluster B was not an appropriate candidate for further analysis. Interestingly, when the expression profiles of the cluster D genes were plotted no coregulation among the whole set of genes could be observed. Nevertheless, the genes um06414 and um06418, which are annotated as polyketide synthases, seemed to be upregulated under the same conditions (Figure 22C). Since no transcription factor was found nearby these genes, it was suggested that a putative activator could be located on a different chromosome.

Taking into account all these elements, the most promising candidates for secondary metabolite gene clusters were cluster A and cluster D. Among these clusters, the only one that harbors a transcriptional regulator was cluster A, which would represent a clear advantage over cluster D, in terms of controlling the expression of the whole gene cluster. Another reason for choosing cluster A was based on the presence of three polyketide synthase genes (*pks3*, *pks4* and *pks5*) which gave us a hint that this cluster could be responsible for the production of more than one compound since many examples in the literature have shown that even a single polyketide synthase can produce several secondary metabolites such as *pksA* in *Aspergillus flavus* which produces four different aflatoxins: AFB₁, AFG₁, AFG₂ and AFB₂ (Yu *et al.*, 2004).

2.2 Upregulation of the Cluster A genes triggers the production of a black-greenish pigment

The analysis of the *U. maydis* genome sequence in combination with gene expression data, allowed the identification of a putative secondary metabolite gene cluster, named in this study as cluster A (Figure 19). Cluster A is located on chromosome 12 and harbors 16 genes encoding for 3 polyketide synthases (*pks3*, *pks4* and *pks5*), 2 transcription factors (*mtf1* and *mtf2*), 6 potential tailoring enzymes (*aox1*, *vbs1*, *omt1*, *pmo1*, *cyp4* and *deh1*) and 5 uncharacterized proteins (*orf1*, *orf2*, *orf3*, *orf4* and *orf5*) (Table 4, Figure 24A). In a previous work, this cluster was identified as msum_11 by analysis of conserved motif seeds in neighboring genes in *U. maydis* (Lee, 2010). msum_11 cluster genes were found to have two co-occurring promoter motif seeds 5'-GGGTAA-3' and 5'GTAn{3}GTT-3'.

Besides the identification of this putative SM gene cluster in *U. maydis* and others in *F. graminearum*, no further characterization has been done, therefore we were interested in exploring the function and biological role of cluster A. As described in Table 2, cluster A possesses two transcription factors, Mtf1 and Mtf2, very likely to act as pathway specific regulators. *mtf1*, annotated as BAS1 transcription factor, consists of 621 aa and contains three SANT domains at positions 7-49, 61-104 and 112-155 aa (Figure 23). The SANT domain is a highly conserved motif that is similar to the Myb DNA-binding domain. The SANT domain consists of three α -helices, each of which contains a corresponding, bulky aromatic residue (Aasland *et al.*, 1996). On the other hand, *mtf2*, a protein with 1,023 aa, encodes a sequence-specific DNA-binding binuclear zinc cluster ($\text{Zn(II)}_2\text{Cys}_6$) protein (Figure 23). Zinc binuclear proteins have been reported to be important for the regulation of secondary metabolism in the ascomycetous fungi *Aspergillus nidulans* (AflR), *Fusarium verticillioides* (Zfr1 and Fum21) and *Magnaporthe grisea* (Pig1p) (Chang *et al.*, 1995; Flaherty and Woloshuk, 2004; Brown *et al.*, 2007; Tsuji *et al.*, 2000).

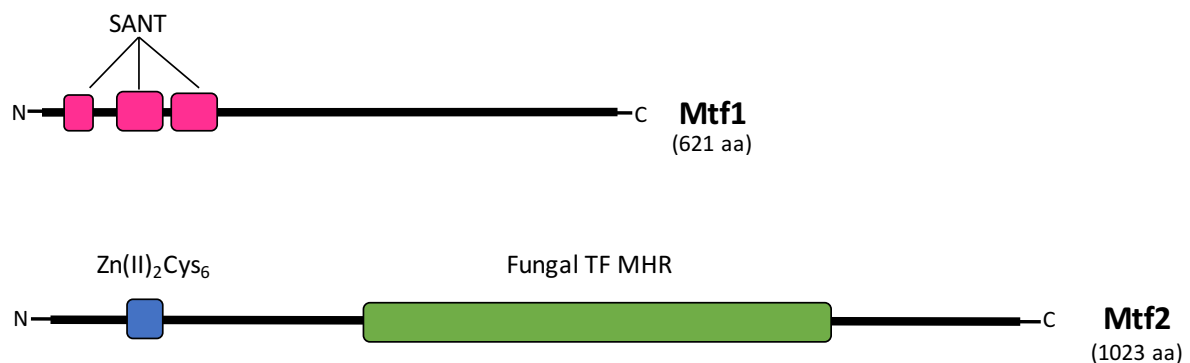


Figure 23. Domain structure of the transcription factors Mtf1 and Mtf2 located within the cluster A. Mtf1 possesses three SANT domains located at the aminoacid positions: 7-49, 61-104 and 112-155 (pink boxes). On the other hand, Mtf2 contains a $\text{Zn(II)}_2\text{Cys}_6$ binuclear cluster domain (blue box) which expands from 129 to 160 aa, and a fungal transcription factor regulatory middle homology region (MHR) located from 429 to 828 aa (green box). N letter represents N-terminal region and C, the C-terminal region from each protein.

Table 4. Cluster A genes in *U. maydis*.

Protein ID	Protein name	Deduced Function	Size [bp/aa]	Location on chromosome XII
um04095	Pks5	Polyketide synthase	3552/1183	3748-7476
um04096	Orf1	Uncharacterized protein	567/188	8330-9085
um04097	Pks4	Polyketide synthase	2256/751	9796-12148
um04098	Orf2	Uncharacterized protein	609/202	12543-13151
um11110	Mtf2	Zn(II) ₂ Cys ₆ transcription factor	3072/1023	14632-17703
um04100	Orf3	Uncharacterized protein	507/168	18695-19201
um04101	Mtf1	BAS1 transcription factor	1866/621	20348-22213
um11111	Aox1	Ascorbate oxidase precursor	1893/630	23340-25553
um11112	Vbs1	Versicolorin B synthase	1800/599	26411-28388
um04104	Orf4	Uncharacterized protein	555/184	29009-29656
um04105	Pks3	Polyketide synthase	5289/1765	30156-35453
um04106	Omt1	O-methyltransferase	1398/465	36350-37747
um04107	Pmo1	Phenol-2-monooxygenase	2145/714	38884-41028
um12253	Orf5	Uncharacterized protein	564/187	41748-42392
um04109	Cyp4	Cytochrome p450	1812/603	43060-44871
um11113	Deh1	NADP (+) dependent dehydrogenase	846/281	47747-48859

In order to gain an insight into the regulation of cluster A genes, we generated strains in which each transcription factor (*mtf1* or *mtf2*) was expressed under the control of the arabinose-inducible *P_{crg}* promoter (MB215 *P_{crg}::mtf1* and MB215 *P_{crg}::mtf2*). The reasoning behind this strategy was to analyze which genes were regulated by which transcription factor. Transcription of *mtf1* and *mtf2* was analyzed by Northern blot (Figure 24B). A substantial amount of the genes *mtf1* and *mtf2* steady state mRNA was detectable in the selected transformants under inducing conditions (I). This mRNA was completely absent under non-inducing conditions (R). Notably, in the MB215 *P_{crg}::mtf1* strain grown under inducing conditions, the three *pks* genes (*pks3*, *pks4* and *pks5*) were substantially transcribed. Likewise, *orf1*, *aox1*, *vbs1*, *orf4*, *omt1*, *pmo1*, *orf5*, *cyp4* and *deh1* genes were only expressed upon induction of *mtf1*. Conversely, no transcription of these genes was detected under non-inducing conditions. This suggests that this cluster is silent when *U. maydis* is grown under normal laboratory conditions and that expression of *mtf1* is sufficient to activate most cluster genes (Figure 24B).

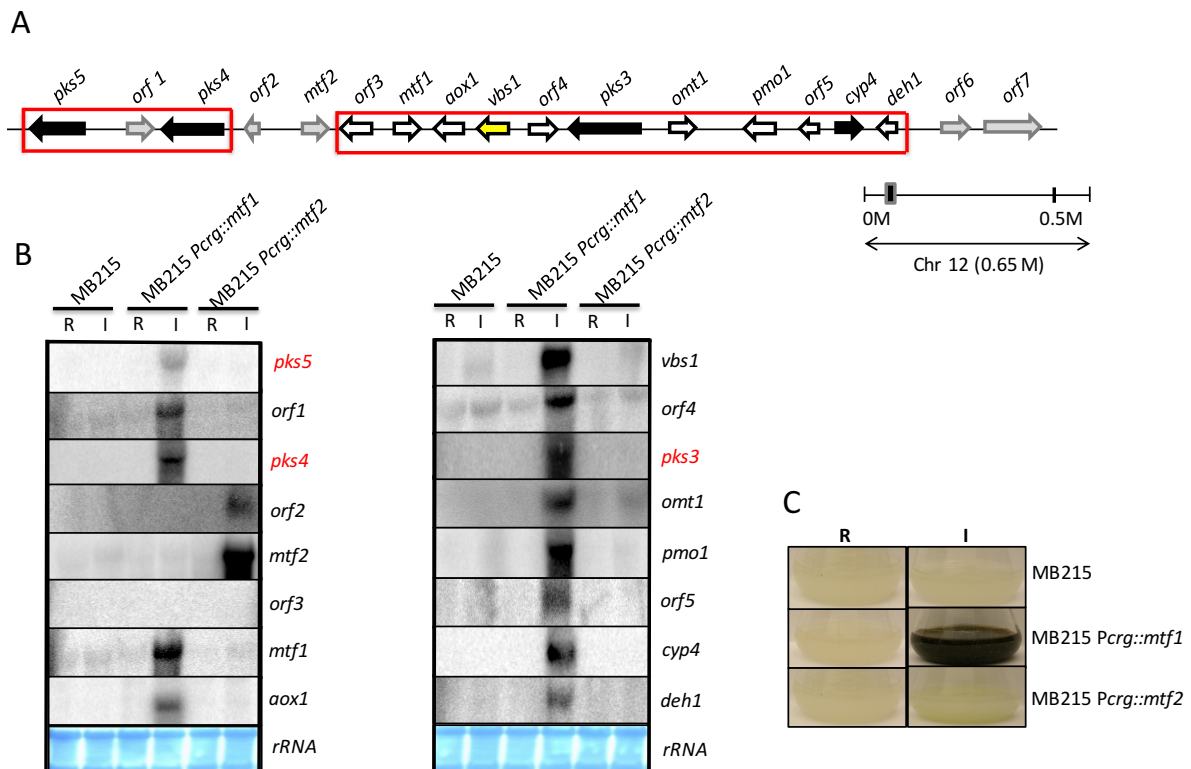


Figure 24. Induction of the silent gene cluster A results in the production of a black-greenish pigment. (A) The cluster A consists of at least 12 coregulated genes. Among these are three polyketide synthases (*pks3*, *pks4* and *pks5*) and several other genes characteristic of secondary metabolism. **(B)** Overexpression of the transcription factor *mtf1* under the control of the arabinose-inducible promoter stimulates transcription of the cluster genes. **(C)** After prolonged induction (I) cells produce a dark pigment, while cultures in which expression of *mtf1* is repressed (R) remain light.

On the other hand, overexpression of *mtf2* upregulated only the *orf2* gene, indicating that activation of *mtf2* has no influence in the expression of the other cluster A genes (Figure 24B). Induced expression of the biosynthetic gene cluster A over the time triggered the production of a black-greenish pigment, which was clearly observed after 24 h of induction (Figure 24C, right side). Moreover, no effect was recorded in MB215 *Pcrg::mtf2* and MB215 strains. In addition, the appearance of the cultures was similar to those grown under repressing conditions (Figure 24C, right side). The same result was detected when the wild-type, MB215 *Pcrg::mtf1* and MB215 *Pcrg::mtf2* strains were spotted in serial dilutions on agar inducing medium (Figure 25). In other words, the activation of cluster A contributes to the biosynthesis of a black-greenish pigment in *U. maydis*.

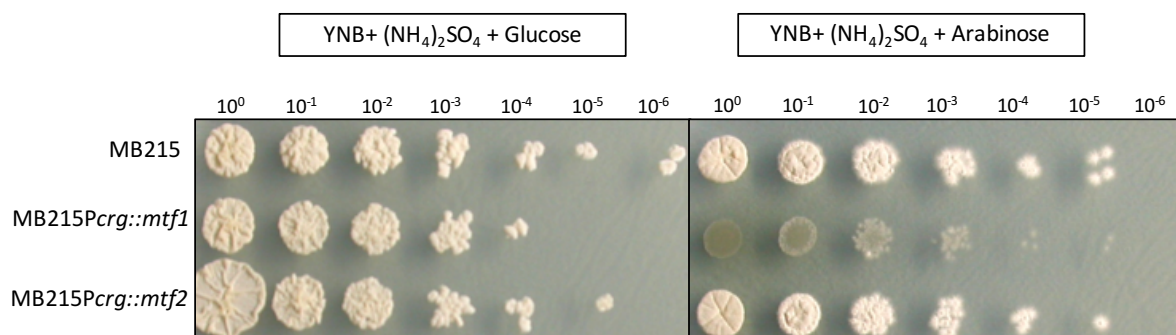


Figure 25. Serial 10 fold-dilutions of cell suspension of MB215, MB215 *Pcrg::mtf1* and MB215 *Pcrg::mtf2* strains on agar inducing medium. The MB215, MB215 *Pcrg::mtf1* and MB215 *Pcrg::mtf2* strains were grown on plates containing YNB, $(\text{NH}_4)_2\text{SO}_4$, and either glucose or arabinose as a carbon source. Strains were grown until an $\text{OD}_{600}=1$, washed twice with $\text{YNB}+(\text{NH}_4)_2\text{SO}_4$ medium without carbon source and spotted onto the corresponding agar plates in serial 10 fold-dilutions (10^0 - 10^{-6}). Left panel, strains grown under non-inducing conditions. Right panel, strains grown under inducing conditions.

Biochemical analysis by HPLC-MS of culture pellets in the wild-type, MB215 *Pcrg::mtf1* and MB215 *Pcrg::mtf2* strains, grown under inducing conditions, revealed the presence of many complex compounds extracted only in the MB215 *Pcrg::mtf1* strain (Figure 26A). Further fragmentation analysis of the chromatogram peaks, identified a common mass of 192, which corresponds to the 1,3,6,8-tetrahydroxynaphthalene (T4HN) (Figure 26B and C). T4HN is an aromatic polyketide that serves as general precursor of fungal melanin. T4HN is derived from acetyl-CoA or malonyl-CoA via polyketide synthase activity. In many fungi, T4HN is subsequently converted to scytalone, 1,3,8-trihydroxynaphthalene, vermeline and 1,8-dihydroxynaphthalene (DHN), which finally polymerizes into melanin (Wheeler, 1983).

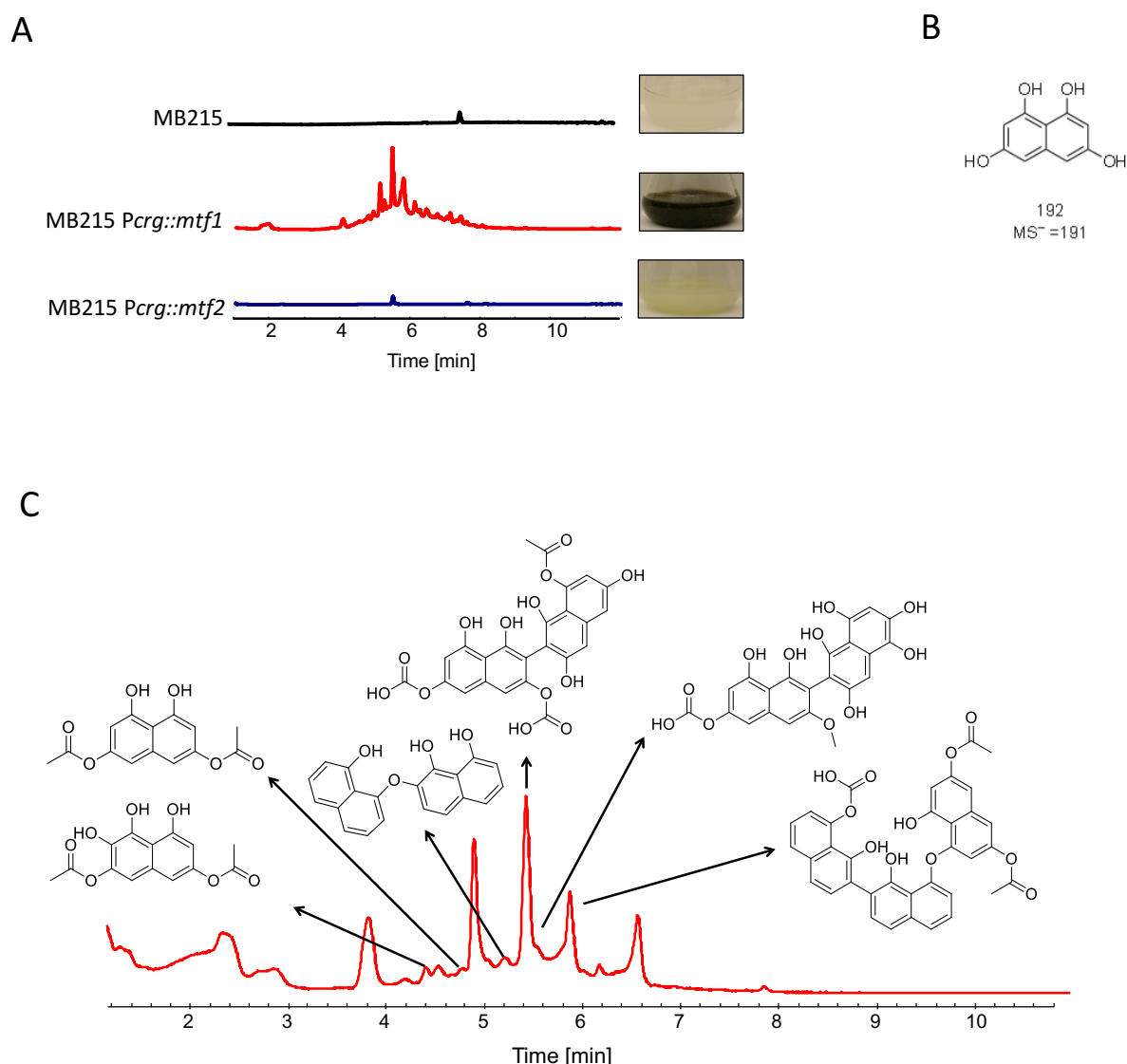


Figure 26. Overexpression of *mtf1* results in the production of many complex compounds derived from T4HN. (A) HPLC chromatograms (272 nm) of the MB215, MB215 *Pcr::mtf1* and MB215 *Pcr::mtf2* extracts. All the strains were cultivated under inducing conditions at 28°C for 96 h. (B) Molecular structure of tetrahydroxynaphthalene (T4HN), a key intermediate in the melanin biosynthesis pathway of many fungi. (C) Proposed structures derived from T4HN and produced as a result of prolonged induction of cluster A.

Due to this finding, we named the cluster A as a melanin-like cluster. For having a better understanding of the biosynthetic pathway controlled by the melanin-like cluster genes in *U. maydis*, a closer analysis of the genes was carried out and is described below.

2.3 Deletion of the *pks3*, *pks4*, *pks5* and *cyp4* genes abolishes the melanin-like pigment production

One of the strategies to investigate the biosynthetic role of the melanin-like cluster genes was to generate single deletion mutants in the MB215 *Pcr::mtf1* background strain by exchanging their coding sequence with a selectable marker gene. Genes considered to be

deleted were those whose expression was activated upon induction of *mtf1* (*pks5*, *orf1*, *pks4*, *aox1*, *vbs1*, *orf4*, *pks3*, *omt1*, *pmo1*, *orf5*, *cyp4* and *deh1*), as well as the *mtf2* gene, which served as a negative control. For all selected mutants, Southern blot hybridization patterns confirmed that they were the result of a single integration event at the targeted locus. All mutant strains were grown in inducing medium for 96 h at 28°C, and the extracts of their cell pellets were analyzed by HPLC-MS (Figure 28).

Single deletion of *pks3*, *pks4*, *pks5* and *cyp4* genes clearly had an effect in the production of the melanin-like pigment compared to the parental strain MB215 *Pcrg::mtf1*. None of the mutants displayed any melanin production (Figure 28), thus indicating the important role of these genes at early stages in the melanin biosynthetic pathway. In the case of the *pks4* gene, the attempts to generate a single deletion mutant in the MB215 *Pcrg::mtf1* background did not succeed. Although a large number of the transformants analyzed by Southern blot analysis showed the expected size of the mutant strain, the wild-type band was always present. For that reason, we suspected that the *pks4* gene could be duplicated in *U. maydis* genome. Duplication events, which have occurred at several times, seem to be the major force in the evolutionary history in fungi, particularly for genes involved in secondary metabolism (Khaldi *et al.*, 2008).

Deletion of a single copy of the *pks4* gene had no effect in melanin biosynthesis, while the induction of the strain in which both copies were deleted (MB215 $\Delta\Delta pks4$ *Pcrg::mtf1*) completely abolished the melanin phenotype (Figure 27B). This result was also reflected in their metabolic profiles where MB215 $\Delta\Delta pks4$ *Pcrg::mtf1* extracts, unlike MB215 *Pcrg::mtf1* and MB215 $\Delta pks4$ *Pcrg::mtf1*, produced no compounds (Figure 27B). In order to rule out the possibility that the colorless phenotype observed in MB215 $\Delta\Delta pks4$ *Pcrg::mtf1* cultures was due to a defect in the expression of those genes whose deletion triggered an albino phenotype (*pks3*, *pks5* and *cyp4*), Northern blot analysis were carried out (Figure 27A). Probes corresponding to the genes *pks3*, *pks4*, *pks5* and *cyp4* were used to analyze their transcript levels in the strains MB215, MB215 *Pcrg::mtf1*, MB215 $\Delta pks4$ *Pcrg::mtf1* and MB215 $\Delta\Delta pks4$ *Pcrg::mtf1*. Neither the single nor the double deletion of the *pks4* copies had an effect in the expression of *pks3*, *pks5* and *cyp4* (Figure 27A), suggesting that the colorless phenotype observed in MB215 $\Delta\Delta pks4$ *Pcrg::mtf1* was attributed to the deletion of both copies of *pks4*. Interestingly, a deletion of a single copy of the *pks4* gene in the background of the FB1 *Pcrg::mtf1* strain was enough to produce no longer melanin. Thus indicating that the gene *pks4* is only duplicated in the MB215 strain and not in FB1.

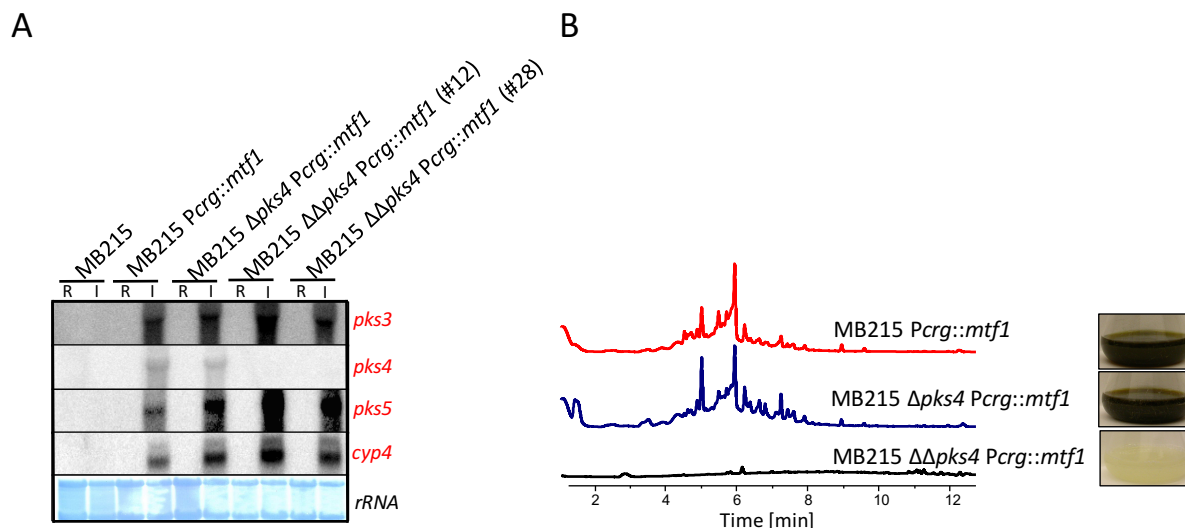


Figure 27. The single deletion of the *pks4* gene has no effect on melanin production. (A) Expression analysis of *pks3*, *pks4*, *pks5* and *cyp4* genes in the induced cultures of the strains MB215 $\Delta pks4$ *Pcrp::mtf1* and MB215 $\Delta\Delta pks4$ *Pcrp::mtf1* by Northern blot. All the tested strains were grown under repressing (R) and inducing (I) conditions at 28 °C for 96 h. Lower panel shows methylene blue-stained ribosomal RNA as an indicator of RNA integrity, loading and relative mobility between the samples. (B) HPLC chromatograms (272 nm) of MB215 *Pcrp::mtf1*, MB215 $\Delta pks4$ *Pcrp::mtf1* and MB215 $\Delta\Delta pks4$ *Pcrp::mtf1* extracts.

Markedly, MB215 $\Delta pks3$ *Pcrp::mtf1* and MB215 $\Delta\Delta pks4$ *Pcrp::mtf1* strains were not able to produce any of the T4HN derivatives shown in the chromatogram of the reference strain (Figure 28). Moreover, HPLC-MS of the MB215 $\Delta cyp4$ *Pcrp::mtf1* extract indicated the presence of three major peaks highlighted in red (Figure 28 and 29).

Single deletion of *vbs1* resulted in a yellowish phenotype (Figure 28). The *vbs1* gene, codes for a protein with sequence similarity to versicolorin B synthase (VBS), previously shown to be involved in the aflatoxin biosynthesis in *Aspergillus parasiticus* (Silva *et al.*, 1996). A closer look at the MB215 $\Delta vbs1$ *Pcrp::mtf1* UV chromatogram at 272 nm revealed the presence of three prominent peaks. The first one (V1, retention time, t_R 1.49 min) showed a m/z of 453.03 ($[M+H]^+$), the second one (V2, t_R 5.8 min) displayed a m/z of 511.32 ($[M+H]^+$), and the third one (V3, t_R 6.6 min) with a m/z of 1050.44 ($[M+H]^+$) (Figure 28).

Moreover, disruption of the *omt1* gene accumulated an orange-yellowish pigment, which was in appearance darker than the MB215 $\Delta vbs1$ *Pcrp::mtf1* culture (Figure 28). Remarkably, the peak named O1, with a retention time of 5.8 min and a m/z = 511.34 ($[M+H]^+$), seemed to be also present in $\Delta vbs1$ extracts as V2 (Figure 28). According to these data, it could be possible that Vbs1 and Omt1 reactions proceed with intermediates produced via Pks3, Pks4, Pks5 and Cyp4.

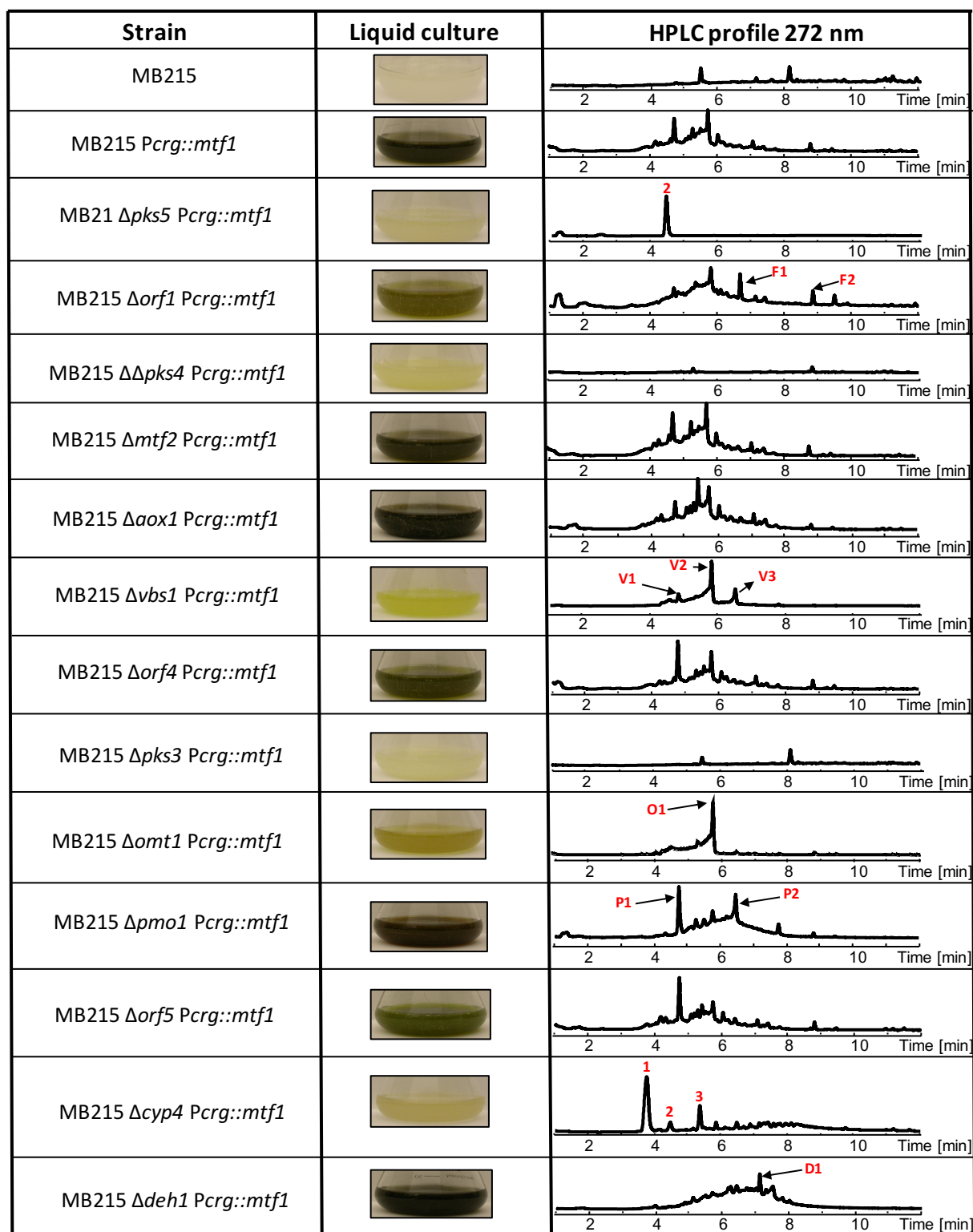


Figure 28. Metabolic profiling of the melanin cluster deletion mutants. Photographs of cultures were taken after 96 h of growth at 28 °C in inducing medium (middle column). Metabolite profiles of culture cells from wild-type (MB215), overexpressing strain (MB215 *Pcrg::mtf1*) and deletion mutants were recorded at 272 nm (right column). Some peaks are labeled and explained in the text.

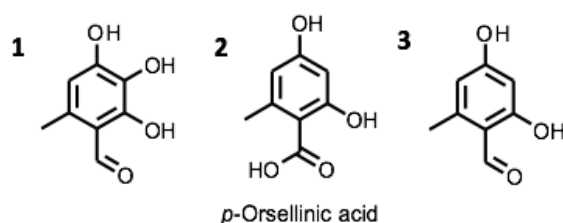


Figure 29. Molecular structure of orsellinic acid and its derivatives identified in the MB215 $\Delta cyp4$ *Pcrg::mtf1* strain.

Unfortunately, it was not possible to elucidate the structure of most these compounds due to their low amounts, instability and rapid polymerization.

The double deletion of *vbs1* and *cyp4* genes (MB215 $\Delta cyp4\Delta vbs1$ *Pcrg::mtf1*) produced OA and its derivative compounds, same compounds observed in the single deletion of *cyp4* (Figure 30). This result represents another indication that Vbs1 catalyzes a downstream reaction of the once catalyzed by Cyp4.

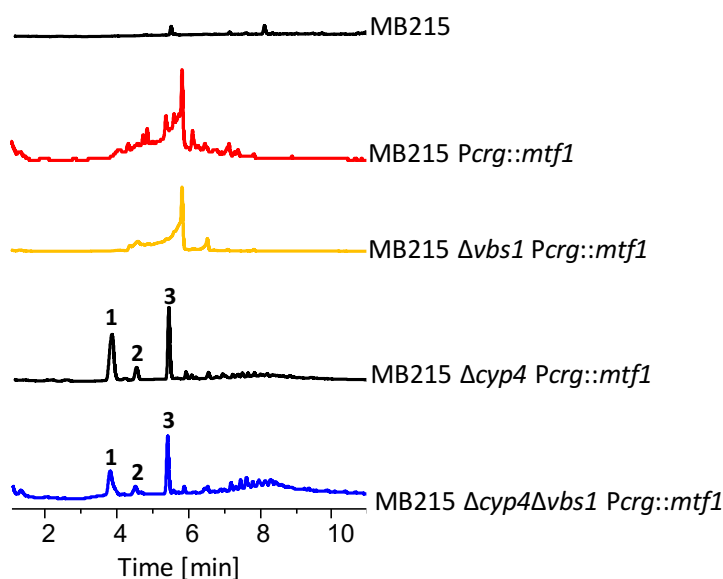


Figure 30. Metabolic profiles of MB215 $\Delta vbs1$ *Pcrg::mtf1*, MB215 $\Delta cyp4$ *Pcrg::mtf1* and MB215 $\Delta cyp4\Delta vbs1$ *Pcrg::mtf1*. The single and double deletion strains MB215 $\Delta cyp4$ *Pcrg::mtf1* and MB215 $\Delta cyp4\Delta vbs1$ produce orsellinic acid (2) and its derivative compounds (1 and 3).

Even though the mutant strains MB215 $\Delta pmol$ *Pcrg::mtf1* and MB215 $\Delta orf1$ *Pcrg::mtf1* exhibited similar melanization phenotype when compared to the reference, their metabolic profiles were different (Figure 28). Deletion of *pmol* generated two peaks that protrude more prominently than the others, one with a retention time of 4.9 minutes (P1) and the other one with 6.7 min (P2). In MB215 $\Delta orf1$ *Pcrg::mtf1* extracts, there were also found two major peaks with retention times of 6.7 min (F1) and 8.8 min (F2). On the other hand, the chromatogram of

the MB215 $\Delta deh1$ *PcrG::mtf1* strain seemed to be shifted to the right in comparison to the reference. Notably, those peaks within retention times between 4-7 minutes did not appear as well defined as in the reference. However, a major peak with retention time of 7.2 min (D1) could be detected. Finally, the chromatograms of the MB215 $\Delta aox1$ *PcrG::mtf1*, MB215 $\Delta orf4$ *PcrG::mtf1* and MB215 $\Delta orf5$ *PcrG::mtf1* mutant strains mimicked the profile of the reference strain. Nevertheless, slight differences in pigmentation were observed in MB215 $\Delta orf4$ *PcrG::mtf1* and MB215 $\Delta orf5$ *PcrG::mtf1*, where the coloration of the cultures appeared to be lighter and more greenish than *PcrG::mtf1*. In summary, disruption mutants of *pks3*, *pks4*, *pks5* and *cyp4* abolished synthesis of the melanin-like pigment, thus indicating the crucial role of these genes in the biosynthetic pathway. Although neither deletion of *vbs1* nor *omt1* produced a colorless phenotype, the participation of the encoded enzymes was confirmed by the yellowish phenotypes and the different metabolic profiles. Small changes in pigmentation were observed in the MB215 $\Delta orf1$ *PcrG::mtf1*, MB215 $\Delta aox1$ *PcrG::mtf1*, MB215 $\Delta orf4$ *PcrG::mtf1*, MB215 $\Delta pmol$ *PcrG::mtf1*, MB215 $\Delta orf5$ *PcrG::mtf1* and MB215 $\Delta deh1$ *PcrG::mtf1* strains if compared with the reference, suggesting a minor involvement of these gene products in the production of the melanin-like pigment.

2.4 Metabolic profiles of strains overexpressing single and multiple genes of the melanization gene cluster

Since there are no available expression data that allow us to assess which genes are regulated by the transcription factor Mtf1, we could not rule out the possibility that other genes, besides those belonging to the melanin-like cluster, could be also induced by *mtf1*. If so, this could indicate that the metabolic profile shown by the MB215 *PcrG::mtf1* strain is not only reflected by the contribution of the genes which are part of the melanin-like cluster (Figure 26A). Therefore, we decided to generate single and multiple overexpressing strains of the melanin-like cluster genes as a strategy to suppress a possible background caused by genes located outside the cluster. The genes that were selected to be overexpressed were those whose deletion showed a clear phenotype if compared with the reference strain. Candidate genes to be overexpressed under the control of the arabinose-inducible *crG* promoter were *pks3*, *pks4*, *pks5*, *cyp4* and *vbs1*, thus generating the strains MB215 *PcrG::pks3*, MB215 *PcrG::pks4*, MB215 *PcrG::pks5*, MB215 *PcrG::cyp4* and MB215 *PcrG::vbs1*, respectively. Using the *crG* promoter for overexpressing the melanin-cluster like genes instead of a constitutive promoter as *etef* or *otef* was due to the idea that having a constitutive upregulation of characteristic secondary metabolite genes could probably affect the transformation process or viability of *U. maydis*,

since many of those metabolites produced by fungi, as defense mechanisms against harsh environments or competitors, could be toxic even for themselves. Cultures were induced for 96 h at 28 °C in YNB medium with 0.1% of ammonium sulfate and 5% of arabinose as a carbon source. Cell pellets were further analyzed by HPLC-MS at 272 nm (Figure 31).


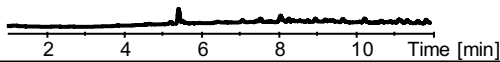
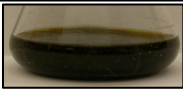
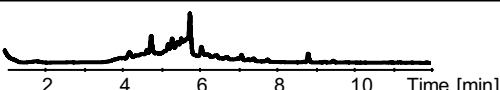
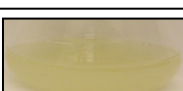
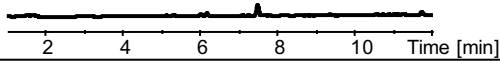
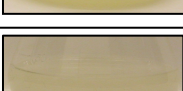
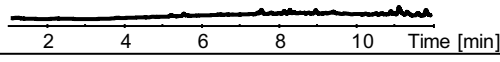
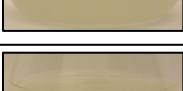
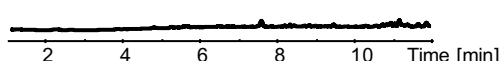
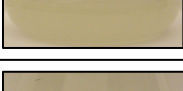
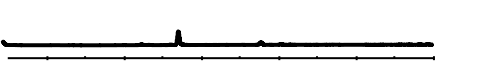


Strain	Liquid culture	HPLC profile 272 nm
MB215		
MB215 <i>Pcrg::mtf1</i>		
MB215 <i>Pcrg::pks3</i>		
MB215 <i>Pcrg::pks4</i>		
MB215 <i>Pcrg::pks5</i>		
MB215 <i>Pcrg::cyp4</i>		
MB215 <i>Pcrg::vbs1</i>		

Figure 31. Metabolic profiling of strains overexpressing single genes of the melanin gene cluster. Photographs of cultures were taken after 96 h of growth at 28 °C in YNB medium with 5% arabinose and 0.1% ammonium sulfate (column 2). Metabolite profiles of culture cells from wild type (MB215) and overexpressing strains (MB215 *Pcrg::mtf1*, MB215 *Pcrg::pks3*, MB215 *Pcrg::pks4*, MB215 *Pcrg::pks5*, MB215 *Pcrg::cyp4* and MB215 *Pcrg::vbs1*) recorded at 272 nm (column 3).

Single overexpression of either *pks3*, *pks4*, *pks5*, *cyp4* or *vbs1* produced no detectable compounds even though deletion of either one of these genes abolished the synthesis of the melanin-like pigment (Figure 31). In the case of the polyketide synthases, the metabolic profiles of their overexpressing strains could be explained by the domain structure of these proteins. Neither Pks3, Pks4 nor Pks5 individually possess all the critical domains from canonical type I PKSs (AT-KS-PP), which would suggest that they very likely work together with another polyketide synthase (Figure 32). A closer look to the domain structure of orsellinic acid polyketide synthases, in fungi and bacteria, revealed the common presence of five domains: KS (β -ketoacyl synthase), AT (acyl transferase), PS-DH (polyketide synthase dehydratase), PP (phosphopantetheine attachment site) and TE (thioesterase). Notably, Pks3 contains all the

necessary domains for the synthesis orsellinic acid, except the AT domain (Figure 32). Therefore, we ask ourselves whether Pks3 could be able to synthesize OA and its derivatives together with Pks4, since this polyketide synthase harbors the AT domain missing in Pks3. Earlier experiments have shown that deletion of *pks3* or *pks4* in the MB215 *Pcrg::mtf1* background produced no compounds, an indication that these genes are involved at early stages in the melanin pathway. If Pks3 and Pks4 catalyze the first reaction of the melanin biosynthetic pathway, OA would be detected if both genes were simultaneously overexpressed. Thus indicating that both polyketide synthases catalyze the first step in the metabolic pathway by a shared contribution of domains. Similarly, in the NRPS-PKS system of the leinamycin biosynthetic gene cluster in *Streptomyces atroolivaceus* S-140, there were found six PKS modules (encoded by the *lnmIJ pks* genes) lacking the AT domain, whose missing activity instead was provided in *trans* by the discrete protein LnmG (Cheng *et al.*, 2002 and 2003). LnmG was biochemically characterized *in vitro* as an AT enzyme, showing that it efficiently and specifically loaded malonyl CoA *in trans* to ACPs from all six LnmIJ PKS modules.

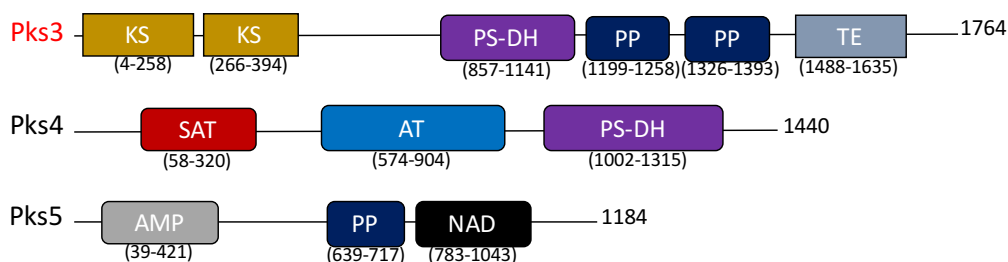


Figure 32. Domain organization of polyketide synthases of the melanin-like gene cluster in *U. maydis*. Protein enzymatic domains are as follows: AT, acyl transferase; AMP, adenylation; KS, β -ketoacyl synthase; NAD, nicotinamide adenine dinucleotide binding; PP, phosphopantetheine attachment site; PS-DH, polyketide synthase dehydratase; SAT, starter unit and TE, thioesterase. Domains were predicted by Protein Families (PFAM) and National Center for Biotechnology Information (NCBI) domain search. Numbers located on the right side of each PKS indicate their length in amino acids, and numbers below each domain represent their localization in the protein.

In order to explore this possibility, we decided to combine the expression of the single *pks* genes and analyze their metabolic profiles. Each *pks* gene was under the control of the *crg* promoter, thus generating the strains: MB215 *Pcrg::pks3+Pcrg::pks4* and MB215 *Pcrg::pks4+Pcrg::pks5* (Figure 33).

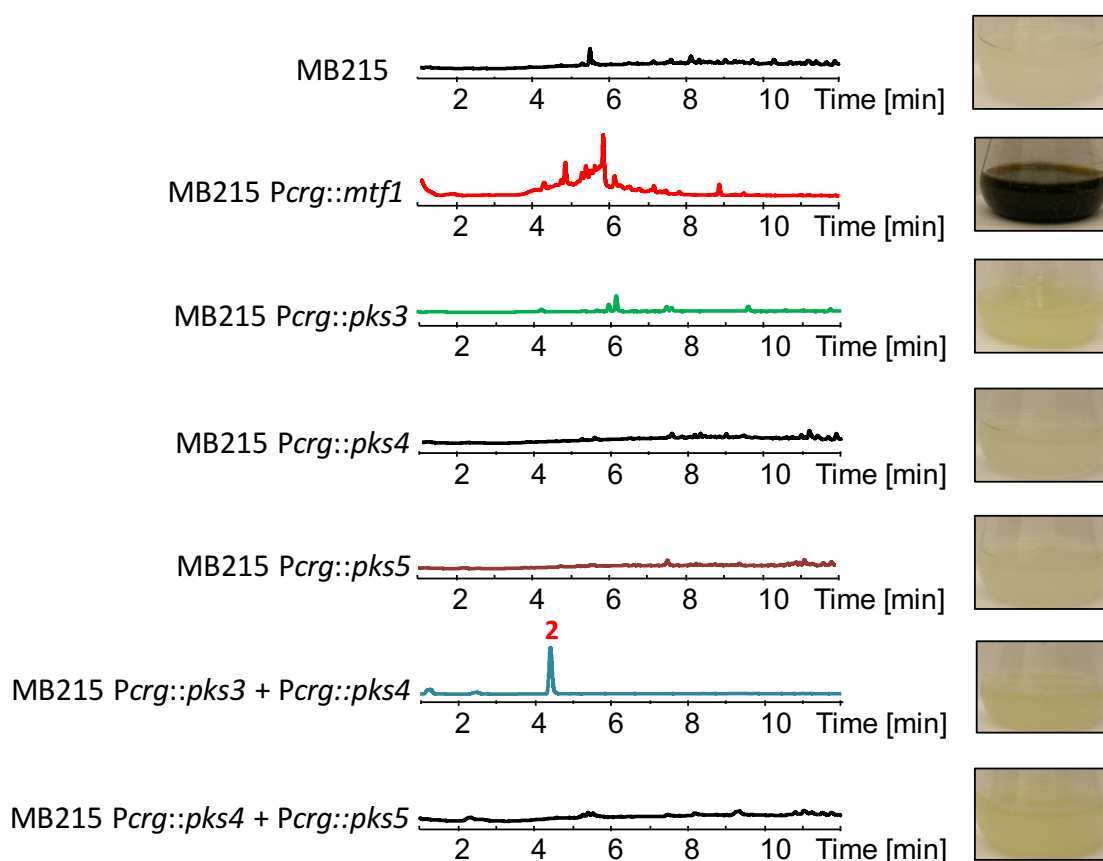


Figure 33. Double overexpression of the *pks3* and *pks4* genes produces orsellinic acid (OA). Metabolic profiles at 272 nm of single (MB215 *Pcr::pks3*, MB215 *Pcr::pks4* and MB215 *Pcr::pks5*) and double (MB215 *Pcr::pks3*+*Pcr::pks4* and MB215 *Pcr::pks4*+*Pcr::pks5*) overexpressing strains were analyzed after 96 h of growth in induction medium at 28 °C. Phenotypes of the strains are shown on the right side of the picture. Simultaneous expression of the *pks3* and *pks4* genes produces a peak with a t_R = 4.4 min identified as orsellinic acid (2) (Figure 29).

Cultures of the double overexpressing strains displayed similar phenotypes as those observed for their single overexpressed genes. Prolonged induction of MB215 *Pcr::pks3*+*Pcr::pks4* triggered the production of a single major compound (2) identified as orsellinic acid (OA). A similar effect was observed when *pks5* was deleted in the MB215 *Pcr::mtf1* background strain (Figure 28), which would indicate that indeed, Pks3 and Pks4 act at earlier stages than Pks5, otherwise no compound would be present in the cell pellets of the MB215 $\Delta pks5$ *Pcr::mtf1* strain. Moreover, the chromatogram given by the MB215 *Pcr::pks4*+*Pcr::pks5* strain showed no compounds (Figure 33). This was an expected result, since Pks4 and Pks5 together do not fulfill the minimal requirement of domains, since both lack the KS domain. Unfortunately, it was not possible to overexpress *pks3* and *pks5* simultaneously. Many *U. maydis* transformation attempts failed, and those that succeeded had very few transformants which turned out to be negative. However, according to the statements

above, cultivation of MB215 *Pcrg::pks3+Pcrg::pks5* in inducing medium would likely produce no detectable compounds.

In spite of the acquired knowledge from these data, the role of *Cyp4* in the melanin-like biosynthesis pathway is not clearly understood yet. Therefore, we decided to analyze the phenotypes and metabolic profiles of double overexpressing strains in which each polyketide synthase (*pks3*, *pks4* and *pks5*) was simultaneously expressed with *cyp4* for a 4-day period (Figure 34).

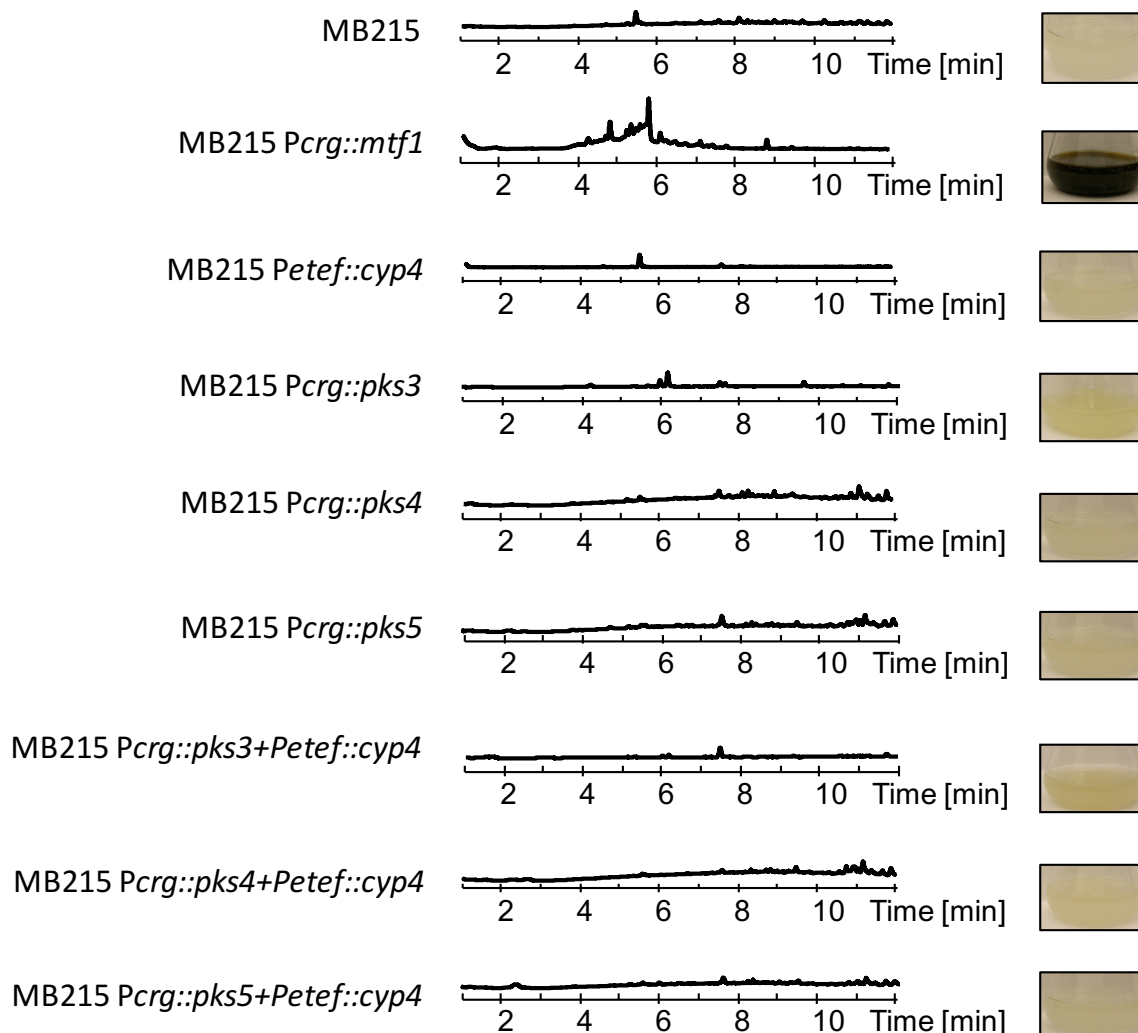


Figure 34. Metabolic profiles of the extracts from the double overexpression strains MB215 *Pcrg::pks3+Petef::cyp4*, MB215 *Pcrg::pks4+Petef::cyp4* and MB215 *Pcrg::pks5+Petef::cyp4* as detected by UV absorption at 272 nm. Photographs of cultures were taken after 96 h of growth at 28 °C in YNB medium with 5% arabinose and 0.1% ammonium sulfate (right side).

Since we previously observed that the single overexpression of *cyp4* produced no compounds, we considered to use an available expression plasmid kindly provided by Julia Ast (pETEF-GFP-Ala6-MMXN-G418) to subclone the *cyp4* gene and generate a plasmid (pETEF-Cyp4-

Tnos-G418), which contains the *cyp4* gene under control of the constitutive *etef* promoter and allowed integration of the desired construct into the *cbx* locus. The pETEF-Cyp4-Tnos-G418 plasmid was transformed into the single *pks* overexpressing strains to generate: MB215 *Pcrg::pks3+Petef::cyp4*, MB215 *Pcrg::pks4+Petef::cyp4* and MB215 *Pcrg::pks5+Petef::cyp4* strains (Figure 34). Analysis of their chromatograms revealed that neither MB215 *Pcrg::pks3+Petef::cyp4*, *Pcrg::pks4+Petef::cyp4* nor MB215 *Pcrg::pks5+Petef::cyp4* exhibited pigmented cultures, which was in accordance with the lack of compounds detected by HPLC. All these data suggest that Pks3, Pks4 and Pks5 participate at early stages in the synthesis of the melanin-like pigment and, very likely, the product derived from these polyketide synthases is used as a substrate by Cyp4.

2.5 Can the overexpression of the *pks1* and/or *pks2* genes rescue the phenotype in the strains MB215 $\Delta pks3$ *Pcrg::mtf1*, MB215 $\Delta\Delta pks4$ *Pcrg::mtf1* and MB215 $\Delta pks5$ *Pcrg::mtf1*?

A previous work in *U. maydis* identified the APSES transcription factor Ust1, whose deletion led to filamentous haploid growth and the production of highly pigmented teliospore-like structures in culture (García-Pedrajas *et al.*, 2010). Transcriptome analysis of the $\Delta ust1$ mutant showed the upregulation of two polyketide synthases, *pks1* (um06414) and *pks2* (um06418), and one putative laccase (um05361) with potential roles in melanin biosynthesis (Islamovic *et al.*, 2015). Interestingly, even though our search for secondary metabolite gene clusters found *pks1* and *pks2* located close to each other in chromosome 23, they were not considered as the perfect cluster candidate since no transcription factor was observed in close proximity to *pks1* and *pks2*. According to the work of Islamovic and collaborators, together with our experimental data, *U. maydis* possesses two gene clusters capable to synthesize melanin. In both cases, each polyketide synthase seems to play a crucial role in the biosynthesis of this natural pigment. Although it was shown that deletion of *ust1* does not influence the expression of *pks3* (Islamovic *et al.*, 2015), we wanted to know whether the transcription factor Mtf1 could be responsible for the regulation of the *pks1* and *pks2* genes. For this reason, we analyzed the expression of *pks1* and *pks2* genes in the strain MB215 *Pcrg:: mtf1* after being cultured for 96 h in inducing medium at 28 °C (Figure 35).

In none of the cases, *pks1* or *pks2* showed increased expression upon induction of *mtf1*, suggesting that *mtf1* does not exert a regulatory effect on *pks1* or *pks2*. Therefore, we asked ourselves whether *U. maydis* polyketide synthases could have complementary functions, if so, the overexpression of either *pks1* or *pks2* could rescue the phenotype of the MB215 $\Delta pks3$

Pcrg::mtf1, MB215 $\Delta\Delta pks4$ *Pcrg::mtf1* or MB215 $\Delta pks5$ *Pcrg::mtf1* mutants. Domain structures of *U. maydis* PKSs and their percentages of identity among them are shown below (Figure 36 and Table 5, respectively).

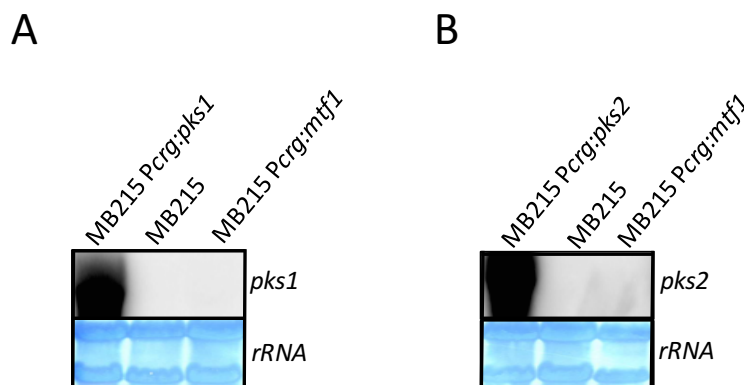


Figure 35. Mtf1 does not control the expression of the *pks1* and *pks2* genes. Expression analysis of (A) *pks1* and (B) *pks2* in the strain MB215 *Pcrg::mtf1*. Lower panel shows methylene blue-stained ribosomal RNA as an indicator of RNA integrity, loading and relative mobility between the samples. The strains MB215, MB215 *Pcrg::pks1*, MB215 *Pcrg::pks2* served as controls.

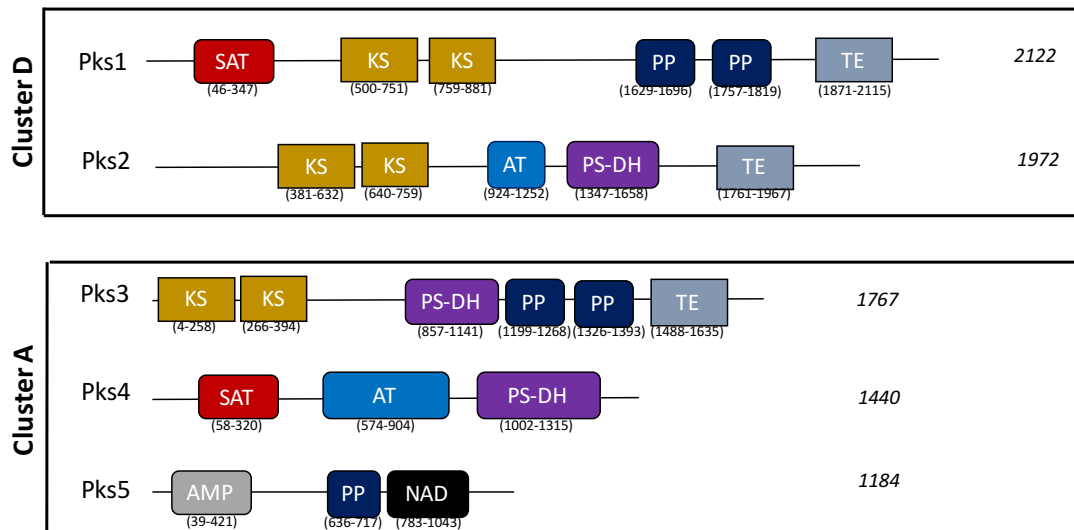


Figure 36. Domain structure of the polyketide synthases identified in the SM gene clusters A and D in *U. maydis*. The domain structures of the 5 polyketide synthases (Pks1-Pks5) identified in *U. maydis* are represented with different colors. Protein enzymatic domains are as follows: AT, acyl transferase; AMP, adenylation; KS, β -ketoacyl synthase; NAD, nicotinamide adenine dinucleotide binding; PP, phosphopantetheine attachment site; PS-DH, polyketide synthase dehydratase; SAT, starter unit and TE, thioesterase. Domains were predicted by Protein Families (PFAM) and National Center for Biotechnology Information (NCBI) domain search. Numbers located on the right side of each PKS indicate their length in amino acids, and numbers below each domain represent their localization in the protein.

Neither Pks1 nor Pks2 have all essential catalytic domains found in fungal PKSs (AT, KS and PP). This suggests that they could work only in a collaborative manner. Pks1 possesses KS and PP domains, while Pks2 contains KS and AT domains (Figure 36). A comparison of Pks1 and Pks2 with the PKSs from the melanin-like cluster indicates that Pks1 and Pks2 are more similar to Pks3 than to Pks4 or Pks5 (Table 5). Despite this observation, the identity percentages among the PKSs from both clusters are not so distant from each other. Therefore, to gain an insight of the biosynthetic potential of Pks1 and Pks2, we first created strains in which either *pks1* or *pks2* were singly overexpressed under the control of the *crg* promoter (MB215 *Pcrg::pks1* and MB215 *Pcrg::pks2*) and afterwards they were analyzed by HPLC-MS at 272 nm (Figure 37).

Table 5. Identity between *U. maydis* PKSs from two different clusters located at chromosome 12 (Pks3, Pks4 and Pks5) and chromosome 23 (Pks1 and Pks2).

Polyketide synthase	Identity ^a	
	Pks1	Pks2
Pks3	16.0%	15.3%
Pks4	12.8%	14.1%
Pks5	9.6%	11.3%

^a The sequences were analyzed by UniProt (www.uniprot.org).

The phenotypes of the single overexpressing strains MB215 *Pcrg::pks1* and MB215 *Pcrg::pks2* were similar to each other and to the one displayed by the strain MB215 *Pcrg::pks3* (Figure 34 and 37). Furthermore, when *pks1* and *pks2* were simultaneously expressed, the cells produced a light greenish pigment. Moreover, no detectable compound was observed in the MB215 *Pcrg::pks1* or MB215 *Pcrg::pks2* strains, while the combined overexpression of *pks1* and *pks2* triggered the production of six major peaks, indicated as PP1 to PP6 (Table 6). Since the *lac1* gene was shown to be involved in the melanization process together with *pks1* and *pks2* (Islamovic *et al.*, 2015), we consider that the triple overexpression of *lac1*, *pks1* and *pks2* will produce a dark pigmentation.

These data suggest that only the combined expression of *pks1* and *pks2* synthesizes compounds that might serve as intermediates for melanin biosynthesis. As it was previously described for Pks3, Pks1 does not possess an AT domain in its structure, which makes us think that this activity could be provided by Pks2, just as we hypothesized that Pks4-AT domain could assist Pks3 in the biosynthesis of OA.

Table 6. Compounds identified by HPLC-MS (272 nm) in extracts of the MB215 *Pcrg::pks1*+*Pcrg::pks2* strain after prolonged induction.

Compound	t_R (min)	m/z ($[M+H]^+$)
PP1	5.9	208.52
PP2	6.2	729.52
PP3	6.8	427.06
PP4	7.3	467.13
PP5	7.7	465.11
PP6	7.9	443.32

On the other hand, we also generated strains in which either *pks1* or *pks2* were co-expressed with *Cyp4* (Figure 37). The analysis of the phenotypes and metabolic profiles given by these strains served as a control to rule out the possibility of an involvement of *Cyp4* in the biosynthesis of the greenish pigment. Neither MB215 *Pcrg::pks1*+*Petef::cyp4* nor MB215 *Pcrg::pks2*+*Petef::cyp4* displayed a different phenotype to the one observed in the MB215 *Pcrg::pks1* or MB215 *Pcrg::pks2* strains (Figure 37). In no case, the double overexpression of either *pks1* or *pks2* with *cyp4* produced a significant peak, indicating that *Cyp4* has no effect in the metabolic profile of MB215 *Pcrg::pks1* or MB215 *Pcrg::pks2*.

Until now, we have shown that the majority of the single or double overexpressing strains of the polyketide synthase genes located within the same cluster produced no compounds. Considering this premise, we decided to explore the complementarity of the PKSs from both gene clusters by combining the expression of their genes and evaluating whether those strains could show a different phenotype. For this purpose, we created six double overexpressing strains in a way that *pks1* and *pks2* could be coexpressed with either *pks3*, *pks4* or *pks5* (Figure 38 and 39)

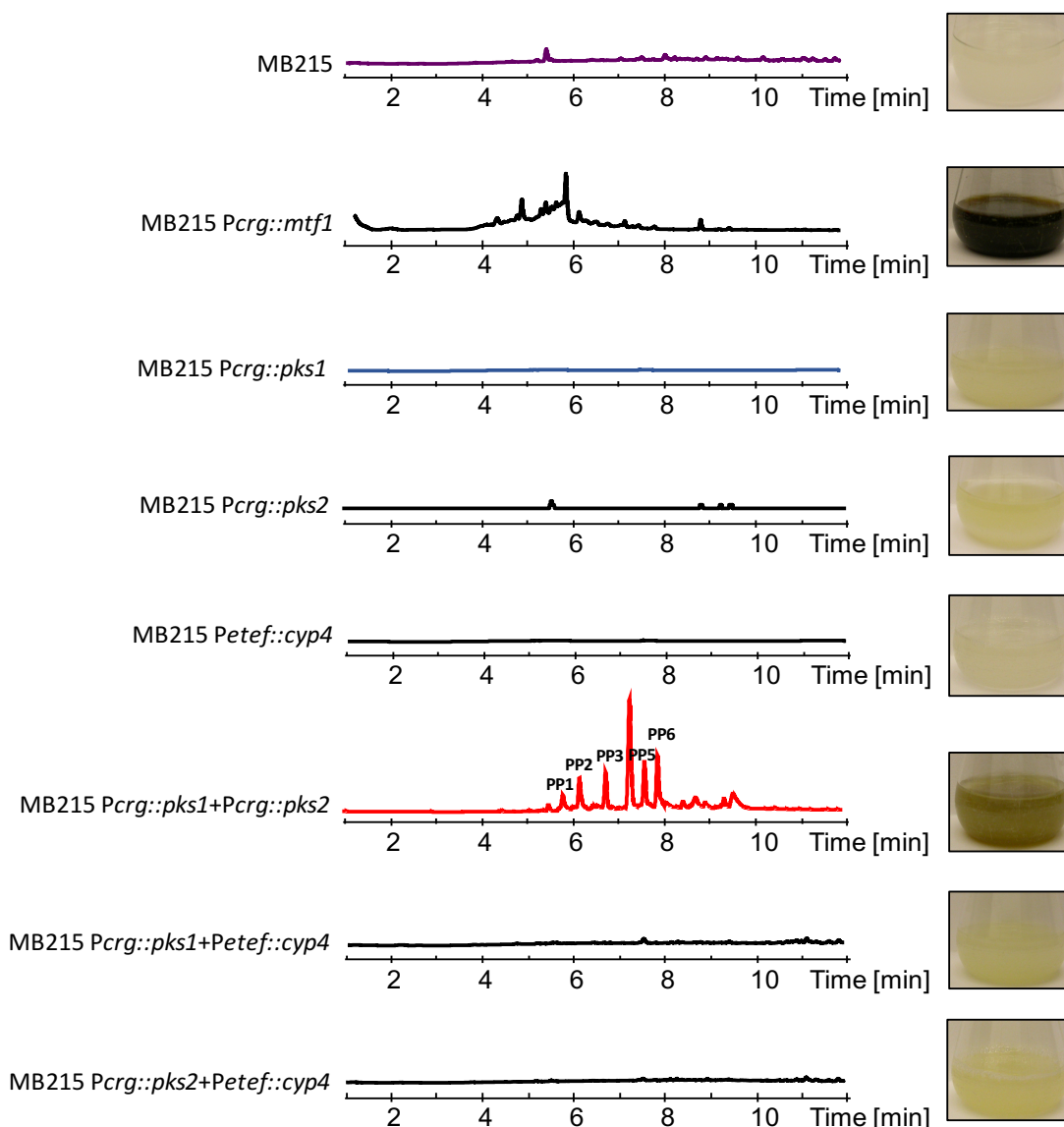


Figure 37. HPLC profiles of the extracts from the double overexpressing strains MB215 *Pcr::pks1+Pcr::pks2*, MB215 *Pcr::pks1+Petef::cyp4* and MB215 *Pcr::pks2+Petef::cyp4* as detected by UV absorption at 272 nm. Photographs of cultures were taken after 96 h of growth at 28 °C in YNB medium with 5% arabinose and 0.1% ammonium sulfate (right side). PP1-PP6 peaks indicate the compounds identified in the strain MB215 *Pcr::pks1+Pcr::pks2*. For more details, consult Table 6.

In the scenario in which *pks1* was overexpressed together with either *pks3*, *pks4* or *pks5* no compounds were produced, thus suggesting that the function of Pks2 can not be complemented by Pks3, Pks4 or Pks5. As expected, similar phenotypes were displayed in the double and single overexpressing strains (Figure 38). Likewise, overexpression of *pks2* in combination with the PKS genes from the melanin-like gene cluster did not produce any new compounds or phenotypes in comparison to those observed in their single overexpressing strains (Figure 39). These data indicate that neither Pks1 nor Pks2 are able to synthesize a greenish pigment if expressed together with either Pks3, Pks4 or Pks5.

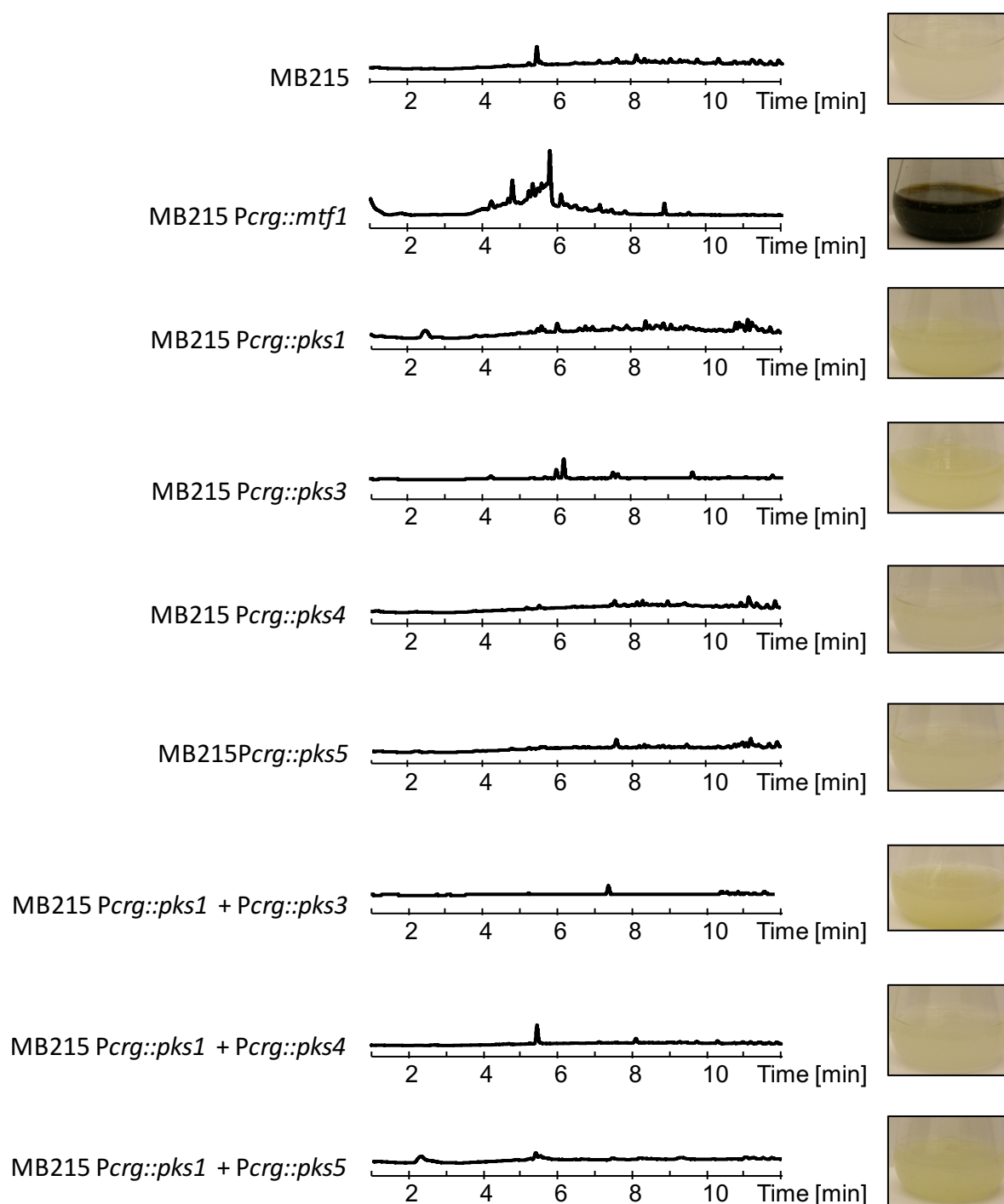


Figure 38. HPLC profiles of the extracts from the double overexpressing strains MB215 *Pcrg::pks1*+*Pcrg::pks3*, MB215 *Pcrg::pks1*+*Pcrg::pks4* and MB215 *Pcrg::pks1*+*Pcrg::pks5* as detected by UV absorption at 272 nm. Photographs of cultures were taken after 96 h of growth at 28 °C in YNB medium with 5% arabinose and 0.1% ammonium sulfate (right side).

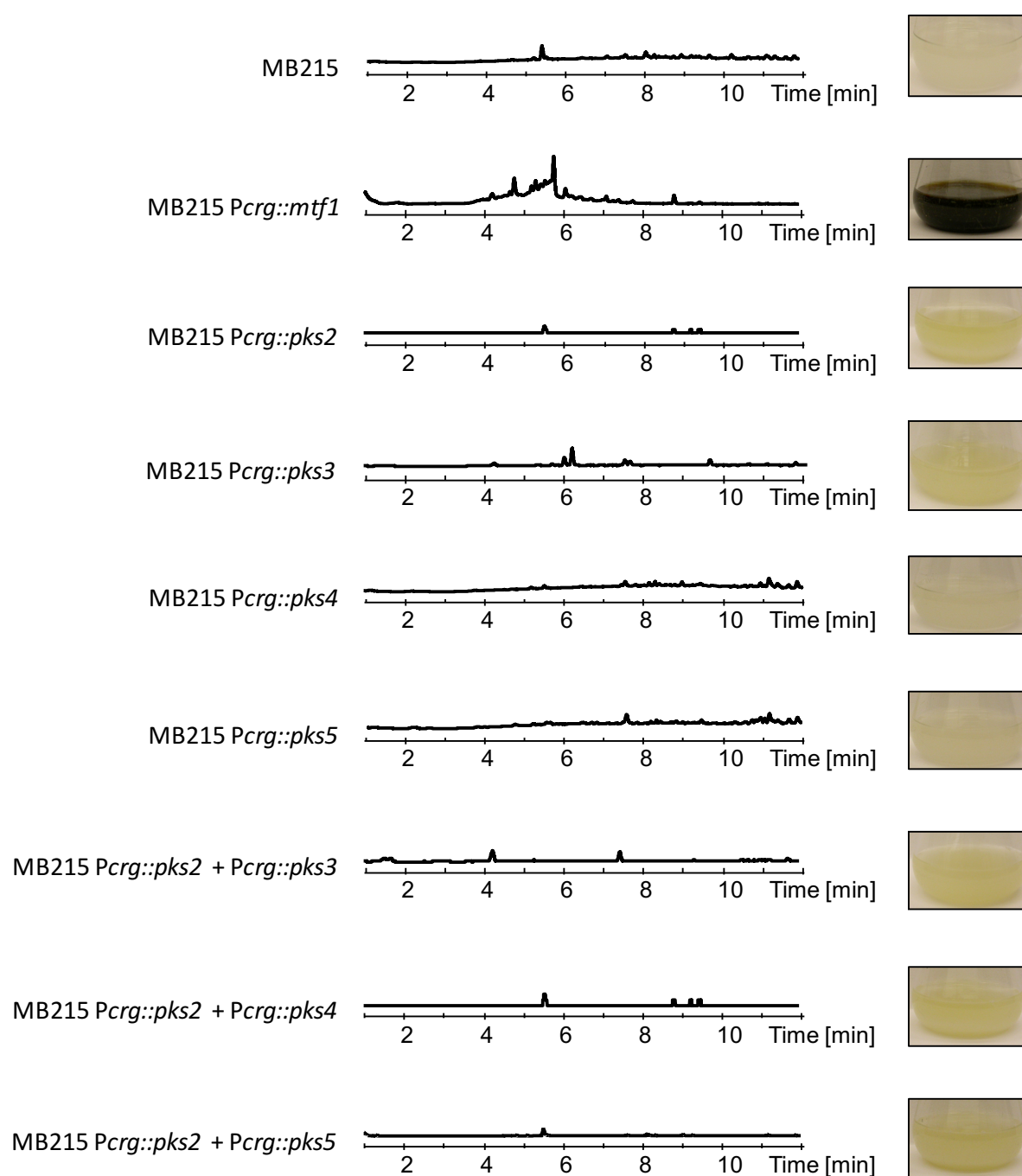


Figure 39. HPLC profiles of the extracts from the double overexpressing strains MB215 *Pcrg::pks2+Pcrg::pks3*, MB215 *Pcrg::pks2+Pcrg::pks4* and MB215 *Pcrg::pks2+Pcrg::pks5* as detected by UV absorption at 272 nm. Photographs of cultures were taken after 96 h of growth at 28 °C in YNB medium with 5% arabinose and 0.1% ammonium sulfate (right side).

Consequently, we considered the possibility that *pks1* and/or *pks2* could rescue the colorless phenotype observed in MB215 $\Delta pks3$ *Pcrg::mtf1*, MB215 $\Delta\Delta pks4$ *Pcrg::mtf1* and MB215 $\Delta pks5$ *Pcrg::mtf1* mutant strains. Six different strains were generated and analyzed in their phenotypes and metabolic profiles (Figure 40). Strains included as controls were: MB215 *Pcrg::mtf1*, MB215 *Pcrg::pks1*, MB215 *Pcrg::pks2*, MB215 $\Delta pks3$ *Pcrg::mtf1*, MB215 $\Delta\Delta pks4$ *Pcrg::mtf1*, and MB215 $\Delta pks5$ *Pcrg::mtf1*.

Interestingly, overexpression of *pks1* rescued the phenotype of the MB215 $\Delta pks3$ *Pcrg::mtf1* strain, which suggests that Pks1 can somehow replace the function of Pks3 since both polyketide synthases harbor the KS and PP domains. In this situation, acyl transferase (AT) and dehydratase (PS-DH) functions are apparently provided by Pks4 (Figure 40). Whether the PS-DH domain is needed or not in Pks3 for the biosynthesis of OA and melanin, has not been investigated yet. Nonetheless, the AT domain represents a critical requirement for any polyketide synthase. By contrast, overexpression of *pks1* in MB215 $\Delta\Delta pks4$ *Pcrg::mtf1* and MB215 $\Delta pks5$ *Pcrg::mtf1* strains had no effect in their phenotypes. None of the expressed PKSs in the strain MB215 $\Delta\Delta pks4$ *Pcrg::mtf1*+*Pcrg::pks1* (Pks1, Pks3 and Pks5) possesses an AT domain, which would match with the no complementation effect. In the same way, due to differences in domain structure between Pks1 and Pks5, MB215 $\Delta pks5$ *Pcrg::mtf1*+*Pcrg::pks1* could not synthesize any T4HN derivatives.

Moreover, overexpression of *pks2* did not rescue the phenotype of the MB215 $\Delta pks3$ *Pcrg::mtf1*, MB215 $\Delta\Delta pks4$ *Pcrg::mtf1* and MB215 $\Delta pks5$ *Pcrg::mtf1* strains. In all cases, their phenotypes mimicked those produced by their single deletion mutants. The missing complementation of the MB215 $\Delta pks3$ *Pcrg::mtf1* strain by overexpression of *pks2* could be explained by the lack of the PP domains in Pks2. The existence of one PP domain in Pks5 appears not to be enough to allow biosynthetic intermediates to be channeled to cognate partner proteins for condensation and further biochemical elaboration. On the other hand, AT-Pks2 domain seemed not enough for replacing AT-Pks4 domain in the MB215 $\Delta\Delta pks4$ *Pcrg::mtf1*+*Pcrg::pks1* strain. Finally, differences in domain structure among Pks2 and Pks5 could not produce melanization in MB215 $\Delta pks5$ *Pcrg::mtf1*+*Pcrg::pks2* cultures. Putting all these data together, Pks1 is capable to participate in the synthesis of the melanin-like pigment in combination with at least two coexpressed PKS genes, *pks4* and *pks5*. Conversely, Pks2 could not complement the albino phenotypes given by the deletion mutants of *pks3*, *pks4* and *pks5* genes, suggesting that Pks2 domains are not enough for replacing their functions.


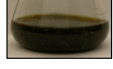
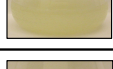
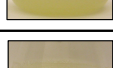
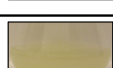
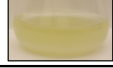
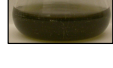





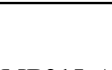
Strain	Active domains	Phenotype
MB215		
MB215 <i>Pcrg::mtf1</i>	PKS3: KS, KS, PS-DH, PP, PP, TE PKS4: SAT, AT, PS-DH PKS5: AMP, PP, NAD	
MB215 $\Delta pks3$ <i>Pcrg::mtf1</i>	PKS4: SAT, AT, PS-DH PKS5: AMP, PP, NAD	
MB215 $\Delta\Delta pks4$ <i>Pcrg::mtf1</i>	PKS3: KS, KS, PS-DH, PP, PP, TE PKS5: AMP, PP, NAD	
MB215 $\Delta pks5$ <i>Pcrg::mtf1</i>	PKS3: KS, KS, PS-DH, PP, PP, TE PKS4: SAT, AT, PS-DH	
MB215 <i>Pcrg::pks1</i>	PKS1: SAT, KS, KS, PP, PP, TE	
MB215 <i>Pcrg::pks2</i>	PKS2: KS, KS, AT, PS-DH, TE	
MB215 $\Delta pks3$ <i>Pcrg::mtf1+Pcrg::pks1</i>	PKS1: SAT, KS, KS, PP, PP, TE PKS4: SAT, AT, PS-DH PKS5: AMP, PP, NAD	
MB215 $\Delta pks3$ <i>Pcrg::mtf1+Pcrg::pks2</i>	PKS2: KS, KS, AT, PS-DH, TE PKS4: SAT, AT, PS-DH PKS5: AMP, PP, NAD	
MB215 $\Delta\Delta pks4$ <i>Pcrg::mtf1+Pcrg::pks1</i>	PKS1: SAT, KS, KS, PP, PP, TE PKS3: KS, KS, PS-DH, PP, PP, TE PKS5: AMP, PP, NAD	
MB215 $\Delta\Delta pks4$ <i>Pcrg::mtf1+Pcrg::pks2</i>	PKS2: KS, KS, AT, PS-DH, TE PKS3: KS, KS, PS-DH, PP, PP, TE PKS5: AMP, PP, NAD	
MB215 $\Delta pks5$ <i>Pcrg::mtf1+Pcrg::pks1</i>	PKS1: SAT, KS, KS, PP, PP, TE PKS3: KS, KS, PS-DH, PP, PP, TE PKS4: SAT, AT, PS-DH	
MB215 $\Delta pks5$ <i>Pcrg::mtf1+Pcrg::pks2</i>	PKS2: KS, KS, AT, PS-DH, TE PKS3: KS, KS, PS-DH, PP, PP, TE PKS4: SAT, AT, PS-DH	

Figure 40. Phenotype of complementation strains MB215 $\Delta pks3$ *Pcrg::mtf1+Pcrg::pks1*, MB215 $\Delta pks3$ *Pcrg::mtf1+Pcrg::pks2*, MB215 $\Delta\Delta pks4$ *Pcrg::mtf1+Pcrg::pks1*, MB215 $\Delta\Delta pks4$ *Pcrg::mtf1+Pcrg::pks2*, MB215 $\Delta pks5$ *Pcrg::mtf1+Pcrg::pks1* and MB215 $\Delta pks5$ *Pcrg::mtf1+Pcrg::pks2*. Protein enzymatic domains are as follows: AT, acyl transferase; AMP, adenylation; KS, β -ketoacyl synthase; NAD, nicotinamide adenine dinucleotide binding; PP, phosphopantetheine attachment site; PS-DH, polyketide synthase dehydratase; SAT, starter unit and TE, thioesterase.

2.6 Orsellinic acid feeding experiment

Orsellinic acid (OA) is a compound produced by prolonged induction of the strains MB215 $\Delta cyp4$ *Pcrg::mtf1*, MB215 $\Delta pks5$ *Pcrg::mtf1* and MB215 *Pcrg::pks3+Pcrg::pks4*. In any case, this molecule seems to be an important intermediate at early stages in the metabolic pathway activated by the melanin-like cluster. Therefore, we examined the impact of the addition of OA to those strains whose gene deletions displayed a different phenotype than the parental strain (MB215 *Pcrg::mtf1*) as MB215 $\Delta pks3$ *Pcrg::mtf1*, MB215 $\Delta\Delta pks4$ *Pcrg::mtf1*, MB215 $\Delta pks5$ *Pcrg::mtf1*, MB215 $\Delta cyp4$ *Pcrg::mtf1* and MB215 $\Delta vbs1$ *Pcrg::mtf1*. Figure 41 (A-D) provides experimental data obtained from the OA feeding experiment performed in those strains under repressing (5 % glucose) and inducing (5 % arabinose) conditions in the presence or absence of 0.5 mM OA. Cell pellets were analyzed by HPLC (272 nm) after 96 h of induction. Phenotypes of the strains are shown for each condition (Figure 41A-D). MB215 and MB215 *Pcrg::mtf1* strains were used as negative and positive controls, respectively. Under repressing conditions, with or without OA, all the phenotypes observed resembled the MB215 and MB215 *Pcrg::mtf1* strains (Figure 41A-B). Regarding the metabolic profiles, no differences were found between the chromatograms of the deletion mutants and the wild type strains in the absence of OA (Figure 41A).

Under the same conditions, but with the addition of OA, a peak with a retention time of 4.5 min (representing the synthetic compound) emerged in all the strains in this category (Figure 41B). On the left bottom side, the phenotypes and profiles given by the deletion strains grown in inducing medium without the addition of OA are indicated (Figure 41C). Data collected by these cultures served as benchmark to determine the effect of the addition of OA to the strains under the same conditions. It can be seen in Figure 41D that the incorporation of OA to the cultures resulted in the chemical complementation of two deletion mutant strains, MB215 $\Delta pks3$ *Pcrg::mtf1* and MB215 $\Delta\Delta pks4$ *Pcrg::mtf1*. Moreover, those strains that did not show complementation (MB215 $\Delta\Delta pks5$ *Pcrg::mtf1*, MB215 $\Delta cyp4$ *Pcrg::mtf1* and MB215 $\Delta vbs1$ *Pcrg::mtf1*) had a much weaker phenotype compared to the cultures in Figure 41C, which could be especially noticed in the MB215 $\Delta vbs1$ *Pcrg::mtf1* where its vivid yellowish color seemed to be diluted with the addition of OA (Figure 41D). Interestingly, the phenotype of MB215 $\Delta\Delta pks4$ *Pcrg::mtf1* was stronger than the one displayed by MB215 $\Delta pks3$ *Pcrg::mtf1* strain. Even though the induction in both cultures started from an $OD_{600}=0.6$, differences in growth rate could have influenced the cell density reached after 96 h (Figure 42).

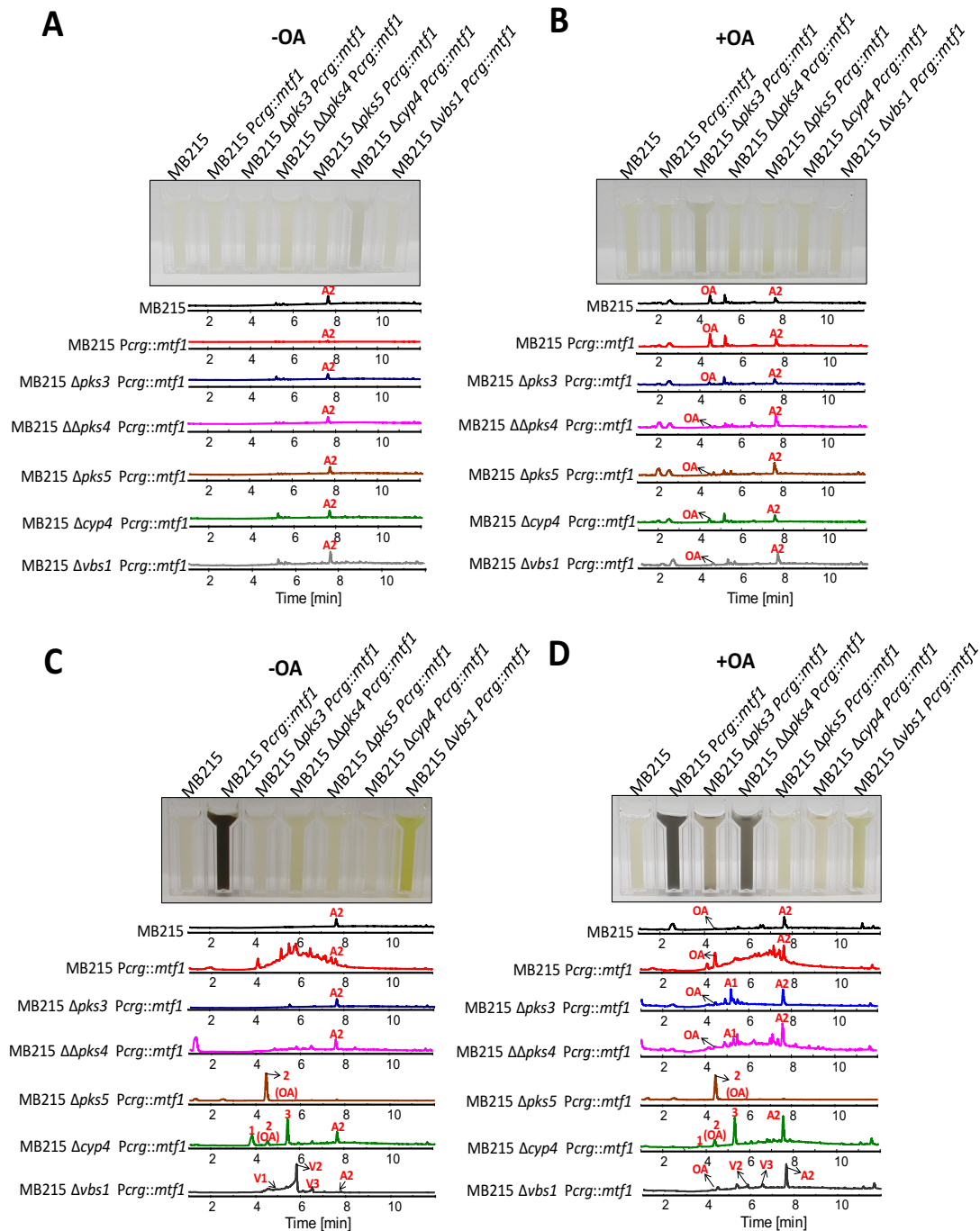


Figure 41. Orsellinic acid feeding experiment in YNB liquid medium. Metabolic profiles (272 nm) of the culture pellets from *U. maydis* MB215, MB215 *Pcrq::mtf1*, MB215 $\Delta pks3$ *Pcrq::mtf1*, MB215 $\Delta\Delta pks4$ *Pcrq::mtf1*, MB215 $\Delta pks5$ *Pcrq::mtf1*, MB215 $\Delta cyp4$ *Pcrq::mtf1* and MB215 $\Delta vbs1$ *Pcrq::mtf1* strains grown under the different conditions: **(A)** Repressing conditions, -OA; **(B)** Repressing conditions, +OA; **(C)** Inducing conditions, -OA and **(D)** Inducing conditions, +OA.

Comparison of their chromatograms with the MB215 *Pcrg::mtf1* strain presented some differences. First of all, the peaks previously observed in the reference strain with retention times between 4-8 min, now appear to lean to the right with retention times between 6-8 min. Furthermore, the chromatograms of MB215 $\Delta pks3$ *Pcrg::mtf1* and MB215 $\Delta\Delta pks4$ *Pcrg::mtf1* were more similar among them than to the MB215 *Pcrg::mtf1* strain (Figure 41D). In both cases it could be noticed the presence of 2 peaks that clearly stood out: A1 with a $m/z= 355.13$ ($[M+H]^+$), $t_R=5.2$ min, and A2 with $m/z= 256.87$ ($[M+H]^+$), $t_R=7.6$ min. Even though the A2 peak had been detected in the MB215 strain, under repressing or inducing conditions, now it seems to be produced in higher amount in all the strains in which OA was added, except for MB215 $\Delta pks5$ *Pcrg::mtf1* (Figure 41D). Remarkably, compounds produced by MB215 $\Delta cyp4$ *Pcrg::mtf1* (1) and MB215 $\Delta vbs1$ *Pcrg::mtf1* (V1, V2 and V3) appeared to be decreased.

Overall, these results support the idea that Pks3 and Pks4 participate at early stages in the melanin pathway, followed by Pks5, Cyp4 and Vbs1. The presence of OA in the MB215 $\Delta pks5$ *Pcrg::mtf1*, MB215 $\Delta cyp4$ *Pcrg::mtf1* and MB215 $\Delta vbs1$ *Pcrg::mtf1* did not restore their phenotype.

In order to get knowledge whether the presence of orsellinic acid influences the growth of the MB215 $\Delta pks3$ *Pcrg::mtf1*, MB215 $\Delta\Delta pks4$ *Pcrg::mtf1* and MB215 $\Delta pks5$ *Pcrg::mtf1* strains, a drop test assay was performed in the presence of 0.25 and 0.5 mM of OA. All the strains were grown to an $OD_{600}=1$ and spotted on YNB agar plate containing 0.1% of ammonium sulfate and 5% arabinose as a carbon source. Four dilution series were considered in this experiment (10^{-1} - 10^{-3}). Figure 42 depicts the assay after the incubation of the strains for 2 days at 28 °C. The inducing agar plate without OA served as control (left side). As it can be seen in the control plate, all strains were affected in their growth when compared with MB215. When they grew on the plate with 0.25 mM of OA those differences were more remarkable, MB215 *Pcrg::mtf1* and MB215 $\Delta pks3$ *Pcrg::mtf1* showed less cell density compared with MB215 $\Delta\Delta pks4$ *Pcrg::mtf1* and MB215 $\Delta pks5$ *Pcrg::mtf1*. Even in the dilution 10^{-3} , the strains MB215 *Pcrg::mtf1* and MB215 $\Delta pks3$ *Pcrg::mtf1* did not grow. Likewise, at the highest concentration of OA (0.5 mM), the growth of all mutant strains seemed to be affected. According to this data we can infer that OA is a compound that can be toxic for *U. maydis* in high concentrations. Those strains that were affected in cell growth like MB215 *Pcrg::mtf1* and MB215 $\Delta pks3$ *Pcrg::mtf1*, can even be more sensitive to it.

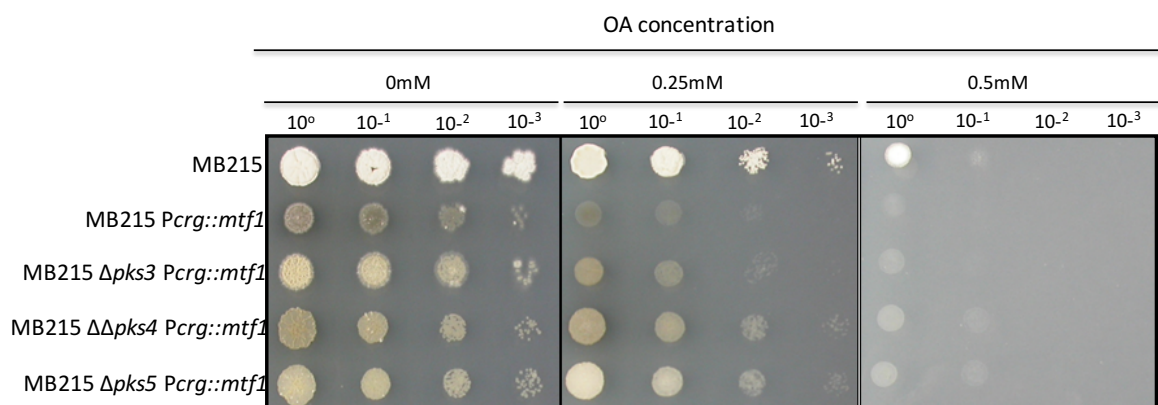


Figure 42. Orsellinic acid feeding experiment on YNB agar plate. The strains MB215, MB215 *PcrG::mtf1*, MB215 $\Delta pks3$ *PcrG::mtf1*, MB215 $\Delta\Delta pks4$ *PcrG::mtf1* and MB215 $\Delta pks5$ *PcrG::mtf1* were grown to an OD₆₀₀=1 and spotted on YNB agar plates supplemented with 0.1% of ammonium sulfate and 5% arabinose. After two days of incubation at 28 °C pictures of the plates were taken. Left side, control plate without OA; middle and right side, plates with 0.25 and 0.5 mM of OA, respectively.

2.7 Effect of tricyclazole on the melanin synthesis

Most fungal melanins are derived from the precursor molecule 1,8-dihydroxynaphthalene (DHN) and are known as DHN-melanins. DHN-melanin pathway has been found in fungi that utilize polyketide metabolites as intermediates as *Botrytis cinerea* (Schumacher, 2016), *Magnaporthe grisea* (Thompson *et al.*, 2000), *T. marneffei* (Sapmak *et al.*, 2015) and *A. fumigatus* (Sugareva *et al.*, 2006). In this pathway, a polyketide synthase catalyzes the formation of the first intermediate, 1,3,6,8-tetrahydroxynaphthalene (T4HN), which is then reduced to scytalone by a tetrahydroxynaphthalene reductase (T4HNR). Dehydration of scytalone by scytalone dehydratase (SD) leads to 1,3,8-trihydroxynaphthalene (T3HN) that is again reduced to vermelone by a trihydroxynaphthalene reductase (T3HNR). DHN is formed by further dehydration by SD, and polymerized to produce DHN-melanin (Figure 43A).

One effective way to study if a given microorganism synthesizes DHN-melanin is by the utilization of inhibitors as tricyclazole (5-methyl-1,2,4-triazolo-(3,4-*b*)-benzothiazole), which blocks the two reduction steps in this biosynthetic pathway (T4HN to scytalone, T3HN to vermelone) (Figure 43A and C). To examine if the black-greenish coloration produced after the induction of the melanin-like cluster is attributed to DHN-melanin, MB215 *PcrG::mtf1* strain was grown in inducing medium (I) supplemented with tricyclazole (50 mg/l in DMSO) (Figure 43B).

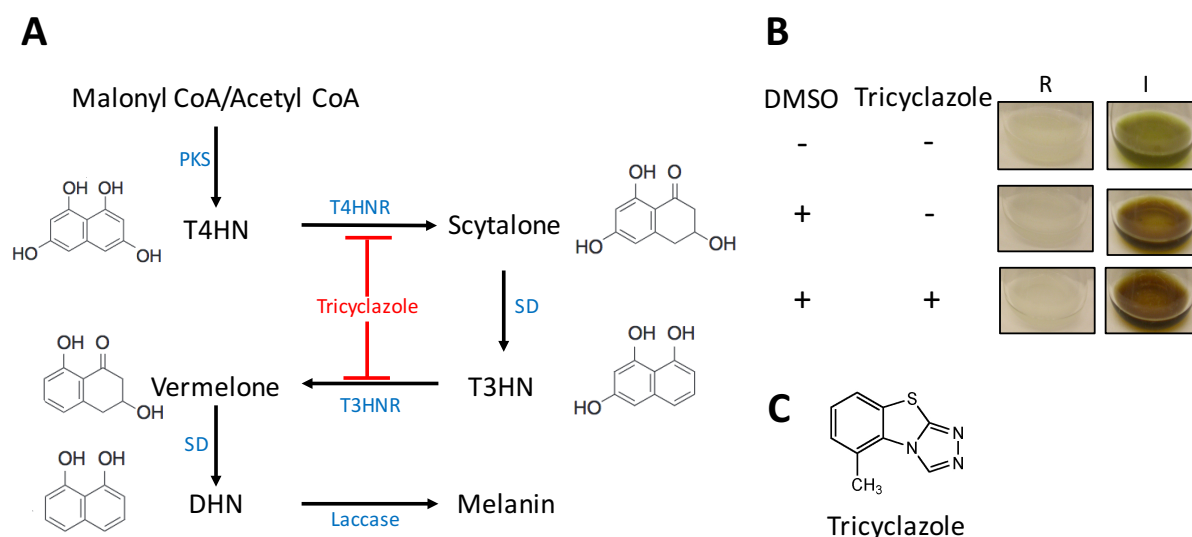


Figure 43. Effect of tricyclazole on the melanin biosynthesis pathway in *U. maydis*. (A) DHN-melanin biosynthesis pathway in fungi. Tricyclazole inhibits the two reduction steps in the DHN-melanin pathway, conversion of T4HN to scytalone and T3HN to vermelone. PKS, polyketide synthase; T4HNR, tetrahydroxynaphthalene reductase; SD, scytalone dehydratase and T3HNR, trihydroxynaphthalene reductase. (B) Effect of tricyclazole on the production of melanin. The strain MB215 *Pcrg::mtf1* was grown under repressing (R) and inducing (I) conditions in the presence and absence of tricyclazole (50 mg/l in DMSO) for 96 h at 28 °C. Addition of tricyclazole did not abolish the production of melanin, indicating an alternative melanin biosynthetic pathway in *U. maydis*. (C) Molecular structure of tricyclazole.

If *U. maydis* synthesizes DHN-melanin, we would expect a reduction in pigmentation due to the inhibition of 2 biosynthetic steps catalyzed by T4HNR and T3HNR. However, no differences in pigmentation were observed in MB215 *Pcrg::mtf1* cultures grown in the presence or absence of tricyclazole, thus indicating that *U. maydis* uses an alternative melanin biosynthesis pathway. A closer inspection to *U. maydis* genome revealed that this pathogenic fungus does not possess T4HNR, T3HNR or scytalone reductase enzymes, which supports the idea that other enzymes are involved in the biosynthesis of this type of melanin.

2.8 Pathogenicity assays

In order to study the role of the melanin-like cluster genes on virulence in maize plants, single deletion mutants in the solopathogenic SG200 background strain were generated. Genes considered to be deleted were those which were activated by the transcription factor Mtf1. Since Mtf1 showed to be responsible for the regulation of at least 12 of these genes, its deletion mutant was also included in this study. In all cases, disease symptoms were scored 13 days after infection according to severity (Kämper *et al.*, 2006) (see methods). Figure 44 provides the evaluation of the plant infection symptoms for the SG200 $\Delta mtf1$ and SG200 $\Delta mtf2$ strains.

Deletion of *mtf1* showed reduced symptoms compared to the solopathogenic strain, especially in the formation of tumors causing stem bending. On the other hand, the infection of SG200 Δ *mtf2* strain did not display any impact in virulence, since severity of the disease symptoms was comparable with SG200. These results gave us a hint that the melanin-like cluster could be somehow implicated in pathogenicity (Figure 44).

To explore in more detail the contribution of each cluster gene during this process, plant infection analysis were made with the single knockout strains (Figure 45). Due to their key role in the biosynthesis of the melanin-like pigment, the first strains that were tested were the deletion mutants SG200 Δ *pks3*, SG200 Δ *pks4* and SG200 Δ *pks5*.

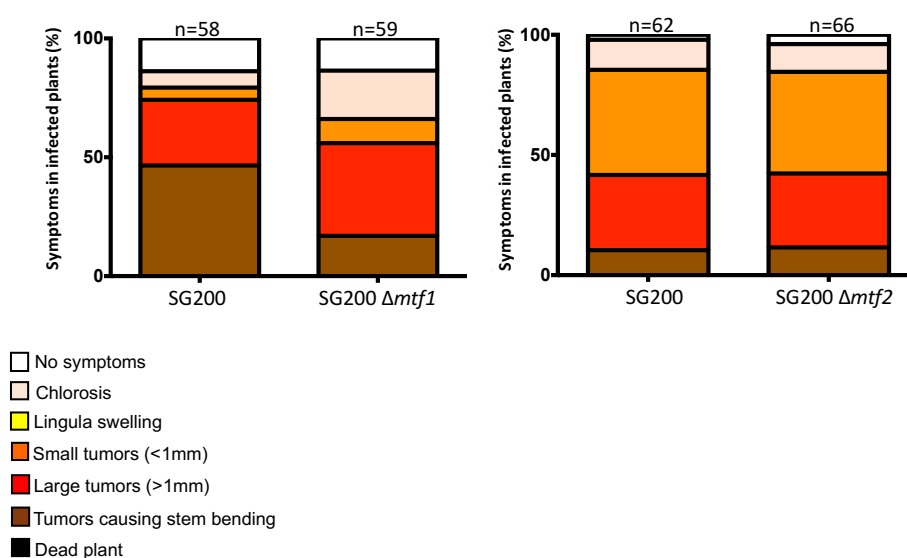


Figure 44. Virulence of the *mtf1* and *mtf2* mutant strains. Maize seedlings were inoculated with the solopathogenic strain SG200 and derivative mutant strains: SG200 Δ *mtf1* and SG200 Δ *mtf2*. Symptoms were scored 13 days after infection (see methods for details). The color code for disease rating is given on the bottom left.

After 13 dpi none of the infected plants presented heavy tumors (tumors causing stem bending) (Figure 27). The most noticeable effect was observed in the SG200 Δ *pks4* strain, around 80% of the infected plants had tumors with sizes less than 2mm, close to 5% had tumors larger than 2mm, and the rest minor symptoms. Even though SG200 Δ *pks3* and SG200 Δ *pks5* exhibited similar phenotype, SG200 Δ *pks5* had higher percentage of plants without symptoms than SG200 Δ *pks3* (Figure 45). These observations are indicative for the importance of these genes during plant-pathogen interaction.

When deletion mutants of the genes encoding for tailoring enzymes (SG200 Δ *aox1*, SG200 Δ *vbs1*, SG200 Δ *omt1*, SG200 Δ *pmo1*, SG200 Δ *cyp4* and SG200 Δ *deh1*) were analyzed, different results were obtained (Figure 45). From the 57 infected plants with SG200 Δ *cyp4* none of them presented heavy tumors or lingula swelling, instead of that, chlorosis was the most

frequent symptom. Concerning to SG200 $\Delta vbs1$ and SG200 $\Delta aox1$, a reduction in large and heavy tumors was observed in both cases. In contrast, SG200 $\Delta omt1$ mutant strain did not show any significant difference compared to the wildtype.

For the SG200 $\Delta pmol$, the symptoms were slightly reduced, the plants had tumors of all sizes with a major proportion of tumors causing stem bending. Deletion of *deh1* also displayed an overall reduction in disease symptoms (Figure 45). An observed trend, though not borne out by statistical analysis, was reduced symptoms in the strains SG200 $\Delta orf1$, SG200 $\Delta orf3$, SG200 $\Delta orf4$ and SG200 $\Delta orf5$. Particularly, a decrease in large and heavy tumors in SG200 $\Delta orf3$, SG200 $\Delta orf4$ and SG200 $\Delta orf5$. Putting together all these data, the single deletion of the melanin-like cluster genes had an effect in virulence of maize plants, which reflects an implication of these genes during the infection process. Further studies need to be done in order to determine at which specific stage of infection those genes are required.

Moreover, deletion of *mtf1* seemed to have a less dramatic effect than other strains as SG200 $\Delta pks4$ or SG200 $\Delta pks5$, just to mention some examples, which could suggest the presence of a second transcription factor that could have regulatory effects on the melanin-like cluster genes.

Since maize seedlings inoculated with the single deletion mutants SG200 $\Delta pks3$ and SG200 $\Delta cyp4$ showed a small reduction in symptoms, we asked ourselves whether the double deletion of *pks3* and *cyp4* could have a more significant effect compared with those strains. As it is depicted in Figure 46, the strain SG200 $\Delta pks3\Delta cyp4$ displayed similar phenotype compared to SG200 $\Delta pks3$ and SG200 $\Delta cyp4$ strains, thus indicating that the double deletion of *pks3* and *cyp4* had no major effect in virulence as the one observed in their single deletion mutants.

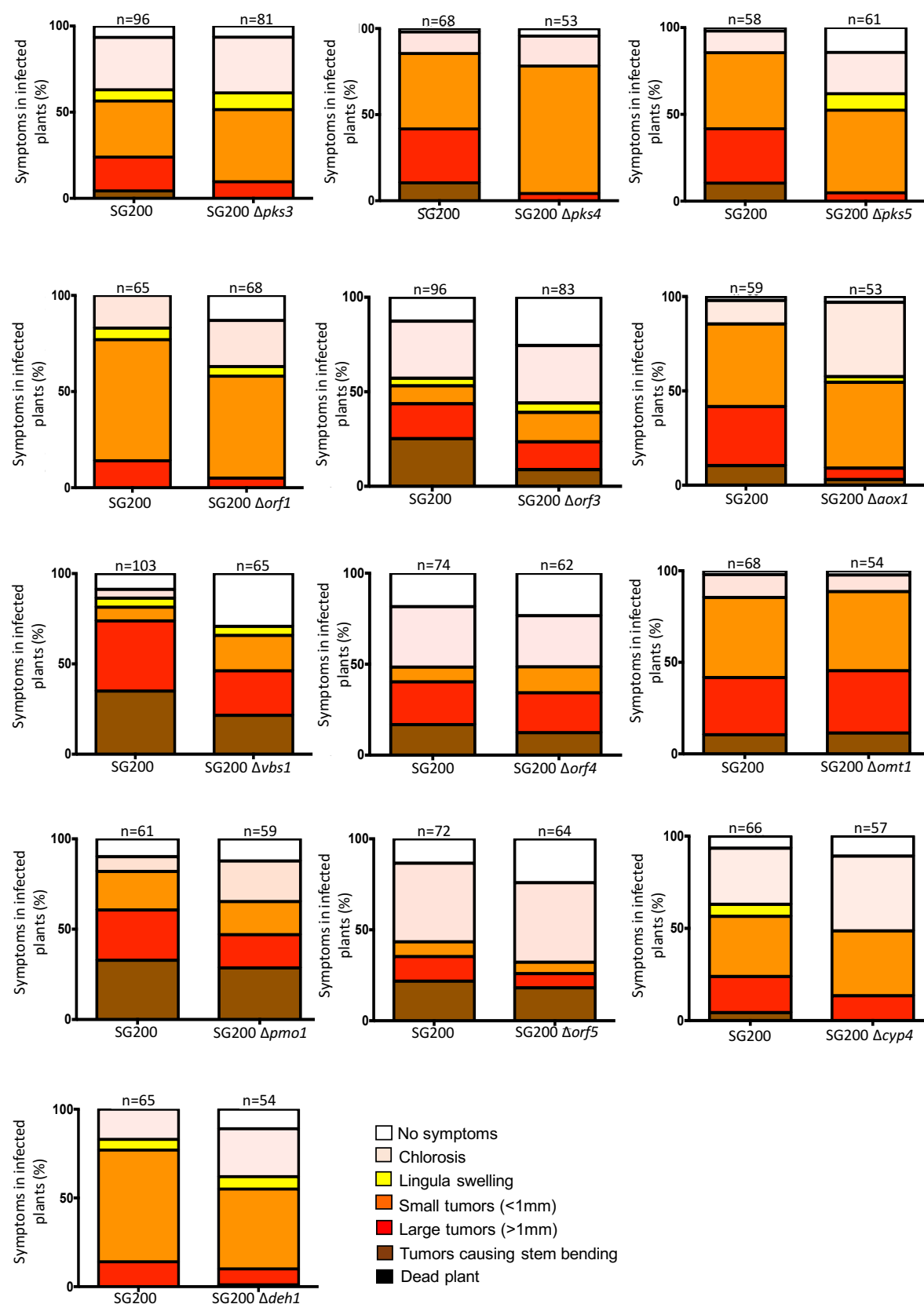


Figure 45. Virulence of the melanin-like single deletion mutants. Maize seedlings were inoculated with the solopathogenic strain SG200 and derivative mutant strains. Symptoms were scored 13 days after infection (see methods for details). The color code for disease rating is given on the bottom.

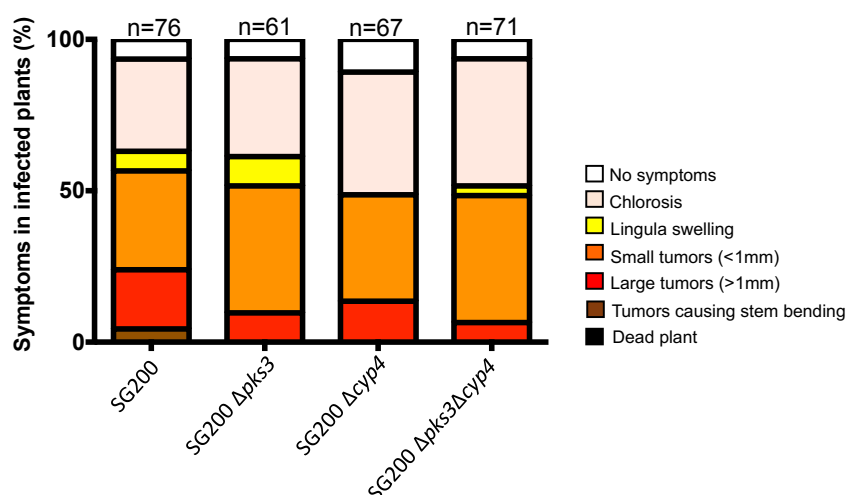


Figure 46. Virulence of the SG200 $\Delta pks3\Delta cyp4$ strain. Maize seedlings were inoculated with the solopathogenic strain SG200 and derivative mutant strains. Symptoms were scored 13 days after infection (see methods for details). The color code for disease rating is given on the right side of the graph.

2.9 H₂O₂ sensitivity assay in *U. maydis*

To determine the role of *pks3*, *pks4* and *pks5* under oxidative stress conditions, deletion mutant strains SG200 $\Delta pks3$, SG200 $\Delta pks4$ and SG200 $\Delta pks5$ were exposed to H₂O₂ on agar plate. Since H₂O₂ is an oxidative agent, prolonged exposure may result in cell death, therefore when cells grow in the presence of H₂O₂ in agar diffusion test, a growth inhibition halo is observed. Strains were grown in YEPS_{light} medium to an OD₆₀₀ = 0.6 and spread onto a PD plate. Filter disks were soaked with 2 μ L H₂O₂ (30% [v/v]) and placed on the plates. After 48 h at 28 °C of incubation, the diameter of the halos were measured and compared to the wildtype (SG200). The larger the diameter was, the more sensitive the strain was considered (Figure 47). The halo size in all cases oscillated between 0.5 to 1 cm.

Among the deletion mutants, SG200 $\Delta pks4$ strain showed to be the most sensitive one. This effect can also be clearly seen in the photographs located above each graph. What is interesting in this data is that SG200 $\Delta pks4$ had stronger phenotype over SG200 $\Delta pks3$ and SG200 $\Delta pks5$, same scenario observed during plant infection (Figure 47). This would mean that the melanin-like cluster genes could be activated under different stress conditions.

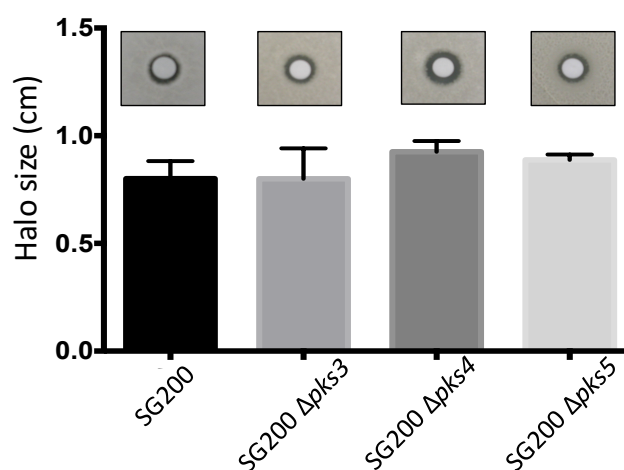


Figure 47. Sensitivity of *U. maydis* wild-type (SG200) and *pks3*, *pks4* and *pks5* mutant strains to oxidative stress. Sensitivity of strains to H_2O_2 was assessed in an agar diffusion test in which a filter soaked with H_2O_2 (30% v/v) was placed on a PD agar plate seeded with the strains indicated on bottom. Halo size was quantified for the SG200 and SG200 $\Delta pks3$, SG200 $\Delta pks4$ and SG200 $\Delta pks5$ strains. Error bars indicate standard deviations derived from three independent experiments consisting of three replicas each.

3 Discussion

3.1 Identification of a coregulated polyketide synthase gene cluster in *U. maydis*

The search of characteristic genes involved in secondary metabolism in *U. maydis* genome, in combination with the analysis of their gene expression data under different conditions, led to the identification of a putative SM gene cluster named in this work as cluster "A". Cluster "A" consists of 16 ORFs including genes encoding for 3 polyketide synthases (*pks3*, *pks4*, and *pks5*), 2 transcription factors (*mtf1* and *mtf2*), 6 tailoring enzymes (*aox1*, *vbs1*, *omt1*, *pmo1*, *cyp4*, and *deh1*) and 5 uncharacterized proteins (*orf1*, *orf2*, *orf3*, *orf4*, and *orf5*) (Figure 24A).

Unlike clusters "B" or "D", cluster "A" is located at the telomeric region on chromosome 12, a feature often found in fungal SM clusters (Bok *et al.*, 2009). Another factor that influenced the selection of cluster "A" was the presence of the two transcription factors, Mtf1 and Mtf2, considered as an important advantage for the manipulation of the cluster genes, since forced expression of transcription factors has constituted an efficient way to uncover secondary metabolites in other fungi; e.g., sterigmatocystin (Fernandes *et al.*, 1998), and aspyridones A and B (Bergmann *et al.*, 2007). Even though, cluster "C" was found at the telomeric region on chromosome 19, it was not contemplated as a promising candidate due to the lack of expression data (Figure 22). As a part of the strategy to identify potential SM gene clusters in *U. maydis*, we also compared the clusters A-D with those detected by the algorithms SMURF and antiSMASH (Table 3). Although most of the clusters ("A", "C" and "D") were detected by these bioinformatic programs, their general trend was either to overpredict the cluster boundaries or to divide a single gene cluster into two different clusters located next to each other (Table 3). For this reason, we considered that the boundaries of clusters A-D should be defined by the manual annotation strategy.

On the other hand, the analysis of the normalized gene expression data extracted from GEO (Gene Expression Omnibus), allowed the identification of groups of 3 to 13 coregulated neighboring genes in *U. maydis* (cluster 1GE - cluster 40GE), whose majority were found to be uncharacterized proteins upregulated during plant infection (Figure S1). Besides the identification of the MEL (21GE) and ferrichrome (6GE) gene clusters, no additional groups of genes involved in secondary metabolism were observed. However, the compendium of

expression data facilitated us the analysis of expression profiles of the genes belonging to the clusters A-D (Figure 22), which supported our decision of selecting the cluster "A" as a matter of this study.

On the other hand, the expression data table constructed in this work can also be used as a valuable tool for the study of genes that are not necessarily located on the same chromosome but participate in related metabolic pathways or cellular processes (e.g., fatty acid biosynthesis) (Figure 21B).

Once the cluster "A" was selected, we decided to analyze the expression of each gene upon the activation of the transcription factor *mtf1* or *mtf2*. Northern blot analysis showed that 12 genes within the cluster "A" (*pks5*, *pks4*, *pks3*, *aox1*, *vbs1*, *omt1*, *pmo1*, *cyp4*, *deh1*, *orf1* and *orf4*) were simultaneously upregulated after the induced expression of *mtf1*. Conversely, overexpression of *mtf2* only upregulated *orf2* (Figure 24B), suggesting that *mtf1* is responsible for the regulation of most of the cluster "A" genes, which are not transcribed when *U. maydis* is grown under standard laboratory conditions. The regulation of cluster "A" can be explained by the three SANT domains of Mtf1 (Figure 23), which are well known for participating in histone acetylation, a process that enhances transcription (Boyer *et al.*, 2002). Increasing the level of histone acetylation at SM clusters was also found to be the molecular basis of how bacterial-fungal cocultivation activates the orsellinic acid gene cluster (ORS) in *A. nidulans* (Schroeckh *et al.*, 2009). Similar case was observed for the White Collar 1 (WC-1) photoreceptor in *N. crassa*, where the histone H3 K14 acetylation by NGF-1 (an homologue of the yeast histone acetyltransferase Gcn5p) was reported as a determinant for the blue light-induced transcription (Grimaldi *et al.*, 2006).

On the other hand, the presence of a second transcription factor (Mtf2) within the cluster "A", seemed not to have an influence in the regulation of the majority of its genes. Markedly, Mtf2 belongs to the family of transcription factors $\text{Zn(II)}_2\text{Cys}_6$, which are considered the most common family of cluster regulators for fungal SM; e.g., CtnA controlling the citrinin cluster in *M. purpureus* (Shimizu *et al.*, 2007), and Zfr1 for fumonisin biosynthesis in *F. verticillioides* (Flaherty and Woloshuk, 2004). In many of these cases, overexpression of $\text{Zn(II)}_2\text{Cys}_6$ proteins can be sufficient to activate silent SM clusters, which could be an indication that *mtf2* is involved in controlling the expression of other SM genes outside the cluster "A" in *U. maydis*. When, where or how this is conducted, remains as an open question.

3.2 Identification of an alternative melanization pathway in *U. maydis*

Induced expression of *mtf1* but not *mtf2* resulted in the accumulation of a dark-greenish pigment (Figure 24C). LC-MS analysis of the cell pellets of the MB215 *Pcrg::mtf1* strain, grown under inducing conditions for a 4-day period, revealed the presence of many complex compounds derived from the 1,3,6,8-tetrahydroxynaphthalene (T4HN) (Figure 26). Unfortunately, it was not possible to elucidate the molecular structure of the T4HN derivatives produced in the MB215 *Pcrg::mtf1* strain, since the pigment was unstable and rapidly underwent polymerization. T4HN is an intermediate in the 1,8-dihydroxynaphthalene-(DHN) melanin biosynthesis pathway in fungi. DHN melanin represents the most common type of fungal melanins, followed by the L-3,4-dihydroxyphenylalanine (L-DOPA) melanin, whose pathway resembles mammalian melanin biosynthesis (Eisenman and Casadevall, 2012). In the DHN pathway, a PKS catalyzes the formation of T4HN from acetyl-CoA or malonyl-CoA precursors. Subsequently, T4HN is reduced to scytalone by a THN reductase (T4HNR), which is then dehydrated by a scytalone dehydratase (SD) to 1,3,8-trihydroxynaphthalene (1,3,8-T3HN). Finally, T3HN is reduced to vermelone by another THN reductase (T3HN), converted to DHN by SD, and polymerized into melanin by a laccase (Wheeler, 1983). Although genes required for the biosynthesis of this type of melanin are highly conserved in fungi, they are missing in the genome of *U. maydis* and other smut fungi as *U. hordei*, *Sporisorium scitamineum* and *S. reilianum*.

The notion of the presence of another type of melanin in *U. maydis* was strengthened by the treatment of the strain MB215 *Pcrg::mtf1* with tricyclazole. The effect of the tricyclazole on the DHN melanin pathway has been well documented for fungi as *Pyricularia oryzae* and *Verticillium dahliae*. In both cases, tricyclazole inhibited the conversion of T4HN to scytalone, and T3HN to vermelone, thus losing their ability to synthesize melanin (Tokousbalides and Sisler, 1979; Wooloshuk *et al.*, 1980). On the contrary, addition of tricyclazole into induced MB215 *Pcrg::mtf1* cultures had no impact on melanin production when compared with the strain grown without treatment (Figure 43), an indication that *U. maydis* uses an alternative pathway for melanin synthesis. This is in line with a recent publication in *Aspergillus terreus*, where the group of Brock and collaborators reported a non-canonical melanin biosynthesis pathway involving an unusual NRPS-like enzyme (MelA) and a tyrosinase (TyrP) (Geib *et al.*, 2016). Interestingly, as in the case of *U. maydis*, *A. terreus* lacks the highly conserved enzymes required for DHN-melanin synthesis (Zaehle *et al.*, 2014; Gressler *et al.*, 2015).

On the other hand, the idea that *U. maydis* could synthesize L-DOPA melanin was ruled out since this pathway does not involve a polyketide synthase, instead, a laccase or tyrosinase

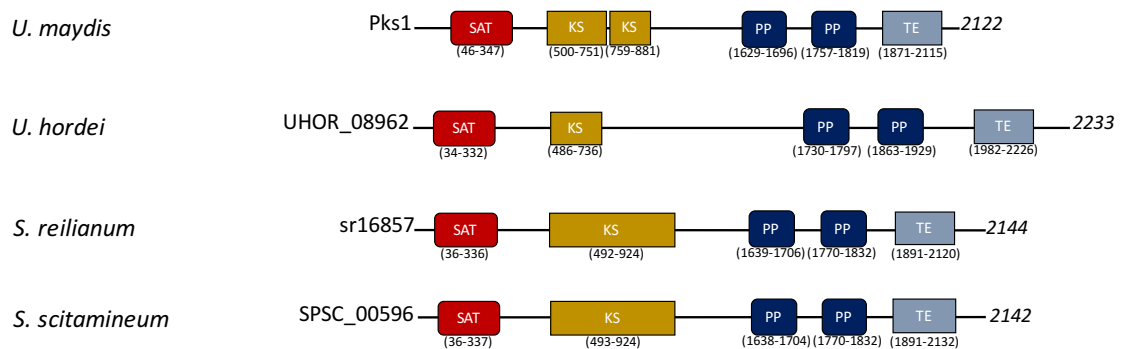
catalyzes the conversion of L-DOPA or tyrosine to dopaquinone, respectively. In addition, no genes encoding for tyrosinases could be identified in *U. maydis*. Markedly, by the time this study was carried out, a publication in *U. maydis* was released, concerning to melanogenic genes involved in teliospore formation. Islamovic and colleagues found two PKS genes (*pks1* and *pks2*), and a putative laccase (*lac1*) to be highly upregulated in a strain deleted for the transcription factor *ust1*, which led to filamentous haploid growth and production of pigmented teliospore-like structures in culture. Moreover, $\Delta pks1$ and $\Delta lac1$ mutants showed less pigmented teliospores in tumors, with a more dramatic effect in the deletion mutant of *pks1*. Even though the $\Delta pks2$ mutant was not tested in planta, they inferred by the transcriptome analysis of the $\Delta ust1$ strain, that *pks1*, *pks2*, and *lac1* participate in the DHN-melanin biosynthesis pathway in *U. maydis* (Islamovic *et al.*, 2016).

It is worth to emphasize that none of the polyketide synthase genes of the melanin-like cluster (*pks3*, *pks4* or *pks5*) were induced in the *ust1* deletion mutant. Likewise, no transcript was detected for the *pks1* or *pks2* genes when the MB215 *Pcrg::mtf1* strain was grown under inducing conditions (Figure 35). All these data suggest that *U. maydis* possesses two PKS gene clusters capable to synthesize melanin using alternative pathways.

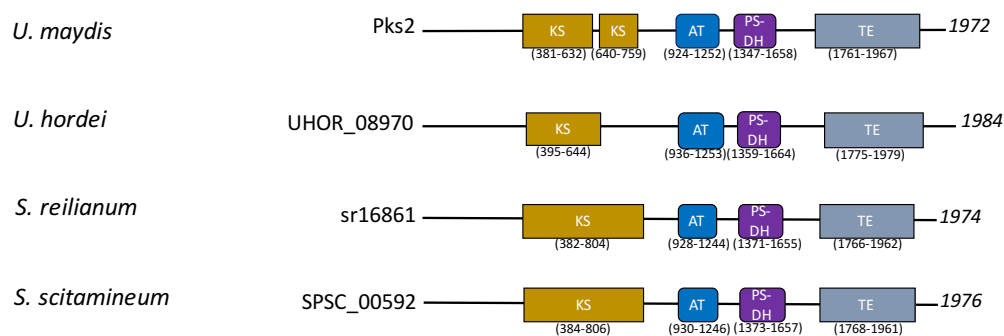
Comparative analysis of *U. maydis*, *U. hordei*, *S. scitamineum* and *S. reilianum* genomes revealed that *U. maydis* possesses 6 PKS genes, while the other smut fungi only 3 of them. Among the *U. maydis* PKSs, Pks1, Pks2 and Pks6 share high sequence similarity to those identified in *U. hordei*, *S. scitamineum* and *S. reilianum* (Figure 48). Interestingly, the counterparts of *U. maydis pks1* and *pks2* genes in *U. hordei* (UHOR_8962 and UHOR_08970), *S. scitamineum* (SPSC_00596 and SPSC_00592) and *S. reilianum* (sr16857 and sr16861) are located on the same chromosome, a similar feature observed for *pks1* and *pks2* in *U. maydis*. Although there are no reports of genes involved in melanization in these smut fungi, the presence of homologs of *U. maydis pks1* and *pks2* in their genomes suggests that they could play an important role in the melanin pathway. Interestingly, although the genes *pks6* (*U. maydis*), UHOR_06950 (*U. hordei*), sr15337 (*S. reilianum*) and SPSC_00985 (*S. scitamineum*) are annotated as polyketide synthases (Figure 48C), none of them contains the characteristic domains found in a PKS gene. Instead, they harbor a NAPRTase (nicotinate phosphoribosyltransferase) domain, which has been shown to be involved in the synthesis of NAD(H) (Heuser *et al.*, 2007). Thus indicating that the function of these genes may differ from the polyketide synthases.

To the best of our knowledge, this study constitutes the first report in which 3 PKS genes (*pks3*, *pks4* and *pks5*) are required for the biosynthesis of a melanin-like pigment. Biological implications of the melanin-like cluster are discussed in the paragraphs below.

A



B



C

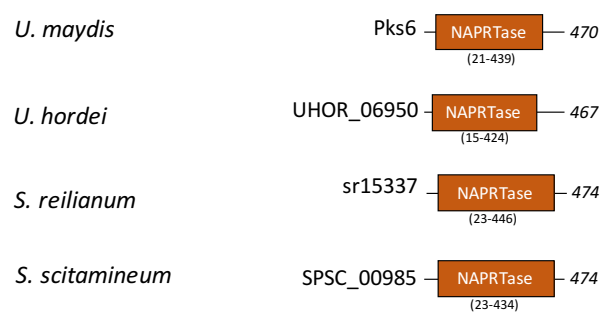


Figure 48. Domain organization of polyketide synthases in *U. maydis*, *U. hordei*, *S. reilianum* and *S. scitamineum*. Comparative analysis of the domain structures of (A) Pks1, (B) Pks2 and (C) Pks6 from *U. maydis* with their counterparts in *U. hordei*, *S. reilianum* and *S. scitamineum*. Protein enzymatic domains are as follows: AT, acyl transferase; AMP, adenylation; KS, β -ketoacyl synthase; NAD, nicotinamide adenine dinucleotide binding; PP, phosphopantetheine attachment site; PS-DH, polyketide synthase dehydratase; SAT, starter unit; TE, thioesterase and NAPRTase, nicotinate phosphoribosyltransferase. Domains were predicted by Protein Families (PFAM) and National Center for Biotechnology Information (NCBI) domain search. Numbers located on the right side of each PKS indicate their length in amino acids, and numbers below each domain represent their localization in the protein.

3.3 Inactivation of *pks3*, *pks4*, *pks5* and *cyp4* genes abolishes melanin pigment biosynthesis

Biochemical analysis by LC-MS revealed the presence of many compounds in the strain MB215 *Pcrg::mtf1*, most of them were derived from T4HN (Figure 26). To examine the role of the melanin-like cluster genes in the pigment production, we generated single deletion mutants that were analyzed for their phenotypes and metabolic profiles (Figure 28). Mutants defective for *pks3*, *pks4*, *pks5* or *cyp4* did not accumulate melanin, which is consistent with observations made for other fungi that synthesize melanin by the DHN pathway. Deletion of the polyketide synthase gene *alb1* in *Penicillium marneffe* was accompanied by the loss of melanin pigment production (Woo *et al.*, 2010). Similar case was reported for *Podospira anserina*, whose pigmentation during all stages of the life cycle was abolished due to inactivation of the *PaPKS1* gene (Coppin and Silar, 2007).

Besides the colorless phenotype displayed in the MB215 $\Delta pks3$ *Pcrg::mtf1* and MB215 $\Delta\Delta pks4$ *Pcrg::mtf1* strains, they were not able to produce any UV-detectable compound, while the chromatogram of the MB215 $\Delta pks5$ *Pcrg::mtf1* strain showed the presence of orsellinic acid (OA) (Figure 29). These results gave us the first indication that Pks3 and Pks4 act at early stages in the metabolic pathway, likely followed by Pks5. This assumption was further supported by the rescue of the melanization defect of the MB215 $\Delta pks3$ *Pcrg::mtf1* and MB215 $\Delta\Delta pks4$ *Pcrg::mtf1* mutants after being fed with orsellinic acid (Figure 41D).

Although the HPLC chromatograms (272nm) of the chemically complemented mutants (MB215 $\Delta pks3$ *Pcrg::mtf1*+OA and MB215 $\Delta\Delta pks4$ *Pcrg::mtf1*+OA) resulted in quite similar peaks among them, the pigmentation of the *pks4* deletion strain was more intense and closer to MB215 *Pcrg::mtf1* strain than what the MB215 $\Delta pks3$ *Pcrg::mtf1* mutant was (Figure 41D). One explanation can be given by the more pronounced growth defect of the MB215 $\Delta pks3$ *Pcrg::mtf1* strain in comparison to the MB215 $\Delta\Delta pks4$ *Pcrg::mtf1* strain (Figure 42). Somehow the addition of OA seems to have a more toxic effect in mutants lacking the *pks3* gene rather than the *pks4*. OA, as many other phenolic compounds produced in fungi, is considered as a potent antioxidant and free radical scavenger. Nevertheless, their accumulation can also have toxic effects for the organism that produces it (Barros-Lopes *et al.*, 2008). In line with these data, the induction of the double overexpressing strain MB215 *Pcrg::pks3*+*Pcrg::pks4* produced OA as well, thus indicating that Pks5 catalyzes the subsequent reaction to the one catalyzed by Pks3 and Pks4 (Figure 33). In the literature there are some examples of fungal PKSs that synthesize OA accompanied by other compounds, e.g., overexpression of the *PKS14*

gene from *F. graminearum* produced orsellinic acid and orcinol (Jørgensen *et al.*, 2014). In addition, the heterologous expression of the *terA* gene (a *pks* gene from *A. terreus*) in *A. niger* yielded a mixture of 4-hydroxy-6-methylpyranone, 6,7-dihydroxymellein and orsellinic acid (Zaehle *et al.*, 2014). However, we found no reports in bacteria or fungi, in which two PKSs would be involved in production of OA. A closer look to the domain structure of Pks3 and Pks4, showed that none of them has the minimal set of required domains for being a functional polyketide synthase, the β -ketoacyl synthase (KS), the acyltransferase (AT), and the acyl carrier protein (ACP) domain (Figure 49). Notably, Pks3 has a similar domain structure to other fungal OA-PKSs, except for the lack of the AT domain, which made us hypothesize that Pks3 does not work alone, and very likely, its mechanism of action is linked to Pks4 due to the presence of an AT domain within its structure. This hypothesis was further supported by the notion of many AT-less type PKSs able to generate SM by using ATs acting in *trans* to select the extender unit and load it onto the ACP domain (Cheng *et al.*, 2003).

Even though there are reports of AT-less type I PKSs especially from *Streptomyces*, *Xanthomonas*, *Bacillus*, *Myxococcus*, *Sorangium* and *Pseudomonas* genera (Cheng *et al.*, 2002, 2003; Huang *et al.*, 2001; Butcher *et al.*, 2007; Simunovic *et al.*, 2006; Menche *et al.*, 2008; Brendel *et al.*, 2007), the only AT-less type I PKS that has been confirmed experimentally is the LNM PKS from *Streptomyces atroolivaceus* S-140 (Figure 50). The LNM biosynthetic gene cluster consists of two PKS genes *lnmI* and *lnmJ*, that encode six PKS modules, none of which contain an AT-domain. Since a PKS module cannot be functional unless its ACP domain is loaded with the extender unit, they proposed that another protein in the cluster with an AT activity (LnmG) could act in *trans* to form a functional type I PKS. Biochemical characterization of LnmG *in vitro* showed that this protein was able to load malonyl-CoA to all six PKS modules in an efficient and specific manner (Cheng *et al.*, 2003), thus providing evidence that the functionality of an AT-less type I PKS can be achieved with the collaboration of another PKS with AT activity. Unlike canonical type I PKSs, the AT-less type I PKS generates polyketides with a high degree of structural diversity, which stems from their evolution by horizontal gene transfer (Lohman *et al.*, 2015).

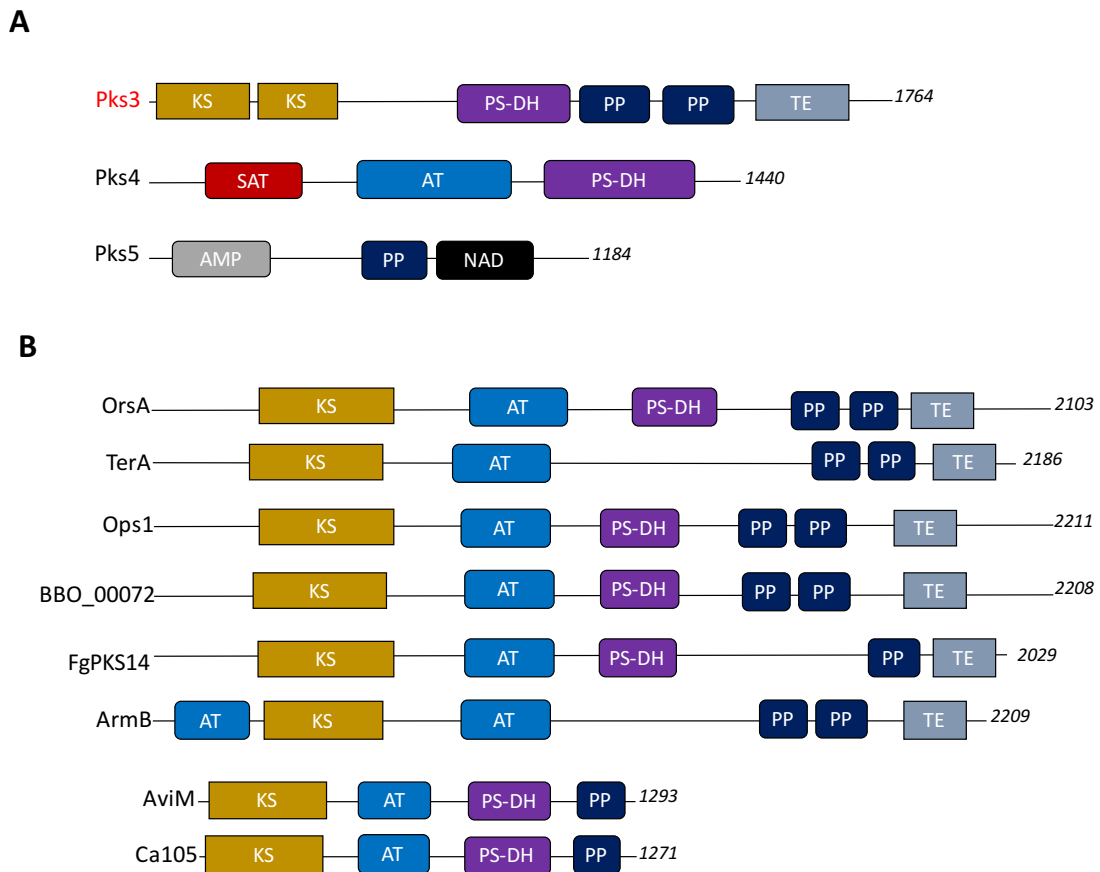


Figure 49. Domain organization of polyketide synthases (PKSs). (A) Domain structure of the PKS enzymes of the melanin-like cluster (Pks3, Pks4 and Pks5) in *U. maydis*. (B) Comparison of the domain structure of different PKSs experimentally verified in biosynthesis of orsellinic acid in different fungi and bacteria. OrsA (AN7909) is from the filamentous fungus *Aspergillus nidulans*; TerA (ATEG_00145) from *A. terreus*; Ops1 (BBA_08179) from *Beauveria bassiana*; BBO_0072, the Ops1 ortholog in *Beauveria brongniartii*; FgPKS14 (FGSG_03964) from *Fusarium graminearum*; ArmB (AFL91703) from the mushroom *Armillaria mellea*; AviM (AAK83194) and Ca105 (AAM70355) are from the bacteria *Streptomyces viridochromogenes* and *Micromonospora echinospora*, respectively. Protein enzymatic domains are as follows: AT, acyl transferase; AMP, adenylation; KS, β -ketoacyl synthase; NAD, nicotinamide adenine dinucleotide binding; PP, phosphopantetheine attachment site; PS-DH, polyketide synthase dehydratase; SAT, starter unit and TE, thioesterase. Domains were predicted by Protein Families (PFAM) and National Center for Biotechnology Information (NCBI) domain search. Numbers located on the right side of each PKS indicate their length in aminoacids. Modified from Feng *et al.*, 2015.

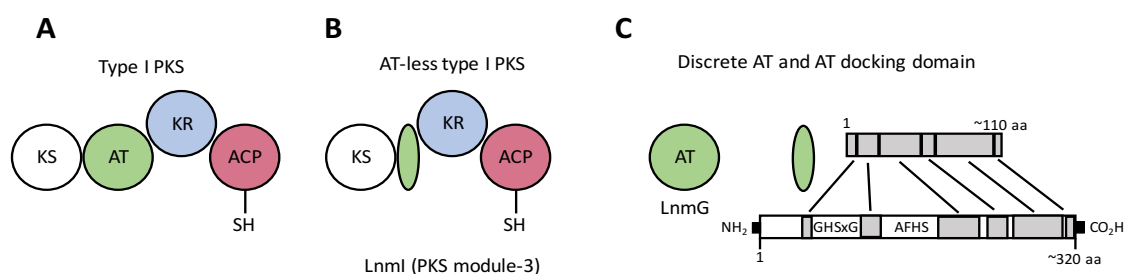


Figure 50. Modular organization of type I polyketide synthases (PKSs). (A) A prototypical type I PKS module contains the cognate AT domain and other domains. (B) An AT-less type I PKS module lacks the cognate AT domain but often contains a short segment of remnant AT residues. (C) The remnant AT segment lacks critical catalytic motifs (GHSxG and AFHS) and is therefore catalytically inactive, but may serve as a docking domain mediating the interactions between the discrete AT (LnmG) and AT-less PKS modules in Lnml and LnmJ. Modified from Tang *et al.*, 2004.

Although there is no information about AT-less type I PKSs in fungi, and even less with respect to such PKSs involved in OA or melanin biosynthesis, the work done by Cheng and coworkers inspired us to speculate that somehow Pks4 provides the missing AT activity *in trans* to Pks3. Gathering all these elements, we could think of some experiments that would help us to get a better understanding of the mechanism of Pks3 and Pks4: (i) the single and double overexpression of the *pks3* and *pks4* genes in an heterologous system as *Saccharomyces cerevisiae* or *Aspergillus niger* with the further LC-MS analysis of the cell pellets and, (ii) biochemical *in vitro* assay with the purified Pks3 and Pks4 proteins to test whether Pks4 can load the malonyl-CoA extender unit onto the Pks3 ACP domains, in a similar way as it was carried out for the LnmI and LnmJ PKSs with LnmG (Cheng *et al.*, 2003).

Our data has shown that *U. maydis* contains a SM cluster with 3 PKSs capable to synthesize orsellinic acid and a melanin-like pigment derived from T4HN, which made us think that this cluster synthesizes either two independent compounds (OA and T4HN) or only T4HN-melanin having OA as an intermediate. In our literature research, we found a report in which the heterologous expression of a polyketide synthase gene (*PKS1*) from *C. lagenarium* in *A. oryzae* produced T4HN and orsellinic acid (Fujii *et al.*, 1999). They considered that the production of OA could have resulted from loose control of the chain-length of the poly β -ketomethylene intermediate and its cyclization; even though the chain-length domain has only been found in bacterial type II PKSs. They also indicated that the aldol-type cyclization could occur between the C-2 and C-7 positions, even at the stage of the tetraketide intermediate, on the *PKS1* enzyme (Figure 51). As in *U. maydis*, the type of melanin synthesized by *C. lagenarium* *PKS1* resulted from the polymerization of unstable T4HN (Fujii *et al.*, 1999), suggesting that both plant-pathogenic fungi could produce similar type of melanin, likely sharing a similar mechanism. Further experiments performed by Watanabe and Ebizuka in 2004, showed that the Claisen condensation domain (TE-like domain) of *C. lagenarium* *PKS1* interferes with the chain length growth by intercepting the polyketomethylene intermediate from the ACP halfway through the condensation reaction. Deletion of the C-terminal TE-like domain of *PKS1* resulted in the production of high amounts of the hexaketide isocumarin, while the wild-type in which the TE-like domain is active, produced pentaketides as major products (Figure 52).

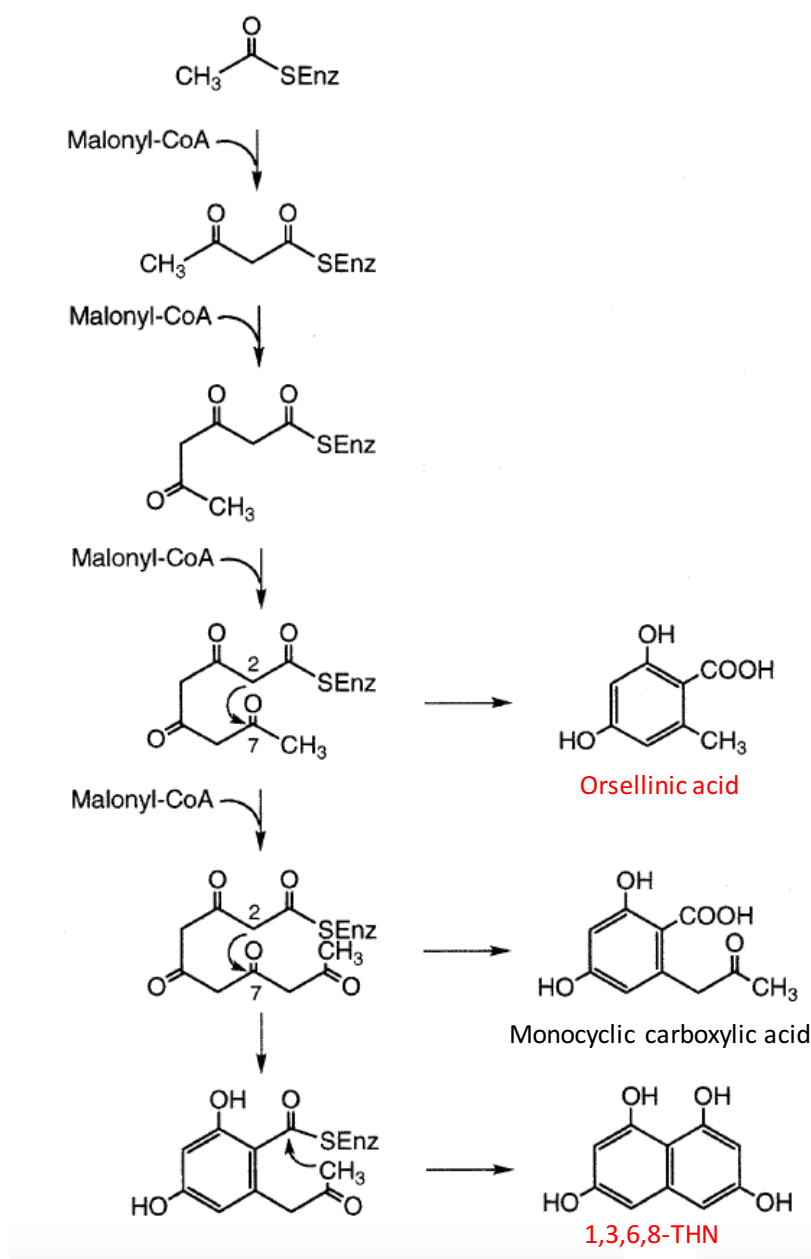


Figure 51. Biosynthetic reaction scheme for T4HN and the by-product orsellinic acid produced by the heterologous expression of the *C. lagenarium* *PKS1* gene in *A. oryzae*. Adapted from Fujii *et al.*, 1999.

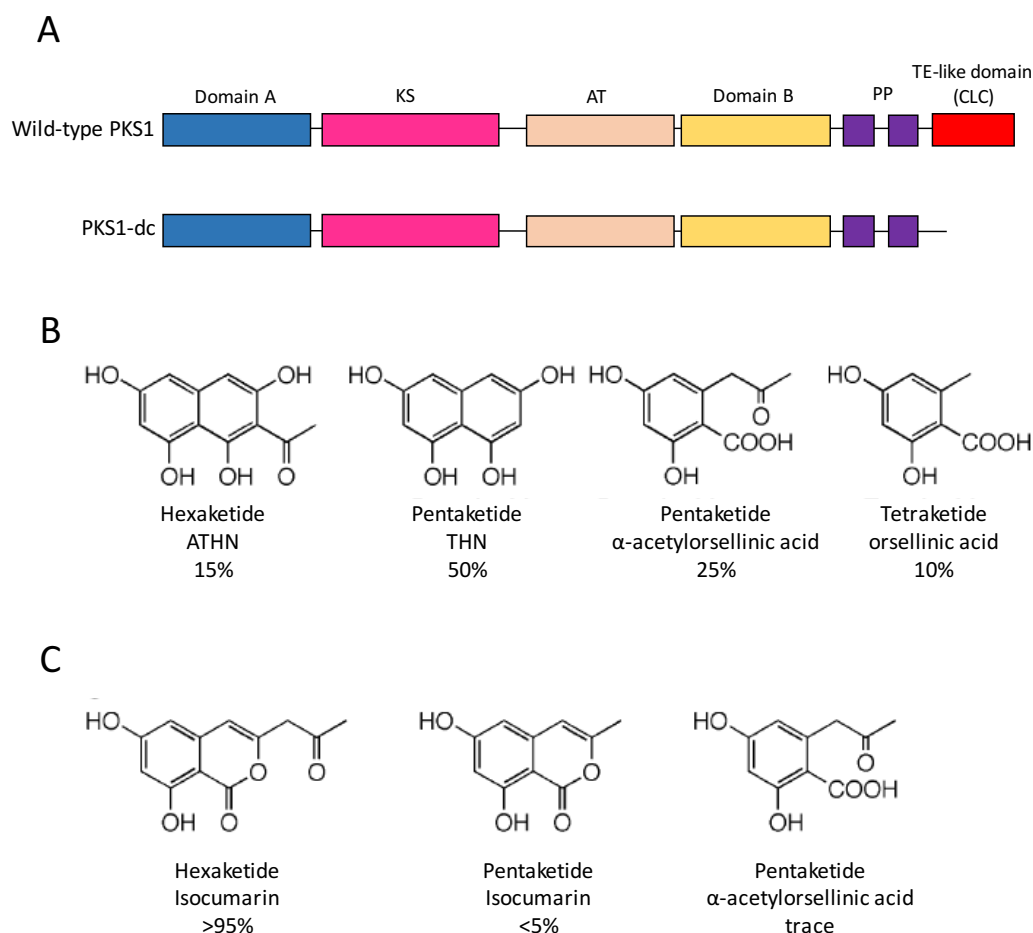


Figure 52. Product identification of the wild-type PKS1 and its mutant in *C. lagenarium*. (A) Domain organization of the wild-type PKS1 and its TE-like domain deletion mutant. (B) Products of the wild-type PKS1. (C) Products of the TE-like domain deletion mutant. The proportion of each compound is shown as the percentage in the total of products. ATHN, 2-acetyl-1,3,6,8-tetrahydroxynaphthalene; THN, tetrahydroxynaphthalene; KS, β -ketoacyl synthase; AT, acyltransferase; PP, phosphopantetheine attachment site; CLC, Claisen-type cyclase. Adapted from Watanabe and Ebizuka, 2004.

These studies are an indication of the versatility of the TE domains in fungal non-reducing iterative PKSs (NR-PKSs), whose activities have been extended to the Claisen cyclase (CLC) chemistry by catalyzing C-C ring closure. However, it is still unclear which component of the NR-PKS is involved in chain release when the CLC is absent. Similar situation has been observed for bacterial type II PKS where there is no obvious mechanism to release the chain from the ACP domain when it has reached its final length. Although speculative, it might be possible that the TE domain of Pks3 had a Claisen condensation activity, just as the TE-like domain of PKS1 from *C. lagenarium*. This would mean that deletion of the TE domain of Pks3 would prevent the synthesis of OA, allowing the growing carbon chain to undergo another elongation step to finally produce T4HN. A way to confirm it would be by overexpressing the

TE-less *pks3* gene under the control of the arabinose-inducible *crg* promoter in the MB215 *Pcrg::pks4* background strain, since the simultaneous expression of the *pks3* and *pks4* genes produces OA. If our assumption is right, the absence of the TE domain in Pks3 will mark a difference in the biosynthesis of polyketides, thus favoring the production of T4HN.

Moreover, mutagenesis experiments in the TE-domain of the aflatoxin B₁ polyketide synthase (PksA), revealed that the residues Ser1937, His2088 and Asp1964 play a crucial role in the CLC activity, since their exchange to S1937A, H2088F, and D1964N led predominantly to the production of pyrone (Korman *et al.*, 2009). In *U. maydis*, the TE-domain of Pks3 contains those conserved residues at positions: Ser1558, His1739, and Asp1587 (Figure 53). Besides the deletion of the TE-domain of Pks3 proposed above, it would be also interesting to study the activity of this domain by mutagenizing these amino acids with the further analysis of their products by HPLC.

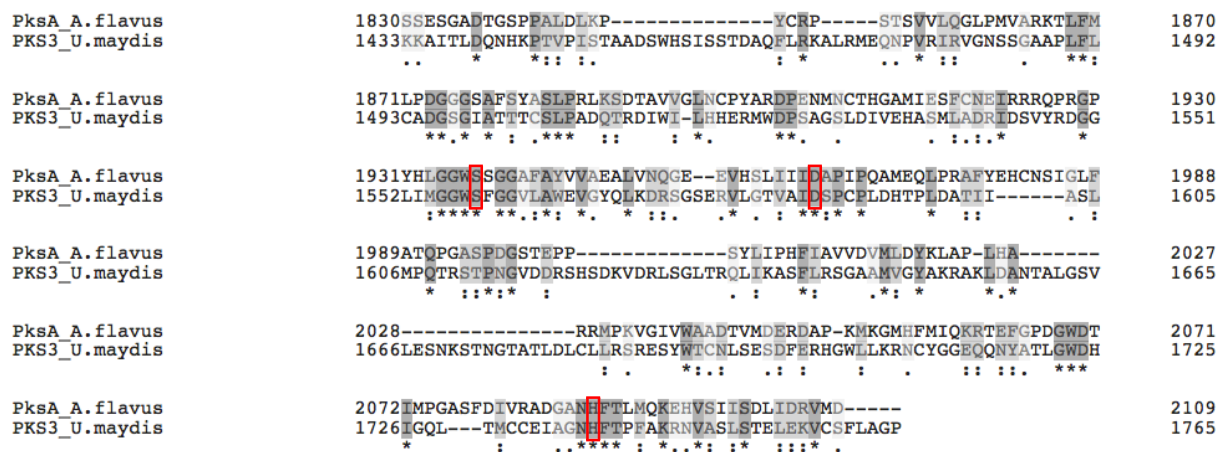


Figure 53. Sequence alignment of the PksA from *A. flavus* and Pks3 from *U. maydis*. The aminoacids belonging to the catalytic triad of the TE-domains of PksA (*A. flavus*) and Pks3 (*U. maydis*) are indicated with a red rectangle. The TE-domain of PksA is located at 1867-2106 aa, while in Pks3 is at position 1488-1635 aa.

On the other hand, in the metabolic profile of the deletion mutant of *cyp4* we detected OA and its derivative compounds, an indication that Cyp4 catalyzes a reaction downstream of the one catalyzed by Pks3 and Pks4. This result was also supported by the non-complementation effect of the MB215 $\Delta cyp4$ *Pcrg::mtf1* strain after the addition of OA (Figure 41). If we take into account that Pks3 and Pks4 catalyze together the first step of the pigment biosynthesis, we could infer that Cyp4 also acts downstream of Pks3 and Pks4, however the reaction steps carried out by Cyp4 are not totally understood yet. Therefore we analyzed the metabolic profiles of the

overexpressing strains in which each PKS gene was simultaneously expressed with *cyp4* (Figure 34). As expected, the double overexpressing strains (*Pcrg::pks3+Petef::cyp4*, *Pcrg::pks4+Petef::cyp4* and *Pcrg::pks5+Petef::cyp4*) exhibited no change in their phenotypes and metabolic profiles when compared with the strains in which their genes were singly overexpressed (Figure 34). Although there are no cases in fungi synthesizing melanin using a PKS and cytochrome P450, we did find a report in the gram-positive bacteria *Streptomyces griseus*. Besides the L-DOPA melanin pathway, *S. griseus* is capable to synthesize HPQ melanin (1,4,6,7,9,12-hexahydroxyperylene-3,10-quinone) by the condensation of malonyl-CoA to generate T4HN by the action of a type III PKS (RppA), followed by the subsequent aryl coupling of T4HN to yield unstable HPQ, a step catalyzed by a cytochrome P450 enzyme (P-450mel) (Funa *et al.*, 2005). As in *U. maydis*, the pigment produced by *S. griseus* was also derived from T4HN and rapidly polymerized. However, they treated the cell extract with trimethylsilyl-diazomethane in order to replace the hydroxyl groups of T4HN by methyl ethers, thus preventing the polymerization. Such a strategy might be considered in the future for the analysis of the cell extracts of the MB215 *Pcrg::mtf1* strain. As for MB215 $\Delta pks3$ *Pcrg::mtf1*, deletion of the *rppA* gene caused the strain to show an albino phenotype. On the other hand, the mutant $\Delta P-450mel$ produced a red-brown pigment as a result of the accumulation of flaviolin as a shunt product (Figure 54). So far, none of our deletion mutants of the melanin-like pigment genes have shown to accumulate only T4HN or flaviolin. Therefore, it would be worthwhile to overexpress *cyp4* under the control of a strong promoter as T7 in *E. coli*, purify it, reconstitute its activity *in vitro* with the ferredoxin and ferredoxin-NADP⁺ reductase from spinach, as it was done for P-450mel in *S. griseus*, incubate it with T4HN and analyze it by HPLC. This experiment could help us somehow to understand whether or not Cyp4 can catalyze the aryl coupling of T4HN. A second alternative would be the heterologous expression of Cyp4 in *S. cerevisiae* as it was performed for the cytochrome P450 enzyme KtnC in *A. niger*, which was shown to be essential for the dimerization of the monomeric coumarin 7-demethylsiderin to orlandin (Mazzaferro *et al.*, 2015).

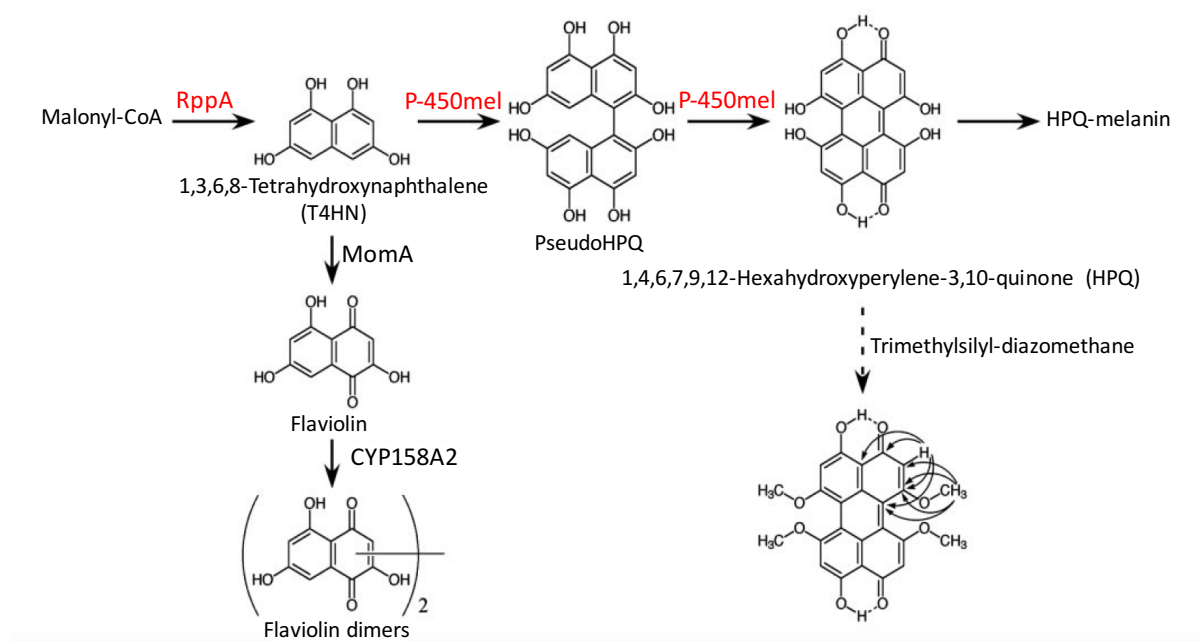


Figure 54. Proposed HPQ melanin biosynthesis pathway in *Streptomyces griseus*. The structure and HMBC correlation of methylated HPQ are also shown. In *S. coelicolor* A3, instead of producing HPQ melanin, CYP158A2 dimerizes flaviolin, which is formed from T4HN by MomA to yield flaviolin dimers. RppA, type III PKS from *S. griseus*; P450-mel, cytochrome P450 involved in the HPQ melanin pathway; CYP158A, cytochrome P450 from *S. coelicolor*. Adapted from Funa *et al.*, 2005.

Gathering all the data concerning to deletion and overexpressing mutants, as well as the previous reports in fungi and bacteria, we propose two different hypothesis. One attractive hypothesis is that Pks3 and Pks4 work together catalyzing the conversion of malonyl-CoA into orsellinic acid only if Pks5 is absent (Figure 55A, steps 1-4A). Since Pks3 does not have the AT domain found in all the OA-PKSs, this function may be provided *in trans* by Pks4.

On the other hand, when *pks5* is expressed together with *pks3* and *pks4* (Figure 55A, steps 1-4B), Pks5 interacts with the complex Pks3-Pks4 by an unknown mechanism, causing a conformational change that masks the catalytic triad of the TE-domain of Pks3 (Ser1558, His1739, and Asp1587), thus disturbing the claisen cyclase activity of TE. Once this occurs, instead of three extension steps that end up with the biosynthesis of OA, there is one additional step that drives the carbon skeleton to the formation of T4HN (Figure 55A, step 4B). Afterwards, it is likely that Cyp4 uses T4HN as a substrate to synthesize the melanin pigment by a similar mechanism as the one describe for HPQ melanin in *S. griseus* (Figure 55A, step 5). None of the experiments carried out so far approve or disapprove the statement that Pks5 uses OA as a direct substrate for the biosynthesis of melanin. Hence, a feeding experiment with OA of the MB215 *Pcrg::pks5* and MB215 *Pcrg::pks5+Petef::cyp4* strains, followed by the LC-

MS analysis of the cell pellets could provide a deeper knowledge about the reaction catalyzed by Pks5.

An important question to be addressed is how the release and cyclization of the carbon chain is carried out to synthesize T4HN. Since we are proposing that Pks5 somehow interferes with the TE activity of Pks3, we had a look to its domain structure and we found that Pks5 possesses a short-chain dehydrogenase/reductase (SDR) domain with the characteristic Rossmann-fold structure and nucleotide binding motif (782-1051aa). Members of the SDR family offer an alternative offloading mechanism by reducing 4'-phosphopantetheine (4'-PPant) arm-tethered peptidyl chain, a thioester, to an aldehyde or an alcohol (Du and Lou, 2010). This finding would suggest that the TE activity needed for the assembly line termination of the polyketide could be given by Pks5. Similar domains are also known from NRPS systems where reductase domains are sometimes used as chain release mechanisms, releasing an aldehyde or primary alcohol. Interestingly, the T4HN and T3HN reductases of *Magnaporthe grisea* are typical members of the SDR family containing the canonical glycine rich NAD (P)-binding site tetrad (Vidal-Cros *et al.*, 1994). Even though *U. maydis* does not possess THN reductases, it seems that the SDR feature is not entirely rare for melanin biosynthetic enzymes. One strategy to study the polyketide intermediate would be by swapping the Pks3-TE domain with the Pks5-SDR domain. By doing so, it could be possible that the combined expression of the chimeric Pks3 and Pks4 (MB215 *Pcrg::pks3*_{SDR-PKS5}+*Pcrg::pks4*) produces T4HN instead of OA.

In the second hypothesis, Pks3 and Pks4 catalyze together the first step of the metabolic pathway in a similar way as described above (Figure 55B, steps 1-4). Afterwards, OA is used as a substrate for Pks5 and Cyp4, which catalyze together its conversion into T4HN (Figure 55B, step 5). Further polymerization of T4HN is accomplished by tailoring enzymes participating in the same pathway, as the ascorbate oxidase Aox1 (Figure 55B, step 6). This hypothesis assumes that neither Pks5 nor Cyp4 are able to convert by themselves OA into T4HN (Figure 55B). It is proposed in this hypothetical model that Pks5 together with Cyp4 act as molecular switches able to convert OA into T4HN. Of course, to validate it, it would be necessary to perform feeding experiments of the strains MB215 *Pcrg::cyp4*, MB215 *Pcrg::pks5* and MB215 *Pcrg::pks5*+*Petef::cyp4* with OA and T4HN, followed by the LC-MS analysis of their cell pellets.

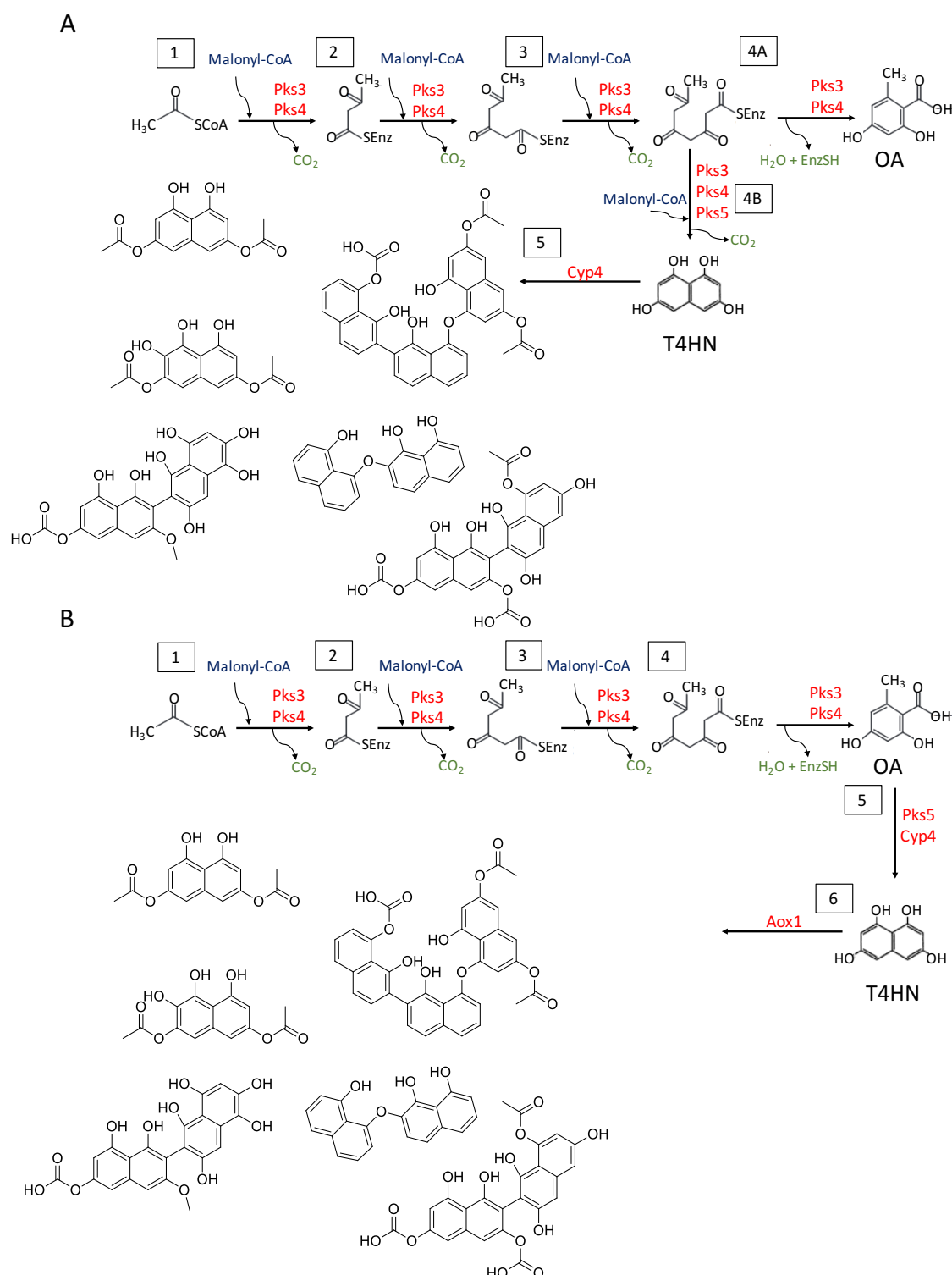


Figure 55. Proposed mechanisms for the first biosynthetic reactions in the melanin pathway in *U. maydis*. (A) First hypothesis. Pks3 and Pks4 catalyze together the conversion of malonyl-CoA into OA (steps 1-4A). If Pks5 is present, as in the MB215 *Pcrg::mtf1* strain, the product derived from the 3rd. step is converted into 1,3,6,8-tetrahydroxynaphthalene (T4HN). Afterwards, Cyp4 polymerizes T4HN into different dimers or trimers. (B) Second hypothesis. The steps 1-4 are carried out in the same way as described for the first hypothesis. Afterwards, Pks5 and Cyp4 convert the OA molecule into T4HN, which is further polymerized by the tailoring enzymes whose genes belong to the melanin-like cluster as ascorbate oxidase (Aox1). Molecular structures shown in the 5th. step in A and 6th. step in B are proposed according the molecular masses detected in the chromatograms of the MB215 *Pcrg::mtf1* cultures.

3.4 Inactivation of *vbs1*, *omt1*, *pmo1* and *deh1* genes influences the biosynthesis of the melanin-like pigment in *U. maydis*.

In addition to the albino phenotypes shown by the deletion mutants of *pks3*, *pks4*, *pks5*, and *cyp4* genes, disruption of *vbs1* and *omt1* genes resulted in a yellowish and orangish phenotypes, respectively. In a similar experiment, disruption of the *vbs1* gene from the aflatoxin pathway in *A. parasiticus*, caused the accumulation of 5'-oxoaverantin (OAVN) and other precursors preceding its formation, thus yielding a yellowish pigment (Sakuno *et al.*, 2004). In *A. parasiticus*, versicolorin B (VBS1) synthase catalyzes two distinct and disconnected reactions. In the first one, versiconal is converted to versicolorin B (VERB) (Yabe *et al.*, 1993), considered as a fundamental step since it closes the bisfuran ring of aflatoxin (McGuire *et al.*, 1996; Silva *et al.*, 1996); and the second one, that involves the conversion of OAVN to (2'S, 5'S)-averunfin (AVR) (Sakuno *et al.*, 2005). Unfortunately, due to the instability of the T4HN, none of the compounds produced in the MB215 $\Delta vbs1$ *Pcrg::mtf1* strain in *U. maydis* (V1, V2, V3) could be isolated and their structures determined (Figure 28). *U. maydis* Vbs1 exhibits an amino acid identity of 28% with the VBS1 from *A. parasiticus*. In addition to that, we did not find reports related to the participation of the *vbs1* gene in any other SM pathway. Therefore, we can only speculate that *U. maydis* Vbs1 might have a similar function to the one observed for the aflatoxin VBS1.

Whether or not *U. maydis* Vbs1 can catalyze more than one metabolic step in the synthesis of melanin is not yet clear, but one way to study it in more detail would be by the overexpression of the *vbs1* gene from *A. parasiticus* in the MB215 $\Delta vbs1$ *Pcrg::mtf1* *U. maydis* strain. If the introduction of *A. parasiticus* *vbs1* gene could rescue the phenotype of the MB215 $\Delta vbs1$ *Pcrg::mtf1* strain, it would mean that both enzymes are capable to catalyze similar reactions, thus contributing to the understanding of this metabolic pathway.

What is clear to us is that Vbs1 catalyzes a downstream reaction of Cyp4, since the double deletion mutant MB215 $\Delta cyp4 \Delta vbs1$ *Pcrg::mtf1* displayed the same phenotype and metabolic profile as the MB215 $\Delta cyp4$ *Pcrg::mtf1* strain did (Figure 30).

On the other hand, deletion of the *omt1* gene triggered a darker phenotype than the one observed in the MB215 $\Delta vbs1$ *Pcrg::mtf1* strain, seeming plausible that the reaction catalyzed by Vbs1 precedes the one catalyzed by Omt1, although it remains to be experimentally demonstrated. As in the case of the V1, V2 and V3 compounds, all the attempts for purifying O1 failed (Figure 28). Hence, a different strategy as the heterologous expression of the *omt1* gene in *A. parasiticus* or *F. fujikuroi* appears to be a feasible solution to gain a better insight into the function of this enzyme. The similarity of Omt1 with the o-methyltransferases Bik3

and AfIO from *F. fujikuroi* and *A. parasiticus*, respectively, promises to be an alternative to study the reactions that could be carried out by Omt1. Bik3 belongs to the bikaverin gene cluster in *F. fujikuroi*, in this pathway a PKS (Bik1) catalyzes the formation of the intermediate pre-bikaverin. The FAD-dependent monooxygenase Bik2 might then be responsible for the oxidation of pre-bikaverin to oxo-pre-bikaverin which is in turn methylated by Bik3 to me-oxo-pre-bikaverin. A further cycle of oxidation and methylation by Bik2 and Bik3 leads to bikaverin (Wiemann *et al.*, 2009). In contrast to the orangish phenotype of the MB215 $\Delta omt1$ *Pcrg::mtf1* strain, the deletion of *bik3* in *F. fujikuroi* resulted in loss of their ability to produce pigmented mycelia as compared with the wild-type strain. Moreover, the encoded protein of the aflatoxin gene *aflO*, catalyzes the conversion of DMST (demethylsterigmatocystin) to ST and DMDHST (demethyldihydrosterigmatocystin) to DHST (Yabe *et al.*, 1989; Kelkar *et al.*, 1996). In the case of Bik3 and AfIO, both enzymes catalyze reactions mostly located at the end of their metabolic pathways probably because the non-methylated derivatives are not toxic for the producer fungi (Medentsev and Akimenko, 1998). In our case, even though the compounds of the MB215 $\Delta omt1$ *Pcrg::mtf1* strain could not be isolated, we infer that Omt1 might participate at later stages in the melanin-like pigment biosynthesis pathway. Same case might be true for those genes whose deletion gave black-greenish phenotypes as *orf1*, *orf4*, *orf5*, *aox1*, *pmo1* and *deh1* (Figure 28). When the metabolic profiles of those deletion mutants were compared with the parental strain, MB215 *Pcrg::mtf1*, some differences were observed but, as described in the previous cases, the respective compounds could not be isolated nor determined. In agreement with this observation, there are many reports in which the monomer units of melanin have been characterized; nevertheless, due to their instability, the arrangement of those subunits in the polymer structure has not been determined (Wakamatsu and Ito 2002).

In contrast to the wild-type phenotype given by the MB215 $\Delta aox1$ *Pcrg::mtf1* strain, deletion of the *abr2* gene, encoding a laccase for conidial pigment in *A. fumigatus*, changed the gray-green conidial pigment to a brown color (Sugareva *et al.*, 2006). A similar case was observed in *T. marneffei*, where the deletion of the laccase gene (*prbB*) for DHN-melanin synthesis in conidia resulted in brown pigmented conidia (Sapmak *et al.*, 2015). One of the reasons why the deletion of the *aox1* gene had not effect on the phenotype could be explained by the presence of another multicopper oxidase gene that has replaced its function. Interestingly, the best self match in *U. maydis* genome, was given by the gene *um05361*, previously identified as *lac1* by Islamovic and coworkers. Because the two genes, *lac1* and *aox1*, are involved in melanogenesis in *U. maydis*, it would not be entirely surprising that they could complement each other's function. One way to confirm this assumption would be by

deleting the *lac1* gene in the MB215 $\Delta aox1$ *Pcrg::mtf1* background, in case of a complementary function of both genes, a reduction of pigmentation in the double deletion mutant (MB215 $\Delta aox1 \Delta lac1$ *Pcrg::mtf1*) might be observed.

Another gene whose deletion seems not to have a strong impact in the pigment biosynthesis is *pmo1*. The *pmo1* gene encoding for a phenol-2-monooxygenase (better known as phenol hydroxylase) belongs to the family of polyphenol oxidases (PPO), in the same way as tyrosinases and laccases do. In contrast to them, phenol hydroxylases are non-copper enzymatic systems. Besides phenol, phenol hydroxylases are also able to catalyze the oxidation of various phenol derivatives including *p*-, *m*- and *o*-cresols, *p*-, *m*- and *o*-chlorophenols, *p*-, *m*- and *o*-aminophenols, orcinol, phloroglucinol, 2-amino-*m*-cresol and β -naphthol (Nakagawa and Takeda, 1962). According to the phenotype of the MB215 $\Delta pmol$ *Pcrg::mtf1* strain, *pmo1* gene may contribute to further modifications of the core structure of the melanin molecule. Similar situation may be true for the dehydrogenase gene *deh1*. Analysis of the domain structure of the Deh1 protein showed a KR domain (at position 11-140 aa) similar to those found in bacterial PKSs. Since the KR domain catalyzes the first step in the reductive modification of the beta-carbonyl centres in the growing polyketide chain, it may be possible that the Deh1-KR domain provides a reductase activity for the melanin PKSs.

No conserved domains were detected for the *orf1*, *orf4*, and *orf5* genes, neither similarities with proteins from other fungi. However, a closer analysis to their amino acid sequences showed certain degree of similarity among them, what makes us suspect that probably *orf1*, *orf4* and *orf5* are paralogs genes residing within the same cluster.

As expected, deletion of the *mtf2* gene had not effect in the pigmentation nor in the metabolic profile of the strain. Besides controlling the expression of the *orf2* gene, it is not known if *mtf2* influences the regulation of other genes outside the melanin-like cluster, since no expression data was found in any of the 144 experiments collected from GEO database.

Even when there is no experimental evidence about the role of *orf1*, *orf2*, *orf5*, *pmo1*, *aox1* and *deh1* genes in the biosynthesis of the melanin-like pigment, their similar phenotypes to the wild-type after being deleted indicate a minor role in the metabolic pathway.

Remarkably, the melanin-like cluster genes in *U. maydis* share similarities with those found in DHN-melanin pathways in other basidiomycetes, while at the same time some of them resemble the aflatoxin genes in *A. parasiticus*. From the evolutionary point of view, it might be possible that *U. maydis* have acquired the melanin and aflatoxin genes by horizontal gene transfer (HGT) events, and during the course of the time those genes belonging to different clusters have fused into one. Most of the HGT events in eukaryotes concerns to the transfer of

single or a few genes from bacterial donors, however there is a perfect example of eukaryote-eukaryote HGT of SM gene clusters. In *Podospira anserina*, the complete gene cluster for sterigmatocystin (a precursor of the aflatoxins) was horizontally transferred from *Aspergillus* (Slot and Rokas, 2011). All the promoter regions of the *Podospira* cluster contain the palindromic sequence 5'-TCG (N₅) CGA-3', which is the binding site of the pathway regulator AfIR. Even though the inspection of such a binding site in the promoter regions of the melanin-like cluster genes did not give a match, the possibility that this cluster has been acquired by HGT can not be entirely ruled out. Comparative genomics and phylogenetic studies need to be done in order to get a deeper understanding in this field.

3.5 Role of the melanin clusters in *U. maydis*

LC-MS analysis of the cell pellets extracts of the strains MB215 *Pcrg::pks1* and MB215 *Pcrg::pks2* produced no compounds, thus indicating that neither Pks1 nor Pks2 are capable to synthesize polyketides by themselves. However, the double overexpression of both accumulated a light-greenish pigment and six compounds (PP1-PP6) which are currently being analyzed (Figure 37). The fact that none of these PKSs can synthesize a polyketide when they are singly overexpressed could be inferred by their domain structures. None of them possess the three minimal domains required to considered a polyketide synthase as functional, AT, ACP and KS (Figure 36). Although it is unknown how these two PKSs interact with each other, our experiments clearly support the idea of complementarity. In addition to *U. maydis*, the biosynthesis of a polyketide generated by two PKSs was previously reported in *Cochliobolus heterostrophus*, the causative agent of the southern corn leaf blight in maize. The synthesis of its T-toxin and the high virulence effect in maize is influenced by *C. heterostrophus* PKS1 and PKS2. Although the mechanism by which both PKSs produce the T-toxin is not well understood, the study suggested that due to each PKS synthesizes a polyketide, one of them may act as the starter unit for the biosynthesis of the mature T-toxin molecule (Baker *et al.*, 2006). Related cases have been also reported for the pair of PKSs in the lovastatin and compactin gene clusters, where the polyketides are joined by an ester, not a carbon-carbon bond as for the T-toxin (Abe *et al.*, 2002; Kennedy *et al.*, 1999).

Since Pks1 and Pks2 were shown to be involved in teliospore pigmentation and our study has presented evidence that suggests that Pks3, Pks4 and Pks5 play a fundamental role in the biosynthesis of a melanin-like pigment, we asked ourselves the possibility of complementarity among them. Coexpression of either *pks1* or *pks2* with each of the PKS genes of the melanin-like cluster (*pks3*, *pks4* and *pks5*) produced no change in the phenotypes or in the metabolic

profiles compared to their single overexpressing strains (MB215 *Pcrg::pks3*, MB215 *Pcrg::pks5* and MB215 *Pcrg::pks4*) (Figure 38 and 39). In some cases, the outcome could be inferred beforehand since not all combinations of PKSs fulfilled the minimum domain requirements for being functional (KS-AT-ACP). Strains that fall within this classification due to the lack of an AT domain are MB215 *Pcrg::pks1+Pcrg::pks3* and MB215 *Pcrg::pks1+Pcrg::pks5*. Another strain that belongs to this category is MB215 *Pcrg::pks2+Pcrg::pks4*, that despite having the KS and AT domains, none of them harbor an ACP domain. In other cases, although the combination of PKSs covered the KS, AT, and ACP domains, they were not able to synthesize detectable compounds (Figure 38 and 39), as for the strain MB215 *Pcrg::pks2+Pcrg::pks3*, MB215 *Pcrg::pks2+Pcrg::pks5* and MB215 *Pcrg::pks1+Pcrg::pks4*. An indication that even though Pks1-Pks5 are implicated in the biosynthesis of a melanin pigment, the specificity of their domains make them to function preferentially with the PKSs from the same gene cluster. However, when *pks1* and *pks2* were individually overexpressed in MB215 $\Delta pks3$ *Pcrg::mtf1*, MB215 $\Delta pks4$ *Pcrg::mtf1* and MB215 $\Delta pks5$ *Pcrg::mtf1* strains, only the overexpression of *pks1* in MB215 $\Delta pks3$ *Pcrg::mtf1* strain could rescue the black-greenish phenotype, thus indicating that Pks1 and Pks3 have complementary functions. Both PKSs harbor the KS, ACP and TE domains, which in combination with Pks4 and Pks5 domains synthesize the melanin-like pigment (Figure 40). Due to the lack of an AT domain in Pks1, it is possible that Pks1 recruits the AT activity *in trans* provided by Pks4, in a similar way as proposed for Pks3. Even though the amino acid sequence analysis of the AT domains of Pks2 and Pks4 is not highly significant (31% identity and 33% similarity), it would seem that Pks1 does not discriminate in using one or the other. Most of the AT domains characterized so far are either malonyl-CoA or (2S)-methylmalonyl-CoA specific; in other rare cases, AT domains are specific for an ACP-tethered extender unit, such as methoxymalonyl-ACP, hydroxymalonyl-ACP, and aminomalonyl-ACP (Chan *et al.*, 2009). In our particular case, AT-domain swaps between Pks2 and Pks4 appears to be an attractive alternative to study their substrate specificity. Moreover, the no complementation effect in the strain MB215 $\Delta pks3$ *Pcrg::mtf1+Pcrg::pks2* could be explained by the absence of the ACP domains in Pks2. Although Pks5 contains an ACP domain, our experiments have previously shown that Pks5 does not participate in the catalysis of the first reaction product for the melanin-like pigment biosynthesis.

On the other hand, the fact that the overexpression of either *pks1* or *pks2* did not complement the phenotype of MB215 $\Delta pks4$ *Pcrg::mtf1* or MB215 $\Delta pks5$ *Pcrg::mtf1* strains can be due to some other reasons. Neither *pks1* nor *pks2* possess the SDR and AMP adenylation

domain of Pks5, which could influence the number of elongation steps carried out by the polyketide intermediate. According to our model, one additional step would drive the reaction towards the biosynthesis of T4HN, which later will polymerize into melanin. In the case of MB215 $\Delta\Delta pks4$ *Pcrg::mtf1*+*Pcrg::pks1* strain can be easily observed that none of the active domains is an AT-domain. In other words, not even together, Pks1, Pks3 and Pks5 accomplish the minimal requirements for a functional PKS (Figure 40). In contrast, although the minimal PKS domains were present in the MB215 $\Delta\Delta pks4$ *Pcrg::mtf1*+*Pcrg::pks2* strain, it was not sufficient for its complementation. Suggesting that Pks3 is not able to use the activity of the AT domain of Pks2, which is in line with the observation that MB215 *Pcrg::pks3*+*Pcrg::pks2* strain produced no detectable compounds. Although it would be premature to speculate on this, it seems that the Pks4-AT domain has less specificity compared with the Pks2-AT domain.

When *pks1* and *pks2* were individually expressed together with *cyp4*, none of the strains displayed a different phenotype than the one observed in the wild-type strain (Figure 37). As formerly mentioned, the strains MB215 *Pcrg::pks1* and MB215 *Pcrg::pks2* produced no compound (s), therefore no intermediates could serve as a substrate for Cyp4. In order to have a better understanding of the role of Cyp4 in the biosynthesis of melanin, it would be necessary to coexpress *pks1*, *pks2* and *cyp4* together (MB215 *Pcrg::pks1*+*Pcrg::pks2*+*Pcrg::cyp4*) and analyzed the extracts by LC-MS. A similar experiment should be also performed using *lac1* instead of *cyp4* (MB215 *Pcrg::pks1*+*Pcrg::pks2*+*Pcrg::lac1*), which would enable to estimate whether Pks1 and Pks2 also synthesize the same kind of T4HN-melanin as Pks3, Pks4 and Pks5. It is possible that *cyp4* could play a role in polymerizing the melanin subunits synthesized by Pks1 and Pks2, in a similar way as suggested for *lac1* by Islamovic and coworkers. In the same publication, it was shown a dramatic and reduced pigmentation phenotype in maize plants when they were infected with $\Delta pks1$ and $\Delta lac1$ mutant strains, respectively. However, they did not test the *pks2* deletion mutant, basically due to its highly induced expression level comparable with *pks1* (Islamovic *et al.*, 2015). Interestingly, experiments performed by Meryem Friedrich in our group showed that plants infected with crosses of the strains FB1 $\Delta pks2$ X FB2 $\Delta pks2$ led to a loss in spore pigmentation compared to wild-type strain (FB1 X FB2) (unpublished data). Thus confirming the role of Pks1 and Pks2 in spore pigmentation and the complementary effect with each other (Figure 56).

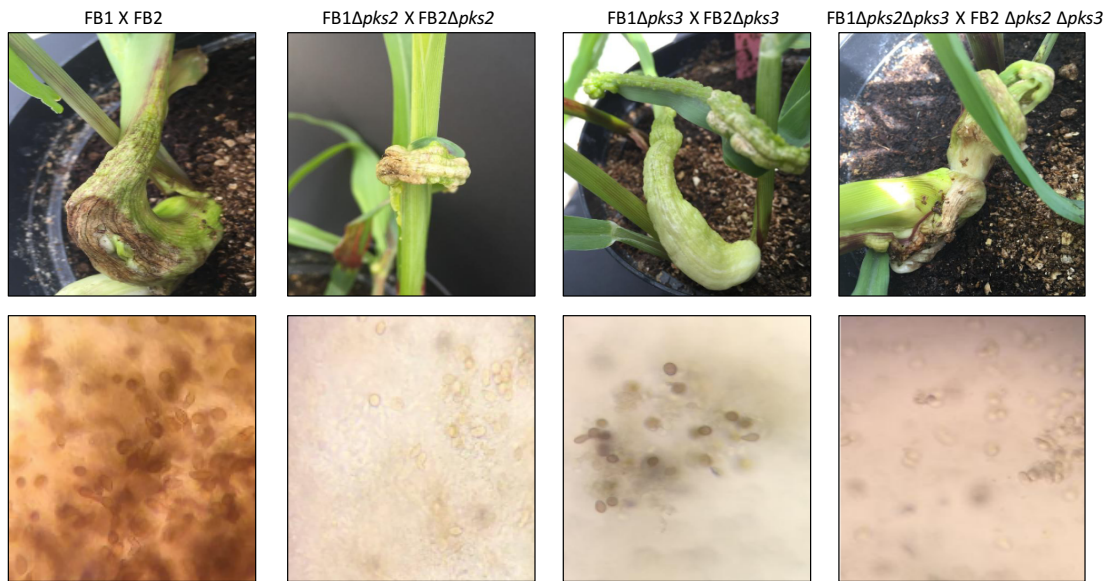


Figure 56. Teliospore development in maize plants induced by the wild-type, $\Delta pks2$, $\Delta pks3$ and $\Delta pks2\Delta pks3$ mutant strains. The upper panel shows the plant tumors induced after 12 dpi by the strains (from left to right): wild-type (FB1 X FB2), $\Delta pks2$ (FB1 $\Delta pks2$ X FB2 $\Delta pks2$), $\Delta pks3$ (FB1 $\Delta pks3$ X FB2 $\Delta pks3$) and $\Delta pks2\Delta pks3$ (FB1 $\Delta pks2\Delta pks3$ X FB2 $\Delta pks2\Delta pks3$). The lower panel indicates the hand sectioned tissues derived from the pictured tumors of the corresponding strains taken by a binocular microscope 4 weeks post-infection. Data kindly provided by Meryem Friedrich and Tobias Deinzer.

In addition, the double deletion mutant of *pks2* and *pks3* genes was also tested for spore pigmentation. Plants inoculated with mixtures of FB1 $\Delta pks3$ X FB2 $\Delta pks3$ showed a slightly impact in virulence and a markedly reduction in spore pigmentation, while the double deletion mutant strain FB1 $\Delta pks2\Delta pks3$ X FB2 $\Delta pks2\Delta pks3$ had a similar effect in virulence and pigmentation compared to the single deletion of the *pks2* gene. (Friedrich *et al.*, unpublished data). Seen in a different way, deletion of *pks3* in the $\Delta pks2$ background strain had no contribution to its phenotype (Figure 56).

Further experiments carried out in the solopathogenic strain SG200 supported the idea of a minor role of the *pks3* gene in virulence (Figure 45). Similar results were exhibited for the strains SG200 $\Delta pks4$ and SG200 $\Delta pks5$, although SG200 $\Delta pks4$ seems to have a stronger impact compared to the deletion of *pks3* and *pks5* genes (Figure 45). This is in line with the observation of RNA-seq data concerning to *U. maydis* PKS genes during maize plant infection, data kindly provided by Daniel Lanver (Figure 57A). In all cases, the transcript levels remain low during the first 24 h post-infection (hpi). At this stage, the filaments of the solopathogenic *U. maydis* strain have formed appressoria on the maize epidermis to penetrate the maize cell wall (Brefort *et al.*, 2009). This is an indication that none of the *U. maydis* PKS-encoding genes seems to play a role during the first stages of infection, unlike other plant pathogenic fungi as *Magnaporthe grisea* (Howard and Valent 1996), *Venturia inaequalis* (Steiner and Oerke 2007),

Diplocarpon rosae (Gachomo *et al.*, 2010) and *Colletotrichum graminicola* (Ludwig *et al.*, 2014), whose polyketide synthases participate in the production of melanized appresoria. Interestingly, at 24 hpi small changes in expression could be observed for *pks1* (Figure 57A, blue line), while for *pks2* those changes started at 6 dpi. As expected, the low expression level of *pks1* and *pks2* in the period between 24 hpi and 2 dpi is because during that time, the penetrated hyphae proliferates intracellularly within the epidermis and mesophyll, having no need to synthesize melanin (Doehlemann *et al.*, 2008). When the tumor induction begins, fungi grow both inter- and intracellularly, normally at 4 dpi. At this stage, cell death is very rarely observed in the plant tissue surrounding aggregates, which indicates that *U. maydis* is actively suppressing plant defense responses during all stages of biotrophic development (Doehlemann *et al.*, 2008). Five to six days after infection, massive fungal proliferation presumably of the diploid form is observed in tumor tissue, therefore *pks1* and *pks2* markedly increase their expression levels at 6 dpi (Figure 57A). That increment continues when fungal hyphae forms large aggregates between the enlarged maize tumor cells (8 dpi). Afterwards, *pks1* and *pks2* register their highest levels in expression at 12 dpi, a period after proliferation where hyphal sections fragment, round up and differentiate into heavily melanized diploid teliospores (Snetselaar and Mims, 1993; Banuett *et al.*, 1996). On the other hand, the expression levels during plant infection of *pks3*, *pks4* and *pks5* remained comparable to those in axenic culture until 8 dpi, thereafter they showed a small increase until 12 dpi (Figure 57A). Comparing the transcript levels of *pks1* and *pks2* with *pks3*, *pks4* and *pks5*, there is a tremendous difference among them, making it clear that *pks1* and *pks2* are involved in the melanization processes of teliospores. Although the role of *pks3*, *pks4* and *pks5* has not been studied in detail during plant infection, probably they contribute to suppress the plant responses by actively detoxifying H₂O₂. We previously showed that overexpression of *mtf1* does not upregulate *pks1* and *pks2*, just as the Δ *ust1* mutant strain does not induce the expression of *pks3*, *pks4* and *pks5* (Islamovic *et al.*, 2015), thus denoting that both gene clusters have distinct mechanisms of regulation and, as a consequence, they are activated under different circumstances. In fungi, most of the studies link one gene cluster to one or more compounds, but very few cases link the same kind of compound with two different gene clusters. For instance, DHN melanogenesis in *Botrytis cinerea* is based on two developmentally regulated PKS-encoding genes. BcPKS13 and BcPKS12 provide the intermediate T4HN in conidia and sclerotia respectively, for further conversion to DHN by the same set of enzymes (Schumacher, 2016). This report provides a perfect example in which PKSs located on distinct chromosomes are able to synthesize the same compound but under different developmental programs. In *A. flavus*, two clusters

harboring non-canonical NRPS genes on chromosome 6 and 8 encode the same set of enzymes involved in the production of a group of piperazines. It was shown that addition of one of the piperazine metabolites, produced almost exclusively by the *lna* cluster, to wild-type cultures greatly increased expression of *lnbA* NRPS. Since both gene clusters shown to be important for sclerotial formation, it was speculated that the occurrence of a functionally duplicated biosynthetic pathway may be due to a mechanism to ensure timely sclerotial production and hence, persistence during unfavorable environmental conditions (Forseth *et al.*, 2013). Alongside these studies, the biosynthesis of endocrocin in *A. fumigatus* (Throckmorton *et al.*, 2016) and conidial pigment in *A. terreus* (Guo *et al.*, 2015) constitute cases in which physically unlinked clusters contribute to the synthesis of the same metabolite in one fungal species. To the best of our knowledge, the work presented here would constitute the first example in *U. maydis* in which two gene clusters located on different chromosomes are able to synthesize the same secondary metabolite, melanin. Although many experiments need to be done in order to clarify under which circumstances the melanin-like cluster is preferentially activated.

In addition to *pks3*, *pks4*, and *pks5* from the melanin-like cluster, we also infected maize plants with the deletion mutants of those genes encoding for tailoring enzymes that also were activated by *mtf1* (Figure 45). Deletion of *mtf1* displayed a reduction in plant symptoms compared to the solopathogenic strain SG200. If we take into account that *mtf1* regulates the expression of *pks3/pks4/pks5* and that the deletion of those genes reduced the symptoms in infected plants, somehow it was expected such a phenotype for SG200 Δ *mtf1*. On the other hand, when maize plants were infected with the strain SG200 Δ *mtf2*, no differences were observed when compared to the wild-type (Figure 44). Besides *orf2*, there are no reports of other genes whose expression is controlled by the transcription factor *mtf2*, but what is clear is that this gene does not seem to play an important role in virulence. A general trend in plants infected with the deletion mutant strains SG200 Δ *aox1*, SG200 Δ *vbs1*, SG200 Δ *pmo1*, SG200 Δ *cyp4*, SG200 Δ *deh1*, SG200 Δ *orf1*, SG200 Δ *orf3*, and SG200 Δ *orf5* was a small reduction in symptoms when compared to the wild-type strain (Figure 45).

Moreover, no significant differences in pathogenicity were observed between SG200 Δ *omt1* and SG200 strains (Figure 45). Although it is not clear the role in melanization of the genes encoding for tailoring enzymes, we have observed that in most of the cases this role is secondary, therefore it may be possible that when any of those genes is deleted, another gene could complement its function. Another important thing to know is whether there is or not a whole contribution of the melanin-like cluster in pathogenicity, hence it would be worth it to

infect maize plants with a strain in which the whole melanin-like cluster has been deleted (SG200 Δmel).

Genes encoding for the tailoring enzymes have a similar trend in their gene expression levels compared to *pks3/pks4/pks5* during plant infection (Figure 45). All of them show a low expression level at early stages with a small increase at 8 dpi, except for *vbs1*, *deh1*, and *pmo1* whose transcript levels raised after 6 days of inoculation. It is not uncommon for coregulated genes part of the same SM gene cluster to show differences in expression under certain condition. In *F. graminearum*, five genes in a cluster with enzymes involved in triacetylfusarin biosynthesis showed differential expression and correlation in their expression profiles during infection (Sieber *et al.*, 2014). Furthermore, the earlier expression increase of *mtf1* (4 dpi) in comparison to the rest of the melanin-like cluster genes can be explained by the idea that its activation may be subjected to an upstream control of other TFs expressed at earlier stages. In addition to this, it is important to note that there can be many steps between mRNA translation of a TF and the actual transcriptional regulation of its target genes. The TF can be post-translationally modified, i.e. it can be methylated, ubiquitinated or phosphorylated. Phosphorylations are often necessary for dimerization and binding to the target gene's promoter (Schacht *et al.*, 2014). As a control, we also included in the analysis the expression of *mtf2* and *orf6*, due to their expression is not dependent of *mtf1*.

Putting all this together, we have observed that the melanin-like cluster genes are coregulated during plant infection, having their highest expression levels at the latest stages. Although *pks1* and *pks2* are leading the spore pigmentation process, the role of the melanin-like cluster genes may be related to help in overcoming the plant responses.

In this work, we also analyzed the gene expression data through 144 experimental conditions downloaded from GEO database. Concerning to the melanin-like cluster genes, we only found information regarding to *vbs1*. In addition to its induction during plant infection, *vbs1* also showed high expression levels in conditions under which the FB1 strain was cultivated in CM-glucose medium with 5 mM of H₂O₂ for 1h (Table S5). Since one of the primary defense reaction mechanisms in planta is the production of ROS, it is not at all unthinkable that melanin is synthesized as a protection shield in the presence of hydrogen peroxide. Therefore, we tested the sensitivity of the strains SG200 $\Delta pks3$, SG200 $\Delta pks4$, and SG200 $\Delta pks5$ to H₂O₂ in an agar diffusion test (Figure 47). Overall, no significant differences in halo size were observed when compared to the wild-type.

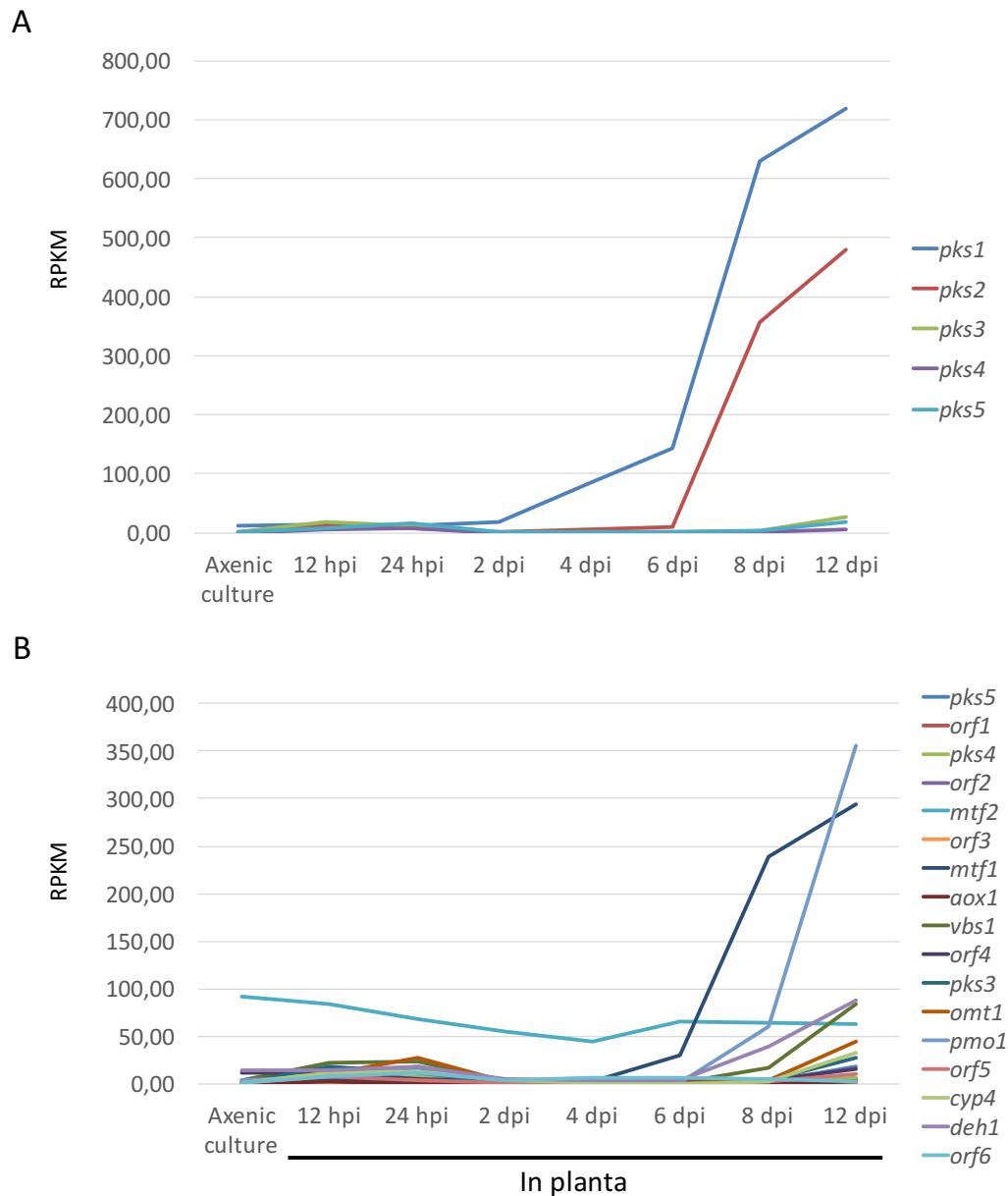


Figure 57. RNA-Seq data of the PKSs and melanin-like cluster genes in *U. maydis* when cultivated in axenic culture and during maize plant infection. (A) RNA-Seq data of *U. maydis* PKS genes *pks1*, *pks2*, *pks3*, *pks4* and *pks5*. The *pks1* and *pks2* genes notably increase their expression level at 6 dpi and continue until 12 dpi. Although both genes are coregulated, it can be noticed a higher expression level in *pks1* compared with *pks2*. On the other hand, the expression levels of *pks3*, *pks4* and *pks5* genes are low in axenic culture and planta; however, small increases in gene expression can be observed at 8 dpi, which is in line with the observation of a reduced virulence effect in maize plants inoculated with SG200 $\Delta pks3$, SG200 $\Delta pks4$ and SG200 $\Delta pks5$ strains. **(B)** RNA-Seq data of the melanin-like cluster genes. Most of the genes increase their expression level at 8 dpi, while some others as *pmo1*, *deh1* and *vbs1* start at 6 dpi. The genes *mtf2*, *orf2* and *orf6* (encoding for a dioxygenase) were included as controls since they were not activated by *mtf1*. Among the melanin-like cluster genes, *mtf1* showed the earliest expression increase in planta at 4 dpi, followed by a higher increase from 6 to 8 dpi. RPKM, reads per kilobase of exon model per million mapped reads; hpi, hours post-infection; dpi, days post-infection. Data kindly provided by Daniel Lanver.

This result seems to be contradictory with the observations in some other fungi such as *Sporothrix schenckii*, *A. fumigatus* and *Paracoccidioides brasiliensis*, which found a decreased resistance to killing by hydrogen peroxide when their melanin-PKS genes were deleted (Romero-Martinez *et al.*, 2000; Tsai *et al.*, 1999; da Silva *et al.*, 2009). A possible explanation for this result in *U. maydis* would be that in the absence of the melanin-like genes, *pks1* and *pks2* could take over the detoxification process. However, when we had a look to the expression levels of *pks1* and *pks2* under the same conditions we noticed that both genes were downregulated (Table S6 and S7), indicating once again that although PKS genes from different clusters participate in the biosynthesis of melanin, the activation of one or other depends on specific conditions. A way to confirm whether *pks1* and *pks2* can be activated in the absence of *pks3* would be by testing the sensitivity to H₂O₂ of the triple deletion mutant strain SG200 $\Delta pks1\Delta pks2\Delta pks3$. Of course, in addition to the melanization process to overcome ROS, there are many other genes implicated in such redox-dependent signaling pathways as the peroxidases *um01947* and *um10672*, whose regulation was shown to be controlled by the transcription factor YAP1 (Molina *et al.*, 2007). According to our expression data, there is not a considerable difference in expression of the PKS genes when FB1 or FB1 $\Delta yap1$ strains were grown in the presence of H₂O₂, suggesting that *yap1* does not exert a regulatory control on the PKS genes when *U. maydis* is grown under oxidative stress conditions. Furthermore, we also noticed that the expression level of *vbs1* decreased in SG200 $\Delta tup1$ strain compared to the wild-type when both were grown on charcoal plates for 48 h, thus indicating that *tup1* somehow positively influences the gene expression of *vbs1* and, likely, also the expression of the other melanin-like genes. Even though Tup1 has been described as a general transcriptional repressor, the deletion of *tup1* in *U. maydis* leads to the down-regulation of the genes that control the dimorphic transition, suggesting an activator role for *tup1* in controlling them (Elías-Villalobos *et al.*, 2011). Although it is not known how *mtf1* is activated, we assume that Tup1 could be its upstream regulator. Therefore, it would be interesting to perform expression analysis of *mtf1* and the melanin-like cluster genes in the background of the $\Delta tup1$ strain. In a recent publication in *U. maydis*, the major regulator of spore formation, Ros1, was found to bind to the promoters of the genes *tup1*, *ust1*, *rum1*, and *hgl1*, suggesting that they could be direct targets (Tollot *et al.*, 2016). Interestingly, the gene encoding for versicolorin B synthase (*vbs1*) was the most upregulated gene involved in secondary metabolism controlled by Ros1. In a similar way, *pks1* and *lac1* were positively regulated by Ros1.

Furthermore, we also explored conditions under which *vbs1* exhibited its lowest expression levels. One of them was found when FB1 $\Delta rak1$ strain was grown in CM medium

with 1% of glucose as a carbon source. Rak1 has been reported to play an important role in cell growth, and cell fusion in *U. maydis* (Wang *et al.*, 2011). In addition, *rak1* participates in the response of cell wall stressors, since the SG200 $\Delta rak1$ strain displayed more sensitivity to congo red and calcofluor white than the wild-type strain. In fungi, Rak1 orthologues are involved in regulation of cell growth and stress responses (Rothberg *et al.*, 2006; Coyle *et al.*, 2009), so it would not be totally surprising that such a process as melanization was controlled by the expression of *rak1*. Indeed, Gib2, the homolog of Rak1 in *Cryptococcus neoformans* required for normal growth and virulence, directly binds to the G α protein (Gpa1), a component of the cAMP-signaling cascade. Deletion of *gpa1* leads to a melanin deficient phenotype (Pukkila-Worley *et al.*, 2005), which can be rescued by the overproduction of Gib2 (Palmer *et al.*, 2006; Wang *et al.*, 2014). Interestingly, the closest relative of Gpa1 in *U. maydis* is Gpa3 (75% identity), whose deletion did not induce disease symptoms in infected corn plants (Regenfelder *et al.*, 1997). Considered as an important gene for teliosporogenesis, *gpa1* showed an increase in its transcript levels, together with *pks1* and *pks2*, in the $\Delta ust1$ mutant (Islamovic *et al.*, 2015). Nonetheless, more comprehensive studies need to be done in order to gain a better knowledge about the regulatory process and the interconnection of both melanin clusters. Given the remarkable conservation in signaling mechanisms among fungal and other eukaryotic organisms, it may be possible that *U. maydis* controls the biosynthesis of the melanin in a similar way.

On the other hand, a low expression level was also reported for *vbs1* when the BW12 strain was grown in minimal medium with 10 μ M of FeSO₄ (Eichhorn *et al.*, 2006). BW12 is a derivative of FB1 strain with a deletion of the *urbs1* open re

ading frame. Urbs1 is a GATA transcription regulator of siderophore biosynthesis in *U. maydis* (Voisard *et al.*, 1993) whose disruption leads to constitutive expression of *sid1* and *sid2* genes, encoding for a L-Orn N⁵-monooxygenase and a siderophore synthase, respectively (Mei *et al.*, 1993; Yuan *et al.*, 2001). Besides *sid1* and *sid2*, Urbs1 also represses the expression of other siderophore genes when *U. maydis* is grown under high iron conditions (Eichhorn *et al.*, 2006). Unlike them, the expression of *vbs1* seems to be oppositely regulated by Urbs1; that is to say, while Urbs1 is a transcriptional repressor for iron-uptake genes, it acts as a positive regulator of *vbs1*. It seems reasonable, that a high concentration of iron can trigger a signal that activates genes involved in melanin biosynthesis, since it is well known that the presence of ferrous iron at high levels catalyzes the production of free radicals that can bind to critical molecules as sugars, aminoacids, phospholipids, DNA bases, and organic acids (Byers *et al.*, 1998). The ability of melanin to prevent the redox cycling of iron ions and their action as

catalysts in Fenton-type reactions has been extensively studied, however there has not been a proper study that links the regulatory network of the siderophore and melanin gene clusters in *U. maydis*. Moreover, when SG200 $\Delta hxt1$ strain was grown in minimal medium with 1% of either glucose or xylose as a carbon source for 6 h, the expression of *vbs1* also dropped down. In *U. maydis*, Hxt1 is a high affinity transporter for monosaccharides important for fungal development during both the saprophytic and the pathogenic stage of the fungus. Besides its function as a transporter, Hxt1 also plays a role as a sensor (Schuler *et al.*, 2015), therefore it is conceivable that $\Delta hxt1$ strains showed decreased symptom development after plant infection. In accordance to this report, deletion of the encoded gene for Hxs1, the counterpart of Hxt1 in *C. neoformans*, had a defect in virulence mainly explained by a defect in melanin production (Liu *et al.*, 2013). Although Schuler and collaborators did not discuss the implication of melanin in the phenotype observed in plants infected with $\Delta hxt1$ strains, it is reasonable to think that the sensing of glucose regulates the production of melanin via the cAMP signaling pathway, just as in *C. neoformans* (Alspaugh *et al.*, 1997; Xue *et al.*, 2006).

Despite the fact that the analysis of 144 experimental conditions was helpful to understand to some extent under which circumstances the melanin-like genes are up- or down-regulated, we can not rule out the possibility of other favorable conditions for the gene cluster activation. In a previous study, Jonkers and collaborators determine the metabolic and transcriptomic changes in *U. maydis* and *F. verticillioides* when both fungi were cocultivated. Seven of the melanin-like cluster genes (*pks5*, *orf1*, *pks4*, *vbs1*, *omt1*, *pmo1* and *cyp4*) showed slightly higher expression levels during cocultivation with *F. verticillioides* than in single cultures, suggesting that *U. maydis* could activate the melanin-like cluster in response to the presence of other competitors as *F. verticillioides* (Jonkers *et al.*, 2012). Also related to this report, the orsellinic acid gene cluster in *A. nidulans* was induced after the cocultivation with *S. hygroscopicus* (Schroeckh *et al.*, 2009). Gathering all this information, it seems reasonable to think that due to the toxic effect of orsellinic acid, *U. maydis* synthesizes it as a defense mechanism during antagonistic interactions. Further experiments need to be carried out in order to gain a better knowledge about the regulation of the melanin-like cluster in *U. maydis*.

3.6 Conclusions and Outlook

In this study we mined the *U. maydis* genome for novel secondary metabolite gene clusters. Among others, we detected a large cluster containing genes encoding for three polyketide synthases (*pks3*, *pks4* and *pks5*), several tailoring enzymes (*aox1*, *vbs1*, *omt1*, *pmo1*, *cyp4*, and *deh1*) and two transcription factors (*mtf1* and *mtf2*). Induced expression of *mtf1* but

not *mtf2* resulted in the accumulation of a dark pigment. Mass spectrometric analysis revealed that this melanin, mainly consisted of crosslinked T4HN, is an unusual finding since most fungal melanins are derived from DHN. In the DHN pathway, the T4HN generated by a PKS undergoes two reduction and two dehydration steps carried out by highly conserved enzymes in fungi but missing in the genome of *U. maydis* as T4HN reductase, T3HN reductase and scytalone dehydratase (SD).

Mutants defective for *pks3*, *pks4*, *pks5* and *cyp4* did not accumulate melanin, but MB215 $\Delta cyp4$ *Pcrg::mtf1* mutants produced OA and two of its derivatives, while MB215 $\Delta pks5$ *Pcrg::mtf1* mutants only OA. Interestingly, feeding experiment of OA rescued the melanization defect of *pks3* and *pks4* deletion mutants, suggesting that Pks3 and Pks4 generate OA, which is then used for chemical conversion into T4HN. Since deletion of the gene encoding for versicolorin B synthase (*vbs1*) results in light yellow coloring, we assume the following preliminary biosynthetic pathway. Pks3 and Pks4 catalyze together the conversion of malonyl-CoA into OA. In the presence of Pks5 orsellinic acid is not synthesized, instead, its intermediate is converted into T4HN, which is further polymerized by Cyp4 into different dimers or trimers, which will be then modified by tailoring enzymes. A second proposed model would be that the OA synthesized by Pks3 and Pks4 is converted by Pks5 and Cyp4 to T4HN, suggesting that Pks5 and Cyp4 act as molecular switchers. Afterwards, the T4HN will be the substrate of enzymes as Vbs1 and Aox1, which will assist in the polymerization of this molecule into T4HN-melanin. An important goal to understand this mechanism would be to fully reconstitute this pathway either in *S. cerevisiae* or in *A. niger*.

Since the transcription of the melanin-like cluster genes was observed under very few conditions as during pathogenic development inside of the plant tissue, on charcoal containing media and in the presence of H₂O₂, information regarding to other stress regimes or environmental signals (light, osmolarity and temperature) would contribute to understand biological context of the melanin-like cluster in *U. maydis*. Along with these experiments, the screening of potential transcriptional regulators as Tup1 would improve our understanding of the regulation process of the melanin-like gene cluster.

4 Materials and Methods

4.1 *E. coli*, *S. cerevisiae* and *U. maydis* strains

4.1.1 *E. coli* strains

For cloning of DNA either the strain DH5 α (Hanahan, 1983) or Top 10 (Invitrogen) was used.

Strain	Genotype
DH5 α	F ⁻ , endA1, hsdR17 (r _K ⁻ , m _K ⁺) supE44, thi-1, gyrA96 (Nal ^r), relA1, recA1, Δ (argF-lacIZYA)U169 (ϕ 80dlacZ Δ M15)
Top10	F ⁻ mcrA Δ (mrr-hsdRMS-mcrBC) ϕ 80lacZ Δ M15 Δ lacX74 recA1 AraD139 Δ (ara-leu)7697 galU galK rpsL (Str ^R) endA1 nupG

4.1.2 *S. cerevisiae* strains

Strain	Genotype	Reference
DF5 his1-1	MATa; his3-D200, leu2-3,2-112, lys2-801, trp1-1 (am), ura3-52, his1-1	Derivative of DF5 (Finley <i>et al.</i> , 1987), kindly provided by Prof. Dr. Hans-Ulrich Mösch.

4.1.3 *U. maydis* strains

4.1.3.1 Lab collection

Strain	Genotype	Core phase	Reference
FB1	<i>a1 b1</i>	Haploid	Banuett and Herskowitz, 1989
FB2	<i>a2 b2</i>	Haploid	Banuett and Herskowitz, 1989
MB215	<i>a2 b13</i>	Haploid	Lab collection (Hewald)
SG200	<i>a1::mfa2 bW2 bE1</i>	Haploid	Kämper <i>et al.</i> , 2006

4.1.3.2 *U. maydis* strains generated in this work.

Strain	Genotype	Transformed construct	Resistance	Recipient strain
MB215 <i>Pcrg::mtf1</i>	<i>a2 b13 Pcrg::um04101</i>	pCRG-Mtf1-Tnos-Cbx	Cbx ^R	MB215
FB1 <i>Pcrg::mtf1</i>	<i>a1 b1 Pcrg::um04101</i>	pCRG-Mtf1-Tnos-Cbx	Cbx ^R	FB1
MB215 <i>Pcrg::mtf2</i>	<i>a2 b13 Pcrg::um11110</i>	pCRG-Mtf2-Tnos-Cbx	Cbx ^R	MB215
MB215 Δ <i>pks5 Pcrg::mtf1</i>	<i>a2 b13 Δum04095 Pcrg::um04101</i>	pRS426- Δ <i>pks5</i> (G418)	Cbx ^R , G418 ^R	MB215 <i>Pcrg::mtf1</i>
MB215 Δ <i>orf1 Pcrg::mtf1</i>	<i>a2 b13 Δum04096 Pcrg::um04101</i>	pRS426- Δ <i>orf1</i> (G418)	Cbx ^R , G418 ^R	MB215 <i>Pcrg::mtf1</i>
FB1 Δ <i>pks4 Pcrg::mtf1</i>	<i>a1 b1 Δum04097 Pcrg::um04101</i>	pRS426- Δ <i>pks4</i> (Hyg)	Cbx ^R , Hyg ^R	FB1 <i>Pcrg::mtf1</i>
MB215 Δ <i>pks4 Pcrg::mtf1</i>	<i>a2 b13 Δum04097 Pcrg::um04101</i>	pRS426- Δ <i>pks4</i> (G418)	Cbx ^R , G418 ^R	MB215 <i>Pcrg::mtf1</i>
MB215 Δ Δ <i>pks4 Pcrg::mtf1</i>	<i>a2 b13 Δum04097 Pcrg::um04101</i>	pRS426- Δ <i>pks4</i> (Hyg)	Cbx ^R , G418 ^R , Hyg ^R	MB215 Δ <i>pks4</i> <i>Pcrg::mtf1</i>
MB215 Δ <i>mtf2 Pcrg::mtf1</i>	<i>a2 b13 Δum11110 Pcrg::um04101</i>	pRS426- Δ <i>mtf2</i> (G418)	Cbx ^R , G418 ^R	MB215 <i>Pcrg::mtf1</i>
MB215 Δ <i>orf3 Pcrg::mtf1</i>	<i>a2 b13 Δum04100 Pcrg::um04101</i>	pRS426- Δ <i>orf3</i> (Hyg)	Cbx ^R , Hyg ^R	MB215 <i>Pcrg::mtf1</i>
MB215 Δ <i>aox1 Pcrg::mtf1</i>	<i>a2 b13 Δum11111 Pcrg::um04101</i>	pRS426- Δ <i>aox1</i> (Hyg)	Cbx ^R , Hyg ^R	MB215 <i>Pcrg::mtf1</i>
MB215 Δ <i>vbs1 Pcrg::mtf1</i>	<i>a2 b13 Δum11112 Pcrg::um04101</i>	pRS426- Δ <i>vbs1</i> (Hyg)	Cbx ^R , Hyg ^R	MB215 <i>Pcrg::mtf1</i>
MB215 Δ <i>orf4 Pcrg::mtf1</i>	<i>a2 b13 Δum04104 Pcrg::um04101</i>	pRS426- Δ <i>orf4</i> (Hyg)	Cbx ^R , Hyg ^R	MB215 <i>Pcrg::mtf1</i>
MB215 Δ <i>pks3 Pcrg::mtf1</i>	<i>a2 b13 Δum04105 Pcrg::um04101</i>	pRS426- Δ <i>pks3</i> (Hyg)	Cbx ^R , Hyg ^R	MB215 <i>Pcrg::mtf1</i>
MB215 Δ <i>omt1 Pcrg::mtf1</i>	<i>a2 b13 Δum04106 Pcrg::um04101</i>	pRS426- Δ <i>omt1</i> (Hyg)	Cbx ^R , Hyg ^R	MB215 <i>Pcrg::mtf1</i>
MB215 Δ <i>pmo1 Pcrg::mtf1</i>	<i>a2 b13 Δum04107 Pcrg::um04101</i>	pRS426- Δ <i>pmo1</i> (Hyg)	Cbx ^R , Hyg ^R	MB215 <i>Pcrg::mtf1</i>
MB215 Δ <i>orf5 Pcrg::mtf1</i>	<i>a2 b13 Δum12253 Pcrg::um04101</i>	pRS426- Δ <i>orf5</i> (Hyg)	Cbx ^R , Hyg ^R	MB215 <i>Pcrg::mtf1</i>

MB215 $\Delta cyp4$ <i>Pcrg::mtf1</i>	<i>a2 b13 $\Delta um04109$ Pcrg::um04101</i>	pRS426- $\Delta cyp4$ (Hyg)	Cbx ^R , Hyg ^R	MB215 <i>Pcrg::mtf1</i>
MB215 $\Delta deh1$ <i>Pcrg::mtf1</i>	<i>a2 b13 $\Delta um11113$ Pcrg::um04101</i>	pRS426- $\Delta deh1$ (Hyg)	Cbx ^R , Hyg ^R	MB215 <i>Pcrg::mtf1</i>
MB215 $\Delta cyp4 \Delta vbs1$ <i>Pcrg::mtf1</i>	<i>a2 b13 $\Delta um04109$ $\Delta um11112$ Pcrg::um04101</i>	pRS426- $\Delta vbs1$ (G418)	Cbx ^R , G418 ^R , Hyg ^R	MB215 $\Delta cyp4$ <i>Pcrg::mtf1</i>
SG200 $\Delta pks5$	<i>a1::mfa2 bW2 bE1 $\Delta um04095$</i>	pRS426- $\Delta pks5$ (G418)	G418 ^R	SG200
SG200 $\Delta orf1$	<i>a1::mfa2 bW2 bE1 $\Delta um04096$</i>	pRS426- $\Delta orf1$ (G418)	G418 ^R	SG200
SG200 $\Delta pks4$	<i>a1::mfa2 bW2 bE1 $\Delta um04097$</i>	pRS426- $\Delta pks4$ (G418)	G418 ^R	SG200
SG200 $\Delta mtf2$	<i>a1::mfa2 bW2 bE1 $\Delta um11110$</i>	pRS426- $\Delta mtf2$ (G418)	G418 ^R	SG200
SG200 $\Delta orf3$	<i>a1::mfa2 bW2 bE1 $\Delta um04100$</i>	pRS426- $\Delta orf3$ (Hyg)	Hyg ^R	SG200
SG200 $\Delta mtf1$	<i>a1::mfa2 bW2 bE1 $\Delta um04101$</i>	pRS426- $\Delta mtf1$ (Hyg)	Hyg ^R	SG200
SG200 $\Delta aox1$	<i>a1::mfa2 bW2 bE1 $\Delta um11111$</i>	pRS426- $\Delta aox1$ (Hyg)	Hyg ^R	SG200
SG200 $\Delta vbs1$	<i>a1::mfa2 bW2 bE1 $\Delta um11112$</i>	pRS426- $\Delta vbs1$ (Hyg)	Hyg ^R	SG200
SG200 $\Delta orf4$	<i>a1::mfa2 bW2 bE1 $\Delta um04104$</i>	pRS426- $\Delta orf4$ (Hyg)	Hyg ^R	SG200
SG200 $\Delta pks3$	<i>a1::mfa2 bW2 bE1 $\Delta um04105$</i>	pRS426- $\Delta pks3$ (Hyg)	Hyg ^R	SG200
SG200 $\Delta omt1$	<i>a1::mfa2 bW2 bE1 $\Delta um04106$</i>	pRS426- $\Delta omt1$ (Hyg)	Hyg ^R	SG200
SG200 $\Delta pmol$	<i>a1::mfa2 bW2 bE1 $\Delta um04107$</i>	pRS426- $\Delta pmol$ (Hyg)	Hyg ^R	SG200
SG200 $\Delta orf5$	<i>a1::mfa2 bW2 bE1 $\Delta um12253$</i>	pRS426- $\Delta orf5$ (Hyg)	Hyg ^R	SG200
SG200 $\Delta cyp4$	<i>a1::mfa2 bW2 bE1 $\Delta um04109$</i>	pRS426- $\Delta cyp4$ (Hyg)	Hyg ^R	SG200
SG200 $\Delta deh1$	<i>a1::mfa2 bW2 bE1 $\Delta um11113$</i>	pRS426- $\Delta deh1$ (Hyg)	Hyg ^R	SG200
MB215 <i>Pcrg::pks1</i>	<i>a2 b13 Pcrg::um06414</i>	pCRG-Pks1-Tnos-Cbx	Cbx ^R	MB215

MB215 <i>Pcrg::pks2</i>	<i>a2 b13 Pcrg::um06418</i>	pCRG-Pks2-Tnos-Cbx	Cbx ^R	MB215
MB215 <i>Pcrg::pks3</i>	<i>a2 b13 Pcrg::um04105</i>	pCRG-Pks3-Tnos-Cbx	Cbx ^R	MB215
MB215 <i>Pcrg::pks4</i>	<i>a2 b13 Pcrg::um04097</i>	pCRG-Pks4-Tnos-Cbx	Cbx ^R	MB215
MB215 <i>Pcrg::pks5</i>	<i>a2 b13 Pcrg::um04095</i>	pCRG-Pks5-Tnos-Cbx	Cbx ^R	MB215
MB215 <i>Pcrg::cyp4</i>	<i>a2 b13 Pcrg::um04109</i>	pCRG-Cyp4-Tnos-Cbx	Cbx ^R	MB215
MB215 <i>Pcrg::vbs1</i>	<i>a2 b13 Pcrg::um11112</i>	pCRG-Vbs1-Tnos-Cbx	Cbx ^R	MB215
MB215 <i>Petef::cyp4</i>	<i>a2 b13 Petef::um04109</i>	pETEF-Cyp4-Tnos-G418	G418 ^R	MB215
MB215 <i>Pcrg::pks1</i> + <i>Pcrg::pks2</i>	<i>a2 b13 Pcrg::um06414</i> + <i>Pcrg::um06418</i>	pCRG-Pks2-Tnos-G418	Cbx ^R , G418 ^R	MB215 <i>Pcrg::pks1</i>
MB215 <i>Pcrg::pks3</i> + <i>Pcrg::pks4</i>	<i>a2 b13 Pcrg::um04105</i> + <i>Pcrg::um04097</i>	pCRG-Pks3-Tnos-G418	Cbx ^R , G418 ^R	MB215 <i>Pcrg::pks4</i>
MB215 <i>Pcrg::pks4</i> + <i>Pcrg::pks5</i>	<i>a2 b13 Pcrg::um04097</i> + <i>Pcrg::um04095</i>	pCRG-Pks4-Tnos-G418-Mig2-6	Cbx ^R , G418 ^R	MB215 <i>Pcrg::pks5</i>
MB215 <i>Pcrg::pks1</i> + <i>Petef::cyp4</i>	<i>a2 b13 Pcrg::um06414</i> + <i>Petef::um04109</i>	pETEF-Cyp4-Tnos-G418	Cbx ^R , G418 ^R	MB215 <i>Pcrg::pks1</i>
MB215 <i>Pcrg::pks2</i> + <i>Petef::cyp4</i>	<i>a2 b13 Pcrg::um06418</i> + <i>Petef::um04109</i>	pETEF-Cyp4-Tnos-G418	Cbx ^R , G418 ^R	MB215 <i>Pcrg::pks2</i>
MB215 <i>Pcrg::pks3</i> + <i>Petef::cyp4</i>	<i>a2 b13 Pcrg::um04105</i> + <i>Petef::um04109</i>	pETEF-Cyp4-Tnos-G418	Cbx ^R , G418 ^R	MB215 <i>Pcrg::pks3</i>
MB215 <i>Pcrg::pks4</i> + <i>Petef::cyp4</i>	<i>a2 b13 Pcrg::um04097</i> + <i>Petef::um04109</i>	pETEF-Cyp4-Tnos-G418	Cbx ^R , G418 ^R	MB215 <i>Pcrg::pks4</i>

MB215 <i>Pcrg::pks5</i> + <i>Petef::cyp4</i>	<i>a2 b13 Pcrg::um04095</i> + <i>Petef::um04109</i>	pETEF-Cyp4- Tnos-G418	Cbx ^R , G418 ^R	MB215 <i>Pcrg::pks5</i>
MB215 Δ <i>pk3</i> <i>Pcrg::mtf1</i> + <i>Pcrg::pks1</i>	<i>a2 b13 Δum04105</i> <i>Pcrg::um04101</i> + <i>Pcrg::um06414</i>	pCRG-Pks1- Tnos-G418	Cbx ^R , G418 ^R , Hyg ^R	MB215 Δ <i>pk3</i> <i>Pcrg::mtf1</i>
MB215 Δ <i>pk3</i> <i>Pcrg::mtf1</i> + <i>Pcrg::pks2</i>	<i>a2 b13 Δum04105</i> <i>Pcrg::um04101</i> + <i>Pcrg::um06418</i>	pCRG-Pks2- Tnos-G418	Cbx ^R , G418 ^R , Hyg ^R	MB215 Δ <i>pk3</i> <i>Pcrg::mtf1</i>
FB1 Δ <i>pks4</i> <i>Pcrg::mtf1</i> + <i>Pcrg::pks1</i>	<i>a1 b1 Δum04097</i> <i>Pcrg::um04101</i> + <i>Pcrg::um06414</i>	pCRG-Pks1- Tnos-G418	Cbx ^R , G418 ^R , Hyg ^R	FB1 Δ <i>pks4</i> <i>Pcrg::mtf1</i>
FB1 Δ <i>pks4</i> <i>Pcrg::mtf1</i> + <i>Pcrg::pks2</i>	<i>a1 b1 Δum04097</i> <i>Pcrg::um04101</i> + <i>Pcrg::um06418</i>	pCRG-Pks2- Tnos-G418	Cbx ^R , G418 ^R , Hyg ^R	FB1 Δ <i>pks4</i> <i>Pcrg::mtf1</i>
MB215 Δ <i>pks5</i> <i>Pcrg::mtf1</i> + <i>Pcrg::pks1</i>	<i>a2 b13 Δum04095</i> <i>Pcrg::um04101</i> + <i>Pcrg::um06414</i>	pCRG-Pks1- Tnos-Hyg	Cbx ^R , G418 ^R , Hyg ^R	MB215 Δ <i>pks5</i> <i>Pcrg::mtf1</i>
MB215 Δ <i>pks5</i> <i>Pcrg::mtf1</i> + <i>Pcrg::pks2</i>	<i>a2 b13 Δum04095</i> <i>Pcrg::um04101</i> + <i>Pcrg::um06418</i>	pCRG-Pks2- Tnos-Hyg	Cbx ^R , G418 ^R , Hyg ^R	MB215 Δ <i>pks5</i> <i>Pcrg::mtf1</i>
MB215 <i>Pcrg::pks1</i> + <i>Pcrg::pks3</i>	<i>a2 b13 Pcrg::um06414</i> + <i>Pcrg::um04105</i>	pCRG-Pks3- Tnos-G418	Cbx ^R , G418 ^R	MB215 <i>Pcrg::pks1</i>
MB215 <i>Pcrg::pks1</i> + <i>Pcrg::pks4</i>	<i>a2 b13 Pcrg::um06414</i> + <i>Pcrg::um04097</i>	pCRG-Pks1- Tnos-G418	Cbx ^R , G418 ^R	MB215 <i>Pcrg::pks4</i>
MB215 <i>Pcrg::pks1</i> + <i>Pcrg::pks5</i>	<i>a2 b13 Pcrg::um06414</i> + <i>Pcrg::um04095</i>	pCRG-Pks1- Tnos-G418	Cbx ^R , G418 ^R	MB215 <i>Pcrg::pks5</i>

MB215 <i>Pcrg::pks2</i> + <i>Pcrg::pks3</i>	<i>a2 b13 Pcrg::um06418</i> + <i>Pcrg::um04105</i>	pCRG-Pks2- Tnos-G418	Cbx ^R , G418 ^R	MB215 <i>Pcrg::pks3</i>
MB215 <i>Pcrg::pks2</i> + <i>Pcrg::pks4</i>	<i>a2 b13 Pcrg::um06418</i> + <i>Pcrg::um04097</i>	pCRG-Pks2- Tnos-G418	Cbx ^R , G418 ^R	MB215 <i>Pcrg::pks4</i>
MB215 <i>Pcrg::pks2</i> + <i>Pcrg::pks5</i>	<i>a2 b13 Pcrg::um06418</i> + <i>Pcrg::um04095</i>	pCRG-Pks2- Tnos-G418	Cbx ^R , G418 ^R	MB215 <i>Pcrg::pks5</i>
MB215 Δ <i>pk3</i> <i>Pcrg::mtf1</i> + <i>Ppks3::pks3</i>	<i>a2 b13 Δum04105</i> <i>Pcrg::um04101</i> + <i>Pum04105::um04105</i>	pMM69-Comp-Pks3- Tnos-G418	Cbx ^R , G418 ^R , Hyg ^R	MB215 Δ <i>pk3</i> <i>Pcrg::mtf1</i>
MB215 Δ <i>cyp4</i> <i>Pcrg::mtf1</i> + <i>Pcyp4::cyp4</i>	<i>a2 b13 Δum04109</i> <i>Pcrg::um04101</i> + <i>Pum04109::um04109</i>	pMM69-Comp-Cyp4- Tnos-G418	Cbx ^R , G418 ^R , Hyg ^R	MB215 Δ <i>cyp4</i> <i>Pcrg::mtf1</i>
MB215 Δ <i>vbs1</i> <i>Pcrg::mtf1</i> + <i>Pvbs1::vbs1</i>	<i>a2 b13 Δum11112</i> <i>Pcrg::um04101</i> + <i>Pum11112::um11112</i>	pMM69-Comp-Vbs1- Tnos-G418	Cbx ^R , G418 ^R , Hyg ^R	MB215 Δ <i>vbs1</i> <i>Pcrg::mtf1</i>
MB215 $\Delta\Delta$ <i>pks4</i> <i>Pcrg::mtf1</i> + <i>Pcrg::pks1</i>	<i>a2 b13 $\Delta\Delta$um04097</i> <i>Pcrg::um04101</i> + <i>Pcrg::um06414</i>	pCRG-Pks1- Tnos-G418	Cbx ^R , G418 ^R , Hyg ^R , Nat ^R	MB215 $\Delta\Delta$ <i>pks4</i> <i>Pcrg::mtf1</i>
MB215 $\Delta\Delta$ <i>pks4</i> <i>Pcrg::mtf1</i> + <i>Pcrg::pks2</i>	<i>a2 b13 $\Delta\Delta$um04097</i> <i>Pcrg::um04101</i> + <i>Pcrg::um06418</i>	pCRG-Pks2- Tnos-G418	Cbx ^R , G418 ^R , Hyg ^R , Nat ^R	MB215 $\Delta\Delta$ <i>pks4</i> <i>Pcrg::mtf1</i>

4.2 Plasmids and primers

4.2.1 Standard plasmids

Plasmid	Resistance	Reference
pJET1.2	Amp	Fermentas
pRS426	Amp, Ura3 (<i>S.cerevisiae</i>)	Sikorski and Hieter, 1989
pETEF-GFP-Ala6-MMXN	Amp, Cbx (<i>U. maydis</i>)	Lab collection
pCRG-GFP-Ala6-MXN	Amp, Cbx (<i>U. maydis</i>)	Lab collection
pMF1-h	Amp, Hyg (<i>U. maydis</i>)	Brachmann <i>et al.</i> , 2004
pMF1-g	Amp, G418 (<i>U. maydis</i>)	Brachmann <i>et al.</i> , 2004
pMM69	Amp, Cbx (<i>U. maydis</i>)	Provided by Marino Moretti
pETEF-GFP-Ala6-MMXN-G418	Amp, G418 (<i>U. maydis</i>)	Provided by Julia Ast
pDL64	Amp, Cbx (<i>U. maydis</i>)	Provided by Marino Moretti
pMM40	Amp, Cbx (<i>U. maydis</i>)	Provided by Marino Moretti

4.2.2 Plasmids created in this study for the transformation of *U. maydis*

pRS426- Δ *pks5* (G418)

This plasmid was used to generate a *pks5*-deletion. 500 bp of the open reading frame of the *pks5* gene were replaced by a geneticin resistance cassette.

Construct:

Left Border

MI287 *pks5* LBfw 5'-gtaacgccagggttttccagtcacgacgaatattatgactgtatcacctcctgctccattcg

MI288 *pks5* LBrv 5'-caattgtcacgcatggtggccatctaggccatcggcattccgatacgagagcgatagggc

Right Border

MI289 *pks5* RBfw 5'-gtgcggccgcattaataggcctgagtggccacaatccaacgctggaggaatcgggcgcaag

MI290 *pks5* RBrv 5'-gcggataacaatttcacacaggaaacagcaatattcgagatatgtcttaagcaagtgtcgtcc

To generate a fragment for the deletion of *pks5*, the 5' and 3' flanking regions of *pks5* were amplified by PCR with the primer combinations MI287 *pks5* LBfw/MI288 *pks5* LBrv and MI289 *pks5* RBfw/MI290 *pks5* RBrv, respectively. The PCR products together with the SfiI-geneticin resistance cassette fragment (digested from the pMF1-g vector) and the KpnI/BamHI pRS426 excised vector were introduced into *S. cerevisiae*. The plasmid pRS426- Δ *pks5* (G418) was generated by the homologous recombination between the borders, the resistance cassette and the pRS426 vector. For transformation of *U. maydis*, the plasmid was linearized with SspI.

pRS426- $\Delta orf1$ (G418)

This plasmid was used to generate a *orf1*-deletion. 406 bp of the open reading frame of the *orf1* gene was replaced by a geneticin resistance cassette.

Construct:

Left Border

MI938 *orf1* LBfw 5'-gtaacgccagggttttcccagtcacgacgaatattcaaagtgaagagagcgtcaagtataagtg

MI939 *orf1* LBrv 5'-caattgtcacgcatggtggccatctaggccagcggcatcaatgagggcccttcttcacactc

Right Border

MI940 *orf1* RBfw 5'-gtgcggccgcattaataggcctgagtggcccgattcgtttgttttcattttctaccaggatc

MI941 *orf1* RBrv 5'-gcggataacaatttcacacaggaaacagcaatattctcccacctcattccattgttgagc

To generate a fragment for the deletion of *orf1*, the 5' and 3' flanking regions of *orf1* were amplified by PCR with the primer combinations MI938 *orf1* LBfw/MI939 *orf1* LBrv and MI940 *orf1* RBfw/MI941 *orf1* RBrv, respectively. The PCR products together with the SfiI-geneticin resistance cassette fragment (digested from the pMF1-g vector) and the KpnI/BamHI pRS426 excised vector were introduced into *S. cerevisiae*. The plasmid pRS426- $\Delta orf1$ (G418) was generated by the homologous recombination between the borders, the resistance cassette and the pRS426 vector. For transformation of *U. maydis*, the plasmid was linearized with SspI.

pRS426- $\Delta pks4$ (Hyg)

This plasmid was used to generate a *pks4*-deletion. 506 bp of the reading frame of the *pks4* gene was replaced by a hygromycin resistance cassette.

Construct:

Left Border

MI469 *pks4* LBfw 5'-gtaacgccagggttttcccagtcacgacgaatattgcaggtgtgtttcgctcgaggacgccatc

MI470 *pks4* LBrv 5'-caattgtcacgcatggtggccatctaggcccaaccacctgtggcccgatactgtctcctggaac

Right Border

MI471 *pks4* RBfw 5'-gtgcggccgcattaataggcctgagtggccattcaatctttcactgtggatctacgcgaac

MI472 *pks4* RBrv 5'-gcggataacaatttcacacaggaaacagcaatattctatcttcaacgcgatgacgacagt

To generate a fragment for the deletion of *pks4*, the 5' and 3' flanking regions of *pks4* were amplified by PCR with the primer combinations MI469 *pks4* LBfw/MI470 *pks4* LBrv and MI471 *pks4* RBfw/MI472 *pks4* RBrv, respectively. The PCR products together with the SfiI-hygromycin resistance cassette fragment (digested from the pMF1-h vector) and the KpnI/BamHI pRS426 excised vector were introduced into *S. cerevisiae*. The plasmid pRS426- $\Delta pks4$ (Hyg) was generated by the homologous recombination between the borders, the resistance cassette and the pRS426 vector. For transformation of *U. maydis*, the plasmid was linearized with SspI.

pRS426- $\Delta pks4$ (G418)

This plasmid was used to generate a *pks4*-deletion. 506 bp of the reading frame of the *pks4* gene was replaced by a geneticin resistance cassette. To generate a fragment for the deletion of *pks4*, the 5' and 3' flanking regions of *pks4* were amplified by PCR with the primer combinations MI469 *pks4* LBfw/MI470 *pks4* LBrv and MI471 *pks4* RBfw/MI472 *pks4* RBrv,

respectively. The PCR products together with the SfiI-geneticin resistance cassette fragment (digested from the pMF1-g vector) and the KpnI/BamHI pRS426 excised vector were introduced into *S. cerevisiae*. The plasmid pRS426- $\Delta pks4$ (G418) was generated by the homologous recombination between the borders, the resistance cassette and the pRS426 vector. For transformation of *U. maydis*, the plasmid was linearized with SspI.

pRS426- $\Delta mtf2$ (Hyg)

This plasmid was used to generate a *mtf2*-deletion. The total open reading frame of the *mtf2* gene was replaced by a hygromycin resistance cassette.

Construct:

Left Border

MG104 *mtf2* LBfw 5'- gtaacgccagggttttccagtcacgacgaatattcttctatcaacgacttctacaagttgtc

MG105 *mtf2* LBrv 5'- caattgtcacgcatggtggccatctaggccagcaaagtacaagagcactgcggcattagatc

Right Border

MG106 *mtf2* RBfw 5'- gtgcggccgcattaataggcctgagtggccacttggttagctcgtgggtcgacgatgcccc

MG107 *mtf2* RBrv 5'- gcggataacaatttcacacaggaaacagcaatattcaggacttggaatgtggatgcgattg

To generate a fragment for the deletion of *mtf2*, the 5' and 3' flanking regions of *mtf2* were amplified by PCR with the primer combinations MG104 *mtf2* LBfw/MG105 *mtf2* LBrv and MG106 *mtf2* RBfw/MG107 *mtf2* RBrv, respectively. The PCR products together with the SfiI-hygromycin resistance cassette fragment (digested from the pMF1-h vector) and the KpnI/BamHI pRS426 excised vector were introduced into *S. cerevisiae*. The plasmid pRS426- $\Delta mtf2$ (Hyg) was generated by the homologous recombination between the borders, the resistance cassette and the pRS426 vector. For transformation of *U. maydis*, the plasmid was linearized with SspI.

pRS426- $\Delta orf3$ (Hyg)

This plasmid was used to generate a *orf3*-deletion. The total open reading frame of the *orf3* gene was replaced by a hygromycin resistance cassette.

Construct:

Left Border

MH416 *orf3* LBfw 5'-gtaacgccagggttttccagtcacgacgaatattgacgaaaccgacacggagcttgatctatatg

MH417 *orf3* LBrv 5'-caattgtcacgcatggtggccatctaggccgctgtatcatgatgcgttcgaatgaaacataaag

Right Border

MH418 *orf3* RBfw 5'-gtgcggccgcattaataggcctgagtggccaccaacagttcccagttaagttactgtacatg

MH419 *orf3* RBrv 5'-gcggataacaatttcacacaggaaacagcaatattggccgccaacgcccttttcactagac

To generate a fragment for the deletion of *orf3*, the 5' and 3' flanking regions of *orf3* were amplified by PCR with the primer combinations MH416 *orf3* LBfw/MH417 *orf3* LBrv and MH418 *orf3* RBfw/MH419 *orf3* RBrv, respectively. The PCR products together with the SfiI-hygromycin resistance cassette fragment (digested from the pMF1-h vector) and the KpnI/BamHI pRS426 excised vector were introduced into *S. cerevisiae*. The plasmid pRS426- $\Delta orf3$ (Hyg) was generated by the homologous recombination between the borders, the

resistance cassette and the pRS426 vector. For transformation of *U. maydis*, the plasmid was linearized with SspI.

pRS426- Δ mtf1 (Hyg)

This plasmid was used to generate a *mtf1*-deletion. The total open reading frame of the *mtf1* gene was replaced by a hygromycin resistance cassette.

Construct:

Left Border

MG108 mtf1 LBfw 5'- gtaacgccagggttttccagtcacgacgaatattgtctatgcaactccgaaggcggcgcg

MG109 mtf1 LBrv 5'- caattgtcacgccatggtggccatctaggccggcgttgagccaagtagcgaactaccagggg

Right Border

MG110 mtf1 RBfw 5'- gtgcggccgcattaataggcctgagtgccgctgatagattcgattgaccgtattctgtaatg

MG111 mtf1 RBrv 5'- gcggataacaatttcacacaggaacagcaatattccagaagcgaccgaccgcacatgttgctc

To generate a fragment for the deletion of *mtf1*, the 5' and 3' flanking regions of *mtf1* were amplified by PCR with the primer combinations MG108 mtf1 LBfw/MG109 mtf1 LBrv and MG110 mtf1 RBfw/MG111 mtf1 RBrv, respectively. The PCR products together with the SfiI-hygromycin resistance cassette fragment (digested from the pMF1-h vector) and the KpnI/BamHI pRS426 excised vector were introduced into *S. cerevisiae*. The plasmid pRS426- Δ mtf1 (Hyg) was generated by the homologous recombination between the borders, the resistance cassette and the pRS426 vector. For transformation of *U. maydis*, the plasmid was linearized with SspI.

pRS426- Δ aox1 (Hyg)

This plasmid was used to generate an *aox1*-deletion. The total open reading frame of the *aox1* gene was replaced by a hygromycin resistance cassette.

Construct:

Left Border

MH420 aox1 LBfw5'- gtaacgccagggttttccagtcacgacgaatattcgacacaaacctcaacgtgttcaacgttg

MH421 aox1 LBrv 5'- caattgtcacgccatggtggccatctaggcccctgtacacagtggtggtcgagcgtaaaaag

Right Border

MH422 aox1 RBfw5'- gtgcggccgcattaataggcctgagtgccaaacacaccaggtacaaagcacgtgatcctgtaaac

MH423 aox1 RBrv 5'- gcggataacaatttcacacaggaacagcaatattagacactgttggtggtgcagcggaacc

To generate a fragment for the deletion of *aox1*, the 5' and 3' flanking regions of *aox1* were amplified by PCR with the primer combinations MH420 aox1 LBfw/MH421 aox1 LBrv and MH422 aox1 RBfw/MH423 aox1 RBrv, respectively. The PCR products together with the SfiI-hygromycin resistance cassette fragment (digested from the pMF1-h vector) and the KpnI/BamHI pRS426 excised vector were introduced into *S. cerevisiae*. The plasmid pRS426- Δ aox1 (Hyg) was generated by the homologous recombination between the borders, the resistance cassette and the pRS426 vector. For transformation of *U. maydis*, the plasmid was linearized with SspI.

pRS426- $\Delta vbs1$ (Hyg)

This plasmid was used to generate a *vbs1*-deletion. The total open reading frame of the *vbs1* gene was replaced by a hygromycin resistance cassette.

Construct:

Left Border

MH424 *vbs1* LBfw 5'- gtaacgccagggttttcccagtcacgacgaatattaccacgccaggcgagagaccgttgg

MH425 *vbs1* LBrv 5'- caattgtcacgccatggtggccatctaggccctgaagaagctcagatgtctagtcagc

Right Border

MH426 *vbs1* RBfw 5'-gtgcggccgcattaataggcctgagtgccgcgtggtgatgacttcagttttactctgtac

MH427 *vbs1* RBrv 5'- gcggataacaatttcacacaggaaacagcaatattcgccagctgtcaattgtacacacctgg

To generate a fragment for the deletion of *vbs1*, the 5' and 3' flanking regions of *vbs1* were amplified by PCR with the primer combinations MH424 *vbs1* LBfw/MH425 *vbs1* LBrv and MH426 *vbs1* RBfw/MH427 *vbs1* RBrv, respectively. The PCR products together with the SfiI-hygromycin resistance cassette fragment (digested from the pMF1-h vector) and the KpnI/BamHI pRS426 excised vector were introduced into *S. cerevisiae*. The plasmid pRS426- $\Delta vbs1$ (Hyg) was generated by the homologous recombination between the borders, the resistance cassette and the pRS426 vector. For transformation of *U. maydis*, the plasmid was linearized with SspI.

pRS426- $\Delta orf4$ (Hyg)

This plasmid was used to generate a *orf4*-deletion. The total open reading frame of the *orf4* gene was replaced by a hygromycin resistance cassette.

Construct:

Left Border

MH428 *orf4* LBfw 5'- gtaacgccagggttttcccagtcacgacgaatattgacactgcttccaccaccaggccaaaac

MH429 *orf4* LBrv 5'-caattgtcacgccatggtggccatctaggccagtagcttgagggtgtacaagttcgag

Right Border

MH430 *orf4* RBfw 5'-gtgcggccgcattaataggcctgagtgccagcaactcaacgtggtccatttcaatatcaatc

MH431 *orf4* RBrv 5'-gcggataacaatttcacacaggaaacagcaatattgcttcgctcatgcctcagacgcgtccac

To generate a fragment for the deletion of *orf4*, the 5' and 3' flanking regions of *orf4* were amplified by PCR with the primer combinations MH428 *orf4* LBfw/MH429 *orf4* LBrv and MH430 *orf4* RBfw/MH431 *orf4* RBrv, respectively. The PCR products together with the SfiI-hygromycin resistance cassette fragment (digested from the pMF1-h vector) and the KpnI/BamHI pRS426 excised vector were introduced into *S. cerevisiae*. The plasmid pRS426- $\Delta orf4$ (Hyg) was generated by the homologous recombination between the borders, the resistance cassette and the pRS426 vector. For transformation of *U. maydis*, the plasmid was linearized with SspI.

pRS426- $\Delta pks3$ (Hyg)

This plasmid was used to generate a *pks3*-deletion. The total open reading frame of the *pks3* gene was replaced by a hygromycin resistance cassette.

Construct:

Left Border

MH432 pks3 LBfw 5'- gtaacgccagggttttcccagtcacgacgaatattggataagagcaagaagctgacgcaagctc
MH433 pks3 LBrv 5'-caattgtcacgccatggtggccatctaggccgccgatagattaccaatgtggctaacgctg

Right Border

MH434 pks3 RB fw 5'-gtgcggccgcattaataggcctgagtgccaaacgatcgagccaatgtgcctgacagacgctc
MH435 pks3 RB rv 5'- gcggataacaatttcacacaggaaacagcaatattctccttactcgaactgtacagccctc

To generate a fragment for the deletion of *pks3*, the 5' and 3' flanking regions of *pks3* were amplified by PCR with the primer combinations MH432 pks3 LBfw/MH433 pks3 LBrv and MH434 pks3 RBfw/MH435 pks3 RBrv, respectively. The PCR products together with the SfiI-hygromycin resistance cassette fragment (digested from the pMF1-h vector) and the KpnI/BamHI pRS426 excised vector were introduced into *S. cerevisiae*. The plasmid pRS426- Δ *pks3* (Hyg) was generated by the homologous recombination between the borders, the resistance cassette and the pRS426 vector. For transformation of *U. maydis*, the plasmid was linearized with SspI.

pRS426- Δ *omt1* (Hyg)

This plasmid was used to generate a *omt1*-deletion. The total open reading frame of the *omt1* gene was replaced by a hygromycin resistance cassette.

Construct:

Left Border

MH436 omt1 LBfw 5'-gtaacgccagggttttcccagtcacgacgaatattccgggatctcgtcgatcgcttgagctccc
MH437 omt1 LBrv 5'-caattgtcacgccatggtggccatctaggccctcaaagaaagaggctagtttccaggaaaac

Right Border

MH438 omt1 RBfw 5'-gtgcggccgcattaataggcctgagtgccgcacctcttgcaagaacgctatcgagttcttc
MH439 omt1 RBrv 5'- gcggataacaatttcacacaggaaacagcaatattcaggtgacaagcatcaccaagtagtattc

To generate a fragment for the deletion of *omt1*, the 5' and 3' flanking regions of *omt1* were amplified by PCR with the primer combinations MH436 omt1 LBfw/MH437 omt1 LBrv and MH438 omt1 RBfw/MH439 omt1 RBrv, respectively. The PCR products together with the SfiI-hygromycin resistance cassette fragment (digested from the pMF1-h vector) and the KpnI/BamHI pRS426 excised vector were introduced into *S. cerevisiae*. The plasmid pRS426- Δ *omt1* (Hyg) was generated by the homologous recombination between the borders, the resistance cassette and the pRS426 vector. For transformation of *U. maydis*, the plasmid was linearized with SspI.

pRS426- Δ *pmo1* (Hyg)

This plasmid was used to generate a *pmo1*-deletion. The total open reading frame of the *pmo1* gene was replaced by a hygromycin resistance cassette.

Construct:

Left Border

MH440 pmo1 LBfw 5'-gtaacgccagggtttccagtcacgacgaatattcagctctccaaccgagcagcccatgg

MH441 pmo1 LBrv 5'-caattgtcacgccatggtggccatctaggccgttttcaagtgccatataatcgagtaaac

Right Border:

MH442 pmo1 RBfw 5'-gtgcggccgcattaataggcctgagtggtggccccacaatcttgaagctttccctcacgcctgtc

MH443 pmo1 RBrv 5'-gcggataacaatttcacacaggaaacagcaatattgaaaacaggaatgccgcgaactagatgac

To generate a fragment for the deletion of *pmo1*, the 5' and 3' flanking regions of *pmo1* were amplified by PCR with the primer combinations MH440 pmo1 LBfw/MH441 pmo1 LBrv and MH442 pmo1 RBfw/MH443 pmo1 RBrv, respectively. The PCR products together with the SfiI-hygromycin resistance cassette fragment (digested from the pMF1-h vector) and the KpnI/BamHI pRS426 excised vector were introduced into *S. cerevisiae*. The plasmid pRS426- Δ *pmo1* (Hyg) was generated by the homologous recombination between the borders, the resistance cassette and the pRS426 vector. For transformation of *U. maydis*, the plasmid was linearized with SspI.

pRS426- Δ *orf5* (Hyg)

This plasmid was used to generate a *orf5*-deletion. The total open reading frame of the *orf5* gene was replaced by a hygromycin resistance cassette.

Construct:

Left Border

MH444 orf5 LBfw 5'-gtaacgccagggtttccagtcacgacgaatattggcagagttgagcaccactatgcggttgc

MH445 orf5 LBrv 5'-caattgtcacgccatggtggccatctaggccgtttcgtctgcagaagagctgctgtatac

Right Border:

MH446 orf5 RBfw 5'-gtgcggccgcattaataggcctgagtggtggccaacacgcgcttgatcgactcactcctcagtcctc

MH447 orf5 RBrv 5'-gcggataacaatttcacacaggaaacagcaatatttcttgaccacacccgaccatgcgcagcac

To generate a fragment for the deletion of *orf5*, the 5' and 3' flanking regions of *orf5* were amplified by PCR with the primer combinations MH444 orf5 LBfw/MH445 orf5 LBrv and MH446 orf5 RBfw/MH447 orf5 RBrv, respectively. The PCR products together with the SfiI-hygromycin resistance cassette fragment (digested from the pMF1-h vector) and the KpnI/BamHI pRS426 excised vector were introduced into *S. cerevisiae*. The plasmid pRS426- Δ *orf5* (Hyg) was generated by the homologous recombination between the borders, the resistance cassette and the pRS426 vector. For transformation of *U. maydis*, the plasmid was linearized with SspI.

pRS426- Δ *cyp4* (Hyg)

This plasmid was used to generate a *cyp4*-deletion. The total open reading frame of the *cyp4* gene was replaced by a hygromycin resistance cassette.

Construct:

Left Border

MH448 cyp4 LBfw 5'-gtaacgccagggtttccagtcacgacgaatattcgatcaacttggtggctagtcaggggc

MH449 cyp4 LBrv 5'-caattgtcacgccatggtggccatctaggccgtcgatcaacaatacacgtccacagcg

Right Border

MH450 cyp4 RBfw 5'-gtgcgggccgcattaataggcctgagtgccaccacacatctttctgcaataggcaatgcg

MH451 cyp4 RBrv 5'-gcggataacaatttcacacaggaaacagcaatattctcgacaggcagcaccgatcctgaagc

To generate a fragment for the deletion of *cyp4*, the 5' and 3' flanking regions of *cyp4* were amplified by PCR with the primer combinations MH448 cyp4 LBfw/MH449 cyp4 LBrv and MH450 cyp4 RBfw/MH451 cyp4 RBrv, respectively. The PCR products together with the SfiI-hygromycin resistance cassette fragment (digested from the pMF1-h vector) and the KpnI/BamHI pRS426 excised vector were introduced into *S. cerevisiae*. The plasmid pRS426- Δ *cyp4* (Hyg) was generated by the homologous recombination between the borders, the resistance cassette and the pRS426 vector. For transformation of *U. maydis*, the plasmid was linearized with SspI.

pRS426- Δ *deh1* (Hyg)

This plasmid was used to generate a *deh1*-deletion. The total open reading frame of the *deh1* gene was replaced by a hygromycin resistance cassette.

Construct:

Left Border

MH452 deh1 LB fw 5'-gtaacgccagggttttccagtcacgacgaatattcgatcgacgctccaatcagcggtggtgc

MH453 deh1 LBrv 5'-caattgtcacgccatggtggccatctaggccttcgtacagcttgcaagatcgagaaagcg

Right Border

MH454 deh1 RB fw 5'-gtgcgggccgcattaataggcctgagtgcccaattcagtcgacgctatccgtttgaatcgcc

MH455 deh1 RB rv 5'-gcggataacaatttcacacaggaaacagcaatattgacggctctggactcaccgccgagggag

To generate a fragment for the deletion of *deh1*, the 5' and 3' flanking regions of *deh1* were amplified by PCR with the primer combinations MH452 deh1 LBfw/MH453 deh1 LBrv and MH454 deh1 RBfw/MH455 deh1 RBrv, respectively. The PCR products together with the SfiI-hygromycin resistance cassette fragment (digested from the pMF1-h vector) and the KpnI/BamHI pRS426 excised vector were introduced into *S. cerevisiae*. The plasmid pRS426- Δ *deh1* (Hyg) was generated by the homologous recombination between the borders, the resistance cassette and the pRS426 vector. For transformation of *U. maydis*, the plasmid was linearized with SspI.

pCRG-Mtf1-Tnos-Cbx

This plasmid was used for expression of the gene *mtf1* under the control of the arabinose-inducible *crg* promoter. The carboxin resistance of the vector pCRG-GFP-Ala6-MXN was used as selection marker for *U. maydis* transformation.

Construct:

MG700 mtf1 XmaI fw 5'-gcatcccgcccatggctggaaaacgtaatcg

MG703 mtf1 NotI rv 5'-atggcgccgctcagaccacggtgttagtgcc

The open reading frame of the *mtf1* gene was amplified from genomic DNA by PCR with the primers MG700 mtf1 XmaI fw and MG703 mtf1 NotI rv, and subsequently cleaved with XmaI/NotI. This fragment was inserted into the plasmid pCRG-GFP-Ala6-MXN, which had

been digested with XmaI/NotI for deleting the GFP insert. For transformation of *U. maydis*, the plasmid was linearized with SspI.

pCRG-Mtf2-Tnos-Cbx

This plasmid was used for expression of the gene *mtf2* under the control of the arabinose-inducible *crg* promoter. The carboxin resistance of the vector pCRG-GFP-Ala6-MXN was used as selection marker for *U. maydis* transformation.

Construct:

MG554 mtf2 XmaI fw	5'-gcatcccgggatgtcttgcacaggatcgc
MG551 mtf2 NotI rv	5'-atgcgcggccgctagtgaaggcggttgccg

The open reading frame of the *mtf2* gene was amplified from genomic DNA by PCR with the primers MG554 mtf2 XmaI fw and MG551 mtf2 NotI rv, and subsequently cleaved with XmaI/NotI. This fragment was inserted into the plasmid pCRG-GFP-Ala6-MXN, which had been digested with XmaI/NotI for deleting the GFP insert. For transformation of *U. maydis*, the plasmid was linearized with SspI.

pCRG-Pks1-Tnos-Cbx

This plasmid was used for expression of the gene *pks1* under the control of the arabinose-inducible *crg* promoter. The carboxin resistance of the vector pCRG-GFP-Ala6-MXN was used as selection marker for *U. maydis* transformation.

Construct:

MI055 pks1 KpnI fw	5'- gcatggtaccccatgagcgctgctatcctcccctcg
MI056 pks1 NotI rv	5'- atggcgccgctagttagcaaggcattccg

The open reading frame of the *pks1* gene was amplified from genomic DNA by PCR with the primers MI055 pks1 KpnI fw and MI056 pks1 NotI rv, and subsequently cleaved with KpnI/NotI. This fragment was inserted into the plasmid pCRG-GFP-Ala6-MXN, which had been digested with KpnI/NotI for deleting the GFP insert. For transformation of *U. maydis*, the plasmid was linearized with SspI.

pCRG-Pks1-Tnos-Cbx-G418

This plasmid was used for expression of the gene *pks1* under the control of the arabinose-inducible *crg* promoter. The geneticin resistance of the vector pETEF-GFP-Ala6-MMXN-G418 was used as selection marker for *U. maydis* transformation.

Construct:

MI756 crg SbfI fw	5'- atatcctgcaggctgggaccataccgtgttc
MI936 pks1 AflIII rv	5'- atatttaagctagttagcaaggcattccgacagg

The *crg* promoter and the open reading frame of the *pks1* gene were amplified from the plasmid pCRG-Pks1-Tnos-Cbx (described above) with the primers MI756 crg SbfI fw and MI936 pks1 AflIII rv. The PCR product was subsequently cleaved with SbfI/AflIII and ligated with the plasmid pETEF-GFP-Ala6-MMXN-G418, which had been previously digested with SbfI/AflIII for removing the pETEF-GFP insert. For transformation of *U. maydis*, the plasmid was linearized with SspI.

pCRG-Pks1-Tnos-Cbx-Hyg

This plasmid was generated by replacing the G418 resistance cassette of the plasmid pCRG-Pks1-Tnos-Cbx-G418 for a hygromycin cassette. The plasmids pCRG-Pks1-Tnos-Cbx-G418 and pMF1-h were digested with NotI to excise the G418 and the hygromycin resistance cassettes, respectively. Subsequently, the digested plasmid and the hygromycin cassette were ligated.

pCRG-Pks2-Tnos-Cbx

This plasmid was used for expression of the gene *pks2* under the control of the arabinose-inducible *crg* promoter. The carboxin resistance of the vector pCRG-GFP-Ala6-MXN was used as selection marker for *U. maydis* transformation.

Construct:

MI10 pks2 XmaI fw	5'- gcatcccgggccatgaaggcccacggccataagg
MI11 pks2 NotI rv	5'- atggcgccgctcactcttgagcactgc

The open reading frame of the *pks2* gene was amplified from genomic DNA by PCR with the combination of primers MI10 pks2 XmaI fw and MI11 pks2 NotI rv, and subsequently cleaved with XmaI/NotI. This fragment was inserted into the plasmid pCRG-GFP-Ala6-MXN, which had been digested with XmaI/NotI for deleting the GFP insert. For transformation of *U. maydis*, the plasmid was linearized with SspI.

pCRG-Pks2-Tnos-Cbx-G418

This plasmid was used for expression of the gene *pks2* under the control of the arabinose-inducible *crg* promoter. The geneticin resistance of the vector pETEF-GFP-Ala6-MMXN-G418 was used as selection marker for *U. maydis* transformation.

Construct:

MI756 crg SbfI fw	5'- atatcctgcaggctgggaccataccgtgttgc
MI937 pks2 AflIII rv	5'- atatcttaagtcactcttgagcactgcgcacgacaagg

The *crg* promoter and the open reading frame of the *pks2* gene were amplified from the plasmid pCRG-Pks2-Tnos-Cbx (described above) with the primers MI756 crg SbfI fw and MI937 pks2 AflIII rv. The PCR product was subsequently cleaved with SbfI/AflIII and ligated with the plasmid pETEF-GFP-Ala6-MMXN-G418, which had been previously digested with SbfI/AflIII for removing the pETEF-GFP insert. For transformation of *U. maydis*, the plasmid was linearized with SspI.

pCRG-Pks2-Tnos-Cbx-Hyg

This plasmid was generated by replacing the G418 resistance cassette of the plasmid pCRG-Pks1-Tnos-Cbx-G418 for a hygromycin cassette. The plasmids pCRG-Pks2-Tnos-Cbx-G418 and pMF1-h were digested with NotI to excise the G418 and the hygromycin resistance cassettes, respectively. Subsequently, the digested plasmid and the hygromycin cassette were ligated.

pCRG-Pks3-Tnos-Cbx

This plasmid was used for expression of the gene *pks3* under the control of the arabinose-inducible *crg* promoter. The carboxin resistance of the vector pCRG-GFP-Ala6-MXN was used as selection marker for *U. maydis* transformation.

Construct:

MH701 pks3 XmaI fw	5'- gcatcccgggccatgtcaagtcaaagtttgc
MH702 pks3 NotI rv	5'- atggcggccgcctactgtgatagtggcttcg

The open reading frame of the *pks3* gene was amplified from genomic DNA by PCR with the primers MH701 pks3 XmaI fw and MH702 pks3 NotI rv, and subsequently cleaved with XmaI/NotI. This fragment was inserted into the plasmid pCRG-GFP-Ala6-MXN, which had been digested with XmaI/NotI for deleting the GFP insert. For transformation of *U. maydis*, the plasmid was linearized with SspI.

pCRG-Pks3-Tnos-Cbx-G418

This plasmid was used for expression of the gene *pks3* under the control of the arabinose-inducible *crg* promoter. The geneticin resistance of the vector pETEF-GFP-Ala6-MMXN-G418 was used as selection marker for *U. maydis* transformation.

Construct:

MI985 crg SbfI fw	5'- atatcctgcaggctgggaccataccgtgttcg
MI986 pks3 AflII rv	5'- atatcttaagaaacttattgccaatgtttg

The *crg* promoter and the open reading frame of the *pks3* gene were amplified from the plasmid pCRG-Pks3-Tnos-Cbx (described above) with the primers MI985 crg SbfI fw and MI986 pks3 AflII rv. The PCR product was subsequently cleaved with SbfI/AflII and ligated with the plasmid pETEF-GFP-Ala6-MMXN-G418, which had been previously digested with SbfI/AflII for removing the pETEF-GFP insert. For transformation of *U. maydis*, the plasmid was linearized with SspI.

pCRG-Pks4-Tnos-Cbx

This plasmid was used for expression of the gene *pks4* under the control of the arabinose-inducible *crg* promoter. The carboxin resistance of the vector pCRG-GFP-Ala6-MXN was used as selection marker for *U. maydis* transformation.

Construct:

MI593 pks4 XmaI fw	5'- gcatcccgggccatgtcttcccactcctctagtc
MH704 pks4 NotI rv	5'- cggatgagctgggatcactatag

The open reading frame of the *pks4* gene was amplified from genomic DNA by PCR with the primers MI593 pks4 XmaI fw and MH704 pks4 NotI rv, and subsequently cleaved with XmaI/NotI. This fragment was inserted into the plasmid pCRG-GFP-Ala6-MXN, which had been digested with XmaI/NotI for deleting the GFP insert. For transformation of *U. maydis*, the plasmid was linearized with SspI.

pCRG-Pks4-Tnos-G418-Mig2-6

This plasmid was used for expression of the gene *pks4* under the control of the arabinose-inducible *crg* promoter. The geneticin resistance of the vector pMM69 was used as selection marker for *U. maydis* transformation.

Construct:

MI985 <i>crg</i> SbfI fw	5' - atatcctgcaggctgggaccataccgtgttgc
MI758 <i>pks4</i> NotI rv	5' - atatgcggccgcctatgcgcaaagcatgg

The *crg* promoter and the open reading frame of the *pks4* gene were amplified from the plasmid pCRG-Pks4-Tnos-Cbx (described above) with the primers MI985 *crg* SbfI fw and MI758 *pks4* NotI rv. The PCR product was subsequently cleaved with SbfI/NotI and ligated with the plasmid pMM69, which had been previously digested with SbfI/NotI for removing the pAM1-mCherry insert. For transformation of *U. maydis*, the plasmid was linearized with EcoNI.

pCRG-Pks5-Tnos-Cbx

This plasmid was used for expression of the gene *pks5* under the control of the arabinose-inducible *crg* promoter. The carboxin resistance of the vector pDL64 was used as selection marker for *U. maydis* transformation.

Construct:

MI823 pDL64 fw	5' - cgtaggggtaggctgctgagcggccgcccggctgcag
MI824 pDL64 rv	5' - ggtgcgtatcgccggcctgcaggcatgcaagcttcagctgctcg
MI825 Pcrgr fw	5' - gctgaagcttgcattgcctgcaggcccgcgatacgcaccttgcaag
MI826 Pcrgr rv	5' - ggaggtgatacagtcattctagacgagttcaccgcaaaccctcgcg
MI827 <i>pks5</i> fw	5' - gcggtgaaactcgtctagaatgactgtatcacctcctgctcc
MI828 <i>pks5</i> rv	5' - cagccggggcgccgctcagcagcctaccctacgacgtgccccgactatgcc ggcgtagtccggcgcatc

The open reading frame of the *pks5* gene was amplified from genomic DNA by PCR with the primers MI827 *pks5* fw and MI828 *pks5* rv. The *crg* promoter and the backbone for the construction of the plasmid pCRG-Pks5-Tnos-Cbx were amplified by PCR using as a template the vectors pMM40 and pDL64, respectively. The primer combinations for each case were: MI825 Pcrgr fw/MI826 Pcrgr rv (*crg*-promoter) and MI823 pDL64 fw/MI824 pDL64 rv (backbone vector). The three PCR fragments were ligated by Gibson assembly. For transformation of *U. maydis*, the plasmid was linearized with SspI.

pCRG-Cyp4-Tnos-Cbx

This plasmid was used for expression of the gene *cyp4* under the control of the arabinose-inducible *crg* promoter. The carboxin resistance of the vector pCRG-GFP-Ala6-MXN was used as selection marker for *U. maydis* transformation.

Construct:

MI059 <i>cyp4</i> XmaI fw	5' - gcatcccgggccatgttcgctctcgaggtagatg
MI060 <i>cyp4</i> NotI rv	5' - atggcgccgctcaatcctttagtagtgatcg

The open reading frame of the *cyp4* gene was amplified from genomic DNA by PCR with the primers MI059 *cyp4* XmaI fw and MI060 *cyp4* NotI rv, and subsequently cleaved with XmaI/NotI. This fragment was inserted into the plasmid pCRG-GFP-Ala6-MXN, which had been digested with XmaI/NotI for deleting the GFP insert. For transformation of *U. maydis*, the plasmid was linearized with SspI.

pETEF-Cyp4-Tnos-Cbx-G418

This plasmid was used for expression of the gene *cyp4* under the control of the constitutive *etef* promoter. The geneticin resistance of the vector pETEF-GFP-Ala6-MMXN-G418 was used as selection marker for *U. maydis* transformation.

Construct:

MI802 cyp4 BamHI fw	5' - atatggatcccatgttcgctctcgaggtagatg
MI803 cyp4 SacIIrv	5' - atatccgcggcgaatcctttagtagtgatcg

The open reading frame of the *cyp4* gene was amplified from the plasmid pCRG-Cyp4-Tnos-Cbx (described above) with the primers MI802 cyp4 BamHI fw and MI803 cyp4 SacIIrv. The PCR product was subsequently cleaved with BamHI/SacII and ligated with the plasmid pETEF-GFP-Ala6-MMXN-G418, which had been previously digested with BamHI/SacII for removing the GFP insert. For transformation of *U. maydis*, the plasmid was linearized with SspI.

pCRG-Vbs1-Tnos-Cbx

This plasmid was used for expression of the gene *vbs1* under the control of the arabinose-inducible *crg* promoter. The carboxin resistance of the vector pCRG-GFP-Ala6-MXN was used as selection marker for *U. maydis* transformation.

Construct:

MI328 vbs1 XmaI fw	5' - gcatcccgggccatggctcaagcagctctgc
MI329 vbs1 NotIrv	5' - atggcgccgctcaatgatgataatgagaag

The open reading frame of the *vbs1* gene was amplified from genomic DNA by PCR with the primers MI328 vbs1 XmaI fw and MI329 vbs1 NotIrv, and subsequently cleaved with XmaI/NotI. This fragment was inserted into the plasmid pCRG-GFP-Ala6-MXN, which had been digested with XmaI/NotI for deleting the GFP insert. For transformation of *U. maydis*, the plasmid was linearized with SspI.

pMM69-Comp-Pks3-G418

For construction of the complementation vector pMM69-Comp-Pks3-G418, the complete gene, including its promoter as one flank (1 kb), were amplified from genomic DNA by PCR with the primers MI796 comp pks3 SbfI fw and MI797 comp pks3 NotIrv. The PCR product was subsequently cleaved with SbfI/NotI and ligated with the plasmid pMM69, which had been previously digested with SbfI/NotI for removing the pAM1-mCherry insert. For transformation of *U. maydis*, the plasmid was linearized with EcoNI.

Construct:

MI796 comp pks3 SbfI fw	5' - atactctgcagggtgacgcaagctcttagctctctc
MI797 comp pks3 NotIrv	5' - atatgcggcgctatggcccgccaagaagaacac

pMM69-Comp-Cyp4-G418

For construction of the complementation vector pMM69-Comp-Cyp4-Gen, the complete gene, including its promoter as one flank (1 kb), were amplified from genomic DNA by PCR with the primers MI798 comp cyp4 SbfI fw and MI799 comp cyp4 NotIrv. The PCR product was subsequently cleaved with SbfI/NotI and ligated with the plasmid pMM69, which had been

previously digested with SbfI/NotI for removing the pAM1-mCherry insert. For transformation of *U. maydis*, the plasmid was linearized with EcoNI.

Construct:

MI798 comp cyp4 SbfI fw 5'- atacctgcaggcgtagattcggatcaacttggtgg
 MI799 comp cyp4 NotI rv 5'- atatgcggccgctcaatccttgtagtagtgatcg

pMM69-Comp-Vbs1-G418

For construction of the complementation vector pMM69-Comp-Vbs-Gen, the complete gene, including its promoter as one flank (1 kb), were amplified from genomic DNA by PCR with the primers MI800 comp vbs1 SbfI fw and MI801 comp vbs1 NotI rv. The PCR product was subsequently cleaved with SbfI/NotI and ligated with the plasmid pMM69, which had been previously digested with SbfI/NotI for removing the pAM1-mCherry insert. For transformation of *U. maydis*, the plasmid was linearized with EcoNI.

Construct:

MI800 comp vbs1 SbfI fw 5'- atacctgcaggatattacccacgccaggcgcag
 MI801 comp vbs1 NotI rv 5'- atatgcggccgctcaatgatgataatgagaagagc

4.2.3 Primers

An additional table (Table S8) with a detailed description of primers used in this study can be found in the supplementary section at the end of this chapter.

4.3 Materials and their sources of supply

4.3.1 Laboratory equipment

Equipment	Company
Balances	Sartorius
Cell Mill	Retsch (Düsseldorf)
Centrifuges	Heraeus
Freezer, -80 °C	Eppendorf
Freezer, -20 °C	Liebherr
Refrigerator, 4 °C	Liebherr
Gel Electrophoresis Chambers	Bio-Rad
Heating Block	Eppendorf
Hot Air Oven	Heraeus
HPLC Instrument	Thermo-Scientific
Microscope	Zeiss
Nanodrop	peQlab
pH-Meter	Schott
Power Supply	Bio-Rad
Shaker	Edmund Bühler GmbH (Hechingen)
Sonicator	Bandelin electronic (Berlin)
Spectrophotometer	Eppendorf

Speed Vac-Concentrator	Eppendorf (Hamburg)
Storm 860	Amersham
Thermocycler	Biometra
Transilluminator	Eppendorf
UV-crosslinker	Stratagene
Vibrax	Kobe
Vortex	MAGV GmbH
Water Bath	GFL mbH

4.3.2 General materials

Material	Company
Baffled Flask	Ochs (Bovenden)
Blotting Paper	Roth (Karlsruhe)
Cryogenic Vials	Sarstedt (Nümbrecht)
Falcon Tubes (15 ml and 50 ml)	Sarstedt (Nümbrecht)
Filter Paper	Neolab (Heidelberg)
Glass Beads	Sigma (Deisenhofen)
Glass Vials (4 ml)	VWR (Darmstadt)
MobiSpin Columns	MoBiTec (Göttingen)
Petri Dishes	Greiner, Sarstedt (Nümbrecht)
Pipette Tips	Biozym, Sarstedt (Nümbrecht)
Plastic Cuvettes	Sarstedt (Nümbrecht)
Round-Bottom Boiling Flask (100 ml)	VWR (Darmstadt)
Screw Cap for Glass Vials	Neolab (Heidelberg)
Screw Cap for Plastic Vials	VWR (Darmstadt)
Screw Cap for Plastic Vials (0.3 ml)	VWR (Darmstadt)
Sterile Filter	Sarstedt (Nümbrecht)
Sterile Syringes and Needles	Braun (Melsungen)

4.3.3 Chemicals

Chemical	Company
Acetic Acid	Roth (Karlsruhe)
Adenine	Sigma (Deisenhofen)
Agarose	Biozym (Hessisch Oldendorf)
Alanine	Serva (Heidelberg)
Ampicillin	Roth (Karlsruhe)
Arabinose	Merck (Darmstadt)
Arginine	Sigma (Deisenhofen)
Asparagine	Sigma (Deisenhofen)
Aspartic Acid	Serva (Heidelberg)
Bacto-Agar	Difco (Detroit)
Boric Acid	Sigma (Deisenhofen)
Calcium Chloride	Merck (Darmstadt)
Carboxin	Riedle-de Haen (Seelze)

Chloroform	Roth (Karlsruhe)
Cobalt (II) Chloride	Merck (Darmstadt)
Copper Chloride	Sigma (Deisenhofen)
Copper Sulfate	Roth (Karlsruhe)
$\alpha^{32}\text{P}$ -dCTP	Hartmann Analytic
DEPC	Roth (Karlsruhe)
Deoxyribonucleotide Triphosphate (dNTPs)	Fermentas
Dimethyl Sulfoxide (DMSO)	Sigma (Deisenhofen)
Disodium Phosphate	Merck (Darmstadt)
Ethylenediaminetetraacetic Acid (EDTA)	Merck (Darmstadt)
Ethanol (Denatured)	Schmidt-GmbH (Dillenburg)
Ethanol (Undenatured)	Roth (Karlsruhe)
Ethidium Bromide	Roth (Karlsruhe)
Ethyl Acetate	Roth (Karlsruhe)
Glucose	Roth (Karlsruhe)
Glycerin	Roth (Karlsruhe)
Herring Sperm DNA	Sigma (Deisenhofen)
Hydrochloric Acid	Roth (Karlsruhe)
Histidine	Merck (Darmstadt)
Hygromycin	Duchefa Biochemie (Haarlem, NL)
Iron (III) Chloride	Roth (Karlsruhe)
Iron (III) Sulfate	Roth (Karlsruhe)
Isoleucine	Merck (Darmstadt)
Isopropanol	Roth (Karlsruhe)
L-Histidine	Roth (Karlsruhe)
Liquid Nitrogen	MPI (Marburg)
Lithium Acetate	Sigma (Deisenhofen)
L-Lysine	Merck (Darmstadt)
Magnesium Chloride	Merck (Darmstadt)
Magnesium Sulfate	Merck (Darmstadt)
Manganese Chloride	Mallinckrodt-Baker (Deventer, NL)
Methanol	VWR (Darmstadt)
Methionine	Merck (Darmstadt)
Methylene Blue	Roth (Karlsruhe)
Molybdic Acid	Sigma (Deisenhofen)
Myo-Inositol	Sigma-Aldrich
Monopotassium Phosphate	Roth (Karlsruhe)
Monosodium Phosphate	Roth (Karlsruhe)
ClonNAT	Werner BioAgents (Jena)
Nickel (II) Chloride	Merck (Darmstadt)
Nutrient Broth	Difco (Detroit, USA)
Orange G	Sigma (Deisenhofen)
Orsellinic Acid	Alfa Aesar (Heysham, England)
p-Amino-Benzoic Acid	Sigma (Deisenhofen)
Peptone	Difco (Detroit, USA)
Potassium Acetate	Merck (Darmstadt)
Potassium Chloride	Merck (Darmstadt)
Potassium Iodide	Roth (Karlsruhe)
Potassium Nitrate	Roth (Karlsruhe)
Phenol	Roth (Karlsruhe)
Phenylalanine	Merck (Darmstadt)

Polyethylene Glycol (PEG 3350)	Merck (Darmstadt)
Proline	Serva (Heidelberg)
Serine	Roth (Karlsruhe)
Sodium Acetate	Merck (Darmstadt)
Sodium Chloride	Roth (Karlsruhe)
Sodium Citrate	Roth (Karlsruhe)
Sodium Dodecyl Sulfate (SDS)	Roth (Karlsruhe)
Sodium Hydroxide	Roth (Karlsruhe)
Sodium Molybdate	Merck (Darmstadt)
Sodium Sulfate	Roth (Karlsruhe)
Sorbitol	Sigma (Deisenhofen)
Sulfuric Acid	Merck (Darmstadt)
Threonine	Sigma (Deisenhofen)
Triazol	Life Technologies
Tris	Roth (Karlsruhe)
Tryptone	GibcoBRL LT (Eggenstein)
Tryptophan	Merck (Darmstadt)
Valine	Merck (Darmstadt)
Yeast Extract	GibcoBRL LT (Eggenstein)
Yeast Nitrogen Base	Difco (Detroit, USA)
Zinc Chloride	Merck (Darmstadt)
Zinc Sulfate	Merck (Darmstadt)

4.3.4 Enzymes

Enzyme	Company
Lysozyme	Boehringer (Mannheim)
KOD Xtreme Hot Start DNA Polymerase	Novagen
Phusion-DNA-Polymerase	Lab Preparation
Restriction Endonucleases	NEB (Schwalbach), Fermentas
RNase A	Serva (Heidelberg)
T4-DNA-Ligase	Roche (Mannheim)

4.3.5 Kits used in this study

Kit	Company
Gel/PCR DNA Fragment Extraction Kit	Geneaid (Taipeh, Taiwan)
Megaprimer Labeling Kit	Amersham (Braunschweig)
ZR Plasmid Miniprep	Classic Zymo Research
Gibson Assembly	Thermo-Scientific

4.4 Cultivation methods

4.4.1 Cultivation of *E. coli*

E. coli cultures were grown in liquid dYT medium with ampicillin (100 µg/ml) and incubated at 37 °C overnight (12-18 h). Glycerin stocks were made from exponentially growing cultures and mixed with dYT-Glycerin-Medium at a 1:1 ratio, in 2 ml screw-cap culture vial, and stored at -80 °C. For growing cultures from glycerin stocks, the desired strains were streaked onto antibiotic containing dYT-agar plates and incubated at 37 °C overnight.

dYT-Medium: 16g/l Tryptone
10g/l Yeast-Extract
5g/l NaCl
in dH₂O
[Agar medium: 2% (w/v) Bactogar]
Autoclave for 20 min at 121 °C

dYT-Glycerin-Medium: 16g/l Tryptone
10g/l Yeast-Extract
5g/l NaCl
69.9 % (v/v) Glycerin
in dH₂O
Autoclave for 20 min at 121 °C

4.4.2 Cultivation of *S. cerevisiae*

S. cerevisiae strains were grown at 28 °C overnight (12-18 h) in YPD medium (Sambrook *et al.*, 1989) or in SC-Medium for auxotrophic selection. Glycerin stocks were made from early stationary phase culture and mixed with NSY-Glycerin-Medium at a 1:1 ratio, in 2 ml screw-cap culture vial, and stored at -80 °C. For growing cultures from glycerin stocks, the desired strains were streaked onto YPD- or SC-URA- agar plates and incubated at 28 °C overnight.

YPD-Medium: 10g/l Yeast-Extract
20g/l Bacto-Peptone
in dH₂O
Autoclave for 20 min at 121 °C
[Agar medium: 2% (w/v) Bactoagar]
2 % (w/v) glucose solution (filter sterilized)

NSY-Glycerin-Medium: 8g/l Nutrient Broth
5g/l Saccharose
1g/l Yeast-Extract
69.9 % (v/v) Glycerin
in dH₂O
Autoclave for 20 min at 121°C

Synthetic Complete-Medium (SC-Medium)

Dropout-Mix –His –Leu –Ade –Trp –Ura –Met

2.0 g	Alanine
2.0 g	Arginine
2.0 g	Aspartic acid
2.0 g	Asparagine
2.0 g	Cysteine
2.0 g	Glutamic acid
2.0 g	Glutamine
2.0 g	Glycine
2.0 g	Inositol
2.0 g	Isoleucine
2.0 g	Lysine

2.0 g	para-Aminobenzoic acid
2.0 g	Phenylalanine
2.0 g	Proline
2.0 g	Serine
2.0 g	Threonine
2.0 g	Tyrosine
2.0 g	Valine
1.7g/l	Yeast Nitrogen Base without (NH ₄) ₂ SO ₄
1.47g/l	Dropout-Mix (depending on the selection marker is additionally added: 0.2 g L-Histidine, 0.1 g Adenine, 0.2 g Leucin, 0.2 g Tryptophan, 0.15g Methionine or 0.2 g Uracil).
	in dH ₂ O, pH 5.6 (with NaOH)
	Autoclave for 20 min at 121 °C
	2 % (w/v) glucose solution (filter sterilized)
	[Agar medium: 2% (w/v) Bactoagar]

4.4.3 Cultivation of *U. maydis*

Ustilago maydis strains were grown at 28 °C in liquid medium (YEPS, YEPS_{light} or YNB) with shaking (200 rpm) to a density of OD₆₀₀ = 0.5 - 0.6. Glycerin stocks were prepared from exponentially growing cultures and mixed with NSY-Glycerin at a 1:1 ratio, in 2 ml screw-cap culture vial, and stored at -80 °C. For growing cultures from glycerin stocks, the desired strains were streaked onto PD-agar plates with the appropriate antibiotic [carboxin (2 µg/ml), hygromycin (200µg/ml) and geneticin (200µg/ml)] and incubated at 28 °C. For the induction of the inducible promoters, *U. maydis* strains were grown at 28 °C in YNB liquid medium (containing 0.1% of ammonium sulfate and 5% of glucose as a carbon source) to exponential phase and then shifted to YNB liquid medium with 5% arabinose instead of glucose. The cultures were centrifuged after 96 h of incubation at 28 °C.

YEPS-Liquid-Medium:	10 g/l Yeast-Extract 20 g/l Peptone 20g /l Saccharose in dH ₂ O, autoclave for 20 min at 121°C
YEPS_{light}-Liquid-Medium:	10 g/l Yeast-Extract 4 g/l Peptone 4 g/l Saccharose in dH ₂ O, autoclave for 20 min at 121°C
YNB-Liquid-Medium:	1.7 g/l Yeast Nitrogen Base 0.1% (w/v) Ammonium sulfate 5.0% (w/v) Glucose or Arabinose in dH ₂ O, adjust pH to 5.6-5.8 with NaOH Autoclave for 20 min at 121°C
PD-Agar:	24 g/l Potato Dextrose Broth 15 g/l Bactoagar in 1:1 H ₂ O with dH ₂ O, adjust pH to 5.6-5.8 with NaOH Autoclave for 20 min at 121°C

4.5 Molecular biological methods

4.5.1 Competent cell preparation and transformation of *E. coli*

A single colony from *E. coli* (Top 10 strain) was picked into 5 ml SOB-Medium and incubated overnight at 37 °C with constant shaking (250 rpm). 100 ml SOB-Medium were inoculated with 1 ml of the overnight culture and incubated at 37 °C (250 rpm) until the cells reached an OD₅₅₀=0.4 (2-3 h). Afterwards, the cells were transferred into two pre-chilled 50 ml falcon tubes and centrifuged for 10 min (4,000 rpm) at 4 °C. Once the supernatant was carefully discarded, the cell pellets were gently resuspended in 30 ml ice-cold CCMB80-Buffer and incubated for 20 min. Subsequently, the centrifugation step was repeated and the cell pellets were resuspended in 3 ml of ice-cold CCMB80-Buffer. Finally, 50-100 µl aliquots were prepared and stored at -80 °C or used immediately for transformation.

SOB-Medium: 20 g/l Bacto-Tryptone
5 g/l Bacto-Yeast-Extract
0.5 g/l NaCl
2.5 mM KCl
in dH₂O, autoclave for 20 min at 121 °C

CCMB80-Buffer: 10 mM KOAc pH 7.0
80 mM CaCl₂
20 mM MnCl₂
10 mM MgCl₂
10% (v/v) Glycerin
Adjust pH to 6.4 with HCl
in dH₂O, autoclave for 20 min at 121 °C

For a single transformation 1 aliquot of bacterial suspension was mixed with 3-5 µl of ligation product in an Eppendorff tube, equalling approximately 1-10 ng of circular plasmid DNA. Immediately, after heat shock (42 °C for 60-90 s) the tube was placed on ice for 2 min. Afterwards, the whole suspension was plated on a dYT-agar plate with ampicillin (100 µg/ml) and incubated at 37 °C over night.

4.5.2 Plasmid preparation from *E. coli*

The *E. coli* strain carrying the desired plasmid was grown in liquid dYT medium with ampicillin (100 µg/ml) overnight under shaking at 37 °C. Cells were harvested by centrifugation (30 s, 13,000 rpm) in a 1.5 ml Eppendorf tube. Depending on the purpose, two different methods were used for the DNA extraction. For high quality plasmid DNA isolation, the ZR Plasmid MiniprepTM-Classic kit was used according to manufacturer's instructions. The alternative used

method was the alkaline lysis. In brief, 100 µl of the Solution A were added into each tube and vortexed until complete resuspension of the cell pellet. 200 µl of lysis buffer (Solution B) were added and gently mixed by inverting the tubes 5-6 times. After 5 min, 150 µl ice-cold Solution C were added and mixed thoroughly (without vortexing). The tubes were incubated for 5 min on ice and centrifuged for 8 min at 13,000 rpm. Carefully, the supernatant was transferred to a new 1.5 ml labeled tube and 500 µl of a phenol:chloroform:isoamyl alcohol (25:24:1) solution were added, vortexed and centrifuged for 2 min at 13,000 rpm. The supernatant was transferred to a fresh reaction tube and 500 µl of chloroform:isoamyl alcohol (24:1) solution were added, vortexed and centrifuged for 2 min at 13,000 rpm. The supernatant was carefully removed and transferred to a new reaction tube. 1 ml of ethanol 96% was added, vortexed and incubated at RT for 2 min. After a centrifugation step (10 min, 13,000 rpm), the supernatant was removed and 1 ml of ethanol 70% was added. After a final centrifugation round (5 min, 13,000 rpm), the supernatant was carefully remove and the pellet was dissolved in 50 µl of TE buffer with RNaseA. DNA was stored at -20 °C for further analysis.

Solution A:	50 mM Glucose 25 mM Tris/HCl-Buffer pH 8.0 10 mM Na ₂ -EDTA 100 µg/ml RNase A in dH ₂ O
--------------------	---

Solution B:	200 mM NaOH 1 % (w/v) SDS in dH ₂ O
--------------------	--

Solution C:	3 M Potassium Acetate in dH ₂ O
--------------------	---

TE-RNase A Buffer:	10 mM Tris/HCl pH 8 1 mM Na ₂ -EDTA 50 µg/ml RNase A in dH ₂ O
---------------------------	---

4.5.3 Restriction enzymatic cleavage of DNA

The restriction enzymatic cleavage of DNA was performed using restriction enzymes from Fermentas or New England Biolabs (NEB). The restriction enzymes were used with the appropriate reaction conditions described by the manufacturers. The digestions were performed under optimal conditions for 2 h or overnight, depending on the subsequent application.

4.5.4 Dephosphorylation of cut plasmid-DNA

In order to prevent self-ligation of plasmid vectors in a ligation reaction, the terminal 5'-phosphate groups were removed by using alkaline phosphatase. To achieve this purpose, closed circular plasmid DNA was digested with the desired restriction enzyme (as describe above) and subsequently dephosphorylated. The reaction was prepared as below:

Linear DNA:	1 µg (~1 pmol termini)
10 X Reaction Buffer:	2 µl
Shrimp Alkaline Phosphatase:	1 µl (1 u)
H₂O (Nuclease-Free):	to 20 µl
Total Volume:	20 µl

The reaction was mixed thoroughly, spun briefly and incubated at 37 °C (30 min for 5'-overhangs or blunt ends, 60 min for 3'overhangs). Finally, the reaction was stop by heating for 15 min at 65 °C.

4.5.5 Agarose gel electrophoresis

Separation of DNA fragments was performed by agarose gel electrophoresis. The gels contained 1-2% agarose dissolved in 1xTAE buffer and 1 µg/ml ethidium bromide. 10 kb DNA ladder (Fermentas) was prepared and run in parallel to the samples. Electrophoresis was carried out in 1xTAE buffer at 90-120 V for 40-60 min. Visualization of DNA was performed by exposure to UV-light using a Dual-Intensity Transilluminator system (UVP).

TAE-Running Buffer:	40 mM Tris/HCl pH 8.3 20 mM Sodium Acetate 2 mM EDTA in dH ₂ O
----------------------------	--

10X DNA Loading Buffer:	0.2% (w/v) Orange G 50% (w/v) Saccharose 1 mM EDTA in dH ₂ O
--------------------------------	--

4.5.6 DNA extraction from agarose gel

The DNA fragments were visualized on a Dual-Intensity Transilluminator (UVP) using the low setting of UV-light. The DNA fragments were cut out from the agarose gel with a clean scalpel. Extraction of the fragments from the gel slice was performed using the Gel/PCR DNA Fragment Extraction Kit (Geneaid) following the manufacturer's protocol. DNA fragments were eluted from the spin column using nuclease-free H₂O.

4.5.7 Ligation of DNA fragments

Ligation of the DNA fragments was performed using T4 DNA ligase (Roche) with supplemented buffer. Ligation took place under optimal reaction conditions according to manufacturer's protocol. 100 ng of vector was used with the molar ratio of vector to insert set at 1:2 or 1:3. In the case of three-fragment ligation, the reaction was performed at equimolar concentrations. The total reaction volume for ligation was 20 µl. The reaction mixture was incubated at 16 °C overnight. Afterwards, 10 µl of ligated mixture was used for transformation into competent bacteria.

An alternative method used in this study for the three-fragment ligation was Gibson Assembly, using the kit from NEB. The following components were set up in a reaction on ice:

Total Amount of Fragments:	0.02-0.5 pmol
Gibson Assembly Master Mix (2X):	10 µl
Nuclease-Free H₂O:	Up to 20 µl

To calculate the number of pmols of each fragment for optimal assembly, based on fragment length and weight, the following formula was used:

$$\text{pmol} = (\text{weight in ng}) \times 1,000 / (\text{base pairs} \times 650 \text{ daltons})$$

The samples were incubated in a thermocycler at 50°C for 15 min. Following incubation, store samples on ice or at -20°C for subsequent transformation. As in the case of the ligation performed with the T4 ligase, 10 µl of the Gibson Assembly reaction were used for transformation into competent bacteria.

4.5.8 PCR amplification of DNA

DNA was amplified by PCR using the Phusion polymerase enzyme for short fragments (< 3 kb) or KOD extreme polymerase for longer fragments (> 3 kb). The reaction setups and thermocycling conditions are described for both cases below:

PCR (Phusion Polymerase)

Reaction Setup		Thermocycling Conditions	
Template DNA:	< 250 ng	1. Initial Denaturation:	95 °C, 2 min
5 X Buffer:	1 X	2. Denaturation:	95 °C, 30 s
dNTP's:	250 µM (1:1:1:1 ratio)	3. Annealing:	55 °C, 30 s
Primer Fw:	1 µM	4. Extension:	72 °C, 30 s per 1 kb
Primer Rv:	1 µM	5. Cycle from step 2 to 4:	30X
DMSO:	5 µl	6. Final Extension:	72 °C, 10 min
Phusion:	1 U	7. Storage:	4 °C
Nuclease-Free H₂O:	up to 50 µl		

PCR (KOD Extreme Polymerase)

Reaction Setup		Thermocycling Conditions	
Template DNA:	10 ng plasmid DNA	1. Initial Denaturation:	95 °C, 2 min
10 X Buffer:	1 X	2. Denaturation:	95 °C, 30 s
dNTP's:	250 µM (1:1:1:1 ratio)	3. Annealing:	65 °C, 15 s
Primer Fw:	1 µM	4. Extension:	72 °C, 30 s/kb
Primer Rv:	1 µM	5. Cycle from step 2 to 4:	40X
KOD:	1 U	6. Final Extension:	70 °C, 25 s/kb
Nuclease-Free H ₂ O:	up to 50 µl	7. Storage:	4 °C

The PCR products were agarose-gel extracted and purified as described in section 4.5.6.

4.5.9 Sequencing of DNA

DNA sequences were delivered to the MPI-Marburg and analyzed by the company Eurofins Genomics. The DNA concentration was adjusted in a total volume of 15 µl as described below:

Purified Plasmid:	50-100 ng/µl
Purified PCR products:	< 0.3 kb (2 ng/µl)
	0.3-1 kb (5 ng/µl)
	> 1 kb (10 ng/µl)

In all cases, the primer concentration was set up to 2 pmol/µl.

4.5.10 Competent cell preparation and transformation of *S. cerevisiae*

The yeast strain of interest was streaked on YPD plate and grown for 2 days at 28 °C before inoculation. Subsequently, one colony was inoculated into 10 ml YPD liquid medium and incubated overnight at 28 °C (shaking speed around 150 rpm). Afterwards, the cells were diluted to an OD₆₀₀ of 0.1 in 20 ml of YPD medium and grown for 6 h at 28 °C. Cells were harvested (2,000 rpm, 3 min), washed once with 0.5 volumes of dH₂O and once with 0.1 volumes of SORB buffer. 450 µl SORB with 50 µl of carrier DNA (salmon sperm DNA, 10 mg/ml, denatured at 100 °C for 10 min, cooled on ice). Aliquots of 45 µl were made and stored at -80 °C. Yeast cells were transformed according to the Lithium Acetate/ss DNA / PEG method proposed by Gietz and Woods (2002). Briefly, to one aliquot of yeast competent cells, the following components were added in the amount indicated:

Component	Amount
Competent Yeast Cells:	1 aliquot (45µl)
Left Border (LB):	Half of the eluted PCR product (15µl)
Right Border (RB):	Half of the eluted PCR product (15µl)
Resistance Cassette:	500 ng
Digested Plasmid pRS426:	200-400 ng
PEG-LA Buffer:	300 µl

The suspension was mixed by flipping the tube and incubated for 30 min at 28 °C and then, at 42 °C for 15 min. Cells were spun (2,000 rpm, 3 min) and resuspended in 200 µl of SC URA⁻ medium prior being spread onto an agar SC URA⁻ plate and incubated at 28 °C for 3 days.

SORB Buffer: 100 mM Lithium Acetate
10 mM Tris
1 mM EDTA
1 M Sorbitol
pH 8 (adjust with acetic acid)
in dH₂O

PEG-LA Buffer: 100 mM Lithium Acetate
10 mM Tris
1 mM EDTA
40% PEG 3350
pH 8 (adjust with acetic acid)
in dH₂O

Carrier DNA: 10 mg/ml Salmon Sperm DNA

4.5.11 Protoplast preparation and transformation of *U. maydis*

For protoplasts preparation, the desired *U. maydis* strains were grown in 50 ml of YEPS_{light} medium at 28 °C until an OD₆₀₀ of 0.3-0.8 was reached. Cells were harvested and resuspended in 25 ml of SCS buffer prior being centrifuged at 3,500 rpm for 5 min. Subsequently, cells were carefully resuspended in 2 ml SCS buffer with 20 mg/ml of lysing enzyme (filter sterilized) and incubated at RT until the 70% of the cells began to form protoplasts (constantly observed under the microscope). Then, 10 ml SCS buffer were added to each sample, centrifuged (2,300 rpm, 10 min) and the supernatant was discarded. The latter procedure was repeated three times. Cell pellets were carefully resuspended in 20 ml STC buffer, centrifuged and the supernatant was discarded. Finally, the pellets were resuspended in 500 µl of STC (ice-cold) and divided into aliquots (50 µl) and used directly for transformation or stored at -80 °C.

Transformation of *U. maydis* was performed as previously described by Schulz *et al.*, 1990. Linearized DNA (5 µg) together with 1 µl of heparin were added to the protoplast aliquot and incubated on ice for 10 min. Subsequently, 500 µl STC/PEG were added to the protoplast mix and then incubated for another 15 min on ice. In the mean time, Reg-agar plates were prepared as follows: 10 ml of the Reg-Agar, containing the selected antibiotic, were poured onto a petri-dish (bottom agar). When the agar cooled it down, another 10 ml of Reg-Agar

without antibiotic were poured on the top of the plate (top agar). Once the plates were ready, the whole mix was spread onto the surface. Plates were incubated at 28 °C for 3 to 7 days. Transformed colonies were singled-out and grown on PD-agar plates containing the appropriate antibiotic.

SCS Buffer:	20 mM Sodium Citrate Buffer pH 5.8 1 M Sorbitol in dH ₂ O
SCS-Lysing-Enzyme Buffer:	30 mg/ml Lysing-Enzyme in SCS Buffer
STC Buffer:	10 mM Tris/HCl pH 7.5 100 mM CaCl ₂ 1 M Sorbitol in dH ₂ O
STC-PEG Buffer:	40% (w/v) Polyethylenglycol/STC
Regeneration-Agar: (Reg-Agar)	10 g/l Yeast-Extract 20 g/l Peptone 2.0% (w/v) Saccharose 182.2 g/l Sorbitol 13 g/l Agar in dH ₂ O, autoclave for 20 min at 121 °C

4.5.12 Genomic DNA isolation of *U. maydis*

For genomic DNA isolation of *U. maydis*, 3 ml of YEPS_{light} were inoculated with a single colony of the selected strain and incubated overnight at 28 °C with constant shaking. Cells were harvested (13,000 rpm, 2 min) in a 2 ml Eppendorf tube. Afterwards, 500 µl of Ustilago-Lysis Buffer, 500 µl of the Phenol:Chloroform (1:1) and the equivalent of 0.2 ml of glass beads were added to each pellet. All the samples were placed on the vibrax for 15 min and then centrifuged at 13,000 rpm for 10 min. Subsequently, 400 µl of the upper phase were transferred to a fresh 1.5 ml Eppendorf tube containing 1 ml of 96% ethanol. Samples were vortexed for short time and centrifuged for 10 min at 13,000 rpm. Supernatant was removed and the pellet washed with 500 µl of 70% ethanol and centrifuged again at 13,000 rpm for 5 min. Once the supernatant was removed, the pellet was dried and resuspended in 100 µl of TE-RNase A Buffer at 50 °C on a thermomixer with constant shaking (600-800 rpm).

Ustilago-Lysis Buffer: 10 mM Tris/HCl pH 8
100 mM NaCl
1 mM EDTA
1 % (w/v) SDS
2 % (w/v) Triton X-100
in dH₂O, autoclave for 20 min at 121 °C

Phenol/Chloroform: 50% (v/v) Phenol
50% (v/v) Chloroform

TE-RNase A Buffer: 10 mM Tris/HCl pH 8
1 mM Na₂-EDTA
50 µg/ml RNase A
in dH₂O

4.5.13 *U. maydis* total RNA isolation from axenic culture

For RNA preparation, *U. maydis* cells were grown overnight at 28 °C to an OD₆₀₀=0.4 in YNB medium containing 5% glucose and 0.1% ammonium sulfate. After centrifugation (3,500 rpm, 10 min), the cells were washed and resuspended in the same volume of fresh YNB medium containing 5% arabinose and 0.1% ammonium sulfate. Cultures were grown for 4 h at 28 °C with constant shaking. Afterwards, the cells were harvested in a 50 ml falcon tube (3,500 rpm/10 min) and the supernatant was discarded. Cell pellets were immersed in liquid nitrogen for 30 s. Thereafter, 1 ml of trizol reagent was added to each sample and the cells were carefully lysed by pipetting up and down several times. Once homogenized, the solution was divided into aliquots in 1.5 ml Eppendorf tubes containing glass beads and subjected to disruption in a cell mill (15 min at maximum speed). 200 µl of chloroform were added to each sample, vortexed and incubated for 3 min at RT. Samples were centrifuged (11,000 rpm for 15 min at 4 °C) and right after, the upper aqueous phase (400-450 µl) was carefully transferred into prepared 1.5 ml Eppendorf tubes containing 500 µl of isopropanol. The samples were mixed by inverting the tube several times and incubated for 10 min at RT. Subsequently, the samples were centrifuged again (11,000 rpm for 15 min at 4 °C). The supernatant was discarded and the pellet washed with 1 ml of ethanol 80%, mixed by inverting the tube several times and centrifuged at 7,500 rpm for 10 min. Carefully, the supernatant was removed and an additional centrifugation step was carried out in order to remove residual ethanol. RNA pellets were dried at RT for 5 min, resuspended in 50-70 µl of RNase-free water and dissolved at 60 °C for 10-30 min. RNA samples were stored at -80 °C for further analysis.

4.5.14 DNA blotting and hybridization (Southern analysis)

Digested genomic DNA was separated at 90 V on a 1% agarose gel in 1X TAE. The gels were then photographed on a UV transilluminator. For depurination, the gel was shaken in 0.25 M HCl for 15 min and denatured for additional 15 min in 0.4 M NaOH solution. Capillary blot was performed to transfer DNA onto Hybond-N⁺ membranes (Sambrook *et al.*, 1989). Blotting was carried out overnight in 0.4 M NaOH. Then, the membrane was dried and cross-linked, followed by incubation in Southern hybridization buffer at 65 °C for 30 min under rotation. The Southern hybridization buffer was discarded and the radioactively labeled probe (see " Probe Labeling ") was added. The membrane was incubated in the probe solution at 65 °C overnight under rotation. After 12-24 h, the membrane was washed with the Southern Wash Buffer (25 ml) for 15 min at 65 °C. Afterwards, the buffer was discarded and the membrane was incubated with another 25 ml of Southern Wash Buffer for 15 min under the same conditions. Finally, the membrane was dried and exposed within a screen cassette for at least 4 h, followed by laser scanning (STORM Phosphorimager).

Breaking Solution: 0.25 M HCl
in dH₂O

Transfer Solution: 0.4 M NaOH
in dH₂O

Southern Hybridization Buffer: 7% (w/v) SDS
500 mM Sodium Phosphate Buffer
pH 7
in dH₂O

Southern Wash Buffer: 1% (w/v) SDS
100 mM Sodium Phosphate Buffer
pH 7
in dH₂O

4.5.15 RNA blotting and hybridization (Northern analysis)

In order to check the RNA quality, all the RNA samples were subjected to electrophoresis through 1% (w/v) agarose gel stained with ethidium bromide. The sample mix was prepared as it follows:

RNA Extract: 1 µl
10X RNA Loading Buffer: 1 µl
RNase-free water: 9 µl

The gel was run at 80 V until the fastest dye moved 2/3 of the gel length and visualized by a UV transilluminator. Prior RNA blotting, the RNA concentrations were determined using a ND-1000 spectrophotometer. Afterwards, 20 µg of each RNA sample were taken and mixed with the following components in a fresh 1.5 ml Eppendorf tube:

10X MOPS:	2 µl
Glyoxal:	2 µl
DMSO:	10 µl
RNA:	20 µg
RNase-free water:	Up to 30 µl

The mixture was incubated at 60 °C for 1 h, and then was transferred on ice for 15 min. 3 µl RNA loading buffer were added to the mixture. The RNA samples were loaded onto a 1% (w/v) agarose gel (in 1X MOPS buffer) at 90 V for 2 h in 1X MOPS buffer. Subsequently, the gel was equilibrated in 20X SSC buffer for 20 min under gentle rotation. The RNA sample in the gel was transferred to a Hybond-NX membrane in 20X SSC buffer by capillary blotting overnight. The dry membrane was UV cross-linked (Stratalinker, STRATA GENE). The membrane was stained in methylene blue solution for 5 min under gentle shaking. Next, the membrane was rinsed in dH₂O for 15 min under gentle rotation, dried and placed into a glass tube for being hybridized. Membrane was pre-hybridize with Northern hybridization buffer for 30 min at 65 °C. The buffer was discarded and the P³² labeled DNA probe (see " Probe Labeling ") was denatured by boiling and then added to the membrane to be incubated overnight at 65 °C. After 12-24 h, the membrane was washed twice with Northern Wash Buffer for 20 min at 65 °C under rotation. Finally, the membrane was dried and exposed to a cassette for at least 4 h, and then the cassette was scanned (STORM Phosphorimager).

10X MOPS Buffer:	20 mM MOPS, pH 7 50 mM Sodium Acetate 10 mM EDTA pH 7 in RNase-free water
-------------------------	---

20X SSC Buffer:	3 M NaCl 0.3 M Sodium Citrate in RNase-free water
------------------------	---

Northern Hybridization Buffer:	50 mM Sodium Phosphate Buffer, pH7 50 mM PIPES, pH 6.7 100 mM NaCl 5 % (w/v) SDS 1 mM EDTA, pH 8 pH 7 in dH ₂ O
---------------------------------------	--

Northern Wash Buffer:	1X SSC 0.1% (w/v) SDS in dH ₂ O
10X RNA Loading Buffer:	1 ml 10X MOPS 5 g Glycerin 50 mg Bromophenol Blue 50 mg Xylene Blue in 10 ml RNase-free water
Methylene Blue Solution:	300 mM Sodium Acetate 0.02 % (w/v) Methylene Blue in RNase-free water

4.5.16 Probe labeling

The generation of radioactive probes for Southern and Northern blot hybridizations was carried out with the Megaprime Labeling System Kit from Amersham Biosciences. As a first step, the DNA template to be labeled and the primer solution (random sequence hexanucleotides) were incubated at 95-100 °C for 5 min as it follows:

DNA Template (400-1000 bp):	25 ng
Primer Solution:	5 µl
diH₂O:	Up to 33 µl

Afterwards, the reaction mix was spun briefly in a microcentrifuge to bring all the contents to the bottom of the tube. Subsequently, the mix was cooled briefly on ice and 10 µl of Reaction Buffer (Buffer solution with all the dNTPs except dCTP), 2 µl of the Klenow Polymerase and 5 µl of α^{32} -P-dCTP were added. The reaction mix was then incubated at 37 °C for 1 h and stopped by the addition of 5 µl of 0.2 M EDTA. The unincorporated dNTP was removed by chromatography on Sephadex G-50 spin column. Prior hybridization, the labeled DNA was denatured by heating to 95-100 °C for 5 min.

4.5.17 Pathogenicity assays

Pathogenicity assays were performed as described by Kämper *et al.*, 2006. For maize (*Zea mays*) infections, cultures of *U. maydis* strains were grown to an OD₆₀₀ of 0.6 in YEPS_{light}, centrifuged and resuspended in distilled water to and OD₆₀₀ of 1 and injected into 7-day-old seedlings of the variety Early Golden Bantam (Olds Seeds, Madison, WI). Plants were kept in the greenhouse with a light-dark cycle of 16 h (28 °C) and 8 h (20 °C). Disease symptoms were scored according to severity 14 days after inoculation. Categories for disease were rated as

follows: (0) no symptoms; (1) chlorosis; (2) lingula swelling; (3) small tumors (<1 mm in diameter); (4) large tumors (> 1 mm in diameter), not associated with bending of stem; (5) tumors associated with bending of infected stems; and (6) dead plants.

4.6 Genetic methods

4.6.1 Generation of deletion mutants in *U. maydis*

For the generation of deletion mutants in *U. maydis*, the open reading frame (ORF) of each gene was replaced by an antibiotic-resistance cassette. The primers LBfw/LBrv and RBfw/RBv were used for amplifying by PCR ~1 kb of the 5' and 3' border regions of the ORF to be deleted, respectively. The 5' extremes of LBfw and RBv were designed with a homologous sequence to the pRS426 vector (blue), while the 5' extremes of LBv and RBfw contained a homologous sequence to the *hph* cassette (red). The method for creating a deletion construct is presented in Figure 58.

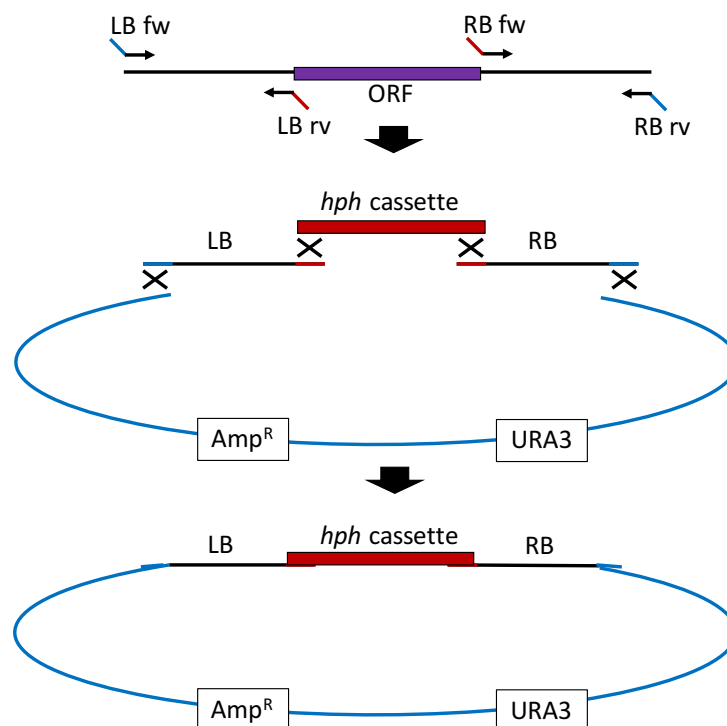


Figure 58. Strategy for creating deletion constructs in *S. cerevisiae*. The right (RB) and left (LB) border regions of the target gene are amplified separately from *U. maydis* genomic DNA with the primers LBfw/LBv and RBfw/RBv, respectively. LB and RB are cotransformed into *S. cerevisiae* along with the *hph* cassette and the gapped yeast shuttle vector. The assembly of all the DNA fragments is carried out by homologous recombination in *S. cerevisiae*.

Briefly, the four DNA fragments comprising the left and right borders of the target gene (LB and RB), the *hph* cassette, and the gapped yeast vector, were assembled in *S. cerevisiae* using endogenous homologous recombination system. A detailed protocol for yeast transformation is described in section 4.5.10. For replicating the plasmid, *E. coli* transformation was carried out with the DNA extracted from those yeast transformants that grew on selection medium (SC –URA-agar plates). After selecting the positive *E. coli* transformants, their plasmids were extracted, and the constructs (LB-resistance cassette-RB) were cut out from the plasmid and used for further transformation in *U. maydis*. The integration of the deletion construct in *U. maydis* is mediated by homologous recombination.

4.6.2 Integration of overexpressing constructs into the *ip*-locus in *U. maydis*

For the generation of overexpressing strains in *U. maydis*, a plasmid carrying the desired gene under the control of the arabinose-inducible (*P_{crg}*) or the constitutive (*P_{tef}*) promoter is integrated into the succinate dehydrogenase (*cbx* or *ip*) genomic locus. A selection of positive transformants is possible due to an amino acid substitution of histidine by leucine at position 257 in the *ip*-gene of the overexpressing vector, which confers to *U. maydis* resistance to the fungicide carboxin. Once the vector is linearized with *Ssp*I and used for transformation in *U. maydis*, both parts of the *ip*-gene are integrated into the genomic *ip*-locus by homologous recombination (Figure 59). Therefore, those transformants that are able to grow on carboxin containing PD-agar plates are considered as potential candidates for successful integration events.

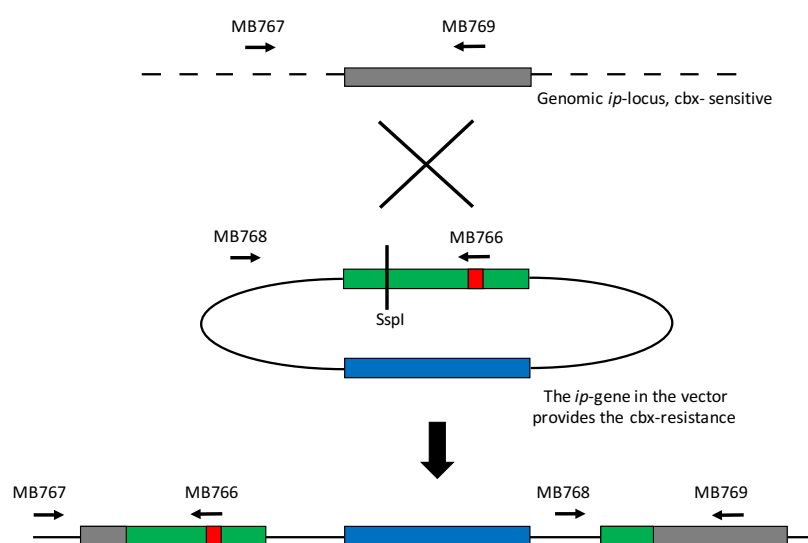


Figure 59. Integration of overexpressing plasmids into the genomic *ip*-locus in *U. maydis*. The overexpressing plasmid carrying the *ip*-gene with an amino acid substitution H257L (which confers *cbx* resistance) is linearized with *Ssp*I and integrated into the genomic *ip*-locus by homologous recombination in *U. maydis*. The combination of primers MB767/MB766 and MB768/MB769 is used to verify that the construct has been successfully integrated into the genomic *ip*-locus.

4.7 Analytical methods

4.7.1 Tricyclazole experiment

U. maydis strains were inoculated in 3 ml of YEPS_{light} medium and incubated at 28 °C ON with constant shaking. Afterwards, the cells were diluted to an OD₆₀₀ of 0.2 in 3 ml of YNB medium with 5% of glucose and 0.1% of ammonium sulfate until an OD₆₀₀ of 0.6 was reached. Subsequently, the cells were washed twice with YNB medium without any carbon source, only containing 0.1% of ammonium sulfate. Cells were immediately transferred to 3 ml volume of YNB medium with 5% of arabinose as a carbon source and 0.1% of ammonium sulfate and incubated, in the presence and absence of tricyclazole in DMSO (50 mg/l), for a 4-day period with constant shaking at 28 °C.

4.7.2 H₂O₂ sensitivity assay

To assay H₂O₂ sensitivity, *U. maydis* strains were grown in YEPS_{light} until the cells reached an OD₆₀₀ of 0.6 and 300 µl were plated on PD medium supplemented with ampicillin (100 µg/ml). Filter disks of Whatman paper (5 mm) were soaked with 2 µl of H₂O₂ (30% [v/v]) and placed on the plates. The halo sizes were measured in four duplicates after 48 h of incubation at 28 °C.

4.7.3 Orsellinic acid (OA) feeding experiment

Strains were grown in YNB medium with 0.1% ammonium sulfate and 5% glucose until they reached an OD₆₀₀=0.5-0.8. Afterwards, the cultures were centrifuged (3,500 rpm, 10 min) and the cells were washed with dH₂O, this procedure was repeated twice. Subsequently, the cells were transferred to 4 ml YNB liquid medium containing 0.1% ammonium sulfate, 5% of carbon source (glucose or arabinose) and depending on the case, with or without 0.5 mM of orsellinic acid in DMSO. Cultures were incubated with shaking for 96 h at 28 °C.

YNB-Agar:

1.7 g/l Yeast Nitrogen Base
0.1% (w/v) Ammonium sulfate
5.0% (w/v) Glucose or Arabinose
2.0% (w/v) Agar
in dH₂O, adjust pH to 5.6-5.8 with NaOH
Autoclave for 20 min at 121°C

4.7.4 Preparation of the extracts for HPLC analysis

The wild-type and mutant strains were grown in YNB medium containing 0.1% of ammonium sulfate and 5% glucose until the cells reached an $OD_{600} = 0.6-0.8$. Afterwards, the cultures were centrifuged (3,500 rpm, 10 min) and the cells were washed with dH_2O , this procedure was repeated twice before they were shifted to 30 ml liquid YNB medium with 0.1% of ammonium sulfate and 5% of arabinose as a carbon source. The strains were grown for 96 h at 28 °C with constant shaking. After completion of the incubation period, the cultures were centrifuged (3,500 rpm/ 10 min) and pellet and supernatant were collected for further analysis. For the pellet fraction, the extracts were prepared as follows. Pellets were transferred to 50 ml glass beakers and stirred with 20 ml acetone for 1 h. The extracts were filtered into 100 ml round bottom flasks and the pellets were washed with a further 10 ml acetone before being concentrated to dryness in a rotary evaporator. Dry extracts were dissolved in 2 ml methanol and transferred to 4 ml glass vials prior of being concentrated to dryness in a speed vacuum (2 h, 28 °C). Extracts were dissolved in 1 ml of methanol (HPLC grade) and centrifuged (16,000 rpm, 20 min) to ensure that no particles were injected onto the HPLC instrument. Finally, 100 μ l of the supernatant was transferred to HPLC plastic vials and subjected to analysis.

4.7.5 HPLC-MS

HPLC-MS analysis was performed with a Dionex UltiMate 3000 system coupled to a Bruker AmaZon X mass spectrometer and an Acquity UPLC BEH C18 1.7 μ m RP column (Waters).

4.8 Bioinformatic analysis

4.8.1 Sequence analysis of DNA and proteins

For the search and comparison of sequences, the following databases were used in this study: National Center of Biotechnology (NCBI; www.ncbi.nlm.nih.gov), MIPS *Ustilago maydis* Data Base (MUMDB; mips.helmholtz-muenchen.de/genre/proj/ustilago), *Saccharomyces* Genome Database (SGD; www.yeastgenome.org), UniProt (www.uniprot.org/align), and ClustalX (Larkin *et al.*, 2007).

4.8.2 Compilation of gene expression data in *U. maydis*

Examination of *U. maydis* gene expression data under a variety of conditions was performed as follows. From GEO (Gene Expression Omnibus) database a total of 144 experiments of *U. maydis*, including annotations, related to microarray platform GPL3681 were downloaded. Using information on probe-ID and chromosomal position the measured gene expression values were mapped along the genome. Each of the 144 experiments (GSM105898, GSM105899, etc.) was added as expression vector of 8,682 genes to a table column, creating thus a data matrix of 8,682 (genes) vs. 144 (samples), stored as Microsoft Excel sheet. The raw expression data were normalized by common operations: log2 transformation of values and z-score transformation along each gene, i.e. mean subtraction followed by a scaling to unit variance. Hierarchical clustering on the normalized data along samples using Euclidean distance with average linkage criterion was used for ordering the 144 experiments by similarity. The mean Pearson correlation coefficient (r) was used as a measure of similarity of co-expression of a gene with its upstream neighboring gene under all the given conditions. All the neighboring genes with an r value higher than 0.75 were considered to be coregulated. Likewise, all the groups from 3 to 13 coregulated neighboring genes were considered as a gene cluster.

5 References

Aasland, R., Stewart, A.F., and Gibson, T. (1996). The SANT domain: a putative DNA-binding domain in the SW1-SNF and ADA complexes, the transcriptional co-repressor N-CoR and TFIIB. *Trends Biochem Sci.* 21:87-88.

Abe, Y., Suzuki, J., Mizuno, T., Ono, C., Iwamoto, K., Hosobuchi, M., and Yoshikawa, H. (2002). Effect of increased dosage of the ML-236B (compactin) biosynthetic gene cluster on ML-236B production in *Penicillium citrinum*. *Mol Genet Genomics.* 268:130-137.

Ahuja, M., Chiang, Y.M., Chang, S.L., Praseuth, M.B., Entwistle, R., Sanchez, J.F., Lo, H.C., Yeh, H.H., Oakley, B.R., and Wang, C.C. (2012). Illuminating the diversity of aromatic polyketide synthases in *Aspergillus nidulans*. *J Am Chem Soc.* 134:8212-8221.

Alspaugh, J.A., Perfect, J.R., and Heitman, J. (1997). *Cryptococcus neoformans* mating and virulence are regulated by the G-protein alpha subunit GPA1 and cAMP. *Genes Dev.* 11:3206-3217.

Amagata, T., Tanaka, M., Yamada, T., Doi, M., Minoura, K., Ohishi, H., Yamori, T., and Numata, A. (2007). Variation in cytostatic constituents of a sponge-derived *Gymnascella dankaliensis* by manipulating the carbon source. *J Nat Prod.* 70:1731-1740.

An, Z., Mei, B., Yuan, W.M., and Leong, S.A. (1997). The distal GATA sequences of the *sid1* promoter of *Ustilago maydis* mediate iron repression of siderophore production and interact directly with Urbs1, a GATA family transcription factor. *EMBO J.* 16:1742-1750.

Anand, S., Prasad, M.V.R., Yadav, G., Kumar, N., Shehara, J., Ansari, M.Z., and Mohanty, D. (2010). SBSPKS: structure based sequence analysis of polyketide synthases. *Nucleic Acids Res.* 38:W487-W496.

Andersen, M.R., Nielsen, J.B., Klitgaard, A., Petersen, L.M., Zachariasen, M., Hansen, T.J., Blicher, L.H., Gotfredsen, C.H., Larsen, T.O., Nielsen, K.F., and Mortensen, U.H. (2013). Accurate prediction of secondary metabolite gene clusters in filamentous fungi. *Proc Natl Acad Sci USA.* 110:E99-E107.

Angell, S., Bench, B.J., Williams, H., and Watanabe, C.M.H. (2006). Pyocyanin isolated from a marine microbial population: synergistic production between two distinct bacterial species and mode of action. *Chem Biol.* 13:1349-1359.

Apel, K., and Hirt, H. (2004). Reactive oxygen species: Metabolism, oxidative stress, and signal transduction. *Annu Rev Plant Biol.* 55:373-399.

Argyropoulos, P., Bergeret, F., Pardin, C., Reimer, J.M., Pinto, A., Boddy, C.N., and Schmeing, T.M. (2016). Towards a characterization of the structural determinants of specificity in the macrocyclizing thioesterase for deoxyerythronolide B biosynthesis. *Biochim Biophys Acta.* 1860:486-497.

- Armaleo, D., Sun, X., and Culberson, C.** (2011). Insights from the first putative biosynthetic gene cluster for a lichen depside and depsidone. *Mycologia*. 103:741-754.
- Ávalos, J., and Limón, C.** (2015). Biological roles of fungal carotenoids. *Curr Genet*. 61:309-324.
- Baker, S.E., Kroken, S., Inderbitzin, P., Asvarak, T., Li, B., Shi, L., Yoder, O.C., and Gillian, T.** (2006). Two polyketide synthase-encoding genes are required for biosynthesis of the polyketide virulence factor, T-toxin by *Cochliobolus heterostrophus*. *Mol Plant Microbe Interact*. 19:139-149.
- Banuett, F., and Herskowitz, I.** (1989). Different *a* alleles of *Ustilago maydis* are necessary for maintenance of filamentous growth but not for meiosis. *Proc Natl Acad Sci USA*. 86:5878-5882.
- Banuett, F., and Herskowitz, I.** (1996). Discrete developmental stages during teliospore formation in the corn smut fungus, *Ustilago maydis*. *Development*. 122:2965-2976.
- Barros-Lopes, T.I., Gomes-Coelho, R., Cristiane-Yoshida, N., and Kika-Honda, N.** (2008). Radical-scavenging activity of orsellinates. *Chem Pharm Bull*. 56:1551-1554.
- Bell, A.A., and Wheeler, M.H.** (1986). Biosynthesis and functions of fungal melanins. *Annu Rev Phytopathol*. 24:411-451.
- Bennett, J.W., and Klich, M.** (2003). Mycotoxins. *Clin Microbiol Rev*. 16:497-516.
- Bergmann, S., Schümann, J., Scherlach, K., Lange, C., Brakhage, A.A., and Hertweck, C.** (2007). Genomics-driven discovery of PKS-NRPS hybrid metabolites from *Aspergillus nidulans*. *Nat Chem Biol*. 3:213-217.
- Blin, K., Medema, M.H., Kazempour, D., Fischbach, M., Breitling, R., Takano, E., and Weber, T.** (2013). AntiSMASH 2.0-a versatile platform for genome mining of secondary metabolite producers. *Nucleic Acids Res*. 41:W204-W212.
- Bode, H.B., Bethe, B., Hofs, R., and Zeeck, A.** (2002). Big effects from small changes: possible ways to explore nature's chemical diversity. *Chem Bio Chem*. 3:619-627.
- Boettger, D., and Hertweck, C.** (2013). Molecular diversity sculpted by fungal PKS-NRPS hybrids. *Chembiochem*. 14:28-42.
- Bok, J.W., and Keller, N.P.** (2004). LaeA, a regulator of secondary metabolism in *Aspergillus* spp. *Eukaryot Cell*. 3:527-535.
- Bok, J.W., Chiang, Y.M., Szewczyk, E., Reyes-Dominguez, Y., Davidson, A.D., Sanchez, J.F., Lo, H.C., Watanabe, K., Strauss, J., Oakley, B.R., Wang, C.C., and Keller, N.P.** (2009). Chromatin-level regulation of biosynthetic gene clusters. *Nat Chem Biol*. 5:462-464.
- Bok, J.W., Soukup, A.A., Chadwick, E., Chiang, Y.M., Wang, C.C., and Keller, N.P.** (2013). VeA and MvIA repression of the cryptic orsellinic acid gene cluster in *Aspergillus nidulans* involves histone 3 acetylation. *Mol Microbiol*. 89:963-974.

- Bomke, C., and Tudzynski, B.** (2009). Diversity, regulation, and evolution of the gibberellin biosynthetic pathway in fungi compared to plants and bacteria. *Phytochemistry*. 70:1876-1893.
- Boyer, L.A., Langer, M.R., Crowley, K.A., Tan S., Denu, J.M., and Peterson, C.L.** (2002). Essential role for the SANT domain in the functioning of multiple chromatin remodeling enzymes. *Mol Cell*. 10:935-942.
- Böhnert, H.U., Fudal, I., Dioh, W., Tharreau, D., Nottéghem, J.-L., and Lebrum, M.-H.** (2004). A putative polyketide synthase/peptide synthetase from *Magnaporthe grisea* signals pathogen attack to resistance rice. *Plant Cell*. 16:2499-2513.
- Bölker, M.** (2001). *Ustilago maydis* – a valuable model system for the study of fungal dimorphism and virulence. *Microbiology*. 1395-1401.
- Bölker, M., Basse, C.W., and Schirawski, J.** (2008). *Ustilago maydis* secondary metabolism—from genomics to biochemistry. *Fungal Genet Biol*. 1:S88-S93.
- Brachmann, A., Köning, J., Julius, C., and Feldbrügge, M.** (2004). A reverse genetic approach for generating gene replacement mutants in *Ustilago maydis*. *Mol Genet Genomics*. 272:216-226.
- Brakhage, A.A., and Liebmann, B.** (2005). *Aspergillus fumigatus* conidial pigment and cAMP signal transduction: significance for virulence. *Med Mycol*. 1:S75-82.
- Brakhage, A.A., Thon, M., Sprote, P., Scharf, D.H., Al-Abdallah, Q., Wolke, S.M., and Hortschansky, P.** (2009). Aspects on evolution of fungal beta-lactam biosynthesis gene clusters and recruitment of trans-acting factors. *Phytochemistry*. 70:1801-1811.
- Brakhage, A.A.** (2013). Regulation of fungal secondary metabolism. *Nat Rev Microbiol*. 11:21-32.
- Brefort, T., Doehlemann, G., Mendoza-Mendoza, A., Reissmann, S., Djamei, A., and Kahmann, R.** (2009). *Ustilago maydis* as a pathogen. *Annu Rev Phytopathol*. 47:423-445.
- Brendel, N., Laila, P., Partida-Martinez, L.P., Scherlach, K., and Hertweck, C.** (2007). A cryptic PKS-NRPS gene locus in the plant commensal *Pseudomonas fluorescens* Pf-5 codes for biosynthesis of an antimiotic rhizoxin complex. *Org Biomol Chem*. 5:2211-2213.
- Brown, D.W., Butchko, R.A.E., Busman, M., and Proctor, R.H.** (2007). The *Fusarium verticillioides* FUM gene cluster encodes a Zn(II)₂Cys₆ protein that affects FUM gene expression and fumonisin production. *Eukaryot Cell*. 6:1210-1218.
- Bruns, S., Seidler, M., Albrecht, D., Salvenmoser, S., Remme, N., Hertweck, C., Brakhage, A.A., Knemeyer, O., and Müller, F.M.** (2010). Functional genomic profiling of *Aspergillus fumigatus* biofilm reveals enhanced production of the mycotoxin gliotoxin. *Proteomics*. 10:3097-3107.
- Bumpus, S.B., Evans, B.S., Thomas, P.M., Ntai, I., and Kelleher, N.L.** (2009). A proteomics approach to discovering natural products and their biosynthetic pathways. *Nat Biotechnol*. 27:951-956.

- Bushley, K.E., and Turgeon, B.G.** (2010). Phylogenomics reveals subfamilies of fungal nonribosomal peptide synthetases and their evolutionary relationships. *BMC Evol Biol.* 10:26.
- Butcher, R.A., Schroeder, F.C., Fischbach, M.A., Straight, P.D., Kolter, R., Walsh, C.T., and Clardy, J.** (2007). The identification of bacillaene, the product of the PksX megacomplex in *Bacillus subtilis*. *Proc Natl Acad Sci. USA* 104:1506-1509.
- Byers, B. R., and Arceneaux, J.E.L.** (1998). Microbial iron transport: iron acquisition by pathogenic microorganisms. *Metal Ions Biol Syst.* 35:37-66.
- Cane, D.E., Wu, Z., Proctor, R.H., and Hohn, T.M.** (1993). Overexpression in *Escherichia coli* of soluble aristolochene synthase from *Penicillium roqueforti*. *Arch Biochem Biophys.* 304:415-419.
- Cane, D.E., and Walsh, C.T.** (1999). The parallel and convergent universes of polyketide synthases and nonribosomal peptide synthetases. *Chem Biol.* 6:R319-R325.
- Carruthers, J., Kang, I., Rynkiewicz, M., Cane, D., and Christianson, D.** (2000). Crystal structure determination of aristolochene synthase from the cheese mold, *Penicillium roquefortii*. *J Biol Chem.* 275:25533-25539.
- Chai, Y.J., Cui, C.B., Li, W.C., Wu, C.J., Tian, C.K., and Hua, W.** (2012). Activation of the dormant secondary metabolite production by introducing gentamicin-resistance in a marine-derived *Penicillium purpurogenum* G59. *Mar Drugs.* 10:559-582.
- Chan, Y.A., Podeveis, A.M., Kevany, B.M., and Thomas, M.G.** (2009). Biosynthesis of polyketide synthase extender units. *Nat Prod Rep.* 26:90-114.
- Chang, P.K., Ehrlich, K.C., Yu, J.J., Bhatnagar, D., and Cleveland, T.E.** (1995). Increased expression of *Aspergillus parasiticus* AflR, encoding a sequence-specific DNA-binding protein, relieves nitrate inhibition of aflatoxin biosynthesis. *Appl Environ Microbiol.* 61:2372-2377.
- Chen, H., Lee, M.H., Daub, M.E., and Chung, K.R.** (2007). Molecular analysis of the cercosporin biosynthetic gene cluster in *Cercospora nicotianae*. *Mol Microbiol.* 64:755-770.
- Chen, M., Shao, C.L., Fu, X.M., Xu, R.F., Zheng, J.J., Zhao, D.L., She, Z.G., and Wang, C.Y.** (2013). Bioactive indole alkaloids and phenyl ether derivatives from a marine-derived *Aspergillus* sp. *Fungus. J Nat Prod.* 76:547-553.
- Chen, H.-J., Awakawa, T., Sun, J.-Y., Wakimoto, T., and Abe, I.** (2013). Epigenetic modifier-induced biosynthesis of novel fusaric acid derivatives in endophytic fungi from *Datura stramonium* L. *Nat Prod Bioprospect.* 3:20-23.
- Cheng, Y.Q., Tang, G.L., and Shen, B.** (2002). Identification and localization of a gene cluster encoding biosynthesis of antitumor macrolactam leinamycin in *Streptomyces atroolivaceus* S-140. *J Bacteriol.* 184:7013-7024.
- Cheng, Y.Q., Tang, G.L., and Shen, B.** (2003). Type I polyketide synthase requiring a discrete acyltransferase for polyketide biosynthesis. *Proc Natl Acad Sci USA.* 100:3149-3154.

- Chiang, Y.M., Chang, S.L., Oakley, B.R., and Wang, C.C.** (2011). Recent advances in awakening silent biosynthetic gene clusters and linking orphan clusters to natural products in microorganisms. *Curr Opin Chem Biol.* 15:137-143.
- Chiang, Y.M., Oakley, C.E., Ahuja, M., Entwistle, R., Schultz, A., Chang, S., Sung, C.T., Wang, C.C.C., and Oakley, B.R.** (2013). An efficient system for heterologous expression of secondary metabolite genes in *Aspergillus nidulans*. *J Am Chem Soc.* 135:7720-7731.
- Christianson, D.W.** (2008). Unearthing the roots of the terpenome. *Curr Opin Chem Biol.* 12:141-150.
- Cichewicz, R.H.** (2010). Epigenome manipulation as a pathway to new natural scaffolds and their congeners. *Nat Prod Rep.* 27:11-22.
- Collemare, J., Billard, A., Böhnert, H.U., Lebrun, M.-H.** (2008). Biosynthesis of secondary metabolites in the rice blast fungus *Magnaporthe grisea*: the role of hybrid PKS-NRPS in pathogenicity. *Mycol Res.* 112:207-215.
- Coppin, E., and Silar, P.** (2007). Identification of PaPKS1, a polyketide synthase involved in melanin formation and its use as a genetic tool in *Podospora anserina*. *Mycol Res.* 111:901-908.
- Cox, R.J., Gold, F., Hurley, D., Lazarus, C.M., Nicholson, T.P., Rudd, B.A., Simpson, T.J., Wilkinson, B., and Zhang, Y.** (2004). Rapid cloning and expression of fungal polyketide synthase gene involved in squalestatin biosynthesis. *Chem Commun (Camb).* 2004:2260-2261.
- Cox, R.J., and Simpson, T.J.** (2009). Fungal type I polyketide synthases. *Methods Enzymol.* 459:49-78.
- Coyle, S.M., Gilbert, W.V., and Doudna, J.A.** (2009). Direct link between RACK1 function and localization at the ribosome *in vivo*. *Mol Cell Biol.* 29:1626-1634.
- Cramer, R.A. Jr., Gamcsik, M.P., Brooking, R.M., Najvar, L.K., Kirkpatrick, W.R., Patterson, T.F., Balibar, C.J., Graybill, J.R., Perfect, J.R., Abraham, S.N., and Steinbach, W.J.** (2006). Disruption of a nonribosomal peptide synthetase in *Aspergillus fumigatus* eliminates gliotoxin production. *Eukaryot Cell.* 5:972-980.
- Cray, J.A., Bell, A.N.W., Bhaganna, P., Mswaka, A.Y., Timson, D.J., and Hallsworth, J.E.** (2013). The biology of habitat dominance; can microbes behave as weeds? *Microb Biotechnol.* 6:453-492.
- Cueto, M., Jensen, P.R., Kauffman, C., Fenical, W., Lobkovsky, E., and Clardy, J.** (2001). Pestalone, a new antibiotic produced by a marine fungus in response to bacterial challenge. *J Nat Prod.* 64:1444-1446.
- da Silva M.B., Thomaz, L., Marques, A.F., Svidzinski, A.E., Nosanchuk, J.D., Casadevall, A., Travassos, L.R., and Taborda, C.P.** (2009). Resistance of melanized yeast cells of *Paracoccidioides brasiliensis* to antimicrobial oxidants and inhibition of phagocytosis using carbohydrates and monoclonal antibody to CD18. *Mem Inst Oswaldo Cruz.* 104:644-648.

- Doehlemann, G., Wahl, R., Horst, R.J., Voll, L.M., Usadel, B., Poree, F., Stitt, M., Pons-Kühnemann, J., Sonnewald, U., Kahmann, R., and Kämper, J.** (2008). Reprogramming a maize plant: transcriptional and metabolic changes induced by the fungal biotroph *Ustilago maydis*. *Plant J.* 56:181-195.
- Dorrestein, P.C., and Kelleher, N.L.** (2006). Dissecting non-ribosomal and polyketide biosynthetic machineries using electrospray ionization Fourier-transform mass spectrometry. *Nat Prod Rep.* 23:893-918.
- dos Santos, V.M., Dorner, J.W., and Carreira, F.** (2003). Isolation and toxigenicity of *Aspergillus fumigatus* from moldy silage. *Mycopathologia.* 156:133-138.
- Dowzer, C.E., and Kelly, J.M.** (1989). Cloning of the *creA* gene from *Aspergillus nidulans*: a gene involved in carbon catabolite repression. *Curr Genet.* 15:457-459.
- Doyle, C.E., Cheung, H.Y.K., Spence, K.L., and Saville, B.J.** (2016). Unh1, an *Ustilago maydis* Ndt80-like protein, controls completion of tumor maturation, teliospore development, and meiosis. *Fungal Genet Biol.* 94:54-68.
- Du, L., and Lou, L.** (2010). PKS and NRPS release mechanisms. *Nat Prod Rep.* 27:255-278.
- Dunn, B.J., Cane, D.E., and Khosla, C.** (2013). Mechanism and specificity of an acyltransferase domain from a modular polyketide synthase. *Biochemistry.* 52:1839-1841.
- Eichhorn, H., Lessing, F., Winterberg, B., Schirawski, J., Kämper, J., Müller, P., and Kahmann, R.** (2006). A ferroxidation/permeation iron uptake system is required for virulence in *Ustilago maydis*. *Plant Cell.* 18:3332-3345.
- Eisenman, H.C., and Casadevall, A.** (2012). Synthesis and assembly of fungal melanin. *Appl Microbiol Biotechnol.* 93:931-940.
- Eley, K.L., Halo, L.M., Song, Z., Powles, H., Cox, R.J., Bailey, A.M., Lazarus, C.M., and Simpson, T.J.** (2007). Biosynthesis of the 2-pyridone tenellin in the insect pathogenic fungus *Beauveria bassiana*. *Chembiochem.* 8:289-297.
- Elías-Villalobos, A., Fernández-Álvarez, A., and Ibeas, J.I.** (2011). The general transcription factor repressor Tup1 is required for dimorphism and virulence in a fungal plant pathogen. *PLoS Pathog.* 7:e1002235.
- Estrada, A.F., Brefort, T., Mengel, C., Díaz-Sánchez, V., Alder, A., Al-Babili, S., and Avalos, J.** (2010). *Ustilago maydis* accumulates β -carotene at levels determined by retinal-forming carotenoid oxygenase. *Fungal Genet Biol.* 46:803-813.
- Evans, B.S., Robinson, S.J., and Kelleher, N.L.** (2011). Surveys of non-ribosomal peptide and polyketide assembly lines in fungi and prospects for their analysis *in vitro* and *in vivo*. *Fungal Genet Biol.* 48:49-61.
- Feng, P., Shang, Y., Cen, K., and Wang, C.** (2015). Fungal biosynthesis of the bibenzoquinone oosporein to evade insect immunity. *Proc Natl Acad Sci USA.* 112:11365-11370.

- Fernandes, M., Keller, N.P., and Adams, T.H.** (1998). Sequence-specific binding by *Aspergillus nidulans* AflR, a C6 zinc cluster protein regulating mycotoxin biosynthesis. *Mol Microbiol.* 28:1355-1365.
- Fetzner, R., Seither, K., Wenderoth, M., Herr, A., and Fischer, R.** (2014). *Alternaria alternata* transcription factor CmrA controls melanization and spore development. *Microbiology.* 160:1845-1854.
- Finking, R., and Marahiel, M.A.** (2004). Biosynthesis of nonribosomal peptides 1. *Annu Rev Microbiol.* 58:453-488.
- Finley, D., Ozkaynak, E., and Varshavsky, A.** (1987). The yeast polyubiquitin gene is essential for resistance to high temperatures, starvation, and other stresses. *Cell.* 48:1035-1046.
- Fisch, K.M., Gillaspay, A.F., Gipson, M., Henrikson, J.C., Hoover, A.R., Jackson, L., Najar, F.Z., Wägele, H., and Cichewicz, R.H.** (2009). Chemical induction of silent biosynthetic pathway transcription in *Aspergillus niger*. *J Ind Microbiol Biotechnol.* 36:1199-1213.
- Fischer, M.J.C., Rustenhloz, C., Leh-Louis, V., and Perrière, G.** (2015). Molecular and functional evolution of the fungal diterpene synthase genes. *BMC Microbiol.* 15:221.
- Flaherty, J.E., and Woloshuk, C.P.** (2004). Regulation of fumonisin biosynthesis in *Fusarium verticillioides* by a zinc binuclear cluster-type gene, ZFR1. *Appl Environ Microbiol.* 70:2653-2659.
- Fleck, C.B., and Brock, M.** (2010). *Aspergillus fumigatus* catalytic glucokinase and hexokinase: expression analysis and importance for germination, growth and conidiation. *Eukaryot. Cell.* 9:1120-1135.
- Flieger, M., Wurst, M., and Shelby, R.** (1997). Ergot alkaloids-sources, structures and analytical methods. *Folia Microbiol (Praha).* 42:3-30.
- Forseth, R.R., Amaike, S., Schwenk, D., Affeldt, K.J., Hoffmeister, D., Schroeder, F.C., and Keller, N.P.** (2013). Homologous NRPS-like gene clusters mediate redundant small-molecule biosynthesis in *Aspergillus flavus*. *Angew Chem Int Ed Engl.* 52:1590-1594.
- Fossati, E., Ekins, A., Narcross, L., Zhu, Y., Falgoutyret, J.P., Beaudoin, G.A., Facchini, P.J., Martin, V.J.** (2014). Reconstitution of a 10-gene pathway for synthesis of the plant alkaloid dihydrosanguinarine in *Saccharomyces cerevisiae*. *Nat Commun.* 5:3283.
- Fox, E.M., Gardiner, D.M., Keller, N.P., and Howlett, B.J.** (2008). A Zn(II)₂Cys₆ DNA binding protein regulates the sirodesmin PL biosynthetic gene cluster in *Leptosphaeria maculans*. *Fungal Genet Biol.* 45:671-682.
- Fujii, I., Ono, Y., Tada, H., Gomi, K., Ebizuka, Y., and Sankawa, U.** (1996). Cloning of the polyketide synthase gene atX from *Aspergillus terreus* and its identification as the 6-methylsalicylic acid synthase gene by heterologous expression. *Mol Gen Genet.* 253:1-10.
- Fujii, I., Mori, Y., Watanabe, A., Kubo, Y., Tsuji, G., and Ebizuka, Y.** (1999). Heterologous expression and product identification of *Colletotrichum lagenarium* polyketide synthase

encoded by the *PKS1* gene involved in melanin biosynthesis. *Biosci Biotechnol Biochem.* 63:1445-1452.

Fujii, I., Yasuoka, Y., Tsai, H.F., Chang, Y.C., Kwon-Chung, K.J., and Ebizuka, Y. (2004). Hydrolytic polyketide shortening by *Ayg1p*, a novel enzyme involved in fungal melanin biosynthesis. *J Biol Chem.* 279:44613-44620.

Funa, N., Ohnishi, Y., Fujii, I., Shibuya, M., Ebizuka, Y., and Horinouchi, S. (1999). A new pathway for polyketide synthesis in microorganisms. 400: 897-899.

Funa, N., Funabashi, M., Ohnishi, Y., and Horinouchi, S. (2005). Biosynthesis of hexahydroxyperylenequinone melanin via oxidative aryl coupling by cytochrome P-450 in *Streptomyces griseus*. (2005). *J Bacteriol.* 187:8149-8155.

Gachomo, E.W., Seufferheld, M.J., and Kotchoni, S.O. (2010). Melanization of appressoria is critical for the pathogenicity of *Diplocarpon rosae*. *Mol Biol Rep.* 37:3583-3591.

Gao, X., Wang, P., and Tang, Y. (2010). Engineered polyketide biosynthesis and biocatalysis. *Appl Microbiol Biotechnol.* 88:1233-1242.

García-Pedrajas, M.D., Baeza-Montañez, L., and Gold, S.E. (2010). Regulation of *Ustilago maydis* dimorphism, sporulation, and pathogenic development by a transcription factor with a highly conserved APSES domain. *Mol Plant Microbe Interact.* 23:211-222.

Gardiner, D.M., Jarvis, R.S., and Howlett, B.J. (2005). The ABC transporter gene in the sirodesmin biosynthetic gene cluster of *Leptosphaeria maculans* is not essential for sirodesmin production but facilitates self-protection. *Fungal Genet Biol.* 42:257-263.

Geib, E., Gressler, M., Viediernikova, I., Hillmann, F., Jacobsen, I.D., Nietzsche, S., Hertweck, C., and Brock M. (2016). A non-canonical melanin biosynthesis pathway protects *Aspergillus terreus* conidia from environmental stresses. *Cell Chem Biol.* 23: 587-597.

Geiser, E., Przybilla, S.K., Friedrich, A., Buckel, W., Wierckx, N., Blank, L.M., and Bölker, M. (2016) *Ustilago maydis* produces itaconic acid via the unusual intermediate *trans*-aconitate. *Microb Biotechnol.* 9:116-126.

Georgiou, C.D., Zervoudakis, G., Tairis, N., and Kornaros, M. (2001). β -carotene production and its role in sclerotial differentiation of *Sclerotium rolfsii*. *Fungal Genet Biol.* 34:11-20.

Gerke, J., Bayram, O., Feussner, K., Landesfeind, M., Shelest, E., Feussner, I. and Braus, G.H. (2012). Breaking the silence: protein stabilization uncovers silenced biosynthetic gene clusters in the fungus *Aspergillus nidulans*. *Appl Environ Microbiol.* 78:8234-8244.

Gietz, R.D., and Woods, R.A. (2002). Transformation of yeast by lithium acetate/single-stranded carrier DNA/polyethylene glycol method. *Methods Enzymol.* 350:87-96.

Gitterman, C.O. (1965). Antitumor, cytotoxic, and antibacterial activities of tenuazonic acid and congeneric tetramic acids. *J Med Chem.* 8:483-486.

- Gold, S., Duncan, G., Barrett, K., and Kronstad, J.** (1994). cAMP regulates morphogenesis in the fungal pathogen *Ustilago maydis*. *Genes Dev.* 8:2805-2816.
- Golinski, P., and Chelkowski, J.** (1992). Biosynthesis of fusarin C by *Fusarium* species. *Microbiol Aliments Nutr.* 10:55-59.
- Gontang, E.A., Gaudencio, S.P., Fenical, W., and Jensen, P.R.** (2010). Sequence-based analysis of secondary-metabolite biosynthesis in marine actinobacteria. *Appl Environ Microbiol.* 76:2487-2499.
- González-Collado, I., Macías-Sánchez, A.J., and Hanson, H.R.** (2007). Fungal terpene metabolites: biosynthetic relationships and the control of the phytopathogenic fungus *Botrytis cinerea*. *Nat Prod Rep.* 24:674-686.
- Grandel, A., Romeis, T., and Kämper, J.** (2000). Regulation of pathogenic development in the corn smut fungus *Ustilago maydis*. *Mol Plant Pathol.* 1:61-66.
- Gressler, M., Hortschansky, P., Geib, E., and Brock, M.** (2015). A new high-performance heterologous fungal expression system based on regulatory elements from the *Aspergillus terreus* terrein gene cluster. *Front Microbiol.* 6:184.
- Gressler, M., Meyer, F., Heine, D., Hortschansky, P., Hertweck, C., and Brock, M.** (2015). Phytotoxin production in *Aspergillus terreus* is regulated by independent environmental signals. *eLife.* 4:e07861.
- Grimaldi, B., Pierluca, C., Filetici, P., Berge, E., Dobosy, J.R., Freitag, M., Selker, E.U., and Ballario, P.** (2006). The *Neurospora crassa* White Collar-1 dependent blue light response requires acetylation of histone H3 lysine 14 by NGF-1. *Mol Biol Cell.* 17:4576-4583.
- Gross, H., Stockwell, V.O., Henkels, M.D., Nowak-Thompson, B., Loper, J.E., and Gerwick, W.H.** (2007). The genomisotopic approach: a systematic method to isolate products of orphan biosynthetic gene clusters. *Chem Biol.* 14:53-63.
- Guo, J.-P., Zhu, C.-Y., Zhang, C.-P., Chu, Y.-S., Wang, Y.-L., Zhang, J.-X., Wu, D.-K., Zhang, K.-Q., and Niu, X.-M.** (2012). Thermolides, potent nematocidal PKS-NRPS hybrid metabolites from thermophilic fungus *Talomyces thermophilus*. *J Am Chem Soc.* 134:20306-20309.
- Guo, C., Sun, W., Bruno, K.S., Oakley, B.R., Keller, N.P., and Wang, C.** (2015). Spatial regulation of a common precursor from two distinct genes generates metabolite diversity. *Chem Sci.* Doi: 10.1039/C5SC01058F.
- Haarmann, T., Machado, C., Lübke, Y., Correia, T., Schardl, C.L., Panaccione, D.G., and Tudzynski, P.** (2005). The ergot alkaloid gene cluster in *Claviceps purpurea*: extension of the cluster sequence intra species evolution. *Phytochemistry.* 66:1312-1320.
- Han, J.R., Zhao, W.J., Gao, Y.Y., Yuan, J.M.** (2005). Effect of oxidative stress and exogenous β -carotene on sclerotial differentiation and carotenoid yield of *Penicillium* sp. PT95. *Lett Appl Microbiol* 40:412-417.

- Hanahan, D.** (1983). Studies on transformation of *Escherichia coli* with plasmid. *J Mol Biol.* 166:557-580.
- Hartmann, H.A., Krüger, J., Friedrich, L., and Kahmann, R.** (1999). Environmental signals controlling sexual development of the corn smut fungus *Ustilago maydis* through the transcriptional regulator Prf1. *Plant Cell.* 11:1293-1306.
- Haskins, R.H.** (1950). Biochemistry of Ustilaginales: I. Preliminary cultural studies of *Ustilago zaeae*. *Can J Res C.* 28:213-223.
- Haskins, R.H., and Thorn, J.A.** (1951). Biochemistry of the ustilaginales. VII. Antibiotic activity of ustilagic acid. *Can J Bot.* 29:585-592.
- Heimel, K., Scherer, M., Vranes, M., Wahl, R., Pothiratana, C., Schuler, D., Vincon, V., Finkernagel, F., Flor-Parra, I., and Kämper, J.** (2010). The transcription factor Rbf1 is the master regulator for *b*-mating type controlled pathogenic development in *Ustilago maydis*. *PLoS Pathog.* 6:e1001035.
- Hendrickson, L., Davis, C.R., Roach, C., Nguyen, D.K., Aldrich, T., McAda, P.C., Reeves, C.D.** (1999). Lovastatin biosynthesis in *Aspergillus terreus*: characterization of blocked mutants, enzyme activities and a multifunctional polyketide synthase gene. *Chem Biol.* 6:429-439.
- Henrikson, J.C., Hoover, A.R., Joyner, P.M, and Cichewicz, R.H.** (2009). A chemical epigenetics approach for engineering the *in situ* biosynthesis of a cryptic natural product from *Aspergillus niger*. 7:435-438.
- Hertweck, C.** (2009). The biosynthetic logic of polyketide diversity. *Angew. Chem. Int. Edit. Engl.* 48:4688-4716.
- Heuser, F., Schroer, K., Lütz, S., Bringer-Meyer, S., and Sahm, H.** (2007). Enhancement of the NAD(P)(H) pool in *Escherichia coli* for biotransformation. *Eng Life Sci.* 7:343-353.
- Hewage, R.T., Aree, T., Mahidol, C., Ruchirawat, S., and Kittakoop, P.** (2014). One strain-many compounds (OSMAC) method for production of polyketides azaphilones, and a isochromanone using the endophytic fungus *Dothideomycete* sp. *Phytochemistry.* 108:87-94.
- Hewald, S., Linne, U., Scherer, M., Marahiel, M.A., Kämper, J., and Bölker, M.** (2006). Identification of a gene cluster for biosynthesis of mannosylerythritol lipids in the basidiomycetous fungus *Ustilago maydis*. *Appl Environ Microbiol.* 72:5469-5477.
- Hoffmeister, D., and Keller, N.P.** (2007). Natural products of filamentous fungi: enzymes, genes, and their regulation. *Nat Prod Rep.* 24:393-416.
- Hohn, T.M., Proctor, R.H., and Desjardins, A.E.** (1991). Biosynthesis of sesquiterpenoid toxins by fungal pathogens. Paper presented at the EMBO workshop on the molecular biology of filamentous fungi, Berlin.
- Hopwood, D.A.** (1997). Genetic contributions to understanding polyketide synthases. *Chem Rev.* 97:2465-2497.

- Hosoya, Y., Okamoto, S., Muramatsu, H., and Ochi, K.** (1998). Acquisition of certain streptomycin-resistant (*str*) mutations enhances antibiotic production in bacteria. *Antimicrob Agents Chemother.* 42:2041-2047.
- Huang, G., Zhang, L., and Birch, R.G.** (2001). A multifunctional polyketide-peptide synthetase essential for albicidin biosynthesis in *Xanthomonas albilineans*. *Microbiology.* 147:631-642.
- Hynes, M.J.** (1975). Studies on the role of the *areA* gene in the regulation of nitrogen catabolism in *Aspergillus nidulans*. *Aust J Biol Sci.* 28:301-313.
- Ichinose, K., Ebizuka, Y., and Sankawa, U.** (2001). Mechanistic studies on the biomimetic reduction of tetrahydroxynaphthalene, a key intermediate in melanin biosynthesis. *Chem Pharm Bull.* 49: 192-196.
- Inglis, D.O., Binkley, J., Skrzypek, M.S., Arnaud, M.B., Cerqueira, G.C., Shah, P., Wymore, F., Wortman, J.R., and Sherlock, G.** (2013). Comprehensive annotation of secondary metabolite biosynthetic genes and gene clusters of *Aspergillus nidulans*, *A. fumigatus*, *A. niger* and *A. oryzae*. *BMC Microbiol.* 13:91.
- Isaka, M., Chinthanom, P., Rachtawee, P., Somyong, W., Luangsa-ard, J., and Hywel-Jones, N.L.** (2013). Cordylactam, a new alkaloid from the spider pathogenic fungus *Cordyceps* sp. BCC 12671. *Phytochem Lett.* 6:162-164.
- Islamovic, E., García-Pedrajas, M.D., Chacko, N., Andrews, D.L., Covert, S.F., and Gold, S.E.** (2015). Transcriptome analysis of a *Ustilago maydis* *ust1* deletion mutant uncovers involvement of laccase and polyketide synthase genes in spore development. *Mol Plant Microbe Interact.* 28:42-54.
- Jakubczyk, D., Caputi, L., Hatsch, A., Nielsen, C.A., Diefenbacher, M., Klein, J., Molt, A., Schröder, H., Cheng, J.Z., Naesby, M., and O'Connor, S.E.** (2015). Discovery and reconstitution of a cycloclavine biosynthetic pathway-enzymatic formation of a cyclopropyl group. *Angew Chem Int Ed Engl.* 54:5117-5121.
- Jenke-Kodama, H., Sandmann, A., Müller, R., and Dittmann, E.** (2005). Evolutionary implications of bacterial polyketide synthases. *Mol Biol Evol.* 22:2027-2039.
- Johnson, E.A.** (2003). *Phaffia rhodozyma*: colorful odyssey. *Int Microbiol.* 6:169-174.
- Jonkers, W., Rodriguez-Estrada, A.E., Lee, K., Breakspear, A., May, G., and Kistler, H.C.** (2012). Metabolome and transcriptome of the interaction between *Ustilago maydis* and *Fusarium verticillioides* in vitro. *Appl Environ Microbiol.* 78:3656-3667.
- Jørgensen, S.H., Frandsen, R.J.N., Nielsen, K.F., Lysøe, E., Sondergaard, T.E., Wimmer, R., Giese, H., Sørensen, J.L.** (2014). *Fusarium graminearum* PKS14 is involved in orsellinic acid and orcinol synthesis. *Fungal Genet Biol.* 70:24-31.
- Kahmann, R., and Kämper, J.** (2004). *Ustilago maydis*: how its biology relates to pathogenic development. *New Phytol.* 164:31-42.

- Kakule, T.B., Lin, Z., and Schmidt, E.** (2014). Combinatorialization of fungal polyketide synthase-peptide synthetase hybrid proteins. *J Am Chem Soc.* 136:17882-17890.
- Kallber, Y., Oppermann, U., Jornvall, H., Persson, B.** (2002). Short chain dehydrogenase/reductase (SDR) relationships: a large family with eight clusters common to human, animal, and plant genomes. *Protein Sci.* 11:636-641.
- Kapur, S., Lowry, B., Yuzawa, S., Kenthirapalan, S., Chen, A.Y., Cane, D.E., and Khosla, C.** (2012). Reprogramming a module of the 6-deoxyerythronolide B synthase for iterative chain elongation. *Proc Natl Acad Sci USA.* 109:4110-4115.
- Katsuyama, Y., and Horinouchi, S.** (2010). *Comprehensive Natural Products II: Chemistry and Biology*, Vol. 1, pp. 147-170, Elsevier Science Publishing Co., Inc., New York
- Kämper, J., Kahmann, R., Bölker, M., Ma, L.J., Brefort, T., Saville, B.J., Banuett, F., Kronstad, J.W., Gold, S.E, Müller, O., Perlin, M.H., Wösten, H.A., de Vries R., Ruiz-Herrera, J., Reynaga-Pena, C.G., Snetselaar, K., McCann, M., Pérez-Martín, J., Feldbrügge, M., Basse, C.W., Steinberg, G., Ibeas, J.I., Holloman, W., Guzman, P., Farman, M., Stajich, J.E., Sentandreu, R., González-Prieto, J.M, Kennell, J.C., Molina, L., Schirawski, J., Mendoza-Mendoza, A., Greilinger, D., Münch, K., Rössel, N., Scherer, M., Vranes, M., Ladendorf, O., Vincon, V., Fuchs, U., Sandrock, B., Meng, S., Ho, E.C., Cahill, M.J., Boyce, K.J., Klose, J., Klosterman, S.J., Deelstra, H.J., Ortiz-Castellanos, L., Li, W., Sanchez-Alonso, P., Schreier, P.H., Häuser-Hahn, I., Vaupel, M., Koopmann, E., Friedrich, G., Voss, H., Schlüter, T., Margolis, J., Platt, D., Swimmer, C., Gnirke, A., Chen, F., Vysotskaia, V., Mannhaupt, G., Güldener U., Münsterkötter, M., Haase, D., Oesterheld, M., Mewes, H.W., Mauceli, E.W., DeCaprio, D., Wade, C.M, Butler, J., Young, S., Jaffe, D.B., Calvo, S., Nusbaum, C., Galagan, J., and Birren, B.W.** (2006). Insights from the genome of the biotrophic fungal plant pathogen *Ustilago maydis*. *Nature.* 444: 97-101.
- Kealey, J.T., Liu, L., Santi, D.V., Betlach, M., and Barr, P.J.** (1998). Production of a polyketide natural product in nonpolyketide-producing prokaryotic and eukaryotic hosts. *Proc Natl Acad Sci USA.* 95:505-509.
- Keating, T.A., and Walsh, C.T.** (1999). Initiation, elongation, and termination strategies in polyketide and polypeptide antibiotic biosynthesis. *Curr Opin Chem Biol.* 3:598-606.
- Keating, T.A., Ehmann, D.E., Kohli, R.M., Marshall, C.G., Trauger, J.M., and Walsh, C.T.** (2001). Chain termination steps in nonribosomal peptide synthetase assembly lines: directed acyl-S-enzyme breakdown in antibiotic and siderophore biosynthesis. *Chem Bio Chem.* 2:99-107.
- Keatinge-Clay, A.T.** (2012). The structures of type I polyketide synthases. *Nat Prod Rep.* 29:1050-1073.
- Kelkar, H.S., Keller, N.P., and Adams, T.H.** (1996). *Aspergillus nidulans* *stcP* encodes an o-methyltransferase that is required for sterigmatocystin biosynthesis. *Appl Environ Microbiol.* 62:4296-4298.
- Keller, N.P., Turner, G., Bennett, J.W.** (2005). Fungal secondary metabolism-from biochemistry to genomics. *Nat Rev Microbiol.* 3:937-947.

- Keller, B., Volkmann, A., Wilckens, T., Moeller, G., Adamski, J.** (2006). Bioinformatic identification and characterization of new members of short chain dehydrogenase/reductase superfamily. *Mol Cell Endocrinol.* 248:56-60.
- Kennedy, J., Auclair, K., Kendrew, S.G., Park, C., Vederas, J.C., and Hutchinson, C.R.** (1999). Modulation of polyketide synthase activity by accessory proteins during lovastatin biosynthesis. *Science.* 248:1368-1372.
- Khalidi, N., Collemare, J., Lebrun, M.-H., and Wolfe, K.H.** (2008). Evidence for horizontal transfer of a secondary metabolite gene cluster between fungi. *Genome Biol.* 9:R18.
- Khalidi, N., Seifunddin, F.T., Turner, G., Nierman, W.C., Wolfe, K.H., and Fedorova, N.D.** (2010). SMURF: Genomic mapping of fungal secondary metabolite clusters. *Fungal Genet Biol.* 47:736-741.
- Kim, H., and Woloshuk, C.P.** (2008). Role of AREA, a regulator of nitrogen metabolism, during colonization of maize kernels and fumonisin biosynthesis in *Fusarium verticillioides*. *Fungal Genet Biol.* 45:947-953.
- Kitamoto, D., Akiba, S., Hioki, C., and Tabuchi, T.** (1990). Extracellular accumulation of mannosylerythritol lipids by a strain of *Candida antartica*. *Agric Biol Chem.* 54:31-36.
- Knox, P.B., and Keller, P.N.** (2015). Key players in the regulation of fungal secondary metabolism. In: Zeilinger, S., Martín, J.-F., García-Estrada, C. (Eds.), *Biosynthesis and Molecular Genetics of Fungal Secondary Metabolites*, Vol. 2 Springer New York, New York, NY, pp. 13-28.
- Koizumi, Y., Arai, M., Tomoda, H., and Omura, S.** (2004). Oxaline, a fungal alkaloid, arrests the cell cycle in M phase by inhibition of tubulin polymerization. *Biochim Biophys Acta.* 1693:47-55.
- Korman, T.P., Crawford, J.M., Labonte, J.W., Newman, A.G., Wong, J., Townsend, C.A., and Tsai, S.** (2010). Structure and function of an iterative polyketide synthase thioesterase domain catalyzing Claisen cyclization in aflatoxin biosynthesis. *Proc Natl Acad Sci USA.* 107:6246-6251.
- Kosman, D.J.** (2003). Molecular mechanisms of iron uptake in fungi. *Mol Microbiol.* 47:1185-1197.
- Kües, U., and Rühl, M.** (2011). Multiple multi-copper oxidase gene families in basidiomycetes- what for? *Curr Genomics.* 12:72-94.
- Lackner, G., Misiek, M., Braesel, J., and Hoffmeister, D.** (2012). Genome mining reveals the evolutionary origin and biosynthetic potential of basidiomycete polyketide synthases. *Fungal Genet Biol.* 49:996-1003.
- Langfelder, K., Jahn, B., Gehringer, H., Schmidt, A., Wanner, G., and Brakhage, A.A.** (1998). Identification of a polyketide synthase gene (*pksP*) of *Aspergillus fumigatus* involved in conidial pigment biosynthesis and virulence. *Med Microbiol Immunol.* 187:79-89.

- Langfelder, K., Streibel, M., Jahn, B., Haase, G., and Brakhage, A.A.** (2003). Biosynthesis of fungal melanins and their importance for human pathogenic fungi. *Fungal Genet Biol.* 38:143-158.
- Lanver, D., Mendoza-Mendoza, A., Brachmann, A., and Kahmann, R.** (2010). Sho1 and Msb2-related proteins regulate appressorium development in the smut fungus *Ustilago maydis*. *Plant Cell.* 22:2085-2101.
- Laureti, L., Song, L., Huang, S., Corre, C., Leblond, P., Challis, G.L., and Aigle, B.** (2011). Identification of a bioactive 51-membered macrolide complex by activation of a silent polyketide synthase in *Streptomyces ambofaciens*. *Proc Natl Acad Sci USA.* 108:6258-6263.
- Lautru, S., and Challis, G.L.** (2004). Substrate recognition by nonribosomal peptide synthetase multi-enzymes. *Microbiology.* 150:1629-1636.
- Lee, I., Oh, J.H., Shwab, E.K., Dagenais, T.R., Andes, D., and Keller, N.P.** (2009). HdaA, a class 2 histone deacetylase of *Aspergillus fumigatus*, affects germination and secondary metabolite production. *Fungal Genet Biol.* 46:782-790.
- Lee, W.** (2010). Comprehensive discovery of fungal gene clusters: unexpected co-work reflected at the genomic level. Ph.D. dissertation. Technische Universität München.
- Letzel, A.C., Pidot, S.J., and Hertweck, C.** (2013). A genomic approach to the cryptic secondary metabolome of the anaerobic world. *Nat Prod Rep.* 30:392-428.
- Li, M.H., Ung, P.M., Zajkowski, J., Garneau-Tsodikova, S., and Sherman, D.H.** (2009). Automated genome mining for natural products. *BMC Bioinformatics.* 10:185.
- Linne, U., Doekel, S., and Marahiel, M.A.** (2001). Portability of epimerization domain and role of peptidyl carrier protein on epimerization activity in nonribosomal peptide synthetases. *Biochemistry.* 40:15824-15834.
- Lim, J., Sun, H., Fan, J.S., Hameed, I.F., Lescar, J., Liang, Z.X., and Yang, D.** (2012). Rigidifying acyl carrier protein domain in iterative type I PKS CalE8 does not affect its function. *Biophys J.* 103:1037-1044.
- Limón, M.C., Rodríguez-Ortiz, R., and Avalos, J.** (2010). Bikaverin production and applications. *Appl Microbiol Biotechnol.* 87:21-29.
- Lin, S.Y., Okuda, S., Ikeda, K., Okuno, T., and Takano, Y.** (2012). *LAC2* encoding a secreted laccase is involved in appressorial melanization and conidial pigmentation in *Colletotrichum orbiculare*. *Mol Plant Microbe Interact.* 25:1552-1561.
- Lin, H.-C., Tsunematsu, Y., Dhingra, S., Xu, W., Fukutomi, M., Chooi, Y.-H., Cane, D.E., Calvo, A.M., Watanabe, K., and Tang, Y.** (2014). Generation of complexity in fungal terpene biosynthesis: discovery of a multifunctional cytochrome P450 in the fumagillin pathway. *J Am Chem Soc.* 136:4426-4436.
- Liu, T.B., Wang, Y., Baker, G.M., Fahmy, H., Jiang, L., and Xue, C.** (2013). The glucose sensor-like protein Hxs1 is a high-affinity glucose transporter and required for virulence in *Cryptococcus neoformans*. *PLoS One.* 8:e64239.

- Lohman, J.R., Ma, M., Osipiuk, J., Nocek, B., Kim, Y., Chang, C., Cuff, M., Mack, J., Bigelow, L., Li, H., Endres, M., Babnigg, G., Joachimiak, A., Phillips Jr., G.N., and Shen, B. (2015). Structural and evolutionary relationships of "AT-less" type I polyketide synthase ketosynthases. *Proc Natl Acad Sci USA*. 112:12693-12698.
- Ludwig, N., Löhner, M., Hempel, M., Mathea, S., Schliebner, I., Menzel, M., Kiesow, A., Schaffrath, U., Deising, H.B., and Horbach, R. (2014). Melanin is not required for turgor generation but enhances cell-wall rigidity in appressoria of the corn pathogen *Colletotrichum graminicola*. *Mol Plant Microbe Interact*. 27:315-327.
- Ma, S.M., Li, J.W.-H., Choi, J.W., Zhou, H., Lee, K.K.M., Moorthie, V.A., Xie, X., Kealey, J.T., Da Silva, N.A., Vederas, J.C., and Tang, Y. (2009). Complete reconstitution of a highly-reducing iterative polyketide synthase. *Science*. 326:589-592.
- Maiya, S., Grundmann, A., Li, X., Li, S.M., and Turner, G. (2007). Identification of a hybrid PKS/NRPS required for pseurotin A biosynthesis in the human pathogen *Aspergillus fumigatus*. *Chembiochem*. 8:1736-1743.
- Marahiel, M., and Essen, L. (2009). Nonribosomal peptide synthetases mechanistic and structural aspects of essential domains. *Methods Enzymol*. 458:337-351.
- Martin, J.F. (2000). Molecular control of expression of penicillin biosynthesis genes in fungi: regulatory proteins interact with a bidirectional promoter region. *J Bacteriol*. 182:2355-2362.
- Mazzaferro, L.S., Hüttel, W., Fries, A., and Müller M. (2015). Cytochrome P450-catalyzed regio- and stereoselective phenol coupling of fungal natural products. *J Am Chem Soc*. 137:12289-12295.
- McGuire, S.M., Silva, J.C., Casillas, E.G., and Townsend, C.A. (1996). Purification and characterization of versicolorin B synthase from *Aspergillus parasiticus*. Catalysis of the stereodifferentiating cyclization in aflatoxin biosynthesis essential to DNA interaction. (1996). *Biochemistry*. 35:11470-11486.
- McDonagh, A., Fedorova, N.D., Crabtree, J., Yu, Y., Kim, S., Chen, D., Loss, O., Cairns, T., Goldman, G., Armstrong-James, D., Haynes, K., Haas, H., Schrettl, M., May, G., Nierman, W.C., and Bignell, E. (2008). Sub-telomere directed gene expression during initiation of invasive aspergillosis. *PLoS Pathog*. 4:e1000154.
- Medema, M.H., Blin, K., Cimermancic, P., de Jager, V., Zakrzewski, P., Fischbach, M.A., Weber, T., Takano, E., and Breitling, R. (2011). antiSMASH: rapid identification, annotation and analysis of secondary metabolite biosynthesis gene clusters in bacterial and fungal genome sequences. *Nucleic Acids Res*. 39:W339-W346.
- Medema, M.H., and Fischbach, M.A. (2015). Computational approaches to natural product discovery. *Nat Chem Biol*. 11:639-648.
- Medentsev, A.G., and Akimenko, V.K. (1998). Naphthoquinone metabolites of the fungi. *Phytochemistry*. 47:935-959.

- Mei, B., Budde, A.D., Leong, S.A.** (1993). *sid1*, a gene initiating siderophore biosynthesis in *Ustilago maydis*: molecular characterization, regulation by iron, and a role in phytopathogenicity. *Proc Natl Acad Sci USA*. 90:903-907.
- Menche, D., Arian, F., Perlova, O., Horstmann, N., Ahlbrecht, W., Wenzel, S.C., Jansen, R., Irschik, H., and Muller, R.** (2008). Stereochemical determination and complex biosynthetic assembly of etnangien, a highly potent RNA polymerase inhibitor from myxobacterium *Sorangium cellulosum*. *J Am Chem Soc*. 130:14234-14243.
- Mendoza-Mendoza, A., Berndt, P., Djamei, A., Weise, C., Linne, U., Marahiel, M., Vranes, M., Kämper, J., and Kahmann, R.** (2009). Physical-chemical plant-derived signals induce differentiation in *Ustilago maydis*. *Mol Microbiol*. 71:895-911.
- Metzger, U., Schall, C., Zocher, G., Unsöld, I., Stec, E., Li, S.M., Heide, L., and Stehle, T.** (2009). The structure of dimethylallyl tryptophan synthase reveals a common architecture of aromatic prenyltransferases in fungi and bacteria. *Proc Natl Acad Sci USA*. 106:14309-14314.
- Miller, F.A., Richtsel, W.A., Sloan, B.J., Ehrlich, J., French, J.C., Bartz, Q.R., and Dixon, G.J.** (1963). Antiviral activity of tenuazonic acid. *Nature*. 200:1338-1339.
- Molina, L., and Kahmann, R.** (2007). An *Ustilago maydis* gene involved in H₂O₂ detoxification is required for virulence. *Plant Cell*. 19:2293-2309.
- Moore, B.S., and Hopke, J.N.** (2001). Discovery of a new bacterial polyketide biosynthetic pathway. *Chembiochem*. 2:35-38.
- Moss, S.J., Martin, C.J., and Wilkinson, B.** (2004). Loss of co-linearity by modular polyketide synthases: a mechanism for the evolution of chemical diversity. *Nat Prod Rep*. 21:575-593.
- Motamedi, H., and Hutchinson, C.R.** (1987). Cloning and heterologous expression of a gene cluster for the biosynthesis of tetracenomycin C, the anthracycline antitumor antibiotic of *Streptomyces glaucescens*. *Proc Natl Acad Sci USA*. 84:4445-4449.
- Mutka, S.C., Bondi, S.M., Carney, J.R., Da Silva, N.A., and Kealey, J.T.** (2005). Metabolic pathway engineering for complex polyketide biosynthesis in *Saccharomyces cerevisiae*. *FEMS Yeast Res*. 6:40-47.
- Nakagawa, H., and Takeda, Y.** (1962). Phenol hydroxylase. *Biochim Biophys Acta*. 62:423-426.
- Nevalainen, K.M.H., Teó, V.S.J., and Bergquist, P.L.** (2005). Heterologous protein expression in filamentous fungi. *Trends Biotechnol*. 23:468-474.
- Nosanchuk, J.D., and Casadevall, A.** (2003). The contribution of melanin to microbial pathogenesis. *Cell Microbiol*. 5:203-223.
- Nosanchuk, J.D., Stark, R.E., and Casadevall, A.** (2015). Fungal melanin: what do we know about structure? *Front Microbiol*. 6:1463.

- Noverr, M.C., Williamson, P.R., Fajardo, R.S., Huffnagle, G.B.** (2004). *CNLAC1* is required for extrapulmonary dissemination of *Cryptococcus neoformans* but not pulmonary persistence. *Infect Immun.* 72:1693-1699.
- Nützmann, H.-W., Reyes-Dominguez, Y., Scherlach, K., Schroeckh, V., Horn, F., Gacek, A., Schümann, J., Hertweck, C., Strauss, J., and Brakhage, A.A.** (2011). Bacteria-induced natural product formation in the fungus *Aspergillus nidulans* requires Saga/Ada-mediated histone acetylation. *Proc Natl Acad Sci USA.* 108:14282-14287.
- Ochi, K., Okamoto, S., Tozawa, Y., Inaoka, T., Hosaka, T., Xu, J., and Kurosawa, K.** (2004). Ribosome engineering and secondary metabolite production. *Adv Appl Microbiol.* 56:155-184.
- Ochi, K. and Hosaka, T.** (2013). New strategies for drug discovery: activation of silent or weakly expressed microbial gene clusters. *Appl Microbiol Biotechnol.* 97:87-98.
- Oh, D., Kauffman, C.A., Jensen, P.R., and Fenical, W.** (2007). Induced production of emericellamides A and B from the marine-derived fungus *Emericella* sp. in competing co-culture. *J Nat Prod.* 70:515-520.
- Okamoto, S., Taguchi, T., Ochi, K., and Ichinose, K.** (2009). Biosynthesis of actinorhodin and related antibiotics: discovery of alternative routes for quinone formation encoded in the act gene cluster. *Chem Bio.* 16:226-236.
- Owens, R.A., Hammel, S., Sheridan, K.J., Jones, G.W., and Doyle, S.** (2014). A proteomic approach to investigating gene cluster expression and secondary metabolite functionality in *Aspergillus fumigatus*. *PLoS One.* 9:e106942.
- Pahirulzaman, K.A., Williams, K., and Lazarus, C.M.** (2012). A toolkit for heterologous expression of metabolite pathways in *Aspergillus oryzae*. *Methods Enzymol.* 517:241-260.
- Palmer, D.A., Thompson, J.K., Li, L., Prat, A., and Wang, P.** (2006). Gib2, a novel G β -like/RACK1 homolog, functions as a G β subunit in cAMP signaling and is essential in *Cryptococcus neoformans*. *J Biol Chem.* 281:32596-32605.
- Palmer, J.M., and Keller, N.P.** (2010). Secondary metabolism in fungi: does chromosomal location matter? *Curr Opin Microbiol.* 13:431-436.
- Paranagama, P.A., Wijeratne, E.M.K., and Gunatilaka, A.A.L.** (2007). Uncovering biosynthetic potential of plant-associated fungi: effect of culture conditions on metabolite production by *Paraphaeosphaeria quadrisepata* and *Chaetomium chiversii*. *J Nat Prod.* 70:1939-1945.
- Park, H.B., Kwon, H.C., Lee, C.H., and Yang, H.O.** (2009). Glionitrin A, an antibiotic-antitumor metabolite derived from competitive interaction between abandoned mine microbes. *J Nat Prod.* 72:248-252.
- Perrin, R.M., Fedorova, N.D., Bok, J.W., Cramer, R.A., Wortman, J.R., Kim, H.S., Nierman, W.C., and Keller, N.P.** (2007). Transcriptional regulation of chemical diversity in *Aspergillus fumigatus* by LaeA. *PLoS Pathog.* 3:e50.

- Pospiech, A., Bietenhader, J., and Schupp, T.** (1996). Two multifunctional peptide synthetases and a O-methyltransferase are involved in the biosynthesis of the DNA-binding antibiotic and antitumor agent saframycin Mx1 from *Myxococcus xanthus*. *Microbiology*. 142:741-746.
- Proctor, R.H. and Hohn, T.M.** (1993). Aristolochene synthase. Isolation, characterization, and bacterial expression of a sesquiterpenoid biosynthetic gene (Ari1) from *Penicillium roqueforti*. *J Biol Chem*. 268:4543-4548.
- Pukkila-Worley, R., Gerrald, Q.D., Kraus, P.R., Boily, M.J., Davis, M.J., Giles, S.S., Cox, G.M., Heitman, J., Alspaugh, J.A.** (2005). Transcriptional network of multiple capsule and melanin genes governed by the *Cryptococcus neoformans* cyclic AMP cascade. *Eukaryot Cell*. 4:190-201.
- Regenfelder, E., Spelling, T., Hartmann, A., Lauenstein, S., Bölker, M., and Kahmann, R.** (1997). G proteins in *Ustilago maydis*: transmission of multiple signals? *EMBO J*. 16:1934-1942.
- Reichmann, M., Jamnischek, A., Weinzierl, G., Ladendorf, O., Huber, S., Kahmann, R., and Kämper, J.** (2002). The histone deacetylase Hda1 from *Ustilago maydis* is essential for teliospore development. *Mol Microbiol*. 46:1169-1182.
- Robinson, S.L., and Panaccione, D.G.** (2015). Diversification of ergot alkaloids in natural and modified fungi. *Toxins*. 7:201-218.
- Rodriguez-Estrada, A.E., Hegeman, A., Kistler, H.C. and May, G.** (2011). *In vitro* interactions between *Fusarium verticillioides* and *Ustilago maydis* through real-time PCR and metabolic profiling. *Fungal Genet Biol*. 48:874-885.
- Romero-Martinez, R., Wheeler, M., Guerrero-Plata, A., Rico, G., and Torres-Guerrero, H.** (2000). Biosynthesis and functions of melanin in *Sporothrix schenckii*. *Infect Immun*. 68:3696-3703.
- Rothberg, K.G., Burdette, D.L., Pfannstiel, J., Jetton, N., Singh, R., and Ruben, L.** (2006). The RACK1 homologue from *Trypanosoma brucei* is required for the onset and progression of cytokinesis. *J Biol Chem*. 281:9781-9790.
- Rutledge, P.J., Challis, G.L.** (2015). Discovery of microbial natural products by activation of silent biosynthetic gene clusters. *Nat Rev Microbiol*. 13:509-523.
- Sakai, K., Kinoshita, H., Shimizu, T., and Nihira, T.** (2008). Construction of a citrinin gene cluster expression system in heterologous *Aspergillus oryzae*. *J Biosci Bioeng*. 106:466-472.
- Sakai, K., Kinoshita, H., and Nihira, T.** (2012). Heterologous expression system in *Aspergillus oryzae* for fungal biosynthetic gene clusters of secondary metabolites. *Appl Microbiol Biotechnol*. 93:2011-2022.
- Sakuno, E., Wen, Y., Hatabayashi, H., Arai, H., Aoki, C., Yabe, K., and Nakajima, H.** (2005). *Aspergillus parasiticus* cyclase catalyzes two dehydration steps in aflatoxin biosynthesis. *Appl Environ Microbiol*. 71:2999-3006.

- Salas, S.D., Bennett, J.E., Kwon-Chung, K.J., Perfect, J.R., and Williamson P.R. (1996). Effect of the laccase gene *CNLACI*, on virulence of *Cryptococcus neoformans*. J Exp Med. 184:377-386.
- Salomon, C.E., Magarvey, N.A., and Sherman, D.H. (2004). Merging the potential of microbial genetics with biological and chemical diversity: an even brighter future for marine natural product drug discovery. Nat Prod Rep. 21:105-121.
- Sambrook, J., Fritsch, E.F., and Maniatis, T. (1989). Molecular cloning: a laboratory manual. Cold Spring Harbor, New York. Cold Spring Harbor Laboratory Press.
- Sapmak, A., Boyce, K.J., Andrianopoulos, A., and Vanittanakom, N. (2015). The *pbrB* gene encodes a laccase required for DHN-melanin synthesis in conidia of *Taromyces (Penicillium) marneffei*. PLoS One. 10:e0122728.
- Schacht, T., Oswald, M., Eils, R., Eichmüller, S.B., and König, R. (2014). Estimating the activity of transcription factors by the effect on their target genes. Bioinformatics. 30:i401-i407.
- Scharf, D.H., Heinekamp, T., Remme, N., Hortschansky, P., Brakhage, A.A., and Hertweck, C. (2012). Biosynthesis and function of gliotoxin in *Aspergillus fumigatus*. Appl Microbiol Biotechnol. 93:467-472.
- Scherlach, K., and Hertweck, C. (2009). Triggering cryptic natural product biosynthesis in microorganisms. Org Biomol Chem. 7:1753-1760.
- Schmaler-Ripcke, J., Sugareva, V., Gebhardt, P., Winkler, R., Kniemeyer, O., Heinekamp, T., and Brakhage, A. (2009). Production of Pyomelanin, a second type of melanin, via the tyrosine degradation pathway in *Aspergillus fumigatus*. Appl Environ Microbiol. 75:493-503.
- Schmidhauser, T.J., Lauter, F.R., Russo, V.E., and Yanofsky, C. (1990). Cloning, sequence, and photoregulation of *al-I*, a carotenoid biosynthetic gene of *Neurospora crassa*. Mol Cell Biol. 10:5064-5070.
- Schneider, A., and Marahiel, M.A. (1998). Genetic evidence for a role of the thioesterase domains, integrated in or associated with peptide synthetases, in nonribosomal peptide biosynthesis in *Bacillus subtilis*. Arch Microbiol. 169:404-410.
- Schroeckh, V., Scherlach, K., Nützmann, H.W., Shelest, E., Schmidt-Heck, W., Schuemann, J., Martin, K., Hertweck, C., and Brakhage, A.A. (2009). Intimate bacterial-fungal interaction triggers biosynthesis of archetypal polyketides in *Aspergillus nidulans*. Proc Natl Acad Sci USA. 106:14558-14563.
- Schulz, B., Banuett, F., Dahl, M., Schlesinger, R., Schäfer, W., Martin, T., Herskowitz, I., and Kahmann, R. (1990). The *b* alleles of *U. maydis*, whose combinations program pathogenic development, code for polypeptides containing a homeodomain-related motif. Cell. 60:295-306.
- Schuler, D., Wahl, R., Wippel, K., Vranes, M., Münsterkötterm, M., Sauer, N., and Kämper, J. (2015). Htx1, a monosaccharide transporter and sensor required for virulence of the maize pathogen *Ustilago maydis*. New Phytol. 206:1086-1100.

- Schumacher, J., Simon, A., Cohrs, K.C., Viaud, M., and Tudzynski, P.** (2013). The transcription factor BcLTF1 regulates virulence and light responses in the necrotrophic plant pathogen *Botrytis cinerea*. *PLoS Genet.* 10:e1004040.
- Schumacher, J.** (2016). DHN melanin biosynthesis in the plant pathogenic fungus *Botrytis cinerea* is based on two developmentally regulated key enzyme (PKS)-encoding genes. *Mol Microbiol.* 99:729-748.
- Schümann, J., and Hertweck, C.** (2006). Advances in cloning, functional analysis and heterologous expression of fungal polyketide synthase genes. *J Biotechnol.* 124:690-703.
- Schwarzer, D., and Marahiel, M.A.** (2001). Multimodular biocatalysis for natural product assembly. *Naturwissenschaften.* 88:93-101.
- Shaw, J.J., Berbasova, T., Sasaki, T., Jefferson-George, K., Spakowicz, D.J., Dunican, B.F., Portero, C.E., Narváez-Trujillo, A., and Strobel, S.A.** (2015). Identification of a fungal 1,8-Cineole synthase from *Hypoxylon* sp. with specificity determinants in common with the plant synthases. *J Biol Chem.* 290:8511-8526.
- Shen, B.** (2000). Biosynthesis of aromatic polyketides. *Curr Top Chem.* 209:1-51.
- Shen, B.** (2003). Polyketide biosynthesis beyond the type I, II and III polyketide synthase paradigms. *Curr Opin Chem Biol.* 7:285-295.
- Shimizu, T., Kinoshita, H., and Nihira, T.** (2007). Identification and *in vivo* functional analysis by gene disruption of *ctnA*, an activator gene involved in citrinin biosynthesis in *Monascus purpureus*. *Appl Environ Microbiol.* 73:5097-5103.
- Shin, C.S., Kim, H.J., Kim, M.J., and Ju, J.Y.** (1998). Morphological change and enhanced pigment production of *Monascus* when cocultured with *Saccharomyces cerevisiae* or *Aspergillus oryzae*. *Biotechnol Bioeng.* 59:576-581.
- Shwab, E.K., Bok, J.W., Tribus, M., Galehr, J., Graessle, S., and Keller, N.P.** (2007). Histone deacetylase activity regulates chemical diversity in *Aspergillus*. *Eukaryot Cell.* 6:1656-1664.
- Sieber, C.M.K., Lee, W., Wong, P., Münsterkötter, M., Mewes, H., Schmeitzl, C., Varga, E., Berthiller, F., Adam, G., and Güldener, U.** (2014). The *Fusarium graminearum* genome reveals more secondary metabolite gene clusters and hints of horizontal gene transfer. *PLoS One.* 9:e110311.
- Sikorski, R.S., and Hieter, P.** (1989). A system of shuttle vectors and yeast host strains designed for efficient manipulation of DNA in *Saccharomyces cerevisiae*. *Genetics.* 122:19-27
- Silakowski, B., Kunze, B., Nordsiek, G., Blöcker, H., Höfle, G., Müller, R.** (2000). The myxochelin iron transport regulon of the myxobacterium *Stigmatella aurantiaca* Sg a15. *Eur J Biochem.* 267:6476-6485.
- Silva, J.C., Minto, R.E., Barry III, C.E., Holland, K.A., and Townsend, C.A.** (1996). Isolation and characterization of versicolorin b synthase gene from *Aspergillus parasiticus*. *J Biol Chem.* 271:13600-13608.

- Smith, S., and Tsai, S.C.** (2007). The type I fatty acid and polyketide synthases: a tale of two megasynthases. *Nat Prod Rep.* 24:1041-1072.
- Sims, J.W., Fillmore, J.P., Warner, D.D., and Schmidt, E.W.** (2005). Equisetin biosynthesis in *Fusarium heterosporum*. *Chem Commun (Camb).* 2:186-188.
- Simunovic, V., Zapp, J., Rachid, S., Krug, D., Meiser, P., and Muller, R.** (2006). Myxovirescin A biosynthesis is directed by hybrid polyketide synthases/nonribosomal peptide synthetase, 3-hydroxy-3-methylglutaryl-CoA synthases, and trans-acting acyltransferases. *Chem Bio Chem.* 7:1206-1220.
- Slot, J.C., and Rokas, A.** (2011). Horizontal transfer of a large and highly toxic secondary metabolic gene cluster between fungi. *Curr Biol.* 21:134-139.
- Snetselaar, K.M., and Mims, C.W.** (1993). Infection of maize stigmas by *Ustilago maydis*: light and electron microscopy. *Phytopathology.* 83:843-850.
- Song, Z., Cox, R.J., Lazarus, C.M., and Simpson, T.J.** (2004). Fusarin C biosynthesis in *Fusarium moniliforme* and *Fusarium venenatum*. *Chembiochem.* 5:1196-1203.
- Staunton, J.** (1997). Biosynthesis of erythromycin and rapamycin. *Chem Rev.* 97:2611-2629.
- Starcevic, A., Zucko, J., Simunkovic, J., Long, P.F., Cullum, J., and Hranueli, D.** (2008). ClustScan: an integrated program package for the semi-automatic annotation of modular biosynthetic gene clusters and in silico prediction of novel chemical structures. *Nucleic Acid Res.* 36:6882-6892.
- Staunton, J., and Weissman, K.J.** (2001). Polyketide biosynthesis: a millennium review. *Nat Prod Rep.* 18:380-416.
- Steiger, M.G., Blumhoff, M.L., Mattanovich, D., and Sauer, M.** (2013). Biochemistry of microbial itaconic acid production. *Front Microbiol.* 4:23.
- Steiner, U., and Oerke, E.C.** (2007). Localized melanization of appresoria is required for pathogenicity of *Venturia inaequalis*. *Phytopathology.* 97:1222-1230.
- Strieker, M., Tanovic, A., and Marahiel, M.A.** (2010). Nonribosomal peptide synthetases: structures and dynamics. *Curr Opin Struct Biol.* 20:234-240.
- Sugareva, V., Härtl, A., Brock, M., Hübner, K., Rohde, M., Heinekamp, T., and Brakhage, A.A.** (2006). Characterisation of the laccase-encoding gene *abr2* of the dihydroxynaphthalene-like melanin gene cluster of *Aspergillus fumigatus*. *Arch Microbiol.* 186:345-355.
- Sugui, J.A., Pardo, J., Chang, Y.C., Müllbacher, A., Zarembek, K.A., Galvez, E.M., Brinster, L., Zerfas, P., Gallin, J.I., Simon, M.M., and Kwon-Chung, K.J.** (2007). Role of *laeA* in regulation of *alb1*, *gliP*, conidial morphology, and virulence in *Aspergillus fumigatus*. *Eukaryot Cell.* 6:1552-1561.
- Sugui, J.A., Kim, H.S., Zarembek, K.A., Chang, Y.C., Gallin, J.I., Nierman, W.C., Kwon-Chung, K.J.** (2008). Genes differentially expressed in conidia and hyphae of *Aspergillus fumigatus* upon exposure to humans neutrophils. *PLoS One.* 3:e2655.

- Szewczyk, E., Chiang, Y.M., Oakley, C.E., Davidson, A.D., Wang, C.C., Oakley, B.R. (2008). Identification and characterization of the asperthecin gene cluster of *Aspergillus nidulans*. *Appl Environ Microbiol.* 74:7607-7612.
- Taguchi, T., Ebizuka, Y., Hopwood, D.A., and Ichinose, K. (2001). A new mode of stereochemical control revealed by analysis of the biosynthesis of dihydrogranaticin in *Streptomyces violaceoruber* T-22. *J Am Chem Soc.* 123:11376-11380.
- Tanaka, Y., Kasahara, K., Hirose, Y., Murakami, K., Kugimiya, R., and Ochi, K. (2013). Activation and products of the cryptic secondary metabolite biosynthetic gene clusters by rifampin resistance (*rpoB*) mutations in actinomycetes. *J Bacteriol.* 195:2959-2970.
- Tang, G.L., Cheng, Y.Q., and Shen, B. (2004). Leinamycin biosynthesis revealing unprecedented architectural complexity for a hybrid polyketide synthase and nonribosomal peptide synthetase. *Chem Biol.* 11:33-45.
- Teichmann, B., Linne, U., Hewald, S., Marahiel, M.A., and Bölker, M. (2007). A biosynthetic gene cluster for a secreted cellobiose lipid with antifungal activity from *Ustilago maydis*. *Mol Microbiol.* 66:525-533.
- Teichmann, B., Liu, L., Schink, K.O., and Bölker, M. (2010). Activation of ustilagic acid biosynthesis gene cluster in *Ustilago maydis* by the C₂H₂ zinc finger transcription factor Rual. *Appl Environ Microbiol.* 76:2633-2640.
- Thompson, J.E., Fahnestock, S., Farrall, L., Liao, D.I., Valent, B., and Jordan, D.B. (2000). The second naphthol reductase of fungal melanin biosynthesis in *Magnaporthe grisea*: tetrahydroxynaphthalene reductase. 275:34867-34872.
- Throckmorton, K., Lim, F.Y., Kontoyiannis, D.P., Zheng, W., and Keller, N.P. (2016). Redundant synthesis of a conidial polyketide by two distinct secondary metabolite clusters in *Aspergillus fumigatus*. 18:246-259.
- Tilburn, J., Sarkar, S., Widdick, D.A., Espeso, E.A., Orejas, M., Mungroo, J., Peñalva, M.A., and Arst, H.N., Jr. (1995). The *Aspergillus* PacC zinc finger transcription factor mediates regulation of both acid- and alkaline-expressed genes by ambient pH. *EMBO J.* 14:779-790.
- Tokousbalides, M.C., and Sisler, H.D. (1979). Site of inhibition by tricyclazole in the melanin biosynthesis pathway of *Verticillium dahliae*. *Pestic Biochem Physiol.* 11:64-73.
- Tollot, M., Assmann, D., Becker, C., Altmüller, J., Dutheil, J.Y., Wegner, C.E., and Kahmann. (2016). The WOPR protein Ros1 is a master regulator of sporogenesis and late effector gene expression in maize pathogen *Ustilago maydis*. *PLoS Pathog.* 12:e1005697.
- Tsai, H.F., Wang, H., Gebler, J.C., Poutler, C.D., Schardl, C.L. (1995). The *Claviceps purpurea* gene encoding dimethylallyltryptophan synthase, the committed step for ergot alkaloid biosynthesis. *Biochem Biophys Res Commun.* 216:119-125.
- Tsai, H.F., Wheeler, M.H., Chang, Y.C., and Kwon-Chung, K.J. (1999). A developmentally regulated gene cluster involved in conidial pigment biosynthesis in *Aspergillus fumigatus*. *J Bacteriol.* 181:6469-6477.

- Tsuji, G., Kenmochi, Y., Takano, J., Sweigard, L. Farrall, I., Furusawa, O., Horino, and Y. Kubo.** (2000). Novel fungal transcriptional activators, Cmr1p of *Colletotrichum lagenarium* and pig1 of *Magnaporthe grisea*, contain Cys2His2 zinc finger and Zn(II)₂Cys₆ binuclear cluster DNA-binding motifs and regulate transcription of melanin biosynthesis genes in a developmentally specific manner. *Mol Microbiol.* 38:940-954.
- Tudzynski, P., Hölter, K., Correia, T., Arntz, C., Grammel, N., and Keller, U.** (1999). Evidence for an ergot alkaloid gene cluster in *Claviceps purpurea*. *Mol Gen Genet.* 261:133-141.
- Tudzynski, B., Homann, V., Feng, B., and Marzluf, G.A.** (1999). Isolation, characterization and disruption of the *areA* nitrogen regulatory gene of *Gibberella fujikuroi*. *Mol Gen Genet.* 261:106-114.
- Twumasi-Boateng, K., Yu, Y., Chen, D., Gravelat, F.N., Nierman, W.C., Sheppard, D.C.** (2009). Transcriptional profiling identifies a role for BrlA in response to nitrogen depletion and for StuA in the regulation of secondary metabolite clusters in *Aspergillus fumigatus*. *Eukaryot Cell.* 8:104-115.
- Vidal-Cros, A., Viviani, F., Labesse, G., Boccara, M., Gaudry, M.** (1994). Polyhydroxynaphthalene reductase involved in melanin biosynthesis in *Magnaporthe grisea*. Purification, cDNA cloning and sequencing. *Eur J Biochem.* 219:985-992.
- Vining, L.C.** (1992). Roles of secondary metabolites from microbes. *Ciba Found Symp.* 171:184-194.
- Voisard, C., Wang, J., McEvoy, J.L., Xu, P., and Leong, S.A.** (1993). *urbs1*, a gene regulating siderophore biosynthesis in *Ustilago maydis*, encodes a protein similar to the erythroid transcription factor GATA-1. *Mol Cell Biol.* 13:7091-7100.
- Vödisch, M., Scherlach, K., Winkler, R., Hertweck, C., Braun, H.P., Roth, M., Haas, H., Werner, E.R., Brakhage, A.A., and Kniemeyer, O.** (2011). Analysis of the *Aspergillus fumigatus* proteome reveals metabolic changes and the activation of pseurotin A biosynthesis gene cluster in response to hypoxia. *J Proteome Res.* 10:2508-2524.
- Wakamatsu, K., and Ito, S.** (2002). Advanced chemical methods in melanin determination. *Pigment Cell Res.* 15:174-183.
- Walsh, C.T., Chen, H., Keating, T.A., Hubbard, B.K., Losey, H.C., Luo, L., Marshall, C.G., Miller, D.A., and Patel, H.M.** (2001). Tailoring enzymes that modify nonribosomal peptides during and after chain elongation on NRPS assembly lines. *Curr Opin Chem Biol.* 5:525-534.
- Wang, J., Budde, A.D., and Leong, S.A.** (1989). Analysis of ferrichrome biosynthesis in the phytopathogenic fungus *Ustilago maydis*: cloning of an ornithine-N⁵-oxygenase gene. *J Bacteriol.* 171:2811-2818.
- Wang, X., Sena-Filho, J.G., Hoover, A.R., King, J.B., Ellis, T.K., Powell, D.R., and Cichewicz, R.H.** (2010). Chemical epigenetics alters the secondary metabolite composition of guttate excreted by an atlantic-forest-soil-derived *Penicillium citreonigrum*. *J Nat Prod.* 73:942-948.

- Wang, L., Berndt, P., Xia, X., Kahnt, J., and Kahmann, R. (2011). A seven-WD40 protein related to human RACK1 regulates mating and virulence in *Ustilago maydis*. *Mol Microbiol.* 81:1484-1498.
- Wang, Y., Shen, G., Gong, J., Shen, D., Whittington, A., Qing, J., Treloar, J., Boisvert, S., Zhang, Z., Yang, C., and Wang, P. (2014). Noncanonical G β Gib2 is a scaffolding protein promoting cAMP signaling through functions of Ras1 and Cac1 proteins in *Cryptococcus neoformans*. *J Biol Chem.* 289:12202-12216.
- Watanabe, A., and Ebizuka, Y. (2004). Unprecedented mechanism of chain length determination in fungal aromatic polyketide synthases. *Chem Biol.* 11:1101-1106.
- Wawrzyn, G.T., Bloch, S.E., and Schmidt-Dannert, C. (2012). Discovery and characterization of terpenoid biosynthetic pathways of fungi. *Methods Enzymol.* 551:83-105.
- Weber, T., Charusanti, P., Musiol-Kroll, E.M., Jiang, X., Tong, Y., Kim, H.U., and Lee, S.Y. (2015). Metabolic engineering of antibiotic factories: new tools for antibiotic production in actinomycetes. *Trends Biotechnol.* 33:15-26.
- Weber, T., and Kim, H.U. (2016). The secondary metabolite bioinformatics portal: computational tools to facilitate synthetic biology of secondary metabolite production. *Synthetic and systems biotech.* 1:69-79.
- Wheeler, M.H. (1983). Comparisons of fungal melanin biosynthesis in ascomycetous, imperfect and basidiomycetous fungi. *Trans Brit Mycol Soc.* 81:29-36.
- White, L.P. (1958). Melanin: a naturally occurring cation exchange material. *Nature.* 182: 1427-1428.
- Wiemann, P., Willmann, A., Straeten, M., Kleigrewe, K., Beyer, M., Humpf, H.U., and Tudzynski, B. (2009). Biosynthesis of the red pigment bikaverin in *Fusarium fujikuroi*: genes, their function and regulation. 72:931-946.
- Wiemann, P., and Keller, N.P. (2014). Strategies for mining fungal natural products. *J Ind Microbiol Biotechnol.* 41:301-313.
- Wight, W.D., Kim, K.H., Lawrence, C.B., and Walton, J.D. (2009). Biosynthesis and role in virulence of the histone deacetylase inhibitor depudecin from *Alternaria brassicicola*. *Mol Plant Microbe Interact.* 22:1258-1267.
- Williams, R.B., Henrikson, J.C., Hoover, A.R., Lee, A.E., and Cichewicz, R.H. (2008). Epigenetic remodeling of the fungal secondary metabolome. *Org Biomol Chem.* 6:1895-1897.
- Williamson, P.R., Wakamatsu, K., and Ito, S. (1998). Melanin biosynthesis in *Cryptococcus neoformans*. *J Bacteriol.* 180:1570-1572.
- Willke, T., and Vorlop, K.D. (2001). Biotechnological production of itaconic acid. *Appl Microbiol Biotechnol.* 56:289-295.
- Winkelblech, J., Fan, A., and Li, S.M. (2015). Prenyltransferases as key enzymes in primary and secondary metabolism. *Appl Microbiol Biotechnol.* 99:7379-7397.

- Winterberg, B., Uhlmann, S., Linne, U., Lessing, F., Marahiel, M.A., Eichhorn, H., Kahmann, R., and Schirawski, J. (2010). Elucidation of the complete ferrichrome A biosynthetic pathway in *Ustilago maydis*. *Mol Microbiol.* 75:1260-1271.
- Woo, P.C., Tam, E.W., Chong, K.T., Cai, J.J., Tung, E.T., Ngan, A.H., Lau, S.K., and Yuen, K.Y. (2010). High diversity of polyketide synthase genes and the melanin biosynthesis gene cluster in *Penicillium marneffe*. *FEBS J.* 277:3750-3758.
- Wooloshuk, C.P., Sisler, H.D., Tokousbalides, M.C., and Dutky, S.R. (1980). Melanin biosynthesis in *Pyricularia oryzae*: site of tricyclazole inhibition and pathogenicity of melanin deficient mutants. *Pestic Biochem Physiol.* 14:256-264.
- Xue, C., Bahn, Y.S., Cox, G.M., Heitman, J. (2006). G protein-coupled receptor Gpr4 senses amino acids and activates the Camp-PKA pathway in *Cryptococcus neoformans*. *Mol Biol Cell.* 17:667-679.
- Yabe, K., Ando, Y., Hashimoto, J., and Hasamasaki, T. (1989). Two distinct *O*-methyltransferases in aflatoxin biosynthesis. *Appl Environ Microbiol.* 55:2172-2177.
- Yabe, K., and Hamasaki, T. (1993). Stereochemistry during aflatoxin biosynthesis: cyclase reaction in the conversion of versiconal to versicolorin B and racemization of versiconal hemiacetal acetate. *Appl Environ Microbiol.* 59:2493-2500.
- Yalpani, N., Altier, D.J., Barbour, E., Cigan, A.L., and Scelonge, C.J. (2001). Production of 6-methylsalicylic acid by expression of a fungal polyketide synthase activates disease resistance in tobacco. *Plant Cell.* 13:1401-1410.
- Yin, W., and Keller, N.P. (2011). Transcriptional regulatory elements in fungal secondary metabolism. *J Microbiol.* 49:329-339.
- Yu, J., Chang, P.K., Ehrlich, K.C., Cary, J.W., Bhatnagar, D., Cleveland, T.E., Payne, G.A., Linz, J.E., Woloshuk, C.P., Bennett, J.W. (2004). The clustered pathway genes in aflatoxin biosynthesis. *Appl Environ Microbiol.* 70:1253-1262.
- Yu, J., and Keller, N. (2005). Regulation of secondary metabolism in filamentous fungi. *Annu Rev Phytopathol.* 43:437-458.
- Yu, D., Xu, F., Zeng, J., and Zhan, J. (2012). Type III polyketide synthases in natural product biosynthesis. *IUBMB Life.* 64:285-295.
- Yuan C., Guo, Y.H., Wang, H.Y., Ma, X.J., Jiang, T., Zhao, J.L., Zou, Z.M., and Ding, G. (2016). Allelopathic polyketides from Endolichenic fungus *Myxotrichum* sp. by using OSMAC strategy. *Sci Rep.* 6:19350.
- Yuan, W.M., Gentil, G.D., Budde, A.D., and Leong, S.A. (2001). Characterization of the *Ustilago maydis* *sid2* gene, encoding a multidomain peptide synthetase in the ferrichrome biosynthetic gene cluster. *J Bacteriol.* 183:4040-4051.
- Yun, C.-S., Motoyama, T., and Osada, H. (2015). Biosynthesis of the mycotoxin tenuazonic acid by a fungal NRPS-PKS hybrid enzyme. *Nat Commun.* 6:8758.

- Zaehle, C., Gressler, M., Shelest, E., Geib, E., Hertweck, C., and Brock, M.** (2014). Terrein biosynthesis in *Aspergillus terreus* and its impact on phytotoxicity. *Chem Biol.* 21:719-731.
- Zhou, R., and Linz, J.E.** (1999). Enzymatic function of the Nor-1 protein in aflatoxin biosynthesis in *Aspergillus parasiticus*. *Appl Environ Microbiol.* 65:5639-5641.
- Zuther, K., Mayser, P., Hettwer, U., Wu, W., Spiteller, P., Kindler, B.L.J., Karlovsky, P., Basse, C.W. and Schirawski, J.** (2008). The tryptophan aminotransferase Tam1 catalyses the single biosynthetic step for tryptophan-dependent pigment synthesis in *Ustilago maydis*.

6 Supplementary data

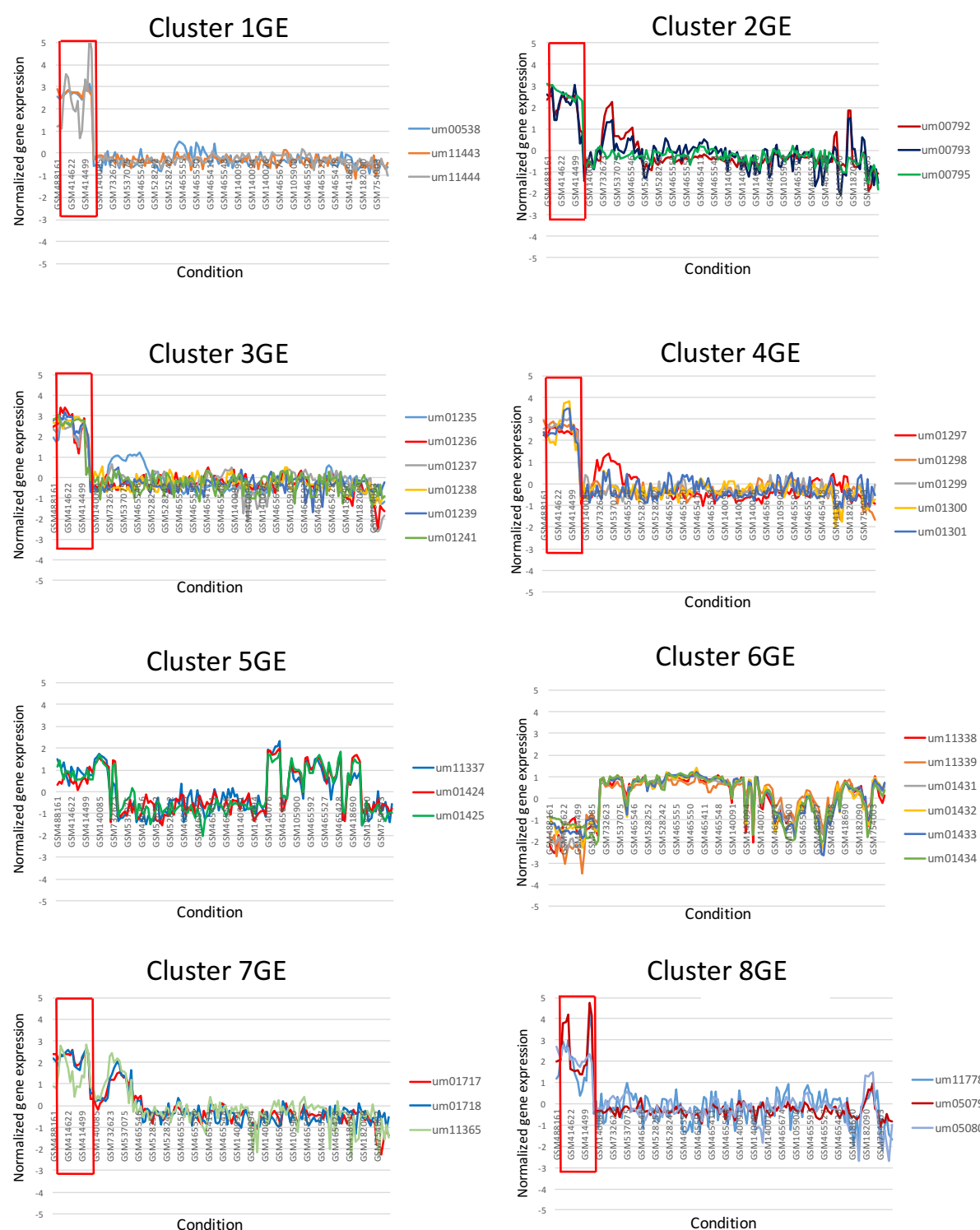


Figure S1, Part1. Overview of the gene expression profiles for all predicted members of the biosynthetic gene clusters of *U. maydis* (Cluster 1GE-Cluster 8GE). The y axis indicates the gene expression index on log₂ scale, and the x axis represents the 144 experimental conditions in the microarray compendium. Regions highlighted with a red rectangle indicate the conditions in which tumor material was analyzed (5dpi and 13 dpi).

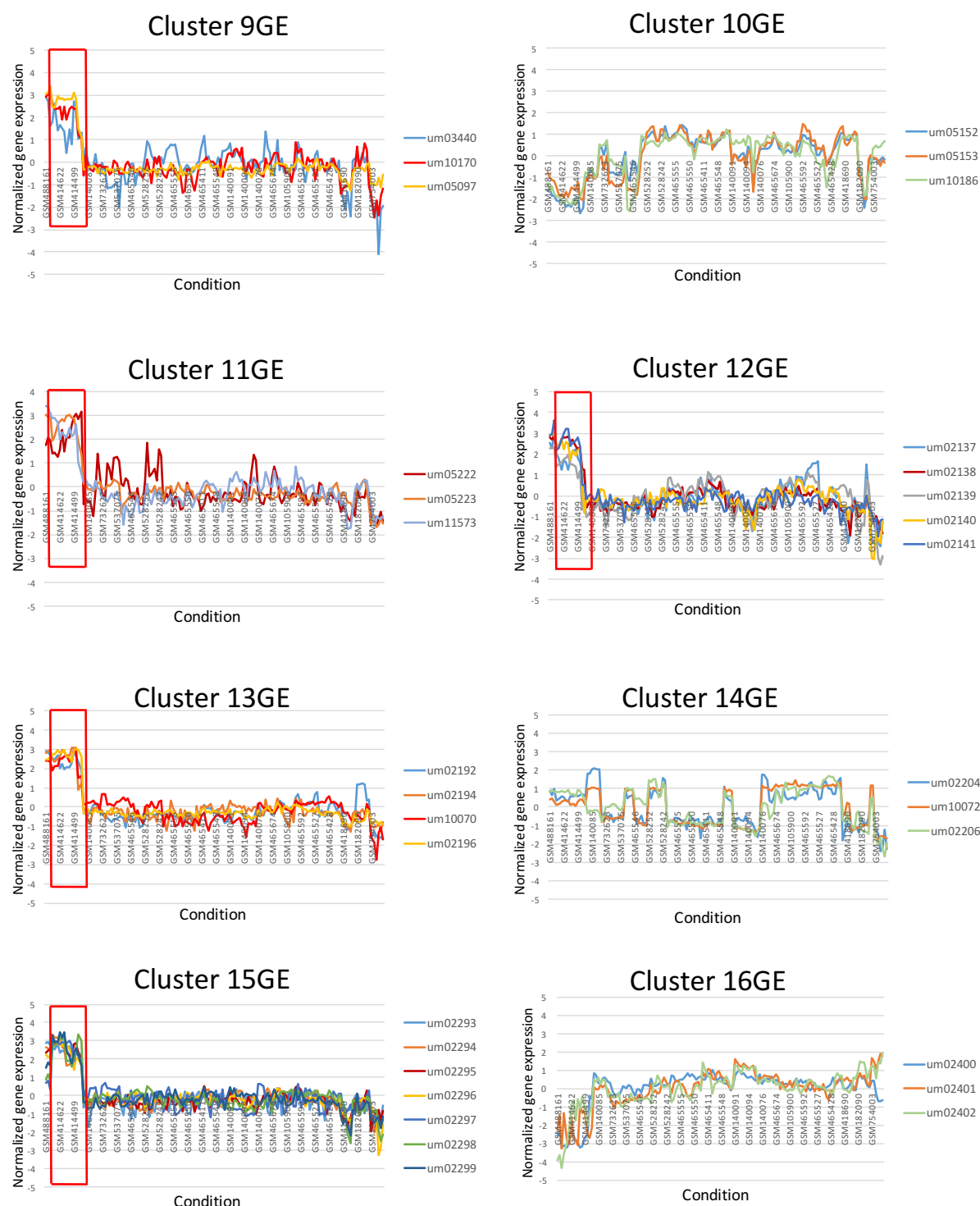


Figure S1, Part2. Overview of the gene expression profiles for all predicted members of the biosynthetic gene clusters of *U. maydis* (Cluster 9GE-Cluster 16GE). The y axis indicates the gene expression index on \log_2 scale, and the x axis represents the 144 experimental conditions in the microarray compendium. Regions highlighted with a red rectangle indicate the conditions in which tumor material was analyzed (5dpi and 13 dpi).

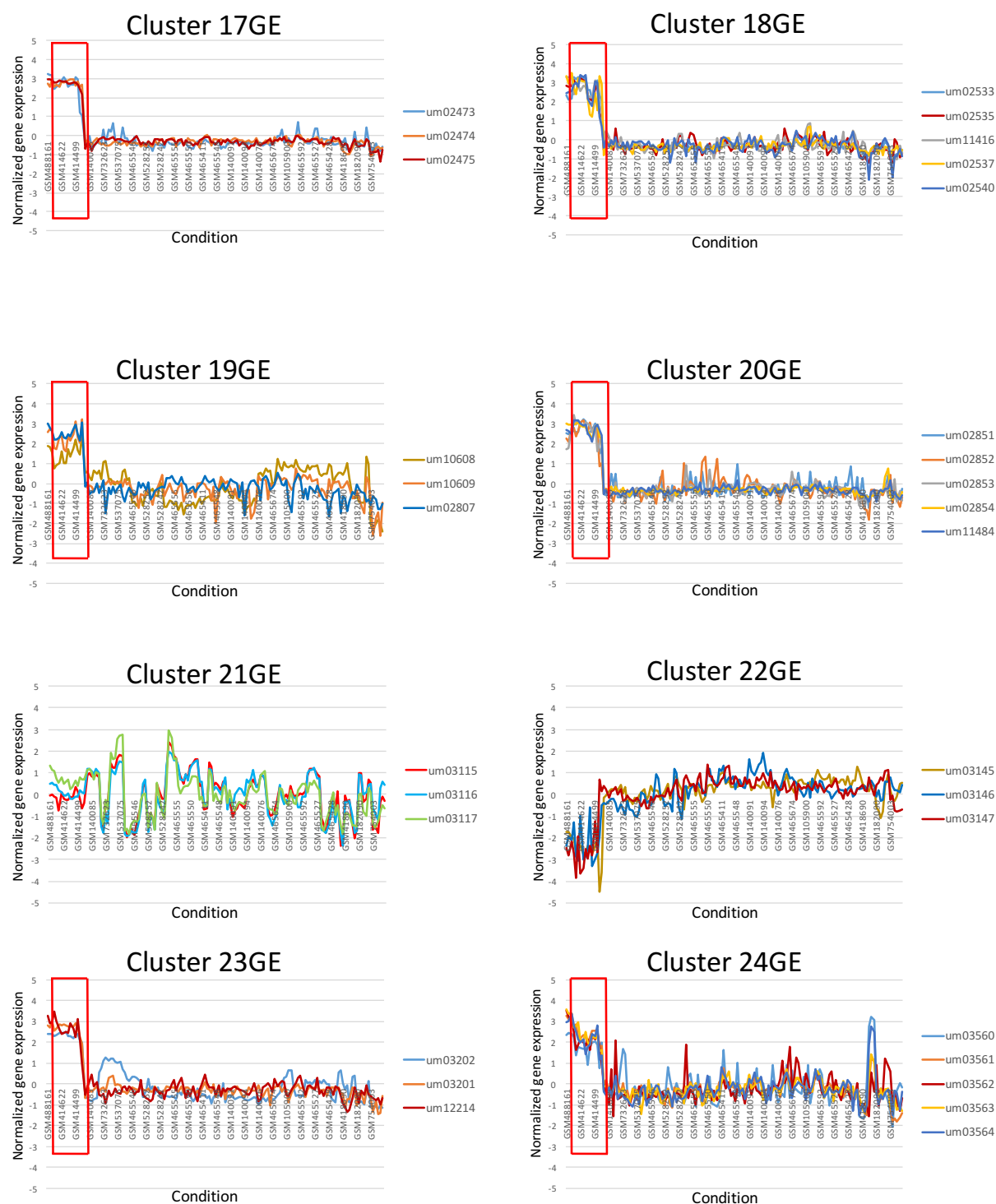


Figure S1, Part3. Overview of the gene expression profiles for all predicted members of the biosynthetic gene clusters of *U. maydis* (Cluster 17GE-Cluster 24GE). The *y* axis indicates the gene expression index on log₂ scale, and the *x* axis represents the 144 experimental conditions in the microarray compendium. Regions highlighted with a red rectangle indicate the conditions in which tumor material was analyzed (5dpi and 13 dpi).

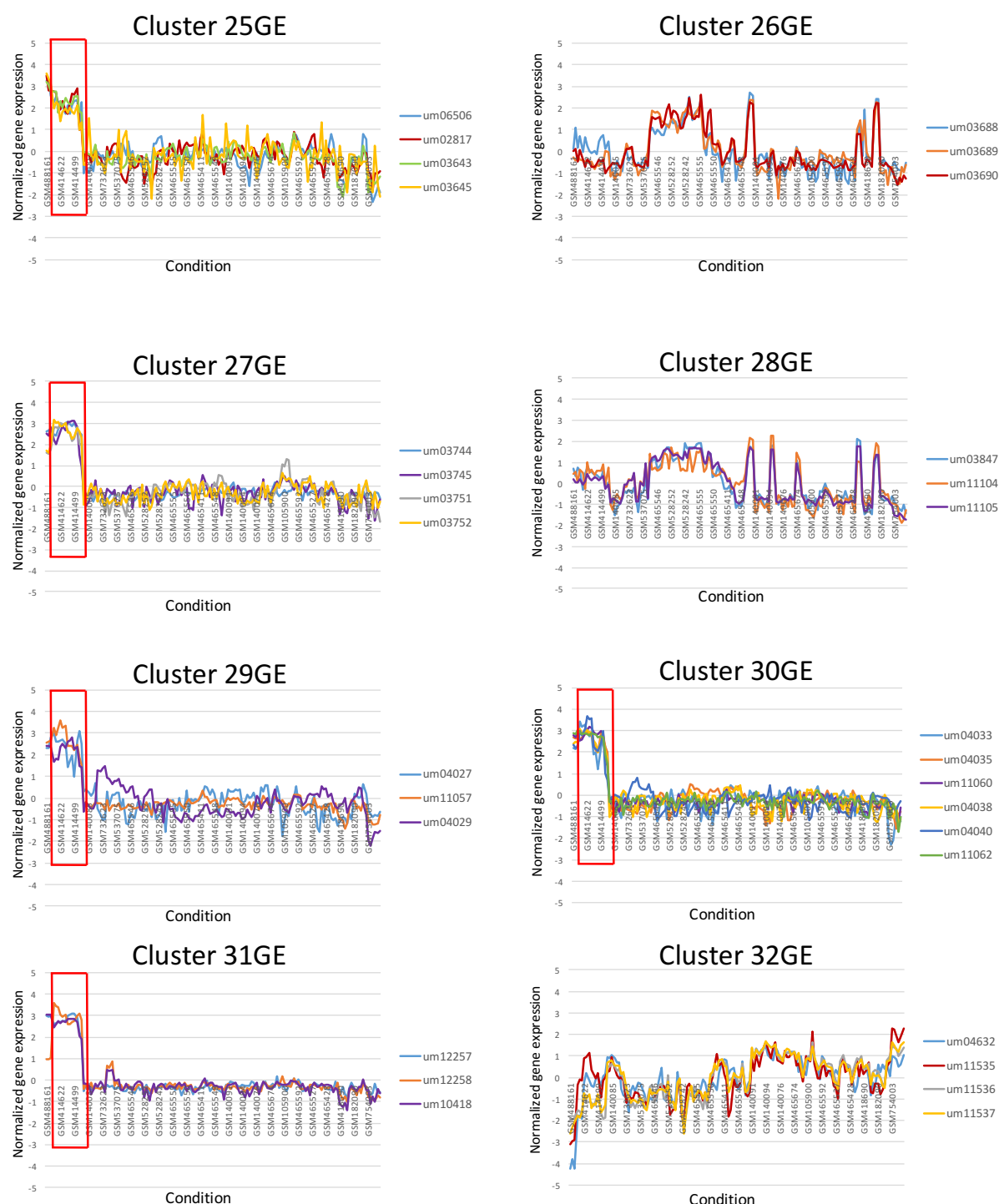


Figure S1, Part4. Overview of the gene expression profiles for all predicted members of the biosynthetic gene clusters of *U. maydis* (Cluster 25GE-Cluster 32GE). The y axis indicates the gene expression index on log₂ scale, and the x axis represents the 144 experimental conditions in the microarray compendium. Regions highlighted with a red rectangle indicate the conditions in which tumor material was analyzed (5dpi and 13 dpi).

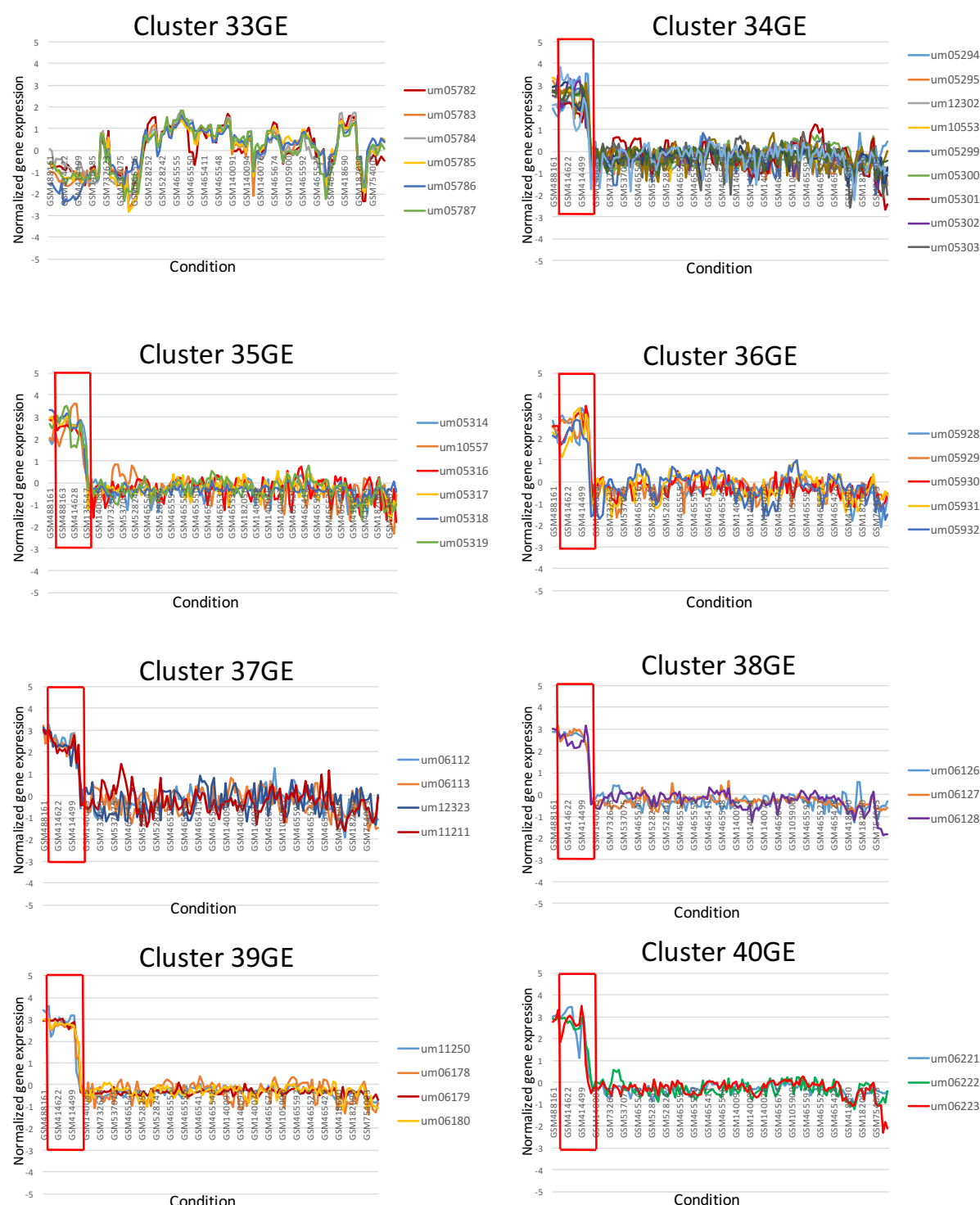


Figure S1, Part5. Overview of the gene expression profiles for all predicted members of the biosynthetic gene clusters of *U. maydis* (Cluster 33GE-Cluster 40GE). The y axis indicates the gene expression index on \log_2 scale, and the x axis represents the 144 experimental conditions in the microarray compendium. Regions highlighted with a red rectangle indicate the conditions in which tumor material was analyzed (5dpi and 13 dpi).

Table S1. Characteristic secondary metabolite genes identified in *U. maydis* by manual inspection.

Backbone Enzymes (BEs)				Tailoring Enzymes (TEs)					Transcription Factors (TFs)	Transporters (T)
PKS	NRPS	DMAT	TC	Cytochrome P450	Dehydrogenase	Transferase	Hydroxylase	Oxygenase	All categories	All categories
um04095 (12)	um10543 (19)			um00005 (1)	um10004 (1)	um00020 (1)	um00319 (1)	um00005 (1)	um00332 (1)	um00034 (1)
um04097 (12)				um00123 (1)	um00108 (1)	um00059 (1)	um01424 (2)	um00029 (1)	um00523 (1)	um00083 (1)
um04105 (12)				um10048 (1)	um00118 (1)	um10015 (1)	um11819 (3)	um11424 (1)	um00533 (1)	um00096 (1)
um10532 (14)				um00202 (1)	um00123 (1)	um10021 (1)	um05074 (4)	um11449 (1)	um00808 (1)	um00103 (1)
um06414 (23)				um00646 (1)	um11421 (1)	um00099 (1)	um05230 (4)	um00708 (1)	um00883 (2)	um00222 (1)
um06418 (23)				um11830 (1)	um00265 (1)	um10032 (1)	um11458 (5)	um00783 (1)	um00922 (2)	um00455 (1)
				um11618 (1)	um00381 (1)	um10043 (1)	um03408 (9)	um00965 (2)	um01371 (2)	um00477 (1)
				um12110 (1)	um00403 (1)	um00265 (1)	um06466 (23)	um01424 (2)	um01523 (3)	um11433 (1)
				um00940 (2)	um00407 (1)	um00280 (1)	um12340 (23)	um01425 (2)	um12167 (3)	um00597 (1)
				um11275 (2)	um00412 (1)	um00288 (1)		um01540 (3)	um01908 (3)	um00679 (1)
				um11645 (2)	um00418 (1)	um00322 (1)		um01714 (3)	um05183 (4)	um00712 (1)
				um01150 (2)	um00424 (1)	um11341 (1)		um11382 (3)	um02405 (5)	um11841 (2)
				um10232 (2)	um00555 (1)	um11347 (1)		um05074 (4)	um02808 (6)	um01051 (2)
				um01424 (2)	um00594 (1)	um00518 (1)		um05084 (4)	um02989 (7)	um01062 (2)
				um11653 (3)	um00694 (1)	um00579 (1)		um10188 (4)	um03074 (7)	um01156 (2)
				um01478 (3)	um11170 (1)	um00594 (1)		um06333 (4)	um03172 (8)	um01341 (2)
				um01723 (3)	um00844 (2)	um00595 (1)		um10062 (5)	um03346 (8)	um11339 (2)
				um11368 (3)	um11256 (2)	um00595 (1)		um10070 (5)	um03557 (9)	um01431 (2)
				um01863 (3)	um01049 (2)	um00605 (1)		um02398 (5)	um03588 (9)	um01435 (2)
				um01896 (3)	um11275 (2)	um00624 (1)		um12229 (9)	um03708 (10)	um01495 (3)
				um01947 (3)	um01099 (2)	um11613 (1)		um03415 (9)	um04101 (12)	um01656 (3)
				um01953 (3)	um01172 (2)	um11617 (1)		um11077 (9)	um04168 (12)	um11359 (3)
				um01980 (3)	um01233 (2)	um00789 (1)		um03728 (10)	um10417 (12)	um01700 (3)
				um12341 (3)	um01245 (2)	um11632 (1)		um03832 (10)	um10426 (12)	um15074 (3)
				um06473 (3)	um01250 (2)	um00872 (2)		um03995 (11)	um10941 (16)	um01756 (3)
				um05074 (4)	um01314 (2)	um10569 (2)		um04107 (12)	um11582 (16)	um01758 (3)
				um06273 (4)	um01328 (2)	um10624 (2)		um12271 (13)	um11176 (18)	um01762 (3)
				um02071 (5)	um01329 (2)	um10586 (2)		um04348 (14)	um10544 (19)	um01813 (3)
				um02377 (5)	um01335 (2)	um00980 (2)		um05586 (18)	um10560 (19)	um12169 (3)
				um02457 (5)	um11323 (2)	um00990 (2)		um05606 (18)	um05338 (19)	um01862 (3)

				um02464 (5)	um11333 (2)	um15057 (2)		um05329 (19)	um12033 (21)	um01868 (3)
				um02477 (5)	um01466 (3)	um11267 (2)		um05812 (20)	um11222 (22)	um01996 (3)
				um10296 (6)	um10804 (3)	um01040 (2)		um05967 (20)	um10971 (22)	um11777 (4)
				um02708 (6)	um11693 (3)	um01080 (2)		um06459 (23)	um15103 (23)	um05079 (4)
				um10835 (8)	um01619 (3)	um01088 (2)				um10761 (4)
				um11097 (9)	um01697 (3)	um01090 (2)				um06349 (4)
				um12241 (10)	um11361 (3)	um01093 (2)				um02037 (5)
				um03775 (10)	um01708 (3)	um01123 (2)				um02081 (5)
				um10507 (10)	um01711 (3)	um01139 (2)				um10072 (5)
				um03845 (10)	um01733 (3)	um01154 (2)				um02258 (5)
				um11288 (11)	um01747 (3)	um01200 (2)				um02365 (5)
				um11743 (11)	um01861 (3)	um01201 (2)				um02374 (5)
				um11744 (11)	um01881 (3)	um01231 (2)				um02387 (5)
				um04109 (12)	um01885 (3)	um10244 (2)				um02568 (6)
				um04189 (12)	um01911 (3)	um11317 (2)				um02583 (6)
				um04237 (12)	um01984 (3)	um11318 (2)				um02598 (6)
				um12269 (13)	um05069 (4)	um11330 (2)				um02686 (6)
				um11534 (13)	um05170 (4)	um01407 (2)				um02723 (6)
				um04362 (14)	um02105 (5)	um11334 (2)				um02806 (6)
				um05664 (16)	um02150 (5)	um01432 (2)				um15032 (6)
				um05791 (16)	um02164 (5)	um01450 (3)				um02900 (7)
				um04702 (17)	um02189 (5)	um11660 (3)				um11500 (7)
				um10682 (17)	um10077 (5)	um11672 (3)				um10320 (7)
				um04802 (17)	um02437 (5)	um01512 (3)				um10330 (7)
				um04818 (17)	um02461 (5)	um01533 (3)				um03034 (7)
				um05465 (18)	um02491-B (5)	um11682 (3)				um03110 (7)
				um12083 (19)	um02491-A (5)	um01621 (3)				um03148 (8)
				um11212 (21)	um02508 (6)	um01623 (3)				um03153 (8)
				um11005 (23)	um10276 (6)	um11885 (3)				um03293 (8)
				um06459 (23)	um02577 (6)	um11136 (3)				um03475 (9)
				um11812 (23)	um10283 (6)	um01726 (3)				um03655 (10)
					um10295 (6)	um11369 (3)				um11105 (10)
					um02683 (6)	um01752 (3)				um11514 (11)
					um10596 (6)	um01787 (3)				um03945 (11)
					um10599 (6)	um01804 (3)				um11057 (11)
					um02778 (6)	um01816 (3)				um04056 (11)

				um10605 (6)	um01818 (3)				um04146 (12)
				um02801 (6)	um01821 (3)				um04162 (12)
				um02888 (7)	um01835 (3)				um04523 (13)
				um03108 (7)	um01843 (3)				um01908 (13)
				um03126 (7)	um01870 (3)				um04680 (13)
				um10402 (8)	um01873 (3)				um04347 (14)
				um10643 (8)	um01875 (3)				um04399 (14)
				um03264 (8)	um01893 (3)				um04410 (14)
				um10825 (8)	um01979 (3)				um04423 (14)
				um03402 (8)	um11776 (4)				um10528 (14)
				um03523 (9)	um05103 (4)				um04444 (14)
				um12236 (9)	um11572 (4)				um11977 (14)
				um03665 (10)	um11784 (4)				um04478 (14)
				um03669 (10)	um05240 (4)				um04982 (15)
				um03761 (10)	um10766 (4)				um05023 (15)
				um10665 (10)	um06295 (4)				um05033 (15)
				um03845 (10)	um10768 (4)				um05642 (16)
				um03854 (10)	um10781 (4)				um05783 (16)
				um03990 (11)	um06329 (4)				um05642 (16)
				um04046 (11)	um06334 (4)				um05783 (16)
				um04061 (11)	um06491 (5)				um05786 (16)
				um11113 (12)	um12074 (5)				um05794 (16)
				um04127 (12)	um11460 (5)				um04811 (17)
				um04182 (12)	um10055 (5)				um05442 (18)
				um04210 (12)	um02124 (5)				um05506 (18)
				um04268 (12)	um10063 (5)				um10896 (18)
				um04300 (12)	um02170 (5)				um05602 (18)
				um12269 (13)	um10080 (5)				um05260 (19)
				um10846 (14)	um02291 (5)				um10210 (19)
				um04378 (14)	um02444 (5)				um05396 (19)
				um04441 (14)	um02500 (5)				um05889 (20)
				um10533 (14)	um02519 (6)				um05951 (20)
				um04480 (14)	um02527 (6)				um05954 (20)
				um11161 (15)	um02567 (6)				um05968 (20)
				um11162 (15)	um02624 (6)				um06093 (21)
				um04930 (15)	um02653 (6)				um06139 (21)

					um05644 (16)	um02657 (6)				um10968 (22)
					um10732 (16)	um02667 (6)				um06461 (23)
					um10735 (16)	um10308 (6)				
					um10938 (16)	um02715 (6)				
					um11583 (16)	um02783 (6)				
					um10581 (17)	um02793 (6)				
					um10682 (17)	um11483 (7)				
					um10695 (17)	um11638 (7)				
					um04833 (17)	um02913 (7)				
					um04873 (17)	um02915 (7)				
					um05598 (18)	um10326 (7)				
					um11181 (18)	um02979 (7)				
					um05600 (18)	um15001 (7)				
					um05610 (18)	um03063 (7)				
					um05252 (19)	um03073 (7)				
					um05275 (19)	um03114 (7)				
					um05407-A (19)	um03116 (7)				
					um05407-B (19)	um03117 (7)				
					um05412 (19)	um10636 (7)				
					um05923 (20)	um03169 (8)				
					um15025 (20)	um03182 (8)				
					um10898 (20)	um10402 (8)				
					um05970 (20)	um03298 (8)				
					um05970 (20)	um10833 (8)				
					um05984 (21)	um03318 (8)				
					um06086 (21)	um11010 (8)				
					um06105 (21)	um11014 (8)				
					um06111-B (21)	um03425 (9)				
					um06111-A (21)	um03515 (9)				
					um06185 (22)	um03537 (9)				
					um06186 (22)	um03538 (9)				
					um11231 (22)	um03543 (9)				
					um10973 (22)	um10571 (9)				
					um11241 (23)	um03621 (9)				

						um03661 (10)				
						um10484 (10)				
						um10659 (10)				
						um03858 (10)				
						um03873 (11)				
						um03937 (11)				
						um03949 (11)				
						um03984 (11)				
						um04081 (11)				
						um04106 (12)				
						um04193 (12)				
						um04198 (12)				
						um04209 (12)				
						um10428 (12)				
						um04209 (12)				
						um10428 (12)				
						um04277 (12)				
						um04496 (13)				
						um04505 (13)				
						um11987 (13)				
						um04562 (13)				
						um10904 (13)				
						um04590 (13)				
						um04649 (13)				
						um04353 (14)				
						um11151 (14)				
						um04374 (14)				
						um04375 (14)				
						um04406 (14)				
						um04420 (14)				
						um10539 (14)				
						um04913 (15)				
						um11770 (15)				
						um11771 (15)				
						um04994 (15)				
						um12293 (15)				

						um05627 (16)				
						um05671 (16)				
						um05678 (16)				
						um05692 (16)				
						um05746 (16)				
						um05769 (16)				
						um05785 (16)				
						um04712 (17)				
						um04714 (17)				
						um04740 (17)				
						um10688 (17)				
						um04801 (17)				
						um10704 (17)				
						um04844 (17)				
						um04881 (17)				
						um10749 (18)				
						um05531 (18)				
						um10357 (18)				
						um05545 (18)				
						um05547 (18)				
						um11792 (18)				
						um05554 (18)				
						um11795 (18)				
						um05569 (18)				
						um05584 (18)				
						um05614 (18)				
						um05293 (19)				
						um05348 (19)				
						um05355 (19)				
						um05433 (19)				
						um05848 (20)				
						um05900 (20)				
						um05915 (20)				
						um12026 (20)				
						um10864 (20)				
						um05994 (21)				

						um11807 (21)				
						um06035 (21)				
						um06047 (21)				
						um06061 (21)				
						um06088 (21)				
						um12068 (21)				
						um11220 (22)				
						um06205 (22)				
						um11231 (22)				
						um06426 (23)				
						um06462 (23)				
						um06467 (23)				

Chromosome location is indicated in brackets followed the ID of each gene.

Table S2. Potential SM gene clusters identified in *U. maydis* by SMURF.

Number of cluster	Gene ID	Annotated Function	Chromosome Location
Cluster 1	um00785	Uncharacterized protein	1
	um00786	Uncharacterized protein	1
	um00787	Probable FUM1-fumarate hydratase	1
	um00788	Uncharacterized protein	1
	um00789	Probable carnitine O-acetyltransferase, mitochondrial precursor	1
	um00790 ^a	Related to coenzyme a synthetase	1
Cluster 2	um01424	Probable cytochrome P450 monooxygenase/phenylacetate hydroxylase	2
	um01425	Probable homogentisate 1,2-dioxygenase	2
	um01426	Uncharacterized protein	2
	um01427	Related to Crg1 protein (Putative arabinase)	2
	um01428	Uncharacterized protein	2
	um01429	Related to high-affinity nickel transport protein nic1	2
	um01430	Related to siderophore iron transporter 3	2
	um01431	Related to ATP-binding cassette transporter protein	2
	um01432	Related to N6-hydroxylysine acetyl transferase	2
	um01433	Related to enoyl-CoA hydratase	2
	um01434 ^a	Siderophore peptide synthetase involved in ferrichrome A biosynthesis	2
	um01435	Related to MCH4-monocarboxylate transporter	2
	um01436	Uncharacterized protein	2
Cluster 3	um01815	Related to carbonyl reductase	3
	um01816	Related to TRM7-tRNA 2'-O-ribose methyltransferase	3
	um01817	Uncharacterized protein	3
	um01818	Related to TAE1-AdoMet-dependent proline methyltransferase	3
	um01819	Uncharacterized protein	3
	um01820	Uncharacterized protein	3
	um01821	Probable KRE2-alpha-1,2-mannosyltransferase	3
	um01822	-	3
	um01823	Uncharacterized protein	3
	um01824	Uncharacterized protein	3
	um01825	Uncharacterized protein	3
	um01826	Uncharacterized protein	3
	um01827	Related to acid phosphatase ACP2 precursor	3
	um01828	-	3
	um01829	Related to alpha-L-arabinofuranosidase I precursor	3
	um01830 ^a	Related to alpha-amino adipate reductase	3
	um01831	Uncharacterized protein	3
	um01832	Uncharacterized protein	3
	um01833	Related to zinc finger DHHC domain containing protein 2	3
	um01834	Uncharacterized protein	3
	um01835	Related to carnitine acetyl transferase FacC	3
	um01836	Uncharacterized protein	3
	um01837	Uncharacterized protein	3
	um01838	-	3
Cluster 4	um02621	-	6
	um02622	Uncharacterized protein	6
	um02623 ^a	Uncharacterized protein	6
	um02624	Related to alpha-1,6-mannosyltransferase	6
	um02625	Probable DUR3-Urea permease	6
	um02626	Uncharacterized protein	6
	um02627	Uncharacterized protein	6
	um02628	Related to DNA-directed RNA polymerase I	6

Cluster 4	um02629	Related to YRO2-Putative plasma membrane protein, transcriptionally regulated by Haa1p	6
	um02630	Uncharacterized protein /related to thiamin pyrophosphokinase	6
	um02631	Uncharacterized protein	6
	um02632	Probable nudC protein	6
	um02633	Probable FBP26-fructose-2,6-biphosphatase	6
	um02634	Uncharacterized protein	6
	um02635	Uncharacterized protein	6
	um02636	Related to LYS2-L-aminoadipate-semialdehyde dehydrogenase, large subunit	6
	um02637	Related to PBP1-Pab1p interacting protein	6
	um02638	Related to GEM1 mitochondrial GTPase EF-hand protein	6
	um02639	Probable ubiquitin-specific processing protease 21	6
Cluster 5	um02960	Probable Ser/Thr protein phosphatase 2A regulatory subunit A	7
	um02961	Uncharacterized protein	7
	um02962	Related to OSH6-member of an oxysterol-binding protein family	7
	um02963	Uncharacterized protein	7
	um02964	Related to Ras-like G protein RagD	7
	um02965	Related to PEX29-peroxisomal integral membrane peroxin	7
	um02966	Related to RPC37-RNA polymerase III subunit C37	7
	um02967	Probable YNK1-nucleoside diphosphate kinase	7
	um02968	Related to LSM1-Sm-like (Lsm) protein	7
	um02969	Probable ubiquitin-conugating enzyme e2-23 kda	7
	um02970	Uncharacterized protein	7
	um02971 ^a	Related to fatty acid synthase, beta and alpha chains	7
	um02972	Uncharacterized protein	7
	um02973	Uncharacterized protein	7
	um02974	Related to AUT4-breakdown of autophagic vesicles inside the vacuole	7
	um02975	Uncharacterized protein	7
	um02976	Uncharacterized protein	7
	um02977	Related to CWC2-involved in mRNA splicing	7
	um02978	Uncharacterized protein	7
	um02979	Related to HPM1-AdoMet-dependent methyltransferase	7
Cluster 6	um03104	Uncharacterized protein	7
	um03105	Uncharacterized protein	7
	um03106	Uncharacterized protein	7
	um03107	Uncharacterized protein	7
	um03108 ^a	Related to aminoadipate-semialdehyde dehydrogenase	7
	um03109	Related to pH-regulated antigen pra1 precursor	7
	um03110	Related to ZRT2-Zinc transporter II	7
	um03111	Uncharacterized protein	7
	um03112	Uncharacterized protein	7
	um03113	Uncharacterized protein	7
	um03114	Acetyltransferase involved in MEL production	7
	um03115	Major facilitator involved in MEL production	7
	um03116	Acyltransferase involved in MEL production	7
	um03117	Erythritol-mannosyl-transferase involved in MEL production	7
	um03118	Uncharacterized protein	7
	um03119	Acetyltransferase involved in MEL production	7
Cluster 7	um04095 ^a	Polyketide synthase	12
	um04096	Uncharacterized protein	12
	um04097	Polyketide synthase	12
	um04116	Uncharacterized protein	12
	um02990	Uncharacterized protein	7
Cluster 8	um04099	Related to HAP1-heme activator protein	12
	um04100	Uncharacterized protein	12
	um04101	Related to BAS1-transcription factor	12

Cluster 8	um04102	Related to ascorbate oxidase precursor	12
	um04103	Related to versicolorin B synthase	12
	um04104	Uncharacterized protein	12
	um04105 ^a	Related to polyketide synthase	12
	um04106	Related to O-methyltransferase B	12
	um04107	Related to phenol-2-monooxygenase	12
	um04108	Uncharacterized protein	12
	um04109	Related to cytochrome P450	12
	um04110	Related to NADP(+)-dependent dehydrogenase	12
	um04111	Uncharacterized protein	12
	um04112	Uncharacterized protein	12
	um04113	Myosin I	12
	um04114	Probable PHO8-repressible alkaline phosphatase vacuolar	12
	um04115	Probable LYS20-homocitrate synthase	12
	um04116	Uncharacterized protein	12
	um04117	Related to CAX4-required for full levels of dolichol-linked oligosaccharides	12
	um04118	Uncharacterized protein	12
	um04119	Uncharacterized protein	12
Cluster 9	um04694	Related to alcohol dehydrogenase class III chi chain	17
	um04695	Probable HNM1-choline permease	17
	um04696	Uncharacterized protein	17
	um04697 ^a	Related to LYS2 alpha aminoadipate reductase	17
	um04698	Uncharacterized protein	17
	um04699	Uncharacterized protein	17
	um04700	Related to ATP23-putative metalloprotease of the mitochondrial inner membrane	17
	um04701	Probable rcd1 protein involved in sexual development	17
	um04702	Related to CYT2-holocytochrome-c1 synthase	17
	um04703	Probable phosphomannomutase	17
	um04704	Related to MRE11-DNA repair and meiotic recombination protein	17
	um04705	Related to ARG2-acetylglutamate synthase	17
Cluster 10	um05165 ^a	Ferrichrome siderophore peptide synthetase	4
	um05166	Related to FUN30-Protein important for chromosome integrity and segregation	4
	um05167	Uncharacterized protein	4
	um05168	Putative histone acetylase	4
	um05169	Related to YAP1802-protein involved in clathrin cage assembly	4
	um05170	Probable formate dehydrogenase	4
	um05171	Related to multifunctional folic acid synthesis protein	4
	um05172	Uncharacterized protein	4
	um05173	Related to DnaJ homolog subfamily C member 3	4
	um05174	Uncharacterized protein	4
	um05175	Uncharacterized protein	4
	um05176	Related to TMS1 protein	4
	um05177	Related to endosomal protein EMP70 precursor	4
	um05178	Related to BET5-component of the TRAPP complex	4
	um05179	Probable MVD1-Mevalonate pyrophosphate decarboxylase	4
Cluster 11	um05245 ^a	Related to NRPS (N-terminal fragment)	19
	um05246	Related to BAS1-Myb-related transcription factor	19
	um05247	Related to methylcrotonyl-CoA carboxylase beta chain, mitochondrial precursor	19
	um05248	Related to TPO3-Polyamine transport protein	19
	um05249	Uncharacterized protein	19
	um05250	Related to methylcrotonyl-CoA carboxylase alpha chain, mitochondrial precursor	19
	um05251	Uncharacterized protein	19
	um05252	Probable NADP-dependent mannitol dehydrogenase	19

	um05253	Related to ATP-binding multidrug cassette transport protein	19
	um05254	Uncharacterized protein	19
	um05255	Uncharacterized protein	19
	um05256	Uncharacterized protein	19
	um05257	Probable histone 3	19
	um05258	Uncharacterized protein	19
	um05259	Uncharacterized protein	19
	um05260	Related to inorganic phosphate transporter	19
Cluster 12	um05781	Uncharacterized protein	16
	um05782	Capsule-associated protein-like protein	16
	um05783	Related to UDP-galactose transporter	16
	um05784	Related to capsular associated protein	16
	um05785	Acyl transferase-like protein	16
	um05786	Related to UDP N-acetylglucosamine transporter	16
	um05787	Uncharacterized protein	16
	um05788	Uncharacterized protein	16
	um05789	Uncharacterized protein	16
	um05790	Uncharacterized protein	16
	um05791	Related to cytochrome P450	16
	um05792	Related to chitin deacetylase precursor	16
	um05793	Uncharacterized protein	16
	um05794	Probable YCF1-vacuolar full size ABC transporter	16
	um05795	Uncharacterized protein	16
	um05796 ^a	Uncharacterized protein	16
Cluster 13	um06407	Probable VIP1-actin cytoskeleton organization and biogenesis-related protein	23
	um06408	Related to IVY1-Phospholipid-binding protein	23
	um06409	Uncharacterized protein	23
	um06410	Related to SFH1-component of the RSC chromatin remodeling complex	23
	um06411	Related to aspartate-tRNA ligase, mitochondrial	23
	um06412	Related to paxillin	23
	um06413	Uncharacterized protein	23
	um06414	Polyketide synthase	23
	um06415	Uncharacterized protein	23
	um06416	Uncharacterized protein	23
	um06417	Related to superoxide dismutase	23
	um06418 ^a	Polyketide synthase	23
	um06419	Uncharacterized protein	23
	um06420	Uncharacterized protein	23
	um06421	Related to Gamm1 protein/Ni-binding urease accessory protein (UreG)	23
	um06422	Uncharacterized protein	23
	um06423	-	23
	um06424	Related to aldehyde dehydrogenase NAD(P)	23
	um06425	Uncharacterized protein	23
	um06426	Related to SLC1-1-acyl-sn-glycerol-3-phosphate acyltransferase	23
	um06427	Related to kinesin-like protein KIF2C	23
	um06428	Related to thiamine-repressible acid phosphatase precursor	23
	um06429	Uncharacterized protein	23
	um06430	Probable heat shock protein HSP104 (endopeptidase Clp ATP-binding chain HSP104)	23
Cluster 14	um06452	Uncharacterized protein	23
	um06453	Related to transaldolase B	23
	um06454	Related to mannose-6-phosphate isomerase	23
	um06455	Uncharacterized protein	23
	um06456	Related to aminopeptidase Y precursor, vacuolar	23
	um06457	-	23

	um06458	Regulator of ustilagic acid biosynthesis	23
	um06459	Cytochrome P450 monooxygenase involved in ustilagic acid production	23
Cluster 14	um06460 ^a	Fatty acid synthase FAS2	23
	um06461	ABC transporter	23
	um06462	Ustilagic acid acyltransferase	23
	um06463	Cytochrome P450 enzyme involved in glycolipid production	23
	um06464	Uncharacterized protein	23
	um06465	Uncharacterized protein	23
	um06466	Ustilagic acid hydroxylase	23

Table S3. Potential SM gene clusters identified in *U. maydis* by anti-SMASH.

Number of cluster	Gene ID	Annotated Function	Chromosome Location
Cluster 1	um00784	Uncharacterized protein	1
	um12356	Uncharacterized protein (N-terminal fragment)	1
	um00785	Uncharacterized protein	1
	um00786	Uncharacterized protein	1
	um10787	Probable FUM1 (fumarate hydratase)	1
	um00788	Uncharacterized protein	1
	um00789	Probable carnitine O-acetyltransferase, mitochondrial precursor	1
	um00790	Related to coenzyme a synthetase	1
	um10788	Probable AAP1-alanine/arginine aminopeptidase	1
	um00792	Uncharacterized protein	1
	um00793	Uncharacterized protein	1
	um00794	Uncharacterized protein	1
	um00795	Uncharacterized protein	1
	um00796	Uncharacterized protein	1
	um15051	Related to SKN1-protein involved in sphngolipid biosynthesis	1
	um00797	Probable adenosine kinase	1
	um00798	Related to RAD5-DNA helicase	1
Cluster 2	um01426-A	Uncharacterized protein	2
	um01426-B	Uncharacterized protein	2
	um01427	Related to Crg1 protein (Putative arabinase)	2
	um01428	Uncharacterized protein	2
	um01429	Related to high-affinity nickel transport protein nic1	2
	um11338	Related to AIF1-mitochondrial cell death effector	2
	um11339	Related to Siderophore iron transporter 3	2
	um01431	Related to ATP-binding cassette transporter protein	2
	um01432	Related to N6-hydroxylysine acetyl transferase	2
	um01433	Related to Enoyl-CoA hydratase	2
	um01434	Siderophore peptide synthetase involved in ferrichrome A biosynthesis	2
	um01435	Related to MCH4-monocarboxylate transporter	2
	um01436	Uncharacterized protein	2
	um01437	Uncharacterized protein	2
	um01438	Uncharacterized protein	2
	um01439	Related to FRE3, ferric reductase	2
	um11873	Uncharacterized protein	2
	um01441	Uncharacterized protein	2
Cluster 3	um01691	Related to ATP-dependent DNA helicase	3
	um01692	Related to CHA1-L-serine/L-threonine deaminase	3
	um11358	Related to MEF2-translation elongation factor, mitochondrial	3
	um11359	Related to BOR1-boron efflux transporter	3
	um01694	Uncharacterized protein	3
	um01695	Uncharacterized protein	3
	um01696	Uncharacterized protein	3
	um01697	Probable LYS2-L-aminoadipate-semialdehyde dehydrogenase, large subunit	3
	um01698	Uncharacterized protein	3
	um01699	Uncharacterized protein	3
	um01700	Related to ABC transporter protein	3
	um01701	Uncharacterized protein	3
	um01702	Uncharacterized protein	3
	um01703	Uncharacterized protein	3

Cluster 4	um12165	Uncharacterized protein	3
Cluster 4	um01826	Uncharacterized protein	3
	um01827	Related to acid phosphatase ACP2 precursor	3
	um12166	Related to SPC1-signal peptidase 10.8 kDa subunit	3
	um12167	Related to PPR1-Zinc finger transcription factor	3
	um12168	Uncharacterized protein	3
	um01829	Related to alpha-L-arabinofuranosidase I precursor	3
	um01830	Related to alpha-aminoadipate reductase	3
	um01831	Uncharacterized protein	3
	um01832	Uncharacterized protein	3
	um01833	Related to zinc finger DHHC domain containing protein 2	3
	um01834	Uncharacterized protein	3
	um01835	Related to carnitine acetyl transferase FacC	3
	um10255	Uncharacterized protein	3
	um01837	Uncharacterized protein	3
	um10256	Uncharacterized protein	3
Cluster 5	um05160	Probable ILS1-isoleucyl-tRNA synthetase	4
	um05161	Related to phosducin	4
	um05162	Probable ADE6-phosphoribosylformyl glycine synthetase	4
	um05163	Uncharacterized protein	4
	Um10188	1-ornithine N5-oxygenase	4
	Um10189	Ferrichrome siderophore peptide synthetase	4
	um05166	Related to FUN30-protein important for chromosome integrity and segregation	4
	um05167	Uncharacterized protein	4
	um10190	Putative histone acetylase	4
	um05169	Related to YAP1802-protein involved in clathrin cage assembly	4
	um05170	Probable formate dehydrogenase	4
	um12158	Uncharacterized protein	4
	um05171	Related to multifunctional folic acid synthesis protein	4
	um12159	Uncharacterized protein	4
	um05173	Related to DnaJ homolog subfamily C member 3	4
	um05174	Uncharacterized protein	4
Cluster 6	um06284	Related to Cut11 or CASP protein	4
	um06285	Related to carbamoyl-phosphate synthase small chain, arginine specific	4
	um10760	Uncharacterized protein	4
	um10761	Related to FLC2-Putative FAD transporter	4
	um06287	Related to Phytoene synthase	4
	um06288	Uncharacterized protein	4
Cluster 7	um02629	Related to YRO2-Putative plasma membrane protein, transcriptionally regulated by Haa1p	6
	um02630	Uncharacterized protein/related to thiamin pyrophosphokinase	6
	um02631	Uncharacterized protein	6
	um02632	Probable nudC protein	6
	um10293	Probable FBF26-fructose-2,6-bisphosphatase	6
	um10294	Uncharacterized protein	6
	um02635	Uncharacterized protein	6
	um10295	Related to LYS2-L-aminoadipate-semialdehyde dehydrogenase, large subunit	6
	um02637	Related to PBP1-Pab1p interacting protein	6
	um02639	Probable ubiquitin-specific processing protease 21	6
	um02640	Uncharacterized protein	6
	um02641	Related to PEX10-peroxisomal assembly protein-peroxin	6
	um02642	Uncharacterized protein	6

Cluster 7	um10296	Probable COX12-cytochrome-c-oxidase, subunit VIB	6
	um10297	Related to pre-mRNA splicing factor 18	6
	um10298	Uncharacterized protein	6
	um02645	Probable DIBB1-17kDa component of the U4/U6aU5 tri-snRNP	6
	um10299	Related to LUC7-essential protein associated with the U1 snRNP complex	6
	um10300	Related to JJJ1 cochaperone required for a late step of ribosome biogenesis	6
	um10301	Uncharacterized protein	6
	um10302	Uncharacterized protein	6
	um02649	Uncharacterized protein	6
	um12194	Related to SWD2-subunit of the COMPASS complex	6
	um02651	Related to dihydroceramide delta (4)-desaturase	6
	um02652	Uncharacterized protein	6
	um02653	Related to alpha-1,3-mannosyltransferase alg2	6
	um02654	Uncharacterized protein	6
	um02655	Related to RNA binding motif protein	6
Cluster 8	um03100	Related to dynein light chain 2B, cytoplasmic	7
	um11948	Related to ubiquitin-like protein Hub1	7
	um03102	Uncharacterized protein	7
	um03103	Probable ribose-5-phosphate isomerase	7
	um10627	Related to triose-phosphate isomerase	7
	um10628	Uncharacterized protein	7
	um10629	Uncharacterized protein	7
	um03105	Uncharacterized protein	7
	um10630	Uncharacterized protein	7
	um10631	Uncharacterized protein	7
	um03108	Related to aminoadipate-semialdehyde dehydrogenase	7
	um10632	Related to pH-regulated antigen pral precursor	7
	um03110	Related to ZRT2-zinc transporter II	7
	um10633	Uncharacterized protein	7
	um10634	Uncharacterized protein	7
	um03112	Uncharacterized protein	7
	um03113	Uncharacterized protein	7
	um03114	Acetyltransferase involved in MEL production	7
	um03115	Major facilitator involved in MEL transport	7
Cluster 9	um03583	Related to HIS2-histidinol-phosphatase	9
	um03584	Related to RPA49-49kDa subunit of DNA-directed RNA polymerase I	9
	um03585	Uncharacterized protein	9
	um03586	Uncharacterized protein	9
	um12235	Uncharacterized protein	9
	um03588	Related to transcription factor medusa	9
	um11959	Uncharacterized protein	9
	um03590	Uncharacterized protein	9
	um12236	Probable NADP(+)-dependent dehydrogenase acting on 3-hydroxy acids	9
	um11960	Uncharacterized protein	9
	um03593	Probable sterol delta 5,6-desaturase	9
	um03595	Uncharacterized protein	9
	um03596	Related to PEX7-peroxisomal import protein-peroxin	9
	um03597	Uncharacterized protein	9
	um03598	Related to ENT2-clathrin binding protein, required for endocytosis	9
	um03599	Probable CDC12-septin	9
Cluster 10	um04095	Related to polyketide synthase	12
	um04096	Uncharacterized protein	12

	um04097	Related to polyketide synthase	12
Cluster 11	um04350	Related to 3-phytase A precursor	14
	um04351	Probable sec7-component of non-clathrin vesicle coat	14
Cluster 11	um04352	Probable MOB1 protein	14
	um04353	Related to glycosyl transferase, group 2 family protein	14
	um04354	Uncharacterized protein	14
	um04355	Related to Sel-1 homolog precursor	14
	um04356	Related to UTP20 component of the small-subunit processome	14
	um04357	Related to endo-1,6-beta-d-glucanase precursor	14
	um04358	Uncharacterized protein	14
	um12262	Related to 4-coumarate-CoA ligase	14
	um11146	Uncharacterized protein	14
	um11147	Uncharacterized protein	14
	um04361	Related to KRI1-KRRI-Interacting protein 1	14
Cluster 12	um04371	Related to eukaryotic translation initiation factor	14
	um04372	Cytoplasmic dynein heavy chain 2	14
	um12263	Uncharacterized protein	14
	um11151	Related to type I protein geranylgeranyltransferase beta subunit	14
	um04374	Farnesyl-diphosphate farnesyltransferase	14
	um04375	Related to hnRNP arginine N-methyltransferase	14
	um04376	Uncharacterized protein	14
	um11152	Related to 2-amino-3-carboxylmuconate-6-semialdehyde decarboxylase	14
	um04378	Related to phenylacetaldehyde dehydrogenase	14
	um04379	Related to gibberellin 20-oxidase	14
Cluster 13	um10543	Related to non-ribosomal peptide synthetase (N-terminal fragment)	19
	um10544	Related to BAS1-Myb-related transcription factor	19
	um05247	Related to methylcrotonyl-CoA carboxylase beta chain, mitochondrial precursor	19
	um05248	Related to TPO3-Polyamine transport protein	19
	um05249	Uncharacterized protein	19
Cluster 14	um06411	Related to aspartate-tRNA ligase, mitochondrial	23
	um06412	Related to paxillin	23
	um06413	Uncharacterized protein	23
	um06414	Related to polyketide synthase	23
	um11239	Uncharacterized protein	23
	um06416	Uncharacterized protein	23
	um06417	Related to superoxide dismutase	23
	um06418	Related to polyketide synthase	23

Table S4. Description of the 144 experiments downloaded from GEO, platform GPL3681.

Condition	GEO ID	Description of the condition	Replicate
1	GSM488161	Tumor material from maize leaves 5 days post FB1Δfox1/FB2Δfox1 mixed infection at 28°C	2nd
2	GSM488162	Tumor material from maize leaves 5 days post FB1Δfox1/FB2Δfox1 mixed infection at 28°C	3rd
3	GSM488160	Tumor material from maize leaves 5 days post FB1Δfox1/FB2Δfox1 mixed infection at 28°C	1st
4	GSM488165	Tumor material from maize leaves 5 days post FB1/FB2 mixed infection at 28°C	3rd
5	GSM488164	Tumor material from maize leaves 5 days post FB1/FB2 mixed infection at 28°C	2nd
6	GSM488163	Tumor material from maize leaves 5 days post FB1/FB2 mixed infection at 28°C	1st
7	GSM414622	Tumor material from maize leaves 5 days post FB1/FB2 mixed infection at 31°C	2nd
8	GSM414621	Tumor material from maize leaves 5 days post FB1/FB2 mixed infection at 31°C	1st
9	GSM414624	Tumor material from maize leaves 5 days post FB1/FB2 mixed infection at 31°C	3rd
10	GSM414629	Tumor material from maize leaves 5 days post RAb1ts/RAb2ts mixed infection at 31°C	3rd
11	GSM414628	Tumor material from maize leaves 5 days post RAb1ts/RAb2ts mixed infection at 31°C	2nd
12	GSM414625	Tumor material from maize leaves 5 days post RAb1ts/RAb2ts mixed infection at 31°C	1st
13	GSM414499	Tumor material from maize leaves 5 days post RAb1ts/RAb2ts mixed infection at 22°C	1st
14	GSM414496	Tumor material from maize leaves 5 days post FB1/FB2 mixed infection at 22°C	1st
15	GSM135548	Tumors induced in corn plants by an infection with the strains FB1 and FB2 (13 dpi)	2nd
16	GSM135547	Tumors induced in corn plants by an infection with the strains FB1 and FB2 (13 dpi)	1st
17	GSM140086	HE140 strain grown for 180 min in CM medium containing 1% (w/v) arabinose	3rd
18	GSM140081	FB1 strain grown for 75 min in CM medium containing 1% (w/v) arabinose	3rd
19	GSM140085	HE140 strain grown for 180 min in CM medium containing 1% (w/v) arabinose	2nd
20	GSM140084	HE140 strain grown for 180 min in CM medium containing 1% (w/v) arabinose	1st
21	GSM140080	FB1 strain grown for 75 min in CM medium containing 1% (w/v) arabinose	2nd
22	GSM140079	FB1 strain grown for 75 min in CM medium containing 1% (w/v) arabinose	1st
23	GSM732626	SG200Δtup1 strain grown for 48 h on charcoal minimal medium	2nd
24	GSM732625	SG200Δtup1 strain grown for 48 h on charcoal minimal medium	1st
25	GSM732623	SG200 strain grown for 48 h on charcoal minimal medium	1st
26	GSM732624	SG200 strain grown for 48 h on charcoal minimal medium	2nd
27	GSM537076	SG200Δrep1 strain grown on NM+ charcoal plates for 48 h	1st
28	GSM537077	SG200Δrep1 strain grown on NM+ charcoal plates for 48 h	2nd
29	GSM537078	SG200Δrep1 strain grown on NM+ charcoal plates for 48 h	3rd
30	GSM537074	SG200 strain grown on NM+ charcoal plates for 48 h	2nd
31	GSM537075	SG200 strain grown on NM+ charcoal plates for 48 h	3rd
32	GSM537073	SG200 strain grown on NM+ charcoal plates for 48 h	1st
33	GSM465433	AB31 strain grown for 12 h in array medium containing 1% (w/v) arabinose	2nd

34	GSM465432	AB31 strain grown for 12 h in array medium containing 1% (w/v) arabinose	1st
35	GSM528243	AB33 strain grown for 12 h in array medium containing 3g/l nitrate and 1% (w/v) arabinose	1st
36	GSM528244	AB33 strain grown for 12 h in array medium containing 3g/l nitrate and 1% (w/v) arabinose	2nd
37	GSM465546	AB33 strain grown for 12 h in array medium containing 3g/l nitrate	2nd
38	GSM465545	AB33 strain grown for 12 h in array medium containing 3g/l nitrate	1st
39	GSM465543	AB33 strain grown for 5 h in array medium containing 3g/l nitrate	1st
40	GSM465544	AB33 strain grown for 5 h in array medium containing 3g/l nitrate	2nd
41	GSM465541	AB33 strain grown for 3 h in array medium containing 3g/l nitrate	1st
42	GSM465542	AB33 strain grown for 3 h in array medium containing 3g/l nitrate	2nd
43	GSM528252	UKH156 strain grown for 12 h in array medium containing 3g/l nitrate and 1% (w/v) arabinose	1st
44	GSM528253	UKH156 strain grown for 12 h in array medium containing 3g/l nitrate and 1% (w/v) arabinose	2nd
45	GSM528255	UKH164 strain grown for 12 h in array medium containing 3g/l nitrate and 1% (w/v) arabinose	2nd
46	GSM528254	UKH164 strain grown for 12 h in array medium containing 3g/l nitrate and 1% (w/v) arabinose	1st
47	GSM528248	UMS84 strain grown for 12 h in array medium containing 3g/l nitrate and 1% (w/v) arabinose	1st
48	GSM528249	UMS84 strain grown for 12 h in array medium containing 3g/l nitrate and 1% (w/v) arabinose	2nd
49	GSM528242	AB33 strain grown for 5 h in array medium containing 3g/l nitrate and 1% (w/v) arabinose	2nd
50	GSM528247	UMS84 strain grown for 12 h in array medium containing 3g/l nitrate and 1% (w/v) arabinose	2nd
51	GSM465554	AB34 strain grown for 3 h in array medium containing 3g/l nitrate	2nd
52	GSM465557	AB34 strain grown for 12 h in array medium containing 3g/l nitrate	1st
53	GSM465558	AB34 strain grown for 12 h in array medium containing 3g/l nitrate	2nd
54	GSM465556	AB34 strain grown for 5 h in array medium containing 3g/l nitrate	2nd
55	GSM465555	AB34 strain grown for 5 h in array medium containing 3g/l nitrate	1st
56	GSM465553	AB34 strain grown for 3 h in array medium containing 3g/l nitrate	1st
57	GSM465552	AB34 strain grown for 2 h in array medium containing 3g/l nitrate	2nd
58	GSM465551	AB34 strain grown for 2 h in array medium containing 3g/l nitrate	1st
59	GSM465540	AB33 strain grown for 2 h in array medium containing 3g/l nitrate	2nd
60	GSM465539	AB33 strain grown for 2 h in array medium containing 3g/l nitrate	1st
61	GSM465550	AB34 strain grown for 1 h in array medium containing 3g/l nitrate	2nd
62	GSM465549	AB34 strain grown for 1 h in array medium containing 3g/l nitrate	1st
63	GSM465538	AB33 strain grown for 1 h in array medium containing 3g/l nitrate	2nd
64	GSM465537	AB33 strain grown for 1 h in array medium containing 3g/l nitrate	1st
65	GSM465434	AB32 strain grown for 0 h in array medium containing 1% (w/v) arabinose	1st
66	GSM465439	AB32 strain grown for 0 h in array medium containing 1% (w/v) arabinose	2nd
67	GSM465411	AB31 strain grown for 0 h in array medium containing 1% (w/v) arabinose	2nd
68	GSM465410	AB31 strain grown for 0 h in array medium containing 1% (w/v) arabinose	1st
69	GSM135545	FB1 strain grown to an OD ₆₀₀ of 0.5 in array medium	1st

70	GSM135546	FB1 strain grown to an OD ₆₀₀ of 0.5 in array medium	2nd
71	GSM465535	AB33 strain grown for 0 h in array medium containing 3g/l nitrate	1st
72	GSM465536	AB33 strain grown for 0 h in array medium containing 3g/l nitrate	2nd
73	GSM465548	AB34 strain grown for 0 h in array medium containing 3g/l nitrate	2nd
74	GSM465547	AB34 strain grown for 0 h in array medium containing 3g/l nitrate	1st
75	GSM465534	AB32 strain grown for 12 h in array medium containing 1% (w/v) arabinose	2nd
76	GSM465533	AB32 strain grown for 12 h in array medium containing 1% (w/v) arabinose	1st
77	GSM465598	AB31Δrbf1 strain grown for 12 h in array medium containing 1% (w/v) arabinose	2nd
78	GSM465597	AB31Δrbf1 strain grown for 12 h in array medium containing 1% (w/v) arabinose	1st
79	GSM140091	HE140 strain grown to an OD ₆₀₀ of 0.5 in CM medium containing 1% (w/v) glucose	2nd
80	GSM182059	FB1 strain grown in CM medium containing 1% (w/v) glucose (without H ₂ O ₂)	2nd
81	GSM182056	FB1 strain grown in CM medium containing 1% (w/v) glucose (without H ₂ O ₂)	1st
82	GSM140082	FB1 strain grown in CM medium containing 1% (w/v) glucose	1st
83	GSM140083	FB1 strain grown in CM medium containing 1% (w/v) glucose	2nd
84	GSM140090	HE140 strain grown to an OD ₆₀₀ of 0.5 in CM medium containing 1% (w/v) glucose	1st
85	GSM140094	FB1 strain grown in CM medium containing 1% (w/v) glucose in the presence of 10mM FeSO ₄	1st
86	GSM140098	BW12 strain grown in CM medium containing 1% (w/v) glucose in the presence of 10mM FeSO ₄	1st
87	GSM140099	BW12 strain grown in CM medium containing 1% (w/v) glucose in the presence of 10mM FeSO ₄	2nd
88	GSM140096	FB1 strain grown to an OD ₆₀₀ of 0.5 in array medium containing 1%(w/v) glucose in the presence of FeSO ₄	2nd
89	GSM140097	FB1 strain grown to an OD ₆₀₀ of 0.5 in array medium containing 1%(w/v) glucose in the absence of FeSO ₄	2nd
90	GSM140095	FB1 strain grown to an OD ₆₀₀ of 0.5 in array medium containing 1%(w/v) glucose in the absence of FeSO ₄	1st
91	GSM140076	FB1 strain grown in CM medium containing 1% (w/v) arabinose for 180 min	1st
92	GSM140077	FB1 strain grown in CM medium containing 1% (w/v) arabinose for 180 min	2nd
93	GSM140078	FB1 strain grown in CM medium containing 1% (w/v) arabinose for 180 min	3rd
94	GSM140089	HE140 strain grown in CM medium containing 1 %(w/v) arabinose for 75 min	3rd
95	GSM140088	HE140 strain grown in CM medium containing 1 %(w/v) arabinose for 75 min	2nd
96	GSM140087	HE140 strain grown in CM medium containing 1 %(w/v) arabinose for 75 min	1st
97	GSM465674	JB2 strain grown in array medium containing 1% (w/v) arabinose for 5 h	1st
98	GSM465675	JB2 strain grown in array medium containing 1% (w/v) arabinose for 5 h	2nd
99	GSM465413	AB31 strain grown in array medium containing 1% (w/v) arabinose for 1 h	2nd
100	GSM465427	AB31 strain grown in array medium containing 1% (w/v) arabinose for 2 h	2nd
101	GSM465426	AB31 strain grown in array medium containing 1% (w/v) arabinose for 2 h	1st
102	GSM105901	JB1-Perg::clp1 strain grown in minimal medium containing 1% (w/v) arabinose for 2 h	2nd
103	GSM105900	JB1-Perg::clp1 strain grown in minimal medium containing 1% (w/v) arabinose for 2 h	1st
104	GSM105899	JB1 strain grown in array medium containing 1% (w/v) arabinose for 2 h	1st
105	GSM105898	JB1 strain grown in array medium containing 1% (w/v) arabinose for 2 h	2nd

106	GSM465412	AB31 strain grown in array medium containing 1% (w/v) arabinose for 1 h	1st
107	GSM465589	AB31Δrbf1 strain grown in array medium containing 1% (w/v) arabinose for 3 h	1st
108	GSM465590	AB31Δrbf1 strain grown in array medium containing 1% (w/v) arabinose for 3 h	2nd
109	GSM465592	AB31Δrbf1 strain grown in array medium containing 1% (w/v) arabinose for 5 h	2nd
110	GSM465591	AB31Δrbf1 strain grown in array medium containing 1% (w/v) arabinose for 5 h	1st
111	GSM465531	AB32 strain grown in array medium containing 1% (w/v) arabinose for 5 h	1st
112	GSM465532	AB32 strain grown in array medium containing 1% (w/v) arabinose for 5 h	2nd
113	GSM465529	AB32 strain grown in array medium containing 1% (w/v) arabinose for 3 h	1st
114	GSM465530	AB32 strain grown in array medium containing 1% (w/v) arabinose for 3 h	2nd
115	GSM465527	AB32 strain grown in array medium containing 1% (w/v) arabinose for 2 h	1st
116	GSM465528	AB32 strain grown in array medium containing 1% (w/v) arabinose for 2 h	2nd
117	GSM465649	CP27 strain grown in array medium containing 1% (w/v) arabinose for 5 h	1st
118	GSM465650	CP27 strain grown in array medium containing 1% (w/v) arabinose for 5 h	2nd
119	GSM465430	AB31 strain grown in array medium containing 1% (w/v) arabinose for 5 h	1st
120	GSM465431	AB31 strain grown in array medium containing 1% (w/v) arabinose for 5 h	2nd
121	GSM465428	AB31 strain grown in array medium containing 1% (w/v) arabinose for 3 h	1st
122	GSM465429	AB31 strain grown in array medium containing 1% (w/v) arabinose for 3 h	2nd
123	GSM528241	AB33 strain grown in array medium containing 3g/l nitrate containing 1 % (w/v) arabinose for 5 h	1st
124	GSM528245	UMS84 strain grown in array medium containing 3g/l nitrate and 1% (w/v) arabinose for 5 h	1st
125	GSM418686	SG200 strain grown in array medium containing 1% (w/v) xylose for 6 h	1st
126	GSM418687	SG200 strain grown in array medium containing 1% (w/v) xylose for 6 h	2nd
127	GSM418690	SG200Δhxt1 strain grown in array medium containing 1% (w/v) xylose for 6 h	1st
128	GSM418691	SG200Δhxt1 strain grown in array medium containing 1% (w/v) xylose for 6 h	2nd
129	GSM418688	SG200Δhxt1 strain grown in array medium containing 1% (w/v) glucose for 6 h	1st
130	GSM418689	SG200Δhxt1 strain grown in array medium containing 1% (w/v) glucose for 6 h	2nd
131	GSM418684	SG200 strain grown in array medium containing 1% (w/v) glucose for 6 h	1st
132	GSM418685	SG200 strain grown in array medium containing 1% (w/v) glucose for 6 h	2nd
133	GSM182090	FB1Δyap1 strain grown in CM-glucose medium containing 5 mM H ₂ O ₂ for 1 h	1st
134	GSM182102	FB1Δyap1 strain grown in CM-glucose medium containing 5 mM H ₂ O ₂ for 1 h	2nd
135	GSM182087	FB1 strain grown in CM-glucose medium containing 5 mM H ₂ O ₂ for 1 h	2nd
136	GSM182061	FB1 strain grown in CM-glucose medium containing 5 mM H ₂ O ₂ for 1 h	1st
137	GSM465526	AB32 strain grown in array medium containing 1% (w/v) arabinose for 1 h	2nd
138	GSM465525	AB32 strain grown in array medium containing 1% (w/v) arabinose for 1 h	1st
139	GSM754003	FB1 strain grown in CM medium with 1% (w/v) glucose to an OD ₆₀₀ of 0.5	2nd
140	GSM754004	FB1 strain grown in CM medium with 1% (w/v) glucose to an OD ₆₀₀ of 0.5	3rd
141	GSM754002	FB1 strain grown in CM medium with 1% (w/v) glucose to an OD ₆₀₀ of 0.5	1st

142	GSM754005	FB1Δrak1 strain grown in CM medium with 1% (w/v) glucose to an OD ₆₀₀ of 0.5	3rd
143	GSM754007	FB1Δrak1 strain grown in CM medium with 1% (w/v) glucose to an OD ₆₀₀ of 0.5	2nd
144	GSM754006	FB1Δrak1 strain grown in CM medium with 1% (w/v) glucose to an OD ₆₀₀ of 0.5	1st

Table S5. Conditions under which the *vbs1* gene is most up- and down-regulated.

Condition	Log2 fold change ^a
Up-regulated	
1. SG200 strain grown for 48 h on charcoal minimal medium	3.47 ^b
2. SG200 strain grown on NM ⁺ charcoal plates for 48 h	3.12 ^c
3. FB1 strain grown in CM-glucose medium containing 5 mM H ₂ O ₂ for 1 h	1.85 ^b
4. Tumors induced in corn plants by an infection with the strains FB1 and FB2 (13 dpi)	1.45 ^b
5. SG200Δtup1 strain grown for 48 h on charcoal minimal medium	0.94 ^b
Down-regulated	
1. FB1Δrak1 strain grown in CM medium with 1% (w/v) glucose to an OD ₆₀₀ of 0.5	-2.06 ^c
2. FB1 strain grown in CM medium with 1% (w/v) glucose to an OD ₆₀₀ of 0.5	-1.59 ^c
3. BW12 strain grown in CM medium containing 1% (w/v) glucose in the presence of 10 mM FeSO ₄	-1.47 ^b
4. SG200Δhxt1 strain grown in array medium containing 1% (w/v) glucose for 6 h	-1.27 ^b
5. SG200Δhxt1 strain grown in array medium containing 1% (w/v) xylose for 6 h	-1.05 ^b

^a Normalized gene expression data extracted from Gene Expression Omnibus.

^b Value calculated from two experimental conditions.

^c Value calculated from three experimental conditions.

Table S6. Conditions under which the *pks1* gene is most up- and down-regulated.

Condition	Log2 fold change ^a
Up-regulated	
1. Tumors induced in corn plants by an infection with the strains FB1 and FB2 (13 dpi)	4.82 ^b
2. Tumor material from maize leaves 5 days post FB1 Δ fox1/FB2 Δ fox1 mixed infection at 28°C	1.93 ^c
3. Tumor material from maize leaves 5 days post FB1/FB2 mixed infection at 28°C	1.93 ^c
4. AB33 strain grown for 5 h in array medium containing 3g/l nitrate	0.76 ^b
5. AB32 strain grown for 12 h in array medium containing 1% (w/v) arabinose	0.71 ^b
Down-regulated	
1. HE140 strain grown for 180 min in CM medium containing 1% (w/v) arabinose	-1.89 ^b
2. FB1 strain grown for 75 min in CM medium containing 1% (w/v) arabinose	-1.47 ^b
3. FB1 strain grown to an OD ₆₀₀ of 0.5 in array medium containing 1%(w/v) glucose in the presence of FeSO ₄	-1.47 ^c
4. FB1 strain grown in CM-glucose medium containing 5 mM H ₂ O ₂ for 1 h	-1.44 ^b
5. FB1 strain grown in CM medium containing 1% (w/v) glucose in the presence of 10 mM FeSO ₄	-0.98 ^b

^a Normalized gene expression data extracted from Gene Expression Omnibus.

^b Value calculated from two experimental conditions.

^c Value calculated from three experimental conditions.

Table S7. Conditions under which the *pks2* gene is most up- and down-regulated.

Condition	Log2 fold change ^a
Up-regulated	
1. Tumors induced in corn plants by an infection with the strains FB1 and FB2 (13 dpi)	5.29 ^b
2. Tumor material from maize leaves 5 days post FB1Δfox1/FB2Δfox1 mixed infection at 28°C	0.95 ^c
3. Tumor material from maize leaves 5 days post FB1/FB2 mixed infection at 28°C	0.92 ^c
4. AB32 strain grown for 12 h in array medium containing 1% (w/v) arabinose	0.89 ^b
5. AB34 strain grown for 3 h in array medium containing 3g/l nitrate	0.83 ^b
Down-regulated	
1. HE140 strain grown for 180 min in CM medium containing 1% (w/v) arabinose	-1.56 ^b
2. FB1 strain grown in CM medium with 1% (w/v) glucose to an OD ₆₀₀ of 0.5	-1.54 ^c
3. HE140 strain grown to an OD ₆₀₀ of 0.5 in CM medium containing 1% (w/v) glucose	-1.43 ^b
4. FB1 strain grown to an OD ₆₀₀ of 0.5 in array medium containing 1% (w/v) glucose in the presence of FeSO ₄	-1.23 ^b
5. FB1 strain grown for 75 min in CM medium containing 1% (w/v) arabinose	-0.88 ^b

^a Normalized gene expression data extracted from Gene Expression Omnibus.

^b Value calculated from two experimental conditions.

^c Value calculated from three experimental conditions.

Table S8. Primers used in this study.

Primer	Sequence	T _m (°C)	Comments
MH86	5' -CGAGCACGGTGTGAGCTCTTG	71.4	Primer forward for the amplification of <i>pks5</i> ORF
MH87	5' -CGCTTGATAGGATAACACCGC	64.4	Primer reverse for the amplification of <i>pks5</i> ORF
MH88	5' -CGACTTCCGTTTTGGTGAGTAGC	68.5	Primer forward for the amplification of <i>orf1</i> ORF
MH89	5' -GCTTCAATGGCCAATACTGCACG	71.2	Primer reverse for the amplification of <i>orf1</i> ORF
MH90	5' -CGTTTCGCCACTGCTATCGATCAAGC	75.1	Primer forward for the amplification of <i>pks4</i> ORF
MH91	5' -CGTAAGCTTGGCGTCCGTCCAGGC	78.1	Primer reverse for the amplification of <i>pks4</i> ORF
MH92	5' -GCTGTTTCTCCATATGATGC	59.7	Primer forward for the amplification of <i>vbs1</i> ORF
MH93	5' -GGATCACAGTCACAAGCTGC	63.6	Primer reverse for the amplification of <i>vbs1</i> ORF
MH94	5' -GCTGCTCAGACGAAAACCC	69.3	Primer forward for the amplification of <i>orf4</i> ORF
MH95	5' -GCATCAATGAGTACTGGATGG	62.0	Primer reverse for the amplification of <i>orf4</i> ORF
MH96	5' -CGGTAGGGCGGAAGGCGTTGC	77.0	Primer forward for the amplification of <i>pks3</i> ORF
MH97	5' -GCTGGAAATGTCCAGGTGTGTGG	71.7	Primer reverse for the amplification of <i>pks3</i> ORF
MH98	5' -GCTCTCCTCGAGAATTACCAGC	65.3	Primer forward for the amplification of <i>omt1</i> ORF
MH99	5' -CGAACCTTGGCCGAGTGCAGG	75.0	Primer reverse for the amplification of <i>omt1</i> ORF
MH100	5' -CGAACCTTCTGGGATACAAGCC	67.6	Primer forward for the amplification of <i>pmo1</i> ORF
MH101	5' -GCATTCTCCTGCTCGGTGTTGC	72.2	Primer reverse for the amplification of <i>pmo1</i> ORF
MH102	5' -CGTCAGCGACACCTGATCTGC	70.7	Primer forward for the amplification of <i>orf5</i> ORF
MH103	5' -CGTGACCCTATCGAGGCCATGACC	75.0	Primer reverse for the amplification of <i>orf5</i> ORF
MH104	5' -CGAATTCCTGGTCCACGTCAACTGC	74.9	Primer forward for the amplification of <i>cyp4</i> ORF
MH105	5' -GAACTGATATCGGCATGCGGCGACG	78.6	Primer reverse for the amplification of <i>cyp4</i> ORF
MH106	5' -CGTTCTCGTCACAGGCAGCACC	73.4	Primer forward for the amplification of <i>deh1</i> ORF
MH107	5' -CGATGGAACCTCGAGCAGAGG	70.4	Primer reverse for the amplification of <i>deh1</i> ORF
MH108	5' -CGTCAGATGGCGGGCTGGGACTCG	81.3	Primer forward for the amplification of <i>orf6</i> ORF
MH109	5' -CGACACGCGATGCGACACCGATGG	82.3	Primer reverse for the amplification of <i>orf6</i> ORF
MH110	5' -GCAACGTCACCAAAGCCTTGACC	72.5	Primer forward for the amplification of <i>orf7</i> ORF
MH111	5' -GGTGTACTCGCCTGCGTACGACG	73.5	Primer reverse for the amplification of <i>orf7</i> ORF
MG1012	5' -CGTTAAACGTATCGAAGCTAGC	61.7	Primer forward for the amplification of <i>mtf2</i> ORF
MG1013	5' -GCAACACAAGATCGTGAGGAGC	68.2	Primer reverse for the amplification of <i>mtf2</i> ORF
MG1014	5' -ATGGATCAGCACAAGCGAGGC	70.8	Primer forward for the amplification of <i>orf2</i> ORF
MG1015	5' -TTAGAACAAAGATGAGAACGTGTCTCCTGC	70.6	Primer reverse for the amplification of <i>orf2</i> ORF
MG1016	5' -ATGAGAAGCGCAGCAATCGAAGC	72.3	Primer forward for the amplification of <i>orf3</i> ORF
MG1017	5' -TCATCCATGTGGACAAGTGGC	68.3	Primer reverse for the amplification of <i>orf3</i> ORF
MG1018	5' -GCTCAAAAAATCTGAATGGACCG	67.4	Primer forward for the amplification of <i>mtf1</i> ORF

MG1019	5' -CGTGCCGGGTCGCCAGCCATGG	84.2	Primer reverse for the amplification of <i>mtf1</i> ORF
MG1020	5' -CGACGAATCAAACAGGTCTACACTGG	70.2	Primer forward for the amplification of <i>aox1</i> ORF
MG1021	5' -CGAAGCGGGCGCGATGCGATCG	83.8	Primer reverse for the amplification of <i>aox1</i> ORF
MH881	5' -CGAGAACGTGGTCAAGTCGATGG	71.8	Primer forward for the amplification of <i>pks1</i> ORF
MH882	5' -GCAGATCGCAGTAATGCTGGGC	71.8	Primer reverse for the amplification of <i>pks1</i> ORF
MH883	5' -CGATGCGGAGATGAGCCAGCC	75.3	Primer forward for the amplification of <i>pks2</i> ORF
MH884	5' -GGTAATCTCTTCAAAGTCTCCAC	59.7	Primer reverse for the amplification of <i>pks2</i> ORF
MH876	5' -GTGAAACTCGATGAGGCC	60.9	Outer primer for downstream of <i>crg1</i> ORF
ME48	5' -GGGGGATGTGCTGCAAGGCG	76.1	Primer forward for sequencing the pRS426 vector
ME49	5' -TCCGGCTCCTATGTTGTGTGG	69.2	Primer reverse for sequencing the pRS426 vector
MI108	5' -GATCCTTCTTCCTGCGACCTTTC	68.0	Primer forward for sequencing the <i>pks2</i> ORF
MI109	5' -GCGGCTGTATCAGAAAATTTTCG	67.3	Primer forward for sequencing the <i>pks2</i> ORF
MI110	5' -GTTAGGCTTCTCAGTCTTCTCTG	60.3	Primer forward for sequencing the <i>pks2</i> ORF
MI111	5' -GACGCTGCAGAAAGCTGGTTACG	70.8	Primer forward for sequencing the <i>pks2</i> ORF
MI112	5' -CCACCAATCATTCGGGAGAATCC	71.2	Primer forward for sequencing the <i>pks2</i> ORF
MI113	5' -CAGACTATCAGAGCAGAGCAAGC	64.5	Primer forward for sequencing the <i>pks2</i> ORF
MI114	5' -CCTTGCAGACGGATGCAACCAAG	73.5	Primer forward for sequencing the <i>pks2</i> ORF
MI115	5' -GTATCGCATGGTAGTAGCCAGCC	67.5	Primer forward for sequencing the <i>pks2</i> ORF
MI116	5' -GCTCCCGCTAATTCTTCGCATG	70.5	Primer forward for sequencing the <i>pks2</i> ORF
MI117	5' -CACAAAGGAGCACGTCACCTAAC	68.0	Primer forward for sequencing the <i>pks2</i> ORF
MI118	5' -CGTCTTTAAGCGAATTCGCCGAG	71.2	Primer forward for sequencing the <i>pks2</i> ORF
MI119	5' -GGAGCTGCTTTGCAGCGTTCAGC	74.9	Primer forward for sequencing the <i>pks2</i> ORF
MI120	5' -CCTGGCTTTGTGGCAACGCGGCG	82.4	Primer forward for sequencing the <i>pks5</i> ORF
MI121	5' -GGGAGCTGATGCTGGCTTTGTATTG	72.0	Primer forward for sequencing the <i>pks5</i> ORF
MI122	5' -CAAAATGCTGGCTGAATGCCGTGC	76.1	Primer forward for sequencing the <i>pks5</i> ORF
MI123	5' -CGTATCGACGACATTATCGTTCTAG	64.4	Primer forward for sequencing the <i>pks5</i> ORF
MI124	5' -GCAACTGCCTTCGTGTCGCACTATG	74.1	Primer forward for sequencing the <i>pks5</i> ORF
MI125	5' -CCGACCTAAGTCAGGCGGAATGG	73.1	Primer forward for sequencing the <i>pks5</i> ORF
MI126	5' -CCAGCTGCCTAGACAGTGTGTGTCG	71.0	Primer forward for sequencing the <i>pks5</i> ORF
MI127	5' -GCTCGATCTGGCCAAAGCCAGGTC	76.1	Primer forward for sequencing the <i>pks5</i> ORF
MI196	5' -CGCTCTCGAGGTAGATGAGAGAAGC	69.4	Primer forward for sequencing the <i>cyp4</i> ORF
MI197	5' -GCACCAAGAGTCAGGGCTACAAG	68.1	Primer forward for sequencing the <i>cyp4</i> ORF
MI198	5' -GGA CTACCGCCGAGGGAGAGATG	76.5	Primer forward for sequencing the <i>cyp4</i> ORF
MI199	5' -GCCAGGGCATGCACATTGCCG	78.6	Primer forward for sequencing the <i>cyp4</i> ORF
MI436	5' -CAAGCATCTTTGGCGCATGCTGTTG	76.4	Primer forward for sequencing the <i>vbs1</i> ORF
MI437	5' -GCAAGCGTTTACGTCAACACG	67.6	Primer forward for sequencing the <i>vbs1</i> ORF

MI438	5' -GCTATCTGGTATTGGACCAGCTC	64.8	Primer forward for sequencing the <i>vbs1</i> ORF
MI439	5' -CGAGTCACGAGGAAGCGTTCGAC	73.1	Primer forward for sequencing the <i>vbs1</i> ORF
MI440	5' -CCGCTACTGCGTGCACACTG	70.4	Primer forward for sequencing the <i>vbs1</i> ORF
MI955	5' -CGAAATGAAGATGAAATTCTTAAG	59.7	Primer forward for sequencing the <i>mtfl</i> ORF
MI956	5' -GTTTCGTCACCTATGTCCGCGTCG	73.5	Primer forward for sequencing the <i>mtfl</i> ORF
MI957	5' -CGAAGACTCTGGTCGCCTCACC	71.5	Primer forward for sequencing the <i>mtfl</i> ORF
MI958	5' -CCATGTTGCGCTTGCCCAATTTTTC	75.4	Primer forward for sequencing the <i>mtfl</i> ORF
MI959	5' -GCGACAAGTGCCCAAGTGTAGTCC	70.9	Primer forward for sequencing the <i>mtfl</i> ORF
MJ180	5' -CGTAAATGTGTTGAGGGTTGTTC	64.2	Primer forward for sequencing the native promoter of <i>pks5</i> ORF
MJ181	5' -GTCGTCAGTATGTACTACCTGAG	57.0	Primer forward for sequencing the native promoter of <i>pks5</i> ORF
MJ182	5' -CGAGAGCAATGCTGGACCATCC	72.1	Primer forward for sequencing the native promoter of <i>pks5</i> ORF
MJ183	5' -CGAGATTAATTTTCAAATGCTG	61.3	Primer forward for sequencing the native promoter of <i>pks5</i> ORF
MJ186	5' -GCTTACTCTCCGGTAAACCAGC	64.9	Primer forward for sequencing the <i>omt1</i> ORF
MJ187	5' -GCTCCCGCCATCAAGAGGCTC	73.4	Primer forward for sequencing the <i>omt1</i> ORF
MJ188	5' -CAGATACTCACGAATGTAAATCC	59.1	Primer forward for sequencing the <i>omt1</i> ORF
MJ189	5' -CTAGCCTCTTTCTTTGAGGATGG	64.1	Primer forward for sequencing the <i>omt1</i> ORF
MJ190	5' -CACGAGAGCTGGACGAGGAGTG	70.8	Primer forward for sequencing the <i>omt1</i> ORF
MJ191	5' -GCAGAGGTGCGACGTGGACACGTAC	72.9	Primer forward for sequencing the <i>omt1</i> ORF
MJ192	5' -CGATGCCGTCTCGAGCCGCACGAC	82.4	Primer forward for sequencing the <i>omt1</i> ORF
MJ197	5' -GTCGATACCGTCGCTTACTGTC	64.7	Primer forward for sequencing the <i>lac1</i> ORF
MJ198	5' -CGTACCTGGGCTATCTCAATGG	66.4	Primer forward for sequencing the <i>lac1</i> ORF
MJ199	5' -CTTTGACTGTCTTCAGCGCTGCC	71.2	Primer forward for sequencing the <i>lac1</i> ORF
MJ200	5' -CCTCTCGACACTGCTCGCCTGGCAG	79.2	Primer forward for sequencing the <i>lac1</i> ORF
MJ201	5' -GCTCTGCAAATGCAAAGTACGTGG	70.3	Primer forward for sequencing the <i>lac1</i> ORF
MJ202	5' -CAGTCAACGCTGTTTGCTATTGC	67.6	Primer forward for sequencing the <i>lac1</i> ORF
MJ203	5' -CTATGTCCAGCAGTGCAAGTTTG	65.7	Primer forward for sequencing the <i>lac1</i> ORF
MJ204	5' -GAGGTGGAAGAGCATCGGCGTCG	76.6	Primer forward for sequencing the <i>lac1</i> ORF
MI924	5' -CGTAAGGTGGACACCTTACTG	61.1	Primer forward for sequencing the <i>crg1</i> ORF
MI925	5' -GCTGACTCCTGTCATGGGCAATG	72.0	Primer forward for sequencing the <i>crg1</i> ORF
MI926	5' -CAGCCGTGCACGAAGATCTCCGG	77.4	Primer forward for sequencing the <i>crg1</i> ORF
MI917	5' -CCTCTTTCTTTGAGGATGGCTTC	66.1	Primer forward for sequencing the native promoter of the <i>pks3</i> ORF
MI918	5' -CGTCCAGCGCGATTTACAAATC	73.2	Primer forward for sequencing the native promoter of the <i>pks3</i> ORF
MI919	5' -GCTCTTTTGCGGACACTGGTAG	66.9	Primer forward for sequencing the native promoter of the <i>pks3</i> ORF
MI920	5' -GTCGATAATCCCGGCCGCGCTCTTG	79.7	Primer forward for sequencing the native promoter of the <i>pks3</i> ORF
MI594	5' -CGGATGAGCTGGGATCACTATAG	65.6	Primer forward for sequencing the <i>pks4</i> ORF
MI595	5' -CCCACTCCTCTAGTCCGAGCTC	67.5	Primer forward for sequencing the <i>pks4</i> ORF

MI596	5' -GTTTTGCCACCTCTTCTTGAC	66.9	Primer forward for sequencing the <i>pks4</i> ORF
MI597	5' -CACCTATCCGACTCCATTATCAGC	66.5	Primer forward for sequencing the <i>pks4</i> ORF
MI598	5' -GTGCCACACCCTCACAGGTCAACG	75.7	Primer forward for sequencing the <i>pks4</i> ORF
MJ049	5' -GTATTGAGCTGGACGAGCGAC	69.2	Primer forward for sequencing the native promoter of the <i>cyp4</i> ORF
MJ050	5' -CGGATGGTGCAATAGCACTTCTC	68.7	Primer forward for sequencing the native promoter of the <i>cyp4</i> ORF
MJ051	5' -CCTCACATCACCACAACACGAG	67.9	Primer forward for sequencing the native promoter of the <i>cyp4</i> ORF
MI930	5' -CGTTTTTTTCATGTTGCATCTCG	67.2	Primer forward for sequencing the <i>crg1</i> ORF
MI931	5' -CATTCCAATCAGTCACGAGTGCAC	69.8	Primer forward for sequencing the <i>crg1</i> ORF
MI932	5' -GCTACTAACTGTCTTTCGCATCTC	62.2	Primer forward for sequencing the <i>crg1</i> ORF
MI933	5' -GCGTGGGCTCGGATATCGGTGG	77.0	Primer forward for sequencing the <i>crg1</i> ORF
MI035	5' -CTCATCCTTCGACAACGCCGTTT	72.6	Primer forward for sequencing the <i>pks1</i> ORF
MI036	5' -CCTGGAAAGCTTTGACGCAACC	70.7	Primer forward for sequencing the <i>pks1</i> ORF
MI037	5' -CTCGCGCCCGAAGCAGATCTGG	77.6	Primer forward for sequencing the <i>pks1</i> ORF
MI038	5' -CTAGACGCGCACTCCTGAGCGG	74.2	Primer forward for sequencing the <i>pks1</i> ORF
MI039	5' -CATTGGTGCAGGCGAAGCGGTGTC	78.7	Primer forward for sequencing the <i>pks1</i> ORF
MI040	5' -GCCTCGGACAAAGATGAGCTGG	71.2	Primer forward for sequencing the <i>pks1</i> ORF
MI041	5' -GCATCAAAAAGGTCAGTGCATTTCG	70.3	Primer forward for sequencing the <i>pks1</i> ORF
MI042	5' -GGTCAAGCTTTCAGTGAAGTCGG	68.1	Primer forward for sequencing the <i>pks1</i> ORF
MI043	5' -GGTGCGTCTGTCAGCTACACGG	71.2	Primer forward for sequencing the <i>pks1</i> ORF
MI044	5' -CGTTGTTTATGGAGTGCACAGC	69.5	Primer forward for sequencing the <i>pks1</i> ORF
MI045	5' -GCAAATCGCGTTCTTTCTTCCACC	72.0	Primer forward for sequencing the <i>pks1</i> ORF
MI046	5' -GTCGATAGCCTCGTTGGCTGGG	72.7	Primer forward for sequencing the <i>pks1</i> ORF
MI950	5' -CCAACCGACCTCGTGCTCTCTG	72.4	Primer forward for sequencing the <i>pks4</i> ORF
MI951	5' -CAGGAACTTGGGATGCTGACGTG	71.8	Primer reverse for sequencing the <i>cyp4</i> ORF
MI952	5' -GACTGGCTCACTCGGCTCATAGTG	70.2	Primer reverse for sequencing the native promoter of the <i>pks3</i> ORF

Acknowledgements

First and foremost, I would like to extend my sincere appreciation and gratitude to my advisor Prof. Dr. Michael Bölker for his guidance, great ideas and enthusiasm for science, which has been contagious and motivational during my PhD studies. I will always be thankful for trusting and giving me the opportunity to be part of his research group, even when my academic training had been focused on a different direction.

I would also like to deeply thank to Prof. Dr. Alfred Batschauer for being the second evaluator of my PhD thesis and dedicate his time and effort in writing the official report of my examination. In addition, I want to express my deeply-felt thanks to Prof. Dr. Regine Kahmann and Prof. Dr. Helge Bode for accepting being part of my PhD thesis committee, their valuable feedback and fruitful discussions during the whole process.

It is also my pleasure to thank Prof. Dr. Helge Bode for generously sharing his time, extraordinary knowledge and facilities in our collaborative work.

Thankfulness is also addressed to Prof. Dr. Johann Heider, Prof. Dr. Regine Kahmann and Dr. Björn Sandrock for the insightful comments, suggestions and hard questions during the committee meetings.

I am really grateful to Dr. Marc Strickert who helped me enormously along my PhD studies, not only for his valuable collaboration in this project but also for all his advice to develop a better scientific criticism.

I am particularly grateful for the assistance given by Dr. Victoria Challinor and Dr. Yi-Ming Shi who shared their expertise in the secondary metabolite extraction and isolation techniques, also for the enriching discussions we had during my working days in Frankfurt. I greatly appreciate the support received from the work that Dr. Zakaria Cheikh Ali and Dr. Peter Grün performed in the NMR spectra interpretation and structure elucidation.

I am deeply grateful to Dr. Björn Sandrock, who first introduced me to *Ustilago maydis* and patiently guided me on the beginning of my laboratory work, sharing all his knowledge and experience in genetics.

I would like to thank to Silke Fröhlich and Marisa Piscator who were always kindly in providing technical assistance during my laboratory work and for their support during my stay here in Germany.

My special words of thanks should also go to Lisa Rosenbecker for having decided to join our project, first as an undergraduate and afterwards as a master student. Thank you Lisa for your dedication and for allowing me to learn how to be a better supervisor.

I would like to thank to Christian Renicke for solving many machine troubles and provide me with yeast strains, plasmids, materials and reagents every time I needed them. Thank you Christian for the constant helps and suggestions you made me when I wanted to used *S. cerevisiae* as a heterologous system for reconstituting the melanin biosynthetic pathway in *U. maydis*.

My deepest appreciation goes to Marino Moretti, who besides being a great friend and an excellent chef, helped me providing me plasmids, primers and strains to make my work smoothly.

I am also hugely appreciative to Gabriel Schweizer, Libera Lo Presti, Pierre Grognet, Lay-Sun, Marie Tollot, Daniel Lanver, Stefanie Reissmann and Stefan Schmidt from Kahmann lab, for their time and effort in answering many questions I made related to *Ustilago maydis*. A very big thank to Annika Brych and Judita Mascarenhas from Batschauer's lab for allow me to make some experiments in their lab, sharing many facilities and reagents.

I appreciate the feedback offered by Johannes Freitag and Thorsten Stehlik during my seminars and informal discussions in the lab. Special thanks to Tobias Deinzer and Meryem Friedrich who contributed to the generation of mutant strains in *U. maydis* for a better understanding of the melanization pathway.

I thank my fellow past and current members from Bölker lab for sharing many hours at work, knowledge, seminars, discussions, life experiences and breakfasts: Alex F., Alex M., Alina, Augustina, Birgit, Britta, Christian, Christopher, Daniel, Darius, Désirée, Domenica, Dr. Escher, Inna, Jens, Johannes, Julia, Laura, Lea, Linda, Marisa, Mathis, Mery Michi, Nicole, Roman, Sandra, Sarah, Saskia, Silke Sonja, Steffi, Tani, Thea, Thorsten, Tina and Tobi.

I am so thankful with all the members of Mösch lab for making my life in Germany much easier and enjoyable. Special thanks to Massi, Didi, Daniel, Vivek, Anne, Nina, Bernard, Sarah W. and Sarah S.

All my friends who supported me in writing, and incented me to strive towards my goal. Thank you Massi for sharing many hours of conversation and dreams (Forza azzurri!), Augustina for being my "bench friend" and for your advice on how to make my life less complicated, Nuria for radiate happiness and positive energy in any circumstance, and Alejandra for giving to Marburg a Mexican taste.

This thesis would have remained a dream had it not been for my parents, Ramona and Cuauhtémoc, and my sister Perla, who have always supported and encouraged me in all the decisions I have taken during my professional career.

Last but not least, I would like to thank to Wei-Hua for making my life more colorful in a broad sense and for make me feel confident to overcome every difficulty I encountered during my PhD studies.

Curriculum Vitae

Esmeralda Za-nicthé Reyes-Fernández

Personal Information

Date of Birth	05.Oct.1984
Nationality	Mexican
Residence	Culiacan, Sinaloa

Education

08.2002 - 06.2007	Bachelor in Biochemical Engineering (Major in Food Science). University of Sinaloa (UAS), Culiacan, Mexico Title of the thesis: Determination of the physical and physicochemical characteristics of fermented common beans (Tempeh).
02.2008 - 06.2010	Master in Biochemical Sciences (Major in Molecular Microbiology). Institute of Biotechnology (IBT-UNAM), Cuernavaca, Mexico Title of the thesis: Analysis of the interaction of the Cry4Ba toxin from <i>Bacillus thuringiensis</i> with its alkaline phosphatase receptor in <i>Aedes aegypti</i> larvae.
10.2011 - 12.2016	PhD in Natural Sciences Marburg University (Genetics Department) Title of the thesis: Genomic analysis of secondary metabolism in <i>Ustilago maydis</i> .